

**GROWTH IN COLD-WATER OCTOCORALS: RATES, MORPHOLOGY AND
ENVIRONMENTAL CONTROLS**

by © Bárbara de Moura Neves (Thesis) submitted to the School of Graduate Studies in
partial fulfillment of the requirements for the degree of

PhD in Biology/Faculty of Sciences

Memorial University of Newfoundland

September 2016

St. John's Newfoundland and Labrador

Abstract

Deep-water corals can have high longevities and slow growth rates. While most studies have been focusing on growth rates of gorgonians, few studies have examined rates and patterns in other octocorals, such as sea pens. Here I studied growth rates and patterns in the sea pens *Halpteria finmarchica*, *Umbellula encrinus*, and *Pennatula grandis*, and in the gorgonians *Primnoa pacifica*, *Primnoa resedaeformis*, and *Keratoisis* sp. Longevity and growth rates were estimated by examining growth rings in their skeletons (axes), whose morphology and composition were also explored. Growth patterns were investigated by examining relationships between colony and axis characteristics. Relationships between colony growth rates and environmental factors were also assessed. The morphology of the axis in sea pens varies among taxa and within colonies, and their carbonate portion is composed in average of 65-85% of magnesian calcite (Ca, Mg)CO₃. Sea pens can have longevities reaching ~70 years in *U. encrinus*. Diametric growth rates in *H. finmarchica*, *U. encrinus*, and *P. grandis* were comparable in magnitude, ranging between 0.13-0.14 mm·yr⁻¹. Using new and published data, diametric growth rates in *P. pacifica* and *P. resedaeformis* averaged 0.43 mm·yr⁻¹ and were not statistically different. In the Arctic populations of *Keratoisis* sp. studied here radial growth rates ranged between 0.010-0.018 mm·yr⁻¹, much slower than in most other populations of this coral. Relationships between growth rates and environmental variables were statistically significant for bottom temperature (*U. encrinus*), chlorophyll a (*P. grandis* and *Primnoa* spp.), and depth (*Primnoa* spp.). Geochemical analyses yielded a number of trace element peaks comparable to the number of growth rings in sea pens. The ¹⁴C curves for the

studied sea pens follow the same patterns seen in the calcite of other octocorals in the region, in which rings are formed annually. Growth rate and longevity data can support conservation efforts for these vulnerable species.

Acknowledgments

I am deeply grateful to my supervisor Dr. Evan Edinger, who provided the opportunity and the resources that allowed me to explore a whole new coral world. I also thank my committee members Dr. Graham Layne, Dr. Annie Mercier, and Dr. Kent Gilkinson for the guidance and valuable comments through the years. The examiner committee members Dr. Robert Hooper, Dr. Stewart Fallon, and Dr. Gary Williams are also thanked for their suggestions and comments.

I thank Dr. Sally Leys (chief scientist), Jackson Chu, Vince Lecours, CCGS *Vector* captain and crew, and the ROPOS team for making possible the 2011 ROV cruise in the Strait of Georgia. I also thank CCGS *Amundsen* captains and crew, chief scientists Dr. Louis Fortier, Dr. Maurice Levasseur, Dr. Philippe Archambault, ROV pilots Ian Murdock, Peter Lockhart, Trevor Shepherd, and Vincent Auger for the 2013-2015 cruises to Baffin Bay.

Vonda Wareham (DFO) provided a great number of the samples used in this thesis, and shared her knowledge and enthusiasm, which were a great incentive to the progress of this work. Dr. Margaret Treble and Dr. Kevin Hedges (DFO), Cindy Grant, Alexis Burt, Brynn Devine, and Laura Wheeland also provided valuable sea pen samples included in this study. Dr. Pål Buhl-Mortensen provided raw unpublished data on *Primnoa resedaeformis*, and Victoria Howse provided *Primnoa* samples from Labrador.

The use of museum specimens was only possible thanks to museum curators and technicians who kindly allowed me to study precious specimens. I sincerely thank Dr. Stephen Cairns and Tim Coffer (Smithsonian Institution) for the *Primnoa* samples, Dr.

Jean-Marc Gagnon (Canadian Museum of Nature) for the *Pennatula grandis* samples, Nathalie Djan-Chékar (The Rooms, St. John's) for access to the collection at The Rooms, and Andrew Cabrinovic (Natural History Museum, London) for access to the *Pennatula* collection.

Several people from the CREAT Network team (Memorial University of Newfoundland) contributed to logistical/methodological aspects of this thesis. Glenn Piercey and Brian Loveridge kindly gave me access to the isomet and rock saws all the times I needed. Glenn also patiently guided me to use the microdrill, performed the trace elements analyses, and also contributed with interesting questions and comments about my study. Michael Shaffer helped with the SEM, David Grant and Dylan Goudie with the polishing machine, and Wanda Aylward provided the XRD analyses.

Vince Lecours and Dave Mercer helped me in my first steps in the world of ArcGIS, and Charlie Conway helped with his advice on mapping and cartography. I also thank Dr. Patrick Gagnon for allowing access and use of equipment in his lab, and the staff at the Biology department for facilitating everything, especially Gary Collins, Cherie Hussey, Alvin Kenny, Shirley Kenny, and also Pam Murphy from the Geography department. I thank Dr. Ted Miller for his great incentive and support along these years.

My research was funded by the Canadian Healthy Oceans Network (CHONe) and by a Doctoral scholarship from the Natural Sciences and Engineering Research Council of Canada (NSERC), which made this project possible.

Finally, my husband David Bélanger could not have been more patient with my incessant biology talk, and I am extremely grateful for his tolerance and support. I also

thank my mom Lúcia and my sisters Débora and Gabriela for the immense support and love.

Table of Contents

Abstract	ii
Acknowledgments	iv
Table of Contents.....	vii
List of figures	xvi
List of tables	xxx
Abbreviations	xxxiv
Co-authorship Statement	xxxv
Appendices	xxxvii
Publications arising	xxxix
1. Introduction	1-1
1.1 Octocoral morphology, skeletal composition, and growth patterns	1-3
1.1.1 Growth patterns in alcyonaceans (order Alcyonacea)	1-5
1.1.2 Growth patterns in sea pens (order Pennatulacea).....	1-10
1.1.3 Growth rings in octocorals	1-14
1.2 Growth rates	1-18
1.2.1 Growth rates in relation to environmental variables	1-19
1.3 Methods for studying growth rates in octocorals	1-20
1.3.1 Aquaria/mesocosm.....	1-21
1.3.2 Ring counting	1-22
1.3.3 Validation techniques.....	1-24
1.4 Limiting factors to octocoral growth.....	1-28

1.5 Conservation perspective	1-29
1.6 Thesis outline	1-30
1.7 References	1-33
2. Decadal longevity and slow growth rates in the deep-water sea pen <i>Halapteris finmarchica</i> (Sars, 1851) (Octocorallia: Pennatulacea): Implications for vulnerability and recovery from anthropogenic disturbance	2-1
Abstract	2-1
2.1 Introduction	2-3
2.2 Materials and Methods	2-6
2.2.1 Study area and sampling.....	2-6
2.2.2 Ring counting and growth rate estimation.....	2-6
2.2.3 Environmental data.....	2-11
2.2.4 Axis composition	2-12
2.2.5 Trace element analysis.....	2-13
2.2.6 Data analysis.....	2-14
2.3 Results	2-15
2.3.1 Axis composition	2-15
2.3.2 Growth rates and age	2-16
2.3.3 Environmental variables	2-22
2.3.4 Trace element analysis.....	2-28
2.4 Discussion	2-31
2.4.1 Growth rates and age in <i>Halapteris finmarchica</i> and comparison between the two species.....	2-31

2.4.2 Growth rates and age in relation to environmental variables	2-37
2.4.3 Trace element ratios and environmental significance.....	2-38
2.5 Conclusions	2-42
2.6 References	2-44
3. Size metrics, and estimates of age and growth rates in one of the tallest known sea pens: <i>Umbellula encrinus</i> (Cnidaria: Pennatulacea) from Baffin Bay	3-1
Abstract	3-1
3.1 Introduction	3-3
3.2. Material and methods	3-5
3.2.1 Sampling.....	3-5
3.2.2 Remark on species identification.....	3-10
3.2.3 Abundance and size-frequency distribution	3-10
3.2.4 Longevity and growth patterns	3-12
3.2.5 Bomb- ¹⁴ C analysis	3-14
3.2.6 Trace elements analysis	3-15
3.2.7 Environmental data.....	3-15
3.2.8 Data analysis.....	3-17
3.3. Results	3-19
3.3.1 Abundance and size-frequency distribution	3-19
3.3.2 Hook size versus colony size.....	3-22
3.3.3 Colony and axis metrics in relation to colony size.....	3-26
3.3.4 Bomb- ¹⁴ C analysis	3-27
3.3.5 Trace element analysis.....	3-30

3.3.6 Longevity and growth rates	3-34
3.3.7 Growth rates in relation to environmental factors	3-38
3.4. Discussion	3-41
3.4.1 Abundance and size-frequency distribution	3-41
3.4.2 Colony and axis metrics in relation to colony size	3-43
3.4.3 Bomb- ¹⁴ C and trace element analysis.....	3-44
3.4.4 Longevity and growth rates	3-46
3.4.5 Vulnerability and conservation	3-51
Acknowledgements	3-52
3.5 References	3-53
4. Growth patterns in the deep-water sea pen <i>Pennatula grandis</i> Ehrenberg, 1834 (Cnidaria: Octocorallia) inferred from growth rings and colony metrics	4-1
Abstract	4-1
4.1 Introduction	4-3
4.2 Material and methods	4-5
4.2.1 Sampling and identification.....	4-5
4.2.2 Colony metrics.....	4-6
4.2.3 Axis characteristics	4-7
4.2.4 Bomb-radiocarbon (¹⁴ C) analysis	4-10
4.2.5 Longevity and growth rates	4-11
4.2.6 Environmental data.....	4-14
4.2.7 Data analysis.....	4-16
4.3. Results	4-17

4.3.1 Colony height versus location and depth.....	4-17
4.3.2 Peduncle metrics and polyp leaves versus colony height.....	4-18
4.3.3 Axis characteristics	4-20
4.3.4 Axis metrics versus colony height	4-25
4.3.5 Bomb-radiocarbon (¹⁴ C) analysis	4-27
4.3.6 Estimated longevity and growth rates	4-29
4.3.7 Growth rates in relation to environmental factors	4-33
4.4. Discussion	4-36
4.4.1 Relationship between peduncle and colony height.....	4-36
4.4.2 Number and density of polyp leaves	4-37
4.4.3 Axis-free space	4-38
4.4.4 Axis composition	4-39
4.4.5 Axis metrics versus colony height	4-42
4.4.6 Bomb radiocarbon (¹⁴ C) analysis.....	4-43
4.4.7 Estimated growth rates	4-44
4.4.8 Summary of growth patterns inferred from colony metrics and growth rings ..	4-45
Acknowledgments.....	4-47
4.5 References	4-48
5. Morphology and composition of the internal axis in two morphologically contrasting deep-water sea pens (Cnidaria: Octocorallia).....	5-1
Abstract	5-1
5.1 Introduction	5-3

5.2 Methods.....	5-5
5.2.1 Sampling.....	5-5
5.2.2 Axis characterization through a vertical gradient	5-5
5.2.3 Axis carbonate composition.....	5-9
5.3 Results	5-11
5.3.1 Axis morphology and metrics.....	5-11
5.3.1.1 <i>Umbellula encrinus</i>	5-11
5.3.1.2 <i>Anthoptilum grandiflorum</i>	5-20
5.3.2 Axis carbonate characterization along a vertical gradient	5-24
5.4 Discussion	5-26
5.4.1 Carbonate composition	5-26
5.4.2. Changes in axis metrics and growth rates along the axis	5-27
5.4.3 Twisting of axis in <i>U. encrinus</i>	5-30
5.4.4 Comparing the axes of <i>U. encrinus</i> and <i>A. grandiflorum</i>	5-32
Acknowledgements	5-37
5.5 References	5-38
6. Growth in the cold-water gorgonians <i>Primnoa pacifica</i> Kinoshita, 1907 and <i>Primnoa resedaeformis</i> (Gunnerus, 1763) (Cnidaria: Octocorallia) in relation to environmental variables	6-1
Abstract	6-1
6.1 Introduction	6-3
6.2 Material and methods	6-5
6.2.1 Study area and sampling.....	6-5

6.2.2 Video analysis (Strait of Georgia): abundance and size structure	6-7
6.2.3 Growth rates and ¹⁴ C analysis	6-9
6.2.4 Environmental data.....	6-12
6.2.5 Data analysis.....	6-15
6.3 Results	6-17
6.3.1 Video analysis (Strait of Georgia): abundance and size structure	6-17
6.3.2 ¹⁴ C analysis	6-19
6.3.3 Colony metrics versus age relationships	6-26
6.3.4 Growth rates	6-26
6.3.5 Growth rates versus environmental variables.....	6-30
6.4 Discussion	6-34
6.4.1 Video analysis (Strait of Georgia): abundance and size structure	6-34
6.4.2 ¹⁴ C data	6-35
6.4.3 Colony metrics versus age relationships	6-36
6.4.4 Growth rates	6-37
Acknowledgements	6-41
6.6 References	6-42
7. Morphology, growth rates, and trace element composition of dense bamboo coral forests in a muddy Arctic environment.....	7-1
Abstract	7-1
7.1 Introduction	7-3
7.2 Material and methods	7-4
7.2.1 Data sampling.....	7-4

7.2.2	Molecular analysis	7-5
7.2.3	Skeleton carbonate composition	7-8
7.2.4	Growth rings and apparent rates	7-8
7.2.5	Trace element analysis	7-9
7.2.6	Palaeotemperature estimation	7-10
7.3	Results	7-12
7.3.1	Molecular analysis	7-12
7.3.2	<i>Keratoisis</i> forests	7-12
7.3.3	Carbonate composition of the skeleton	7-13
7.3.4	Growth rings and apparent rates	7-13
7.3.5	Trace element analysis	7-14
7.3.6	Palaeotemperature estimation	7-22
7.4	Discussion	7-24
7.4.1	Forests	7-24
7.4.2	Growth rings and apparent rates	7-26
7.4.3	Trace elements analysis	7-27
7.4.4	Palaeotemperature estimation	7-30
	Acknowledgements	7-31
7.6	References	7-33
8.	General conclusions	8-1
8.1	Growth rates	8-1
8.2	Validation of ring formation periodicity	8-11
8.3	Morphology and growth in sea pens and <i>Keratoisis</i> sp. “kerD2d”	8-13

8.4 Final considerations.....	8-15
8.5 References	8-19

List of figures

Figure 1-1. Current classification of Octocorallia and Hexacorallia by Kayal et al. (2013).

Orders for Hexacorallia not shown. 1-1

Figure 1-2. Diversity of octocoral growth forms. A-F: order Alcyonacea, G-J: Order

Pennatulacea. A) *Paragorgia arborea* (Nova Scotia), B) *Paramuricea* sp. (Nova

Scotia), C) *Keratoisis grayi* (Nova Scotia), D) *Acanella arbuscula* and

Acanthogorgia armata (Southwest Grand Banks), E) *Anthomastus* sp. (Southwest

Grand Banks), F) c.f. Nephtheidae (Scott Inlet, Baffin Bay), G) *Halipterus*

finmarchica (Southwest Grand Banks), H) *Pennatula* sp. (Nova Scotia), I) *Pennatula*

grandis, and J) *Umbellula encrinus* (Scott Inlet, Baffin Bay). Letters in H), I) and J)

refer to: pl = polyp leaves, r = rachis, b = bulb, ax = axis, p = peduncle, st = stalk.

Credits: A-E, G-H: DFO-CSSF, F, J: ArcticNet-CSSF-DFO, I: BMN..... 1-4

Figure 1-3. Cross section of the internal axis of *Umbellula encrinus* seen under regular

light (A) and UV light in a stereomicroscope (B) and in an SEM (C), with

correspondent magnified lobes for details (D-F). Scale bar = 1 mm (photo sizes are

slightly different). 1-26

Figure 2-1. Map showing the locations included in this study. Circles are the locations of

Halipterus finmarchica samples from the Northwest Atlantic, and triangles are

locations of *H. willemoesi* from the Bering Sea (from Wilson et al., 2002).2-11

Figure 2-2. *Halipterus finmarchica* showing: whole colony (A), whole axis only (B), cross

section under ultraviolet (UV) light (C). Scale bar = 1 mm. 2-16

Figure 2-3. Box-plots showing: diametric (A) and linear growth rates (B) in *Halipteris finmarchica* from the Northwest Atlantic and *H. willemoesi* from the Bering Sea (cf. Wilson et al., 2002)..... 2-18

Figure 2-4. Observed and estimated number of rings in *Halipteris finmarchica* per colony: average number of rings (observed, A), estimated number of rings based on axis diameter (using the regression equation produced by Wilson et al. (2002) for *H. willemoesi*, B), estimated number of rings based on colony height (based on the relationship between size at maturity for *H. finmarchica* from Baillon et al. (2014), our estimated linear growth rates and age at maturity, C). The number of rings based on height was not estimated for colonies of incomplete size. 2-19

Figure 2-5. Relationships between: colony height and axis diameter (A), number of rings and axis diameter (B), colony height and number of rings (C), where the dashed line represents the regression through the origin..... 2-20

Figure 2-6. Diametric and linear growth rates in *Halipteris finmarchica* in relation to colony height (A), linear growth rates in relation to colony height in *H. finmarchica* (circles, B) and in *H. willemoesi* (triangles; data from Wilson et al., 2002). In b *H. willemoesi* showed the best fit when adding a cubic term to the regression..... 2-21

Figure 2-7. Relationships between diametric growth rates and: depth (A), latitude (B), temperature (C), chlorophyll a concentration (D), particulate organic carbon (POC, E), and particulate inorganic carbon (PIC, F) for *Halipteris finmarchica* (circles) and *H. willemoesi* (cf. Wilson et al., 2002; triangles). 2-23

Figure 2-8. Environmental data from the locations of *Halipteris finmarchica* (Northwest Atlantic) and *H. willemoesi* (Bering Sea; from Wilson et al., 2002): mean annual

chlorophyll a concentration (A), particulate organic carbon (POC, B), and particulate inorganic carbon (PIC, C) from the periods ranging 1997-2010 (chlorophyll a; excluding 2008-2009) and 2002-2013 (POC and PIC).	2-25
Figure 2-9. Relationships between linear growth rates and: depth (A), latitude (B), temperature (C), chlorophyll a concentration (D), particulate organic carbon (POC, E), and particulate inorganic carbon (PIC, F) for <i>Halipteris finmarchica</i> (circles) and <i>H. willemoesi</i> (cf. Wilson et al., 2002; triangles).	2-26
Figure 2-10. Number of rings (age) in <i>Halipteris finmarchica</i> in relation to: depth (A), latitude (B), temperature (C), chlorophyll a concentration (D), particulate organic carbon (POC, E), and particulate inorganic carbon (PIC, F).	2-27
Figure 2-11. Trace element ratios (Mg/Ca, Sr/Ca, Ba/Ca, and Na/Ca) in the axis of three colonies of <i>Halipteris finmarchica</i> (one transect per axis/colony).	2-28
Figure 2-12. Distribution of trace element ratios across the axes radius of <i>Halipteris finmarchica</i> : Sr/Ca and Mg/Ca in relation to distance from core for sample 035B (A), correlation between Sr/Ca and Mg/Ca for sample 035B ($r=-0.54$, $p<0.05$, B), Ba/Ca and Na/Ca in relation to distance from core for all three analyzed samples (C). Error bars are $\pm 1\sigma$	2-30
Figure 2-13. Distribution of Mg/Ca peaks along the radius of one colony of <i>Halipteris finmarchica</i> (sample 035B): cross section of axis showing rings (identified by black dots) and direction of SIMS transect (A), distribution of Mg/Ca along the SIMS transect, with filled red dots emphasizing positive peaks and x representing the first sample of a transect that has an extreme value (B). Error bars are $\pm 1\sigma$. Stars represent every 10 points. Scale bar in A = 1 mm.	2-31

Figure 3-1. Map of study area. 3-7

Figure 3-2. Colonies of *Umbellula encrinus*: *in situ* at Scott Inlet (A-B), at Qikiqtarjuaq (C-D), freshly caught sample from Jones Sound (E). Scale bars = 6 cm. Credits: ArcticNet-CSSF-DFO (A-D) and Laura Wheeland (E). 3-13

Figure 3-3. Colonies of *Umbellula encrinus* *in situ*. Size cannot be indicated in all photos because the scaling lasers are not visible at these distances. Scale bars = 6 cm. Top-left photo shows a colony estimated to measure ~2 m. Credits: ArcticNet-CSSF-DFO. 3-20

Figure 3-4. Density of *Umbellula encrinus* colonies from trawl, longline and video surveys by site in Baffin Bay (Left to right: north-south). 3-23

Figure 3-5. Size frequency distribution of *Umbellula encrinus* from Baffin Bay. 3-25

Figure 3-6. Colony height in relation to hook size for samples of *Umbellula encrinus* caught as longline bycatch at Cumberland Sound, Qikiqtarjuaq, and Jones Sound (Baffin Bay). In Cumberland Sound only hook size 14 was used. Black horizontal bars inside the boxes represent the median, boxes are limited by minimum and maximum values, and circles are outliers. 3-26

Figure 3-7. Peduncle and axis metrics in relation to colony size in *Umbellula encrinus* from Baffin Bay: A) peduncle length, B) peduncle proportion, C) axis radius, D) axis area. Fit lines and confidence intervals (dashed lines) are for reference only, as the regression equation also included depth as a covariate. All observations shown, including the ones not included in the statistical analysis due to missing depth information. 3-28

Figure 3-8. $\Delta^{14}\text{C}$ for the axis of a live-collected colony of *Umbellula encrinus* sampled in 2014 at Jones Sound (red circles) in relation to year. The data is overlaid with $\Delta^{14}\text{C}$ data from the calcite and gorgonin from *Keratoisis grayi* from the SW Grand Banks (Sherwood et al., 2008), calcite and gorgonin from *Primnoa resedaeformis* from the Hudson Strait (HS) and NE Channel (NC) (Sherwood et al., 2008), and calcite from the otoliths of the Greenland halibut *Reinhardtius hippoglossoides* (Walbaum, 1792) from NAFO zone 0B (Treble et al., 2008). 3-29

Figure 3-9. Growth rings and Mg/Ca profile in the axis of *Umbellula encrinus*: A) Cross section of the axis seen under Scanning Electron Microscope (SEM) showing SIMS transect, growth rings (indicated by black dots), and Mg/Ca peaks (red dots); B) Mg/Ca peaks with distance from core, with red dots corresponding to red dots shown in A. 3-31

Figure 3-10. Trace elements distribution with distance from core along the axis radius of three *Umbellula encrinus* colonies (samples 028, 029, and 030F)..... 3-32

Figure 3-11. Relationship between Mg/Ca and Sr/Ca ratios in the axis of *Umbellula encrinus* for all three analyzed samples. 3-33

Figure 3-12. Cross section of the internal axis of *Umbellula encrinus* seen under UV light (stereomicroscope). Red dots indicate growth rings. Scale bars = 1 mm. 3-34

Figure 3-13. Growth rates in *Umbellula encrinus* per site. Black horizontal bars inside the boxes represent the median, boxes are limited by minimum and maximum values, and circles are outliers. Left to right: north-south. 3-35

Figure 3-14. Growth rates in relation to colony height in *Umbellula encrinus* from Baffin Bay: A) Radial growth rates, and B) linear growth rates. Fit lines and confidence

intervals (dashed lines) are for reference only, as the regression equation also included depth as a covariate.....	3-36
Figure 3-15. Number of rings in relation to A) colony height, and B) axis radius in <i>Umbellula encrinus</i> from Baffin Bay. Error bars = standard deviations of average number of rings and average radius. R ² is shown for both linear (gray) and power equations.....	3-37
Figure 3-16. Radial growth rates in <i>Umbellula encrinus</i> in relation to environmental variables. Fit lines and confidence intervals (dashed lines) are for reference only, as the regression equation also included depth as a covariate.	3-40
Figure 3-17. 3D-plot of the relationship between radial growth rates in <i>Umbellula encrinus</i> , colony height, and sea surface temperature (SST).	3-41
Figure 4-1. Map of study area.	4-8
Figure 4-2. A) <i>Pennatula grandis</i> colony, B) piece of axis subsampled for ¹⁴ C analysis, C) longitudinal section of the axis, D) axis being micromilled for ¹⁴ C analysis, E) resulting drilled axis. Scale bar = 2 mm.	4-13
Figure 4-3. Colony height in <i>Pennatula grandis</i> from the Northwest Atlantic by location. Black horizontal bars inside the boxes represent the median, boxes are limited by minimum and maximum values, and circles are outliers. Left to right: north-south. 4-19	
Figure 4-4. Colony metrics in relation to colony height in <i>Pennatula grandis</i> : A) peduncle length, B) proportion of peduncle length, C) number of pairs of polyp leaves, and D) density of pairs of polyp leaves. Fit lines and confidence intervals (dashed lines) are for reference only, as the regression equation also included depth as a covariate. 4-20	

Figure 4-5. Results on the EDX analysis on a transect from the center (near the core) to the edge in a cross section of the axis of *Pennatula grandis* (sample 074, inset).
Black arrows point to main peaks (N = 23) in the distribution of Ca. 4-22

Figure 4-6. Axis composition and carbonate proportion in relation the colony height in colonies of the sea pen *Pennatula grandis* from the NW Atlantic. 4-23

Figure 4-7. Axis of the sea pen *Pennatula grandis* after extraction from the colony, showing A) cross sections along its length, B) before, and C) after treatment with HCl, and D) another axis after treatment with H₂O₂. Pe: peduncle. 4-24

Figure 4-8. Axis-free space in *Pennatula grandis* in relation to colony height in terms of A) space length (A) and B) number of pairs of polyp leaves. Inset in A shows extension of axis visible through the tissue. 4-25

Figure 4-9. Axis metrics in relation to colony height in *Pennatula grandis*: A) axis weight, B) axis area, C) axis diameter, and D) axis proportion (in weight, N= 10)..... 4-26

Figure 4-10. $\Delta^{14}\text{C}$ for axis of two *Pennatula grandis* colonies from the Gulf of St-Lawrence (red symbols) in relation to year, overlaid with $\Delta^{14}\text{C}$ data from calcite and gorgonin in *Keratoisis grayi* from the SW Grand Banks (Sherwood et al., 2008), gorgonin in *Primnoa resedaeformis* from the Northeast Channel – Nova Scotia (Sherwood et al., 2005), and otolith from American plaice *Hippoglossoides platessoides* (Fabricius, 1780) from the Southern Gulf of St. Lawrence for reference (Morin et al., 2013). 4-28

Figure 4-11. Cross sections of the axis in *Pennatula grandis* under UV light at the base (A, specimen 011) showing a porous aspect, and above the peduncle area (B,

specimen 075) showing growth rings depicted by 14 black dots. Photos were not taken from the same colony. Scale bars = 1 mm.	4-30
Figure 4-12. Number of rings in relation to A) colony height, and B) axis diameter in <i>Pennatula grandis</i> . Fit lines and confidence intervals (dashed lines) are for reference only, as the regression equation also included depth as a covariate.	4-31
Figure 4-13. Growth rates in relation to colony height in <i>Pennatula grandis</i> . A) Diametric growth rates ($\text{mm}\cdot\text{yr}^{-1}$), and B) Linear growth rates ($\text{cm}\cdot\text{yr}^{-1}$). Fit lines and confidence intervals (dashed lines) are for reference only, as the regression equation also included depth as a covariate.	4-31
Figure 4-14. Diametric and linear growth rates in <i>Pennatula grandis</i> from the NW Atlantic by site (left to right: north-south). Black horizontal bars inside the boxes represent the median, boxes are limited by minimum and maximum values, and circles are outliers.	4-32
Figure 4-15. Diametric growth rates in the sea pen <i>Pennatula grandis</i> from the NW Atlantic in relation to environmental variables by size class. Fit lines and confidence intervals (dashed lines) are for reference only, as the regression equation also included height as a covariate. POC and PIC had the same patterns as chlorophyll a, with chlorophyll a and POC strongly correlated (Pearson's $r = 0.98$, $N=42$, unique values only including data on all size classes).	4-35
Figure 5-1. Map of study area.	5-6
Figure 5-2. A-D) <i>Umbellula encrinus</i> : A) whole colony <i>in situ</i> , B) whole colony, C) piece of stem and corresponding extracted axis, D) axis cross sectioning scheme. E-H) <i>Anthoptilum grandiflorum</i> : E) whole colony <i>in situ</i> , F) whole colony, G) whole axis,	

H) axis cross sectioning scheme. au: autozooids, p: peduncle, s: stalk, r: rachis. Scale bars = 10 cm. A-B and E-F are not the same colonies. Colony in A) measures ~81 cm. Size not available for E). 5-9

Figure 5-3. Pieces of axis showing surface at different sections of a same specimen of *Umbellula encrinus* (052). Scale bar = 5 cm (refers to bottom photos).5-11

Figure 5-4. *Umbellula encrinus*. A) Twisting of axis, B) colony *in situ* (Scott Inlet, Baffin Bay, at 520 m) with inset showing twisting of stalk, C) colony *in situ* standing in a ~90° position (Qikiqtarjuaq, Baffin Bay, at 680 m, estimated to be ~2 m tall)..... 5-12

Figure 5-5. The internal axes from five *Umbellula encrinus* colonies seen as cross sections along a gradient (every 10 cm) from base to tip. Changes in the position of red dots indicate changes in lobe position due to axis twisting. *cracked samples. Cross sections were photographed under UV light. Scale bar = 2 mm. 5-13

Figure 5-6. Axis radius in each of the four lobes in five colonies of *Umbellula encrinus*. 5-16

Figure 5-7. Radial growth rates in relation to distance from base in five colonies of *Umbellula encrinus*. 5-19

Figure 5-8. Axis area and relative weight in relation to distance from base in five colonies of *Umbellula encrinus* (A-B), and eight colonies of *Anthoptilum grandiflorum* (C-D). The vertical arrows indicate maximum peduncle length among the studied colonies. 5-20

Figure 5-9. Pieces of axis showing surface at different sections of a same specimen of *Anthoptilum grandiflorum* from base to tip. Pencil marking is seen in red. Scale bar = 2 cm. 5-21

Figure 5-10. Cross sections of the internal axis of eight *Anthoptilum grandiflorum* colonies along a gradient (every 5 cm) from the base to the distal tip. Cross sections were photographed under UV light. Scale bar = 2 mm. 5-22

Figure 5-11. *Anthoptilum grandiflorum*: whole colony and its extracted axis before being sectioned, showing position of cross sections (arrows) along the axis, and in relation to the peduncle (p). 5-23

Figure 5-12. Axis composition in *Umbellula encrinus* and *Anthoptilum grandiflorum*: proportion of axis components (A-B), carbonate proportion in relation to distance from base (C-D), and carbonate proportion at base and tip. The vertical arrows in C and D indicate maximum peduncle length among the studied colonies. 5-25

Figure 6-1. Map of sample locations for *Primnoa pacifica* and *P. resedaeformis* colonies included in this study. 6-8

Figure 6-2. Colonies of *Primnoa pacifica* collected in 2011 at the Coral Knoll (A-E) and Sabine Channel (F-L) in the Strait of Georgia (NE Pacific) using the ROV ROPOS. 6-9

Figure 6-3. *In situ* colonies of *Primnoa pacifica* at the Coral Knoll (A-F) and Sabine Channel (G-L), Strait of Georgia, British Columbia (NE Pacific). High suspension of sediments can be noticed in several photos. Colonies of *Paragorgia arborea* (Linnaeus, 1758) are also seen (C-D, H-J, L: dark red colonies). 6-18

Figure 6-4. Size frequency distribution of *Primnoa pacifica* colonies (N=17) in the Sabine Channel (Strait of Georgia, NE Pacific). 6-19

Figure 6-5. $\Delta^{14}\text{C}$ in relation to year (ring count) in colonies of *Primnoa pacifica* from the Strait of Georgia (NE Pacific), from otoliths of yelloweye rockfish from Southeast

Alaska (Kerr et al., 2004), canary rockfish from the Oregon coast (Piner et al., 2005), and from dorsal spines of spiny dogfish from the NE Pacific (Campana et al., 2006). Sample identifications in bold as well as dashed lines in the figure represent dead-collected colonies. For these colonies, year of the outermost ring was estimated based on the expected year for the ^{14}C value associated to that ring. Sample R1513-BR-0024 was partially alive when sampled. PC1 and PC2 are different pieces of the same colony. Different symbols refer to different samples. 6-24

Figure 6-6. Skeletons of dead-collected *Primnoa pacifica* showing bioerosion in two colonies (A-C, and D-E). Skeleton shown in C is part of A (side not seen). Note cross section of D shown in E), with a hole containing the arm of a brittle star. 6-25

Figure 6-7. Relationship between A) colony height versus colony age, and B) stem diameter versus colony age in *Primnoa pacifica* and *Primnoa resedaeformis*. 6-28

Figure 6-8. Cross section of the base of *Primnoa pacifica* under UV light where alternating bands of calcite (pale) and gorgonin (dark) rings, as well as the calcite core can be identified. Sample 12261 USNM. Scale bar = 1 mm. 6-29

Figure 6-9. Growth rates in *Primnoa pacifica* and *Primnoa resedaeformis* by location. Black horizontal bars inside the boxes represent the median, boxes are limited by minimum and maximum values, circles are outliers, and stars are extreme values... 6-31

Figure 6-10. Diametric growth rates in *Primnoa pacifica* and *P. resedaeformis* in relation to chlorophyll a, dissolved oxygen, depth, and latitude. 6-32

Figure 6-11. Diametric growth rates in *Primnoa* spp. in relation to environmental variables not included in the GLM model: bottom temperature (world ocean database

– WOD, and world ocean atlas - WOA), bottom salinity, surface salinity from the SODA database (not available for the Strait of Georgia – SoG site), particulate organic carbon (POC), and surface current velocity. Figure in previous page..... 6-34

Figure 7-1. A) location of surveyed area (rectangle) showing Canada’s Exclusive Economic Zone (EEZ), B) fishing effort (shrimp and Greenland Halibut; 2004-2005; Edinger et al. 2007) and coral records from Fisheries and Oceans Canada (DFO) scientific surveys (circles; 1999, 2001, 2006, 2008, 2010, 2012) and the Fisheries Observer Program (FOP) datasets (2005-2007) (triangles, Gass & Willison, 2005, Wareham, 2009) near the surveyed area (positional error ~ 100 m), C) location of *Keratoisis* sp. from previous surveys, *Keratoisis* sp. forests observed in this study, and fragments of dead colonies in relation to the 1999 trawl path. Buffer zones represent areas of long-term monitoring. Figure shown in the previous page. 7-7

Figure 7-2. Fragments of *Keratoisis* sp. used to estimate growth rates and for the trace elements analysis. A-B) sample 1, C-D) sample 2. Arrows point to locations from where cross sections were made. Note orange polyps still present in both samples. 7-11

Figure 7-3. A-C) Forests of *Keratoisis* sp. “kerD2d” (arrow in C points to a flatfish), D) close up of polyps showing ruler used to estimate size, E) polyps and node (arrow), F) branched root-like structures, G) coral fragments close to the 1999 trawl path, and H) sparse rocks. 7-15

Figure 7-4. Cross section of the stem in *Keratoisis* sp. “kerD2d”. A-C: sample 1, D-E: sample 2. Grey spots/stains in A and B are from the impregnated polishing liquid. Residues of the gold coating can still be seen in the samples (B and E), which were

completely covered with gold before using acetone to dissolve the Crazy Glue™.

Scale bars = 1 mm (A-B, D-E), and 0.5 mm (C and F)..... 7-16

Figure 7-5. Comparison of radial growth rates among specimens of the genus *Keratoisis* from this study and published data. Growth rates from Andrews et al. (2009), Sherwood & Edinger (2009), Thresher (2009), Thresher et al. (2009), Hill et al. (2011), Sinclair et al. (2011), and Farmer et al. (2015). Values from Hudson Strait to Bear Seamount (green dots) are all from the North Atlantic region..... 7-17

Figure 7-6. Trace elements/Ca ratios (Sr/Ca, Mg/Ca) in the calcite of *Keratoisis* sp. “kerD2d” in relation to distance from core for sample 1 (A) and 2 (B). Error bars are 1SD. Where error bars are not seen the error is smaller than the marker..... 7-19

Figure 7-7. Trace elements/Ca ratios (Na/Ca, Ba/Ca) in the calcite of *Keratoisis* sp. “kerD2d” in relation to distance from core for sample 1 (A) and 2 (B). Error bars are 1SD. Where error bars are not seen the error is smaller than the marker..... 7-20

Figure 7-8. Relationships between Mg/Ca and Sr/Ca in the calcite of *Keratoisis* sp. “kerD2d” stem in sample 1 (A) and 2 (B). Error bars are 1SD..... 7-21

Figure 7-9. Estimated water temperature (°C) from Mg/Ca ratios from A) samples 1a-b, and B) samples 2a-b of *Keratoisis* sp. “kerD2d”, according to the equation by Sherwood et al. (2005). Smoothed lines produced using a moving average (5 intervals)..... 7-23

Figure 8-1. A) radial and B) linear growth rates in the four genera included in this study, including *Halipterus finmarchica*, *H. willemoesi* (Wilson et al., 2002), *Pennatula grandis*, *Umbellula encrinus*, *Keratoisis* sp. (radial growth rates only), *Primnoa pacifica* and *P. resedaeformis*..... 8-2

Figure 8-2. Growth rates in octocorals from shallow and deep waters by temperature classes: A) radial growth, and B) linear growth. 8-5

Figure 8-3. Radial growth rates in octocoral species from shallow and deep-water. Stars (*) indicate new data produced as a result of this thesis. Alc: Alcyoniidae, Chrys: Chrysogorgiidae, Gorg: Gorgoniidae, and Plexaurid: Plexauridae. When radial growth rates were not available, diametric growth rates were used as a proxy by dividing them by 2. Radial growth rates for *Paragorgia arborea* are not shown for a better visualization of the data (0.83 mm·yr⁻¹, Sherwood & Edinger, 2009). Figure shown in the previous page. 8-7

Figure 8-4. Linear growth rates in octocoral species from shallow and deep-water. Stars (*) indicate new data produced as a result of this thesis. Briar: Briareidae, Acant: Acanthogorgiidae, Chrys: Chrysogorgiidae, Gorg: Gorgoniidae, Melit: Melithaeidae, Parag: Paragorgiidae, Primn: Primnoidae, and Suberg: Subergorgiidae. Linear growth rates for *Pseudopterogorgia acerosa* are not shown for a better visualization of the data (31 cm·yr⁻¹, Cadena & Sánchez, 2010). Figure shown in the previous page. 8-9

List of tables

Table 2-1. Sampling information, colony measurements, age, and growth rates for <i>Halipteris finmarchica</i> from the Northwest Atlantic.....	2-9
Table 2-2. Results of linear regression analyzes using permutation techniques on growth rates and number of rings (age) for <i>Halipteris finmarchica</i> only, and for both species pooled (<i>H. finmarchica</i> and <i>H. willemoesi</i>) in relation to environmental variables... 2-24	24
Table 2-3. Results from the Mann-Whitney U test on the relationship between Sr/Ca, Mg/Ca, Na/Ca and Ba/Ca (mmol/mol) ratios per sample of <i>Halipteris finmarchica</i> colonies.....	2-29
Table 3-1. General sample information for colonies of <i>Umbellula encrinus</i> included in this study.....	3-8
Table 3-2. Specifications of ROV video-transects.....	3-10
Table 3-3. Descriptive statistics for the size structure of <i>Umbellula encrinus</i> from Baffin Bay.....	3-24
Table 3-4. $\Delta^{14}\text{C}$ values from the axis of a live-collected colony of <i>Umbellula encrinus</i> sampled in 2014. The year associated to the core region was determined as the average number of rings visually counted (N= 68) subtracted from 2014. The years for the intermediate regions were estimated as the number of rings between core and edge, divided by the number of regions.	3-30
Table 3-5. Trace elements distribution in the axes of three <i>Umbellula encrinus</i> colonies.	3-30

Table 3-6. Results from the Mann-Whitney test on the comparison of trace element ratios between colonies of *Umbellula encrinus*. 3-33

Table 3-7. Comparison between observed (Obs) number of rings in *Umbellula encrinus* from visual counting and number of rings estimated from equations on the relationship between number of rings and colony size (EstH = $0.8094 * \text{height}^{0.7228}$), and axis radius (EstR = $16.646 * \text{radius}^{0.7887}$) when using 25% of the data (hold-out sample). 3-38

Table 4-1. Summary of axis composition in *Pennatula grandis* (N=10). 4-22

Table 4-2. Results of ^{14}C analysis in the axis of two *Pennatula grandis* colonies. Samples were collected in 1983 (edge region). The year for the core region equals 1983 minus the number of rings visually counted. The years for the middle regions were estimated as the number of rings between core and edge, divided by the number of regions. CAMS is the Center for Accelerator Mass Spectrometry analytical identifier. 4-27

Table 4-3. Results of the GLM analysis between diametric growth rates and environmental factors in *Pennatula grandis* by size class (small, medium, and large), with colony height as a co-variable. Interaction indicates a significant interaction between the environmental variable and colony height. 4-34

Table 5-1. Sampling information on *Umbellula encrinus* and *Anthoptilum grandiflorum* from the NW Atlantic. Latitude (N) and longitude (W) are in decimal degrees. Ped = peduncle length. 5-7

Table 5-2. Axis cross-sectional area (mm^2) per colony and start height of twisting in *Umbellula encrinus*. Cross section interval was 10 cm and twisting could have

started between the previous cross section and the one where twisting was first reported.....	5-14
Table 5-3. Results from the paired <i>t</i> -test on difference in lobe radii among lobes in five different colonies of <i>Umbellula encrinus</i> . Boxes in grey highlight pairs where differences in radii were not statistically significant at $\alpha = 5\%$	5-15
Table 5-4. Average number of rings and radial growth rates (Rgrowth) in five colonies of <i>Umbellula encrinus</i>	5-17
Table 5-5. Axis cross-sectional area (mm ²) in <i>Umbellula encrinus</i> and <i>Anthoptilum grandiflorum</i> near the base (largest) and near the distal tip (smallest), and percentage reduction of axis cross-sectional area (degree of tapering).	5-18
Table 6-1. Location and reservoir age used for ¹⁴ C calibration from McNeely et al. (2006) for samples collected in the Strait of Georgia (British Columbia, Canada).	6-13
Table 6-2. Specifications of environmental data used in this study.....	6-15
Table 6-3. ¹⁴ C concentration and ages per sample of <i>Primnoa pacifica</i> , including ¹⁴ C reservoir corrected ages (¹⁴ C age –reservoir) and calibrated ages in calendar years. 6-21	
Table 6-4. Estimation of time <i>post-mortem</i> on the bottom for colonies of <i>Primnoa pacifica</i> from the Strait of Georgia (NE Pacific). na = not applicable.	6-23
Table 6-5. Results from the statistical analysis on diametric growth rates in <i>Primnoa</i> spp. in relation to environmental variables.	6-32
Table 7-1. Summary of trace element ratios (mmol·mol ⁻¹) for the calcite of <i>Keratoisis</i> sp. “kerD2d”.	7-17

Table 7-2. Number of peaks in the trace elements in relation to the extrapolated number of growth rings in *Keratoisis* sp. “kerD2d” 7-22

Table 7-3. Estimated water temperature (°C) from Mg/Ca ratios from the calcite of *Keratoisis* sp. “kerD2d” according to the equation by Sherwood et al. (2005). 7-22

Abbreviations

AIC – Akaike Information Criteria

ANCOVA – Analysis of covariance

CMN – Canadian Museum of Nature

CSSF – Canadian Scientific Submersible Facility

DFO – Fisheries and Oceans Canada

EDX – Energy Dispersive X-Ray

GLM – General Linear Model

IRLS – Integrated Real-time Logging System

MODIS - Moderate-resolution Imaging Spectroradiometer

OSCAR – Ocean Surface Currents Analysis – Real time

POC – Particulate Organic Carbon

PIC – Particulate Inorganic Carbon

ROPOS – Remotely Operated Platform for Ocean Sciences

ROV – Remotely Operated Vehicle

SEM – Scanning Electron Microscope

SODA – Simple Ocean Data Assimilation

SoG – Strait of Georgia

SST – Sea Surface Temperature

SuMo – Super Mohawk ROV

VME – Vulnerable Marine Ecosystem

XRD – X-Ray Diffraction

WOA – World Ocean Atlas

WOD – World Ocean Database

Co-authorship Statement

This thesis was written by me, Bárbara de Moura Neves. I lead the definition of most research questions, methodologies, and choice of the targeted organisms, with guidance from my supervisor Dr. Evan Edinger and my supervisory committee. I collected part of the studied specimens, I collected and analysed the data, and I am the lead author in all contributions emerging from this thesis. However, contributions by several co-authors helped to improve each individual chapter, and they are listed below.

- Dr. Evan Edinger co-authored all Chapters (2-7), provided assistance with the definition of research questions and methodologies, provided intellectual, financial and logistic support, and reviewed all chapters.
- Vonda Wareham co-authored Chapters 2-5, and 7, provided specimens of sea pens, and reviewed the manuscripts published from Chapters 2 and 7.
- Dr. Graham Layne co-authored Chapters 2-3, and 7 (partial), and provided advice and guidance with the interpretation of the trace elements analysis, as well as reviewed the manuscripts.
- Brynn Devine and Laura Wheeland will be co-authors of the publication emerging from Chapter 3. They provided sea pen samples, some colony measurements, and will participate in the manuscript review.
- Dr. Pål Mortensen and Dr. Lene Buhl-Mortensen will be co-authors of the publication emerging from Chapter 6, and provided unpublished data on *Primnoa* growth rates.

- Chapter 7 was partially co-authored by Dr. Claude Hillaire-Marcel who reviewed the manuscript and provided financial support, and by Dr. Scott France and Esprit Saucier who performed the molecular analysis of the studied specimens, and reviewed the manuscript. It was also co-authored by Dr. Margaret Treble (DFO) who reviewed the published portion of the chapter.

Appendices

- Appendix 2-1** X-Ray Diffraction analysis for the carbonate portion of the axis in *Halipterus finmarchica*. Overlap between the axis in *H. finmarchica* axis (black), magnesian calcite (red), and calcite (blue). Note that the axis of *H. finmarchica* follows the same pattern as magnesian calcite. 2-55
- Appendix 4-1** List of colonies of *Pennatula grandis* and associated depth and location. Latitude and longitude are in decimal degrees. 4-56
- Appendix 4-2** Carbonate composition of the axis in ten specimens of *Pennatula grandis* from the Northwest Atlantic. Samples are from the same location and depth. Red: length reduction (%), Wgt: weight, Org: organic material. 4-58
- Appendix 4-3** Results on the GLM analysis on the relationships between certain colony metrics and colony height for *Pennatula grandis* by locations in the Northwest Atlantic. 4-59
- Appendix 4-4** X-Ray Diffraction analysis for the carbonate portion of the axis in *Pennatula grandis*. Overlap between the axis in *P. grandis* (black), magnesian calcite (red), and calcite (blue). Note that the axis of *P. grandis* follows the same pattern as magnesian calcite. 4-60
- Appendix 5-1** X-Ray Diffraction analysis for the carbonate portion of the axis in *Umbellula encrinus*. Overlap between the axis in *U. encrinus* axis (black), magnesian calcite (red), and calcite (blue). Note that the axis of *U. encrinus* follows the same pattern as magnesian calcite. 5-45

Appendix 5-2 X-Ray Diffraction analysis for the carbonate portion of the axis in <i>Anthoptilum grandiflorum</i> . Overlap between the axis in <i>A. grandiflorum</i> (black), magnesian calcite (red), and calcite (blue). Note that the axis of <i>A. grandiflorum</i> follows the same pattern as magnesian calcite.	5-46
Appendix 6-1. Sample identification and associated information. Latitude (N) and longitude (W) are in decimal degrees. Depth in meters, height in cm, age in years. Rgrowth: radial growth rates ($\text{mm}\cdot\text{yr}^{-1}$), Dgrowth: diametric growth rates ($\text{mm}\cdot\text{yr}^{-1}$), Lgrowth: linear growth rates ($\text{cm}\cdot\text{yr}^{-1}$).	6-51
Appendix 7-1 X-Ray Diffraction analysis for the carbonate portion of the stem in <i>Keratoisis</i> sp. (“kerD2d”). Overlap between the stem in <i>Keratoisis</i> sp. (black) and magnesian calcite (red). Note that the stem of <i>Keratoisis</i> sp. follows the same pattern as magnesian calcite.	7-40
Appendix 7-2 Annual surface chlorophyll a from the MODIS sensor in the Aqua satellite for the years 2008-2013, for Baffin Bay near the sampled site (central green square). Red represents the highest values for chlorophyll a, while dark blue represents the lowest values. Data from NASA Goddard Space Flight Center, Ocean Biology Processing Group (2015).	7-41
Appendix 8-1 Published octocoral growth rates.	8-23

Publications arising

Chapter 2: Neves, B. M., E. Edinger, G. Layne & V. E. Wareham, 2015. Decadal longevity and slow growth rates in the deep-water sea pen *Halipterus finmarchica* (Sars, 1851) (Octocorallia: Pennatulacea): Implications for vulnerability and recovery from anthropogenic disturbance. *Hydrobiologia* 759 (1): 147-170.

Chapter 3: Neves, B. M., E. Edinger, V. E. Wareham, B. Devine, L. Wheeland & G. Layne (in prep). Size metrics and estimates of age and growth rates in one of the tallest known sea pens: *Umbellula encrinus* (Cnidaria: Pennatulacea) from Baffin Bay. For submission to *Canadian Journal of Fisheries and Aquatic Sciences*.

Chapter 4: Neves, B. M., E. Edinger & V. E. Wareham (in prep). Growth patterns in the deep-water sea pen *Pennatula grandis* Ehrenberg, 1834 (Cnidaria: Octocorallia) inferred from growth rings and colony metrics. For submission to *Acta Zoologica*.

Chapter 5: Neves, B. M., E. Edinger & V. E. Wareham (in prep). Morphology and composition of the internal axis in two morphologically contrasting deep-water sea pens (Cnidaria: Octocorallia). For submission to *Journal of Natural History*.

Chapter 6: Neves, B. M., E. Edinger, P. Buhl-Mortensen & L. Buhl-Mortensen (in prep). Growth in the cold-water gorgonians *Primnoa pacifica* Kinoshita, 1907 and *Primnoa*

resedaeformis (Gunnerus, 1763) (Cnidaria: Octocorallia) in relation to environmental variables. For submission to Deep Sea Research Part I.

Chapter 7: Partially published. Neves, B. M., E. Edinger, C. Hillaire-Marcel, E. Saucier, S. C. France, M. A. Treble & V. E. Wareham, 2014. Deep-water bamboo coral forests in a muddy arctic environment. *Marine Biodiversity* 45(4): 867-871.

1. Introduction

Deep-water corals have been known for over a century. A number of deep-water coral species known today were described for the first time as a result of some of the earliest oceanographic expeditions, including the HMS *Challenger* (1872-1876) and even earlier expeditions (Roberts et al., 2009). As deep-water species, they inhabit the continental shelf and beyond (Gage & Tyler, 1991). As corals, they are cnidarians with a calcium carbonate and/or proteinaceous skeleton classified in either the Anthozoa (Octocorallia or Hexacorallia, Fig. 1-1), or in the Hydrozoa (hydrocorals) (Cairns, 2007).

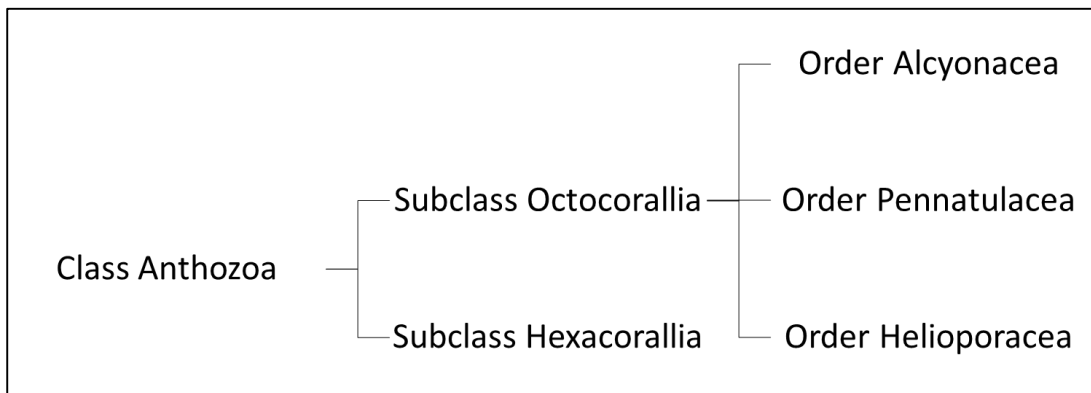


Figure 1-1. Current classification of Octocorallia and Hexacorallia by Kayal et al. (2013). Orders for Hexacorallia not shown.

Corals in the Octocorallia (i.e. octocorals) comprise sessile or sedentary anthozoans living associated to hard or soft substrates. Differently from all other coral taxa, they are unique in having polyps with exclusively eight tentacles (mostly pinnate) and eight mesenteries (Kayal et al., 2013). Their mainly sessile nature makes them

vulnerable to physical disturbance, as usually a dislodged coral cannot reattach to the substrate. And those which can (e.g. sea pens) might be more vulnerable after re-anchoring into the substrate, as colonies can be dislodged again without further disturbance (e.g. Malecha and Stone, 2009).

As their vulnerability to anthropogenic activities – especially bottom fisheries – became evident in the past decades (Hutchings, 1990, Jones, 1992, Hall–Spencer et al., 2002, Thrush & Dayton, 2002, Wassenberg et al., 2002, Troffe et al., 2005, Althaus et al., 2009, Malecha & Stone, 2009, Rooper et al., 2011, Jørgensen et al., 2015), there was an increase in the interest to determine deep-water coral longevity and growth rates, as proxies for recovery time. In the 21st century the number of studies on deep-sea octocoral growth rapidly increased, with several studies revealing growth rates in large octocorals such as *Primnoa* spp. (e.g. Andrews et al., 2002, Risk et al., 2002, Sherwood et al., 2005), bamboo corals (e.g. Roark et al., 2005, Noé et al., 2008, Andrews et al., 2009, Sherwood & Edinger, 2009), and arborescent hexacorals such as black corals (e.g. Goldberg, 1991, Love et al., 2007, Prouty et al., 2011).

Combined, these studies indicated that several deep-water corals are slow growing organisms with high longevities, which can reach centuries (Sherwood & Edinger, 2009), and in some cases millennia (Roark et al., 2009). As a result, the vulnerability of several deep-water coral species has been verified in the past years, among other things by these slow growth rates and high longevity estimates.

This thesis is the result of a project focused on octocoral growth. Besides looking at longevity, growth rates and patterns, I have investigated relationships between octocoral growth rates and environmental variables.

1.1 Octocoral morphology, skeletal composition, and growth patterns

Octocorals are currently classified in three orders: Alcyonacea (e.g. gorgonians, and soft corals), Pennatulacea (sea pens), and Helioporacea (blue corals) (Fig. 1-1, Kayal et al., 2013). They present an array of shapes and growth patterns, including the tree-like robust body of gorgonians, and the more fleshy bodies of soft corals and sea pens (Fig. 1-2). Gorgonians can have arborescent forms growing from a single point of attachment to the substrate, or they grow through stolons and root-like systems, with variable branching arrangements. Soft corals can also have a number of different branching patterns, which can be taxonomically important (Bayer, 1973). Sea pens can also vary from the pen-like erect forms of variable shapes to completely flattened colonies laying on the bottom (Williams, 1995).

All octocorals have a hydrostatic skeleton, which is seen at the colonial level in sea pens and soft corals, and at the polyp level in all taxa. Besides a hydrostatic skeleton, all octocorals have some other type of skeletal support. Gorgonians have CaCO_3 sclerites and an axial skeleton which can be proteinaceous, calcareous, or a combination of both materials (Bayer, 1981). Soft corals do not have an axial skeleton, and CaCO_3 sclerites are the single calcareous component of their skeleton.

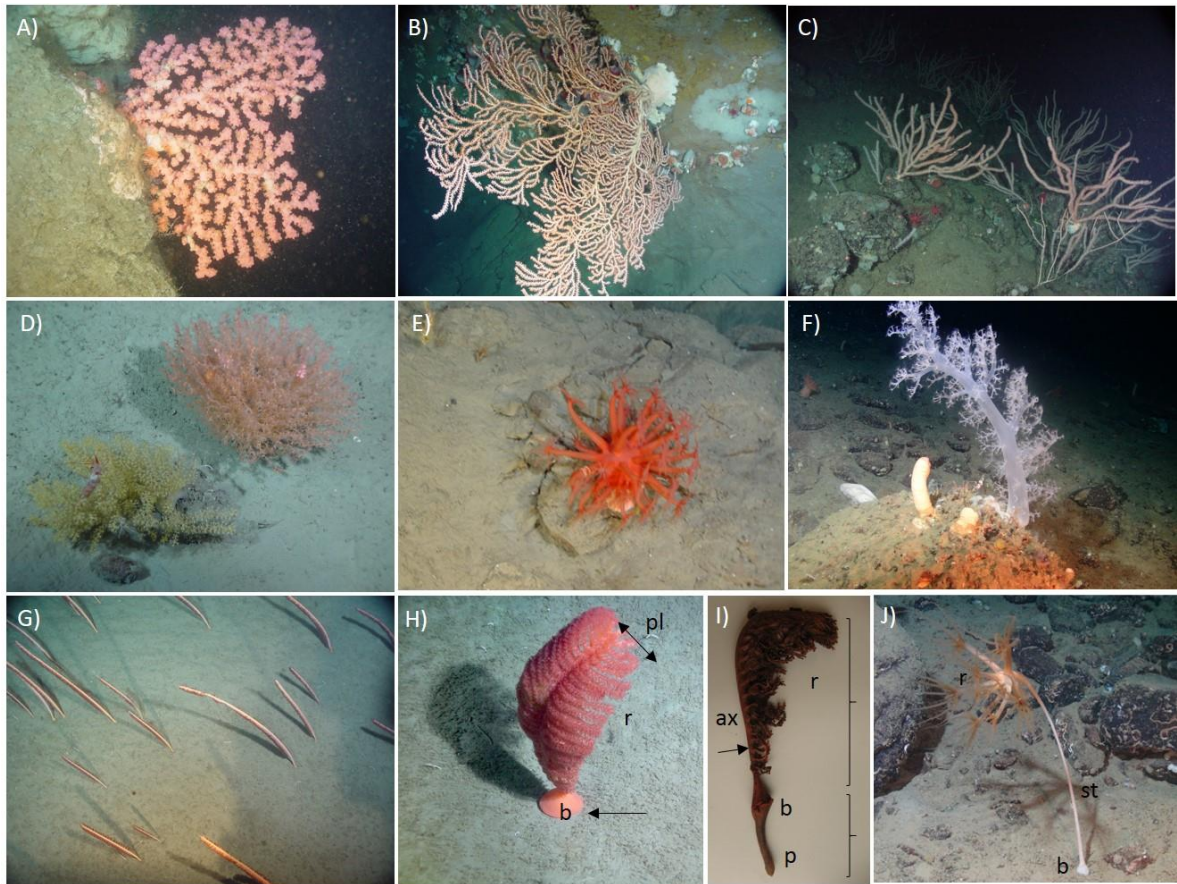


Figure 1-2. Diversity of octocoral growth forms. A-F: order Alcyonacea, G-J: Order Pennatulacea. A) *Paragorgia arborea* (Nova Scotia), B) *Paramuricea* sp. (Nova Scotia), C) *Keratoisis grayi* (Nova Scotia), D) *Acanella arbuscula* and *Acanthogorgia armata* (Southwest Grand Banks), E) *Anthomastus* sp. (Southwest Grand Banks), F) c.f. Nephtheidae (Scott Inlet, Baffin Bay), G) *Halipteris finmarchica* (Southwest Grand Banks), H) *Pennatula* sp. (Nova Scotia), I) *Pennatula grandis*, and J) *Umbellula encrinus* (Scott Inlet, Baffin Bay). Letters in H), I) and J) refer to: pl = polyp leaves, r = rachis, b = bulb, ax = axis, p = peduncle, st = stalk. Credits: A-E, G-H: DFO-CSSF, F, J: ArcticNet-CSSF-DFO, I: BMN.

Most sea pens have an internal axis composed of a mix of calcite and protein. Blue corals (order Helioporacea) are unique among octocorals in that they produce a calcareous skeleton composed of aragonite, like their counterparts the scleractinians (Daly et al., 2007), but these will not be considered here.

1.1.1 Growth patterns in alcyonaceans (order Alcyonacea)

The order Alcyonacea comprises gorgonians and soft corals. It is the largest Octocorallia order, comprising over 30 families (Van Ofwegen & McFadden, 2009, Breedy et al., 2012, Kayal et al., 2013, McFadden & Van Ofwegen, 2012, 2013). The order has been subdivided in two suborders based on the type of skeleton: Calcaxonia and Holaxonia (Fabricius & Alderslade, 2001). Calcaxonia is represented by octocorals whose skeleton is composed of gorgonin (a protein) and non-scleritic calcite, without a hollow cross-chambered central core (e.g. Isididae, Primnoidae). Holaxonia is represented by those octocorals with a skeleton primarily composed of gorgonin, but with some non-scleritic calcite present and a hollow cross-chambered central core (e.g. Acanthogorgiidae, Gorgoniidae).

As with other cnidarians, colonial growth begins with the settlement of a planula in a suitable substrate – although there are rare records of planula to polyp metamorphosis occurring without attachment to the substratum (e.g. Linares et al., 2008, Sun et al., 2010). Larval settlement can occur from 1 to several days post release (e.g. Sebens, 1983, Linares et al., 2008, Sun et al., 2010). After metamorphosis starts, the first polyp to be formed is called a primary zooid (Bayer, 1973), and the process of polyp development is relatively fast. In the Mediterranean *Paramuricea clavata* (Risso, 1826) the primary zooid

already had pinnate tentacles (tentacles with lateral extensions) in the 2-3 days after beginning metamorphosis. In the temperate soft corals *Drifa glomerata* Verrill, 1869 and *Drifa* sp. the primary zooid had 8 mesenteries and tentacle buds within only 24 hours post settlement (Sun et al., 2010).

Production of new polyps is continuous throughout the life of the colony, and although in most cases polyps in a single colony are anatomically identical (autozooids), some alcyonaceans present polymorphism, where more than one anatomical type of polyp can be found (Bayer, 1973). Although not very prevalent among alcyonaceans, polymorphism in this order can be found in the families Corallidae and Paragorgiidae (Bayer, 1981, Daly et al., 2007). In monomorphic colonies, autozooids are involved in all colony activities including growth. However, not all polyps in a colony are necessarily involved in growth. For instance, in the shallow-water tropical soft coral *Briareum asbestinum* (Pallas, 1766) only polyps near the tip of branches were found to be involved in branch growth, with polyps away from the base and tips being involved in reproduction only (Brazeau & Lasker, 1992).

Growth in alcyonaceans has been studied in terms of changes over time in overall colony length (Brazeau & Lasker, 1992, Goh & Chou, 1995, Matsumoto, 2004, Cadena & Sánchez, 2010, Rossi et al., 2011, Sartoretto & Francour, 2012, Peck & Brockington, 2013), weight (Khalesi et al., 2007), area (Garrabou, 1999), stalk diameter (Cordes et al., 2001), and stem radius and diameter (Mistri & Ceccherelli, 1993, Mortensen & Buhl-Mortensen, 2005, Matsumoto, 2007, Sherwood & Edinger, 2009, Luan et al., 2013, Chapters 6-7). In a few other studies authors have considered colony growth in terms of

polyp addition and branching events as well (Brazeau & Lasker, 1992, Fabricius et al., 1995, Bramanti et al., 2005, Khalesi et al., 2007, Mosher and Watling, 2009).

While in several alcyonaceans juveniles and adults are morphologically similar, in some cases there are large differences between life stages, with juveniles and adults being morphologically distinct. Mosher and Watling (2009) showed that colonies of the deep-water gorgonian *Metallogorgia melanotrichos* (Wright & Studer, 1889) undergoes a significant morphological change as it grows. In other species like *Paragorgia johnsoni* Gray, 1862 the similarity between younger and older stages of the colony is such that juveniles look like miniature versions of the adults (Watling et al., 2011).

Although gorgonians grow by the addition of new polyps, the branch is the functional module in their growth (Sánchez et al., 2004). To maintain colony shape, all the mother branches in a gorgonian should increase/decrease branching at the same rhythm (Sánchez et al., 2004). In a single colony, certain branches can have a determinate growth, while others might continue growing indeterminately over the colony life span (Lasker et al., 2003).

Polyp addition in soft corals can be related to flow intensity: in the shallow-water *Dendronephthya hemprichi* Klunzinger, 1877 polyp addition increases food intake under intermediate flow (12-16 cm.s⁻¹), while under high flow (25-32 cm.s⁻¹) polyp addition is replaced by an increase in polyp strength (Fabricius et al., 1995). In *Sinularia flexibilis* (Quoy & Gaimard, 1833) specific growth rates and the number of protruding branches was higher at intermediate (7 and 11 cm.s⁻¹) flows, when compared to slow (3 cm.s⁻¹) and fast (15 and 19 cm.s⁻¹) flows. High water velocities can cause colony retraction and reduction in exposed area, leading to a reduction in food intake (Khalesi et al., 2007).

Variations in growth forms in octocorals have been frequently associated to responses to hydrodynamic forces (e.g. Mistri & Ceccherelli, 1993). Shallow-water reef gorgonians can direct their bodies and bend to withstand wave motion as they grow. Larger gorgonians - which are more exposed to stronger currents - seem to have a different orientation than smaller ones (Wainwright & Dillon, 1969). In the case of the stoloniferous octocoral *Carijoa riisei* (Duchassaing & Michelotti, 1860) (published as *Telesto*), a switch from vertical to lateral growth was also observed as a response to unidirectional currents. Colonies acquired a flabellate growth form, instead of bushy forms found where colonies are more protected from currents (Rees, 1972).

Gorgonians can also assume different shapes as a response to colony size and the resulting changes in hydrodynamic conditions. The frequency of concave shapes in the deep-water *Paragorgia arborea* (Linnaeus, 1758) increased with colony size. Mortensen & Buhl-Mortensen (2005) suggested that this indicates a transition from the turbulent environment experienced by small colonies to an environment dominated by unidirectional currents when colonies are larger. Food availability provided by these currents also seem to be a factor determining colony shape in this octocoral.

Modes of growth and flow regime can also have an influence on resource capture, and these factors together can influence octocoral morphology (Kim & Lasker, 1998, Goffredo & Lasker, 2006) and growth (Fabricius et al., 1995). In many cases as a colony grows, polyps formed at more exposed parts of the colony might have more access to food than polyps restricted to other parts (more hidden) of the colony (McFadden, 1991, Kim & Lasker, 1997, 1998). This condition is analogous to self-shading in plants, where

light is the limiting resource as new leaves are formed and over-shade older leaves (Kim & Lasker, 1997, 1998).

In terms of skeletal growth, the axial skeleton in octocorals is a specialized part of the coenenchyma, being the product of the colony as a whole, not individual polyps (Bayer, 1973). Skeletons containing both calcareous and proteinaceous parts have an important role in giving the colony both strength and flexibility. A very interesting case of such specialization can be found in the family Isididae (bamboo corals), where the skeleton vertically alternates into regions of Mg-calcite (internodes) and protein (nodes) as the colony grows (Noé & Dullo, 2006, Noé et al., 2008).

Noé & Dullo (2006) identified six growth stages in bamboo corals. Growth starts with the secretion of an organo-mineralic axis followed by a calcitic growth band. The layer (ring) formed in the first internode becomes restricted to this area. After a new node is formed, the following new internode will contain only the layers formed hereinafter. In this way, the colony grows vertically with new layers being secreted around the entire skeleton, but with the main stem accumulating all layers, while the tips (youngest parts) only have the most recent layer (ring).

In the case of these bamboo corals, the pattern shown by Noé & Dullo (2006) indicates that the production of the organic node seems to be the trigger point for the addition of new layers to the skeleton. In other gorgonians, new branching takes place at approximately fixed distances from the mother branch tip (Sánchez et al., 2004) and there is no separation into organic node and inorganic internode.

Growth patterns in alcyonaceans have also been determined in terms of growth curves. Although several growth curves have been used to describe growth patterns in

many organisms (Kaufmann, 1981), the Von Bertalanffy growth curve is the most applied curved in studies on octocoral growth (e.g. Grigg, 1974, Mistri & Ceccherelli, 1993, Mistri, 1995a, 1995b, Goffredo & Lasker, 2006, Sartoretto & Francour, 2012, Munari et al., 2013, Doughty et al., 2014). According to this model, size increases with time and growth rates are faster at the beginning, and decrease continually until an asymptote is reached (von Bertalanffy, 1938).

Another growth curve that has been used in the study of octocorals is the Gompertz model. In contrast to the von Bertalanffy model, the Gompertz model predicts slow initial growth, with a more rapid growth when colonies reach an intermediate size, followed by reaching an asymptote (Kaufmann, 1981). Cordes et al. (2001) justified the use of a Gompertz model when studying the deep-water *Anthomastus ritteri* Nutting, 1909 based on the relationship between feeding rate and surface area in this soft coral. In this sense, very small colonies with few polyps have limited food input, and they will have slower initial growth rates, which will increase as the animals' feeding capacity also increases. Early growth has also been shown to be very slow in neptheid soft corals, with no or rare budding occurring throughout several months of observation after larval settlement (Sun et al., 2010, 2011).

1.1.2 Growth patterns in sea pens (order Pennatulacea)

The order Pennatulacea comprises approximately 200 sea pen species (Williams, 2011). Sea pens are octocorals characterized by having a muscular peduncle unique among octocorals. The peduncle anchors the colony in the soft substrate (Williams, 1995), although a few species are known to have adapted to a life on hard substrate

(Williams & Alderslade, 2011). Colonies have a proximal peduncle, a distal rachis that contains autozooids (Fig. 2-1) and sometimes other types of polyps (e.g. siphonozooids and mesozooids).

Differently from gorgonians and some other alcyonaceans, sea pens usually have fleshy and flexible bodies, with many species having a skeleton composed of an internal axis and CaCO₃ sclerites (Williams, 1995). Sea pens are sedentary but not necessarily sessile organisms, as some species are able to perform some movement thanks to powerful muscles in the peduncle area (Musgrave, 1909). In fact, several species are even capable of completely withdrawing into the sediment, and although the reasons for that are still unclear (Langton et al., 1990, Ambroso et al., 2013), predation by other species is one of the possible triggers to this behavior (Wyeth & Willows, 2006).

After settlement, the juvenile of a sea pen develops into an oozoid, the first polyp of the colony, which will differentiate in the peduncle. The subsequent polyps will develop by budding of the oozoid, which will become the greater part of the rachis and stalk of the adult colony (Hickson, 1916). After three days of settlement, the young sea pen *Ptilosarcus gurneyi* (Gray, 1860) already has eight tentacles, and in nine days it has developed a peduncle (Chia & Crawford, 1973). In the same species, an 18-day-old oozoid has what Chia & Crawford (1977) called “style cells” or large interstitial cells in the endoderm of the peduncle septum, which will differentiate to form the style, or the internal axis. Style cells were not present in the planula (Chia & Crawford, 1977).

Berg (1941) gives detailed descriptions on the development biology, colony formation, and organization of *Funiculina quadrangularis* (Pallas, 1766), which in the NW Atlantic is usually found at depths > 180 m (Wareham and Edinger, 2007), but in

Berg's study colonies were from shallow-water environments (25-50 m). Eight projections that will represent the tentacles are formed just after the larvae has settled. At around 7-8 weeks after the primary polyp is formed, it will shift to the side and budding of the primary polyp will take place (Berg, 1941). This migration of the primary polyp has also been reported for *Umbellula* sp. (Willemoes-Suhm, 1875).

Differently from alcyonaceans, sea pens present a high degree of polymorphism, with most species having both an oozoid, autozooids and siphonozooids (Williams, 1995). Autozooids are the main polyps, which are responsible for feeding and reproducing in most species, while siphonozooids are smaller and delicate polyps with a function in the water transport in the colony and sometimes in reproduction (Bayer, 1973, Williams et al., 2012). Some species in the genus *Pennatula* have a fourth type of polyp called mesozoid, and a fifth type (acrozoid) has also been identified in the genus *Pteroeides* (Williams et al., 2012).

Sea pens can grow by the addition of autozooids directly in the surface of the colony (suborder Sessiliflorae), or by creating polyp leaves and raised pads, where new autozooids (and sometimes siphonozooids and mesozoids) grow (suborder Subsessiliflorae). Colonies can be cordate (heart-shaped) with a flattened rachis (e.g. Renillidae), or have more cylindrical or elongate growth forms (Williams, 1995).

Few studies have specifically examined growth in sea pens. In some species new polyps are added near the basal part of the rachis, above the peduncle (Soong, 2005, Baillon et al., 2016). In certain taxa including the Umbellulidae and Chunellidae families, a very different growth pattern occurs, where a cluster of polyps is found at specific parts of the colony (Williams, 1995).

The arctic species *Umbellula encrinus* Linnaeus, 1758 grows in three stages, which are characterized by (1) the presence of terminal zooids that produce small processes that will become secondary autozooids, (2) the growth of these processes and appearance of siphonozooids, (3) the development of the secondary autozooids, and increased distinction of siphonozooids (López-González & Williams, 2011). Willemoes-Suhm (1875) described the initial growth in *Umbellula antarctica* to begin with an initial central polyp, the appearance of two lateral polyps, and the migration of the central polyp to the sides as a fourth polyp is added.

The internal axis of sea pens is usually a mix of carbonate and organic material (Franc et al., 1975, 1985, Wilson et al., 2002, Chapters 2-5), and it frequently follows the whole length of the colony, from the proximal to the distal extremities (Williams, 1995). In some species the axis does not fully extend throughout the whole colony (e.g. *Pennatula aculeata* Danielssen, 1860, Baillon et al., 2016). Growth rings can be identified in the axis of several species (Birkeland, 1974, Wilson et al., 2002, Chapters 2-5), although there are species where rings have not been observed at all (Soong, 2005). The internal axis of sea pens can have different shapes and textures (Hickson, 1916), and are an important component of a sea pen growth.

Prior to this study, only two other studies have shown growth rates in sea pens, one of which focused on a shallow-water species (Birkeland, 1974), and the other one on a deep-water species from Pacific waters (Wilson et al., 2002). Both studies have shown that as other deep-sea octocorals, sea pens also grow at slow rates and have longevities at the decadal scale. In this thesis, I present data on growth patterns and rates of three additional species of deep-water sea pens common in the Northwest Atlantic. The

widespread presence of these sea pens indicates that they are an important component of the benthic environment in this region. Knowledge of their growth rates and longevity can help to infer about recovery time. Knowledge of other aspects of colony growth (e.g. morphological relationships) and the influence of environmental factors on growth rates is also important to better assess their vulnerability. In the Northwest Atlantic sea pens inhabit environments increasingly exposed to anthropogenic threats (e.g. bottom fisheries), which can heavily impact them.

1.1.3 Growth rings in octocorals

Growth lines or rings can be defined as “abrupt or repetitive changes in the character of an accreting tissue” (Clark, 1974). In corals, these lines are not continuously deposited like in trees; deposition is rather limited to the portion of the skeleton in contact with the tissue (Clark, 1974). In octocorals, growth rings can be found both in horny and calcareous skeletons. In calcareous skeletons, growth rings might be more difficult to visualize, becoming more discernible with the aid of a stain such as toluidine (Marschal et al., 2004). In the case of species with a mixed skeleton, growth rings sometimes can be identified in both regions (e.g. in *Primnoa pacifica* Kinoshita, 1907, Risk et al., 2002).

The recognition that several octocoral species lay down growth rings is not new. Growth rings in gorgonians were already described by Linnaeus. Referring to Zoophyta he said that these organisms “...are increased every year under their bark, like trees, as appears from the annual rings in a section of the trunk of a gorgonian” (Johnston, 1847). Ellis (1753) illustrated the presence of growth rings in the axis of the sea pen *Umbellula*

encrinus. Wainwright and Dillon (1969) recognized that the presence of layers in the axial skeleton of gorgonians indicate the age of the organism.

The study of periodicities stored in accreted hard parts and skeletons of an organism is called sclerochronology (reviewed in Helmle & Dodge, 2011). Modern studies on growth rings in corals mainly focused on scleractinians, which were the first corals recognized to lay down growth rings at a temporal scale that could be traced (Sorauf & Jell, 1977, Lazier et al., 1999). Later, black corals, gorgonians and sea pens were also recognized to lay down growth bands of known periodicity in their skeletons (Wainwright & Dillon, 1969, Birkeland, 1974, Grigg, 1974). Sclerochronology has gained an important role in the study of octocoral growth rates, longevity and paleoceanography.

Grigg (1974) and Birkeland (1974) were the first to show that growth rings in some octocorals are formed annually. Since these studies, a few teams have been able to determine ring formation periodicity in other octocoral species. Ring periodicity has been confirmed to be annual in several species including *Primnoa pacifica* (Risk et al., 2002), *Primnoa resedaeformis* (Gunnerus, 1763) and *Keratoisis grayi* (Wright, 1869) (Sherwood et al., 2005, Sherwood & Edinger, 2009), and *Corallium rubrum* (Linnaeus, 1758) (Marschal et al., 2004). Validating ring formation periodicity in deep-sea corals presents several challenges, and the level of difficulty depends on factors that include type and arrangement of skeletal material, accessibility to living colonies for monitoring, colony age, and availability of geochemical tools for validation. This topic will be discussed in section 1.3.3.

Most of the information available on the process of ring formation in octocorals come from a few studies on shallow-water species. The formation of growth rings in

different coral taxa has been mainly associated to tanning processes and changes in skeletal density. The sequence of deposition of the axial skeleton in two species of the shallow-water gorgonians *Muricea fruticosa* Verrill, 1869 and *Muricea californica* Aurivillius, 1931 was determined by Szmant-Froelich (1974). As in some other octocorals, alternating light and dark bands can be distinguished in the axial proteinaceous skeleton of *Muricea* spp. Lighter bands are formed during times of favorable and faster growth, while dark bands are formed when growth rates are reduced. That is because of the time of contact between the recently formed band and the axial epithelium: the longer the contact with the epithelium (slower growth) the longer the epithelium's tanning action is, which makes the bands darker.

In the Mediterranean gorgonian *Leptogorgia sarmentosa* (Esper, 1789) the same pattern can be observed, of light bands being formed during summer time (Mistri & Ceccherelli, 1993). In *Corallium rubrum* colonies from a shallow-water population in the Mediterranean a dark band is formed in the calcareous skeleton during late autumn and winter, also corresponding to the slowest growth rates (Marschal et al., 2004). In *C. rubrum* the formation of a dark band is associated to a high concentration of organic matrix.

In the cold-water octocorals *Primnoa pacifica* and *P. resedaeformis*, in which rings alternate as carbonate and proteinaceous bands (a couplet equals one year) (Risk et al., 2002, Sherwood et al., 2005) the production of the dark proteinaceous band is thought to be related to particulate organic matter (Sherwood et al., 2005). Differently from the species described above, the dark band in *Primnoa* is believed to be formed during periods of the year of higher primary productivity (i.e. annual spring phytoplankton

bloom), and the switching to calcite is thought to be a response to a decrease in food availability (Risk et al., 2002).

In the early stage of axis formation in *P. pacifica* a calcareous core is deposited before the proteinaceous layer. It has been suggested that the growth mode of skeletal deposition in this species started with the carbonate mode and then switched to the carbonate/gorgonin couplet mode (Matsumoto, 2007). In *Corallium rubrum*, the axis core (medullar region) contains no rings and it is first formed by the fusion of sclerites. The region where rings are observed (annular region) is formed from a secretion by the skeletogenic epithelium allowing centrifugal growth (Debreuil et al., 2011).

In the sea pens *Halopteris finmarchica* (Sars, 1851) and *Umbellula encrinus* the association between the number of rings visually determined and the number of peaks in the trace element ratios indicates that alternating bands (light and dark) have a different geochemistry, which is related to changes in the physical characteristics of the rings (Chapters 2-3).

In scleractinians, contrasting growth rings are visible due to changes in skeletal density. In these corals, although it is not clear yet whether its environmental and/or endogenous factors that cause annual density banding in their skeletons, factors including temperature, light, productivity, and reproduction have all been suggested to play a role in banding formation. Density banding in the skeletons of scleractinians is caused by a periodic thickening and/ or coalescing of skeletal structures, which can be taxa-specific (Helmle & Dodge, 2011).

1.2 Growth rates

Deep-water octocorals are generally considered slow growing organisms when compared to their shallow-water counterparts. Growth rates in these animals have been mainly estimated in terms of radial, diametric and linear growth rates, although some studies have also considered growth in terms of biomass increment over time (e.g. Rossi et al., 2011), and polyp/branch addition as discussed in section 1.1.1.

In a biological context, growth rate is the increase of an organic system (e.g. in length) over time (von Bertalanffy, 1938). Radial growth rates are a measure of how fast the stem/axis grows radially and in diameter, respectively, while linear growth rates – also called axial growth rates by some authors (e.g. Sherwood & Edinger, 2009, Watling et al., 2011) – represent extension in colony height over time.

Growth rates and longevity are better known for gorgonians than for other octocorals. This is probably due to their potential high longevities and vulnerability, but also because of their potential as palaeoceanographic proxies of environmental change (reviewed in Robinson et al., 2014). The skeletons of long-lived species can be particularly useful to allow a characterization and better understanding of changes in oceanographic conditions over time. Gorgonians whose skeletons preserve well after death such as bamboo corals and primnoids, and commercially exploited species such as the precious coral *Corallium* spp., have been the focus of most studies. There is only a single published study on growth rates of a soft coral (*Anthomastus ritteri*, Cordes et al., 2001), and few studies on sea pens as mentioned in the previous sections.

In the next subsection a number of environmental factors that might influence growth rates in cold-water octocoral species are discussed.

1.2.1 Growth rates in relation to environmental variables

The influence of environmental factors on cold-water octocoral growth is not yet well understood, but it is believed that temperature, current strength and food availability are important factors influencing growth (Roberts et al., 2009). Growth is among the processes heavily affected by low temperatures (Peck, 2016). In well-studied shallow-water zooxanthellate scleractinians, growth rates are believed to be mainly controlled by temperature and light, although no isolate factors have been demonstrated to explain growth in these organisms yet (Helmle & Dodge, 2011).

Thresher (2009) identified temperature and depth as important factors influencing radial growth rates in deep-water bamboo corals. Colonies grew faster at temperatures between 2-5 °C; outside of this range colony growth rates reached a plateau (both below and above these ranges). Recently Farmer et al. (2015) showed that no relationships were identified between growth rates and several environmental variables in the deep-water bamboo-coral *Keratoisis* spp., including temperature and proxies of primary productivity. The contrast between the studies by Thresher (2009) and Farmer et al. (2015) can be explained by the inclusion of additional specimens of *Keratoisis* sp. in the latter study. These additional specimens came from areas of higher temperatures (> 5 °C) but with modest growth rates.

Colonies of *Primnoa pacifica* from Japan, living in waters at 0.6-0.7 °C had growth rates slower than those estimated for colonies from sites where temperature is

much higher. This was suggested to indicate that temperature might influence growth rates in this species (Matsumoto, 2007). However, because in other locations of higher temperature growth rates were still very slow, factors other than temperature are believed to influence growth in these gorgonians. In Chapter 6, I show additional results on the growth rates of *Primnoa pacifica* and *P. resedaeformis* using published data and new data in relation to environmental variables, including proxies of primary productivity, which have been suggested to play a role in growth rates in these octocorals (Aranha et al., 2014).

Primnoella scotiae Thomson & Ritchie, 1906 from shallow Antarctic waters showed very slow average linear growth rates of $< 1 \text{ cm}\cdot\text{yr}^{-1}$ (Peck & Brockington, 2013). While life in temperatures frequently below zero might explain these slow growth rates, temperate and even tropical species have shown similar rates in previous studies (Chapter 8).

In this thesis, I also show that for the studied species and using the environmental data used, we did not find strong relationships between growth rates and environmental variables. Whether we are looking at the wrong variables or whether intrinsic factors are more influential on growth rates than environmental factors is still under discussion.

1.3 Methods for studying growth rates in octocorals

Methods used to study growth rates in deep-water octocorals are usually more restricted than those used to study shallow-water species. That is because the application of straightforward techniques such as the marking and monitoring of colonies over time

become very demanding when studying deep-sea environments. Therefore, growth rates in deep-water octocorals have been mainly studied by examining growth rings formed in their skeletons, as outlined in section 1.1.

1.3.1 Aquaria/mesocosm

Small deep-water scleractinian corals have been successfully kept in aquaria and mesocosm; but among octocorals the only published study on growth rates so far was that by Cordes et al. (2001) on the soft coral *Anthomastus ritteri*. Although soft corals and sea pens can be successfully kept in aquaria, they have not yet been the subject of a growth study in this type of setting, except for a handful of studies on early growth in soft corals (e.g. Sun et al., 2011).

The problem with large and long-lived gorgonians is obvious, as keeping very large colonies in a tank for long periods of time (necessary for growth studies) can be very challenging. Keeping deep-water species in controlled environments presents additional challenges, as certain environmental conditions (e.g. absence of light and low temperatures) are difficult to maintain. Williams and Grottoli (2008) attempted to keep deep-water gorgonians in a tank for a growth study, but colonies died within two weeks of experiment. However, keeping small octocorals in aquaria for growth studies is one of the obvious future directions to be taken, especially for ends of validation of growth ring formation (section 1.3.3).

1.3.2 Ring counting

Most studies on growth rates of deep-water corals have been focused on gorgonians and black corals, which lay down growth rings in their skeletons. In several taxa, periodicity of growth rings has been confirmed to be annual (Risk et al., 2002, Sherwood et al., 2005). The gorgonian *Paragorgia arborea* can reach large sizes (e.g. 2.4 m, Watanabe et al., 2009) and it is potentially a species with very high longevities (Mortensen & Buhl-Mortensen, 2005, Sherwood & Edinger, 2009). However, it does not lay down clear and defined rings, and therefore it cannot be aged by the ring counting technique. In sea pens, growth rings can also be observed in the axis of several species, which will be explored in Chapters 2-5.

Finer scale rings have also been identified in several species, although the nature and frequency of formation of these rings remains conjectural. In *Keratoisis* sp. macroscopic bands are produced on an annual basis, while their microscopic sub-units are produced on sub-annual frequencies (Noé & Dullo, 2006). The formation of intra-annual rings possibly has a monthly lunar periodicity in *Primnoa pacifica* (Risk et al., 2002), and in certain bamboo corals (Roark et al., 2005, Tracey et al., 2007). The influence of the moon on deep-sea organisms might be related to fluxes of particulate matter, moonlight (disphotic zone), and tidal currents; however, these remain elusive (Mercier & Hamel, 2014).

Growth rings in marine benthic invertebrates can be formed at variable temporal scales including daily (solar or lunar periodicity), following a synodic month (28.51 days), fortnightly (tidal cycles), annually, etc. (Clark, 1974). Although in many cases the

formation of growth lines follows environmental cues, there are also cases where an internal biological clock might trigger the formation of a growth line (Clark, 1974).

In octocoral sclerochronology, by determining the number of growth rings (i.e. age) seen in the skeleton, growth rates can be calculated by simply considering how much the organism grew over time. In some studies, authors have preferred to ask colleagues with no previous experience to visually count rings after a basic training (e.g. Sherwood et al., 2005), while in other studies rings have been counted by specially trained personnel (Gallmetzer et al., 2010), and in other cases authors counted rings themselves (Chapters 2-5). Whatever the case is, it seems reasonable that rings should be counted more than once and averaged, in order to account for any variations that might result from the technique. Furthermore, in the case of the same person counting rings more than once in the same specimen, it should be performed at non-consecutive times to avoid any bias.

Some studies show comparisons between the uses of light microscopy versus Scanning Electron Microscopy (SEM) when working with the ring counting technique. Mortensen and Buhl-Mortensen (2005) found a 97% correspondence between ring counts using both techniques in *Primnoa resedaeformis*, and Tracey et al. (2007) found that in the skeleton of the bamboo coral *Keratoisis* sp. major events (rings) could be clearly identified using both techniques. Major growth rings in many species can be readily identified when seen under a light microscope or stereoscope. The use of an SEM provides detailed observation of more discrete intra-annual rings.

In the case of *Primnoa resedaeformis* (Sherwood et al., 2005) and based on my experience with sea pens, the visualization of growth rings is highly improved when the stem/axis is photographed under UV light, followed by a Photoshop treatment (e.g.

sharpening of image). Figure 1-3 shows a comparison between a cross section of the axis from the sea pen *Umbellula encrinus* seen under stereomicroscope in regular light, UV light, and SEM. As observed by the aforementioned authors, the main rings are conspicuous when seen under both microscopes, but rings are better seen under UV light than under regular light, at least in *Primnoa* and sea pens.

1.3.3 Validation techniques

Validation techniques have been widely used as attempts to corroborate or determine frequency of ring formation in deep-water octocorals. Among the validation methods most frequently applied to deep-water octocorals are radiometric techniques, of which ^{14}C and ^{210}Pb have been particularly recurrent. Besides radiometric techniques, validation can be obtained by creating a visual marker (e.g. stain) in the newest region of the skeleton and following growth afterwards. Growth ring periodicity can be also corroborated by studying organisms growing on structures of known age (Squires, 1960, Davis et al., 2000, Marschal et al., 2004, Gass & Roberts, 2006, Larcom et al., 2014), which are not frequently available or reported.

Radiometric techniques. In *Primnoa pacifica* annual growth ring formation was validated by applying the bomb- ^{14}C technique (Sherwood et al., 2005). Atomic bomb testing that occurred during the 1950s and 1960s led to an abnormal increase in the ^{14}C amount in the atmosphere and in the oceans. In the NW Atlantic, the ^{14}C concentration in the water peaked in ~1970s. Organisms with a hard skeleton that were alive at that time should have incorporated this increase, which should be captured in a ^{14}C analysis (Campana, 1997). By knowing the age of an organism collected alive whose year of

collection is also known, it is possible to estimate the year of formation of the specific ring that corresponds to a peak in ^{14}C . If the curve closely matches the bomb- ^{14}C depletion curve, then a periodicity can be determined (Sherwood et al., 2005).

^{14}C analysis with aims of age determination has also been performed in other species that do not form evident growth rings, such as in *Paragorgia* spp. and *Paramuricea* spp., which have relatively porous skeletons (Sherwood & Edinger, 2009, Prouty et al., 2014). In both species, the analyses showed that rings (when visible) are not annual in nature. Therefore, estimation of age from growth rings in the genus *Paragorgia* will be imprecise (e.g. Andrews et al., 2005, Sherwood & Edinger, 2009), and this might also be the case in the different species of *Paramuricea* that have not been tested yet. In such cases, extraction of material for radiometric analysis is not based on individual rings, but rather on specific areas of the stem (e.g. core, middle, edge). This will frequently be the case for octocorals with a porous skeleton, where rings are not clearly identifiable.

^{210}Pb has been used aiming to validate growth ring formation periodicity in fewer deep-water octocorals than in comparison to ^{14}C . The method is based on the radioactive decay of ^{210}Pb over time. In the sea pen *Halopteris willemoesi* K lliker, 1870 this technique was not successful due to the presence of exogenous material in the sample (Wilson et al., 2002), and it did not work well for *Paragorgia* sp. (Andrews et al., 2005). The technique was also used to date bamboo coral colonies from the calcified internodes without counting rings (Andrews et al., 2009), which are more difficult to visualize in the calcite of bamboo corals (Sherwood & Edinger, 2009). ^{210}Pb was also used in combination to ^{14}C to determine ring periodicity in colonies of *Keratoisis grayi*, which was confirmed to be annual (Sherwood et al., 2008).

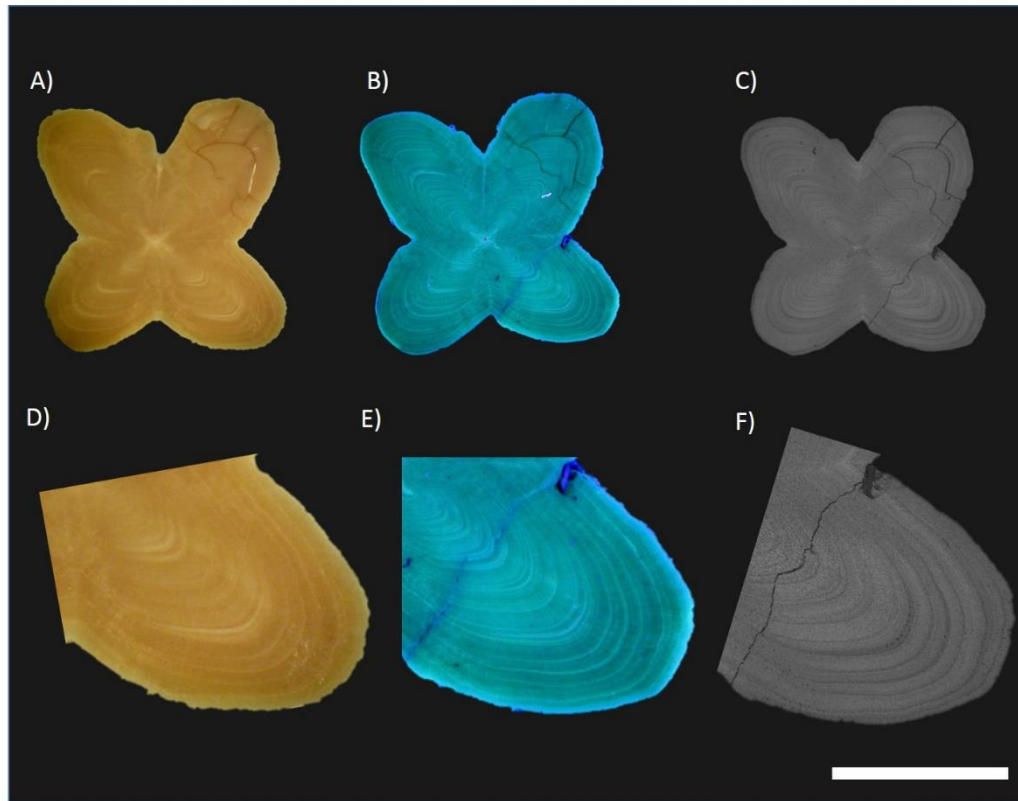


Figure 1-3. Cross section of the internal axis of *Umbellula encrinus* seen under regular light (A) and UV light in a stereomicroscope (B) and in an SEM (C), with correspondent magnified lobes for details (D-F). Scale bar = 1 mm (photo sizes are slightly different).

To validate frequency of ring formation in species that are not very long-lived is challenging, as radiometric techniques become more limited. In terms of analyses based on radioactive decay, the lower limit of the ^{14}C method is ~ 300 calendar years (Taylor & Bar-Yosef, 2014), and that of ^{210}Pb is 100-120 years (Andrews et al., 2009). Furthermore,

as the bomb-¹⁴C peak in the 1970s stays farther behind in time, fewer specimens alive at the present were alive at that time.

Perhaps the arrival of other unplanned human-induced activities will function as markers for future studies. For example, the Deepwater Horizon oil spill that took place in the Gulf of Mexico in 2010 exposed several populations of deep-water corals to oil and other chemicals (White et al., 2012). It is very likely that there were changes in the geochemistry of the skeletons associated to the chemicals present in the water during the spill in 2010, setting a potential new time marker in the region.

Staining techniques. Staining techniques have also been applied to determine the frequency of ring formation in some cold-water octocoral species (e.g. Marschal et al., 2004). Although this method works well in shallow-water settings, it becomes more challenging for studies *in situ* in deep-water environments, due to some of the constraints related to deep-water studies. Calcein and alizarin red (Marschal et al., 2004, Williams & Grottoli, 2008, Brooke & Young, 2009) are among the stains used in this context.

The use of stains in aquaria could work well for relatively small octocorals such as sea pens. Adding a stain as a marker to validate how long it takes for one ring couplet to be formed is a future direction in the study of these organisms. A drawback of this type of study is that adding a stain to the water might somehow affect the colonies and preclude using them for other types of study (e.g. reproduction). Furthermore, at the end of the experimental period the sea pen (s) will be sacrificed for a detailed examination of the axis.

1.4 Limiting factors to octocoral growth

An array of studies on the distribution of cold-water corals has been showing that coral distribution is strongly controlled by environmental variables including temperature, appropriate substratum, and current velocity (Roberts et al., 2009). Although these studies are not focused on measures of growth rates or patterns of individual colonies, they indicate where octocorals might grow. Predictive modelling has been very useful in testing and identifying environmental factors that have the strongest influence on the distribution of these organisms.

Yesson et al. (2012) identified several environmental factors influencing the global distribution of cold-water octocorals, including temperature, salinity, productivity, oxygen, and calcite saturation. In a smaller scale, Bryan & Metaxas (2006) identified temperature, slope and currents as primary environmental factors influencing the distribution of Paragorgiidae and Primnoidae octocorals in the continental shelf/slope of the Atlantic and Pacific coasts of North America. Substrate (mud and gravel content), minimum salinity, and depth were the most important variables explaining the distribution of three sea pen species in Scotland (Greathead et al., 2014).

In the study by Bryan & Metaxas (2006) members of Paragorgiidae preferred steepest slopes and slowest currents than primnoids. Similarly, requirements to gravel content differed among sea pen species, with *Pennatula phosphorea* Linnaeus, 1758 being absent where gravel content was > 30%, which was not limiting to *Virgularia mirabilis* (Müller, 1776) (Greathead et al., 2014). Therefore, certain environmental variables determine the susceptibility of a site to the growth of octocorals. Furthermore,

the ranges within each of these variables (e.g. temperature, salinity, current strength) are taxa-specific.

Substrate availability and size have an important influence on octocoral growth. Coral larvae depend on a hard substrate so that a colony can fully grow, even if the initial structure is a grain of sand (Roberts et al., 2009). Furthermore, substrate size (e.g. boulder size) will also determine how large a coral can grow, as octocoral maximum size has been found to be related to the size of the attachment substrate in some cases (Tunncliffe & Syvitski, 1983, Mortensen & Buhl-Mortensen, 2005).

1.5 Conservation perspective

The recognition of several species of deep-water corals as slow growing has been an important addition to the knowledge on these organisms, which has contributed to include them as part of the United Nations (UN) definition of Vulnerable Marine Ecosystems (VMEs). Being included in this definition is a very important step for the conservation of deep-water corals.

Just as some species can have very slow growth and longevities of centuries and millennia, other species seem to have decadal longevities. For instance, sea pens have longevities at the scale of decades, as do other marine suspension feeding invertebrates including brittle stars (Dahm & Brey, 1998, Gage 1990) and bryozoans (Barnes, 1995, 2007, Brey, 1999). It is important to emphasize that an invertebrate that lives decades already has a very important connection and function in the ecosystem (Buhl-Mortensen

et al., 2010), and that shorter longevities compared to other organisms (e.g. other corals) should not be seen as less important.

1.6 Thesis outline

Besides this introductory Chapter (1) this thesis contains six data Chapters (2-7) and a conclusions Chapter (8). Chapters 2-5 are focused on sea pen growth, and Chapters 6-7 on gorgonians. In Chapter 2 I present the study on growth rates and longevity of the sea pen *Halipteris finmarchica* in relation to environmental factors, and in comparison with published data of the Pacific species *H. willemoesi*. Trace elements analysis was performed in the axis of *H. finmarchica* and the results are discussed in light of growth ring formation periodicity.

In Chapter 3 I focus on size structure and growth rates of *Umbellula encrinus* from Baffin Bay through the examination of specimens and video data. I also included the aspect of fishing gear used and size of caught colonies in the context of the size structure study. Furthermore, ^{14}C and trace element analyses were performed, also as attempts to validate ring formation periodicity.

Chapter 4 is on growth rates and patterns in the sea pen *Pennatula grandis* Ehrenberg, 1834. In this study I determined growth rates, longevity, and growth patterns based on interpretations of certain morphological traits and their relationships (e.g. colony size vs. number of polyp leaves). I also examined the relationship between growth rates and environmental factors. Additionally, samples were analyzed for ^{14}C aiming to validate frequency of ring formation.

Chapter 5 is the study of the morphology and carbonate composition of the internal skeletons (axes) of the sea pens *Umbellula encrinus* and *Anthoptilum grandiflorum* (Verrill, 1879). I have analyzed cross sections of the axes along their lengths in terms of shape, diameter, weight, and carbonate proportion. For *U. encrinus* I also determined growth rates along the axis.

Species identification for *P. grandis* and *U. encrinus* were performed by the author, mostly by following available general and specific literature (detailed in the chapters). These identifications are considered tentative, as a revision of species in all studied genera is still necessary in order to confirm species identities (Dr. G. Williams, personal communication). In the case of *H. finmarchica* and *A. grandiflorum*, species identities were determined based on common local knowledge.

In Chapter 6 I present the results of a study on growth rates in the gorgonians *Primnoa pacifica* and *P. resedaeformis* using new data and published data in relation to environmental variables. I also examined the size structure and abundance of *P. pacifica* from the Strait of Georgia using remotely operated vehicle (ROV) video data obtained in 2011.

In Chapter 7 I report the existence of dense forests of the bamboo coral *Keratoisis* sp. “kerD2d” in Southeast Baffin Bay, as well as an estimate of growth rates based on growth ring counting. I have also used results of trace element analysis to calculate water palaeotemperatures using a published equation on the relationship between Mg/Ca ratios and temperature.

The last is a closing chapter that includes a summary of the other chapters’ results, main conclusions, and points to new questions on growth in octocorals. In this chapter I

also included a comparison between growth rates in octocorals using most of the published data available and my own data, yielding a database of over 550 observations (mostly individual coral growth rates). This comparison had the single objective of drawing a more comprehensive picture of growth rates between cold versus warm water environments and among taxa. This comparison places the growth rates of the six main taxa presented in this thesis: *H. finmarchica*, *U. encrinus*, *P. grandis*, *Primnoa pacifica* and *P. resedaeformis*, and *Keratoisis* sp. “kerD2d” into a broader ecological and taxonomic context.

1.7 References

- Althaus, F., A. Williams, T. A. Schlacher, R. J. Kloser, M. A. Green, B. A. Barker, N. J. Bax, P. Brodie & Schlacher-Hoenlinger M. A., 2009. Impacts of bottom trawling on deep-coral ecosystems of seamounts are long-lasting. *Marine Ecology Progress Series* 397: 279-294.
- Ambroso, S., C. Dominguez-Carrió, J. Grinyó, López-González Pablo J., J. Gili, A. Purroy, S. Requena & T. Madurell, 2013. In situ observations on withdrawal behaviour of the sea pen *Virgularia mirabilis*. *Marine Biodiversity* 43: 257-258.
- Andrews, A. H., R. P. Stone, C. C. Lundstrom & A. P. DeVogelaere, 2009. Growth rate and age determination of bamboo corals from the northeastern Pacific Ocean using refined ^{210}Pb dating. *Marine Ecology Progress Series* 397: 173-185.
- Andrews, A. H., G. M. Cailliet, L. A. Kerr, K. H. Coale, C. Lundstrom & A. P. DeVogelaere, 2005. Investigations of age and growth for three deep-sea corals from the Davidson Seamount off central California. In Freiwald, A. & J. M. Roberts (eds), *Cold-water corals and ecosystems*. Springer: 1021-1038.
- Andrews, A. H., E. E. Cordes, M. M. Mahoney, K. Munk, K. H. Coale, G. M. Cailliet & J. Heifetz, 2002. Age, growth and radiometric age validation of a deep-sea, habitat-forming gorgonian (*Primnoa resedaeformis*) from the Gulf of Alaska. *Hydrobiologia* 471: 101-110.
- Aranha, R., E. Edinger, G. Layne & G. Piercey, 2014. Growth rate variation and potential paleoceanographic proxies in *Primnoa pacifica*: Insights from high-resolution

trace element microanalysis. *Deep Sea Research Part II: Topical Studies in Oceanography* 99: 213-226.

Baillon, S., M. English, J. Hamel & A. Mercier, 2016. Comparative biometry and isotopy of three dominant pennatulacean corals in the Northwest Atlantic. *Acta Zoologica*: in press.

Barnes, D. K. A., K. E. Webb & K. Linse, 2007. Growth rate and its variability in erect Antarctic bryozoans. *Polar Biology* 30: 1069-1081.

Barnes, D., 1995. Seasonal and annual growth in erect species of Antarctic bryozoans. *Journal of Experimental Marine Biology and Ecology* 188: 181-198.

Bayer, F. M., 1981. Key to the genera of Octocorallia exclusive of Pennatulacea (Coelenterata: Anthozoa), with diagnoses of new taxa. *Proceedings of the Biological Society of Washington* 94: 902-947.

Bayer, F. M., 1973. Colonial organization in octocorals. In Boardman, R. S., A. H. Cheetham & W. A. Oliver (eds), *Animal colonies: Development and function through time*. Dowden, Hutchinson, and Ross, Stroudsburg, PA: 69-93.

Berg, S. E., 1941. Die Entwicklung und Koloniebildung bei *Funiculina quadrangularis* (Pallas). *Zoologiska bidrag fran Uppsala* 20: 1-100.

Birkeland, C., 1974. Interactions between a sea pen and seven of its predators. *Ecological Monographs* 44: 211-232.

Bramanti, L., G. Magagnini, L. D. Maio & G. Santangelo, 2005. Recruitment, early survival and growth of the Mediterranean red coral *Corallium rubrum* (L 1758), a 4-year study. *Journal of Experimental Marine Biology and Ecology* 314: 69-78.

Brazeau, D. A. & H. R. Lasker, 1992. Growth rates and growth strategy in a clonal marine invertebrate, the Caribbean octocoral *Briareum asbestinum*. The Biological Bulletin 183: 269-277.

Breedy, O., L. P. Van Ofwegen & S. Vargas, 2012. A new family of soft corals (Anthozoa, Octocorallia, Alcyonacea) from the aphotic tropical eastern Pacific waters revealed by integrative taxonomy. Systematics and Biodiversity 10: 351-359.

Brey, T., D. Gerdes, J. Gutt, A. Mackensen & A. Starms, 1999. Growth and age of the Antarctic bryozoan *Cellaria incula* on the Weddell Sea shelf. Antarctic Science 11: 408-414.

Brooke, S. & C. Young, 2009. In situ measurement of survival and growth of *Lophelia pertusa* in the northern Gulf of Mexico. Marine Ecology Progress Series 397: 153-161.

Bryan, T. L. & A. Metaxas, 2006. Distribution of deep-water corals along the North American continental margins: Relationships with environmental factors. Deep Sea Research Part I: Oceanographic Research Papers 53: 1865-1879.

Cadena, N. J. & J. A. Sánchez, 2010. Colony growth in the harvested octocoral *Pseudopterogorgia acerosa* in a Caribbean coral reef. Marine Ecology 31: 566-573.

Cairns, S. D., 2007. Deep-water corals: an overview with special reference to diversity and distribution of deep-water scleractinian corals. Bulletin of Marine Science 81: 311-322.

Campana, S. E., 1997. Use of radiocarbon from nuclear fallout as a dated marker in the otoliths of Haddock *Melanogrammus aeglefinus*. Marine Ecology Progress Series 150: 49-56.

Chia, F. S. & B. J. Crawford, 1973. Some observations on gametogenesis, larval development and substratum selection of the sea pen *Ptilosarcus guernei*. *Marine Biology* 23: 73-82.

Chia, F. & B. Crawford, 1977. Comparative fine structural studies of planulae and primary polyps of identical age of the sea pen, *Ptilosarcus guernei*. *Journal of Morphology* 151: 131-157.

Clark, G. R., 1974. Growth lines in invertebrate skeletons. *Annual Review of Earth and Planetary Sciences* 2: 77-99.

Cordes, E. E., J. W. Nybakken & G. VanDykhuisen, 2001. Reproduction and growth of *Anthomastus ritteri* (Octocorallia: Alcyonacea) from Monterey Bay, California, USA. *Marine Biology* 138: 491-501.

Dahm, C. & T. Brey, 1998. Determination of growth and age of slow growing brittle stars (Echinodermata Ophiuroidea) from natural growth bands. *Journal of the Marine Biological Association of the United Kingdom* 78: 941-951.

Daly, M., M. R. Brugler, P. Cartwright, A. G. Collins, M. N. Dawson, D. G. Fautin, S. C. France, C. S. McFadden, D. M. Opresko, S. Rodriguez, S. L. Romano & J. L. Stake, 2007. The phylum Cnidaria: A review of phylogenetic patterns and diversity 300 years after Linnaeus. *Zootaxa* 1668: 127-182.

Davis, D. S., A. Hebda & L. Pezzack, 2000. Early records of deep sea corals from submarine telegraph cables recovered off Nova Scotia. Poster, Museum of Natural History, Halifax, Canada.

Debreuil, J., S. Tambutté, D. Zoccola, N. Segonds, N. Techer, C. Marschal, D. Allemand, S. Kosuge & É Tambutté, 2011. Specific organic matrix characteristics in skeletons of *Corallium* species. *Marine Biology* 158: 2765-2774.

Doughty, C. L., A. M. Quattrini & E. E. Cordes, 2014. Insights into the population dynamics of the deep-sea coral genus *Paramuricea* in the Gulf of Mexico. *Deep Sea Research Part II: Topical Studies in Oceanography* 99: 71-82.

Ellis, J., 1753. A letter from Mr. John Ellis to Mr. Peter Collinson, FRS concerning a cluster-polype, found in the sea near the coast of Greenland. *Philosophical Transactions* 48: 305-308.

Fabricius, K. K. & P. P. Alderslade, 2001. Soft corals and sea fans: a comprehensive guide to the tropical shallow water genera of the central-west Pacific, the Indian Ocean and the Red Sea. Australian Institute of Marine Science (AIMS), Townsville.

Fabricius, K. E., A. Genin & Y. Benayahu, 1995. Flow-dependent herbivory and growth in zooxanthellae-free soft corals. *Limnology and Oceanography* 40: 1290-1301.

Farmer, J. R., L. F. Robinson & B. Hönisch, 2015. Growth rate determinations from radiocarbon in bamboo corals (genus *Keratoisis*). *Deep Sea Research Part I: Oceanographic Research Papers* 105: 26-40.

Franc, S., A. Huc & G. Chassagne, 1975. Calcite and collagen in the skeleton of the Cnidaria *Veretillum cynomorium* Pall. (Anthozoa. Pennatulidae): 65-69.

Franc, S., P. W. Ledger & R. Garrone, 1985. Structural variability of collagen fibers in the calcareous axial rod of a sea pen. *Journal of Morphology* 184: 75-84.

Gage, J. D. & P. A. Tyler, 1991. Deep-sea biology: a natural history of organisms at the deep-sea floor. Cambridge University Press, Cambridge England; New York, NY, USA.

Gage, J. D., 1990. Skeletal growth markers in the deep-sea brittle stars *Ophiura ljunghmani* and *Ophiomusium lymani*. Marine Biology 104: 427-435.

Gallmetzer, I., A. Haselmair & B. Velimirov, 2010. Slow growth and early sexual maturity: Bane and boon for the red coral *Corallium rubrum*. Estuarine, Coastal and Shelf Science 90: 1-10.

Garrabou, J., 1999. Life-history traits of *Alcyonium acaule* and *Parazoanthus axinellae* (Cnidaria, Anthozoa), with emphasis on growth. Marine Ecology Progress Series 178: 193-204.

Gass, S. E. & J. M. Roberts, 2006. The occurrence of the cold-water coral *Lophelia pertusa* (Scleractinia) on oil and gas platforms in the North Sea: Colony growth, recruitment and environmental controls on distribution. Marine Pollution Bulletin 52: 549-559.

Goffredo, S. & H. R. Lasker, 2006. Modular growth of a gorgonian coral can generate predictable patterns of colony growth. Journal of Experimental Marine Biology and Ecology 336: 221-229.

Goh, N. K. C. & L. M. Chou, 1995. Growth of five species of gorgonians (Subclass Octocorallia) in the sedimented waters of Singapore. Marine Ecology 16: 337-346.

Goldberg, W. M., 1991. Chemistry and structure of skeletal growth rings in the black coral *Antipathes fiordensis* (Cnidaria, Antipatharia). Hydrobiologia 216: 403-409.

Greathead, C., J. M. González-Irusta, J. Clarke, P. Boulcott, L. Blackadder, A. Weetman & P. J. Wright, 2014. Environmental requirements for three sea pen species: relevance to distribution and conservation. *ICES Journal of Marine Science: Journal du Conseil* 72: 576-586.

Grigg, R. W., 1974. Growth rings: annual periodicity in two gorgonian corals. *Ecology* 55: 876-881.

Hall–Spencer, J., V. Allain & J. H. Fosså, 2002. Trawling damage to Northeast Atlantic ancient coral reefs. *Proceedings of the Royal Society of London. Series B: Biological Sciences* 269: 507-511.

Helmle, K. P. & R. E. Dodge, 2011. Sclerochronology. In Hopley, D. (ed), *Encyclopedia of Modern Coral Reefs*. Springer Netherlands: 958-966.

Hickson, S. J., 1916. *The Pennatulacea of the Siboga Expedition: with a general survey of the order*. Late EJ Brill.

Hutchings, P., 1990. Review of the effects of trawling on macrobenthic epifaunal communities. *Marine and Freshwater Research* 41: 111-120.

Johnston, G., 1847. *A history of the British zoophytes*. John Van Voorst, London.

Jones, J. B., 1992. Environmental impact of trawling on the seabed: A review. *New Zealand Journal of Marine and Freshwater Research* 26: 59-67.

Jørgensen, L. L., B. Planque, T. H. Thangstad & G. Certain, 2015. Vulnerability of megabenthic species to trawling in the Barents Sea. *ICES Journal of Marine Science: Journal du Conseil* 73: i84-i97.

Kaufmann, K., 1981. Fitting and using growth curves. *Oecologia* 49: 293-299.

Kayal, E., B. Roure, H. Philippe, A. G. Collins & D. V. Lavrov, 2013. Cnidarian phylogenetic relationships as revealed by mitogenomics. *BMC Evolutionary Biology* 13: 1-18.

Khalesi, M. K., H. H. Beeftink & R. H. Wijffels, 2007. Flow-dependent growth in the zooxanthellate soft coral *Simularia flexibilis*. *Journal of Experimental Marine Biology and Ecology* 351: 106-113.

Kim, K. & H. R. Lasker, 1998. Allometry of resource capture in colonial cnidarians and constraints on modular growth. *Functional Ecology* 12: 646-654.

Kim, K. & H. R. Lasker, 1997. Flow-mediated resource competition in the suspension feeding gorgonian *Plexaura homomalla* (Esper). *Journal of Experimental Marine Biology and Ecology* 215: 49-64.

Langton, R., E. Langton, R. Theroux & J. Uzmann, 1990. Distribution, behavior and abundance of sea pens, *Pennatula aculeata*, in the Gulf of Maine. *Marine Biology* 107: 463-469.

Larcom, E. A., D. L. McKean, J. M. Brooks & C. R. Fisher, 2014. Growth rates, densities, and distribution of *Lophelia pertusa* on artificial structures in the Gulf of Mexico. *Deep Sea Research Part I: Oceanographic Research Papers* 85: 101-109.

Lasker, H., M. Boller, J. Castanaro & J. Sanchez, 2003. Determinate growth and modularity in a gorgonian octocoral. *Biological Bulletin* 205: 319-330.

Lazier, A. V., J. E. Smith, M. J. Risk & H. P. Schwarcz, 1999. The skeletal structure of *Desmophyllum cristagalli*: The use of deep-water corals in sclerochronology. *Lethaia* 32: 119-130.

Linares, C., R. Coma, S. Mariani, D. Díaz, B. Hereu & M. Zabala, 2008. Early life history of the Mediterranean gorgonian *Paramuricea clavata*: implications for population dynamics. *Invertebrate Biology* 127: 1-11.

López-González, P. & G. Williams, 2011. A new deep-sea pennatulacean (Anthozoa: Octocorallia: Chunellidae) from the Porcupine Abyssal Plain (NE Atlantic). *Helgoland Marine Research* 65: 309-318.

Love, M. S., M. M. Yoklavich, B. A. Black & A. H. Andrews, 2007. Age of black coral (*Antipathes dendrochristos*) colonies, with notes on associated invertebrate species. *Bulletin of Marine Science* 80: 391-399.

Luan, N. T., M. A. Rahman, T. Maki, N. Iwasaki & H. Hasegawa, 2013. Growth characteristics and growth rate estimation of Japanese precious corals. *Journal of Experimental Marine Biology and Ecology* 441: 117-125.

Malecha, P. W. & R. P. Stone, 2009. Response of the sea whip *Halipteris willemoesi* to simulated trawl disturbance and its vulnerability to subsequent predation. *Marine Ecology Progress Series* 388: 197-206.

Marschal, C., J. Garrabou, J. Harmelin & M. Pichon, 2004. A new method for measuring growth and age in the precious red coral *Corallium rubrum* (L.). *Coral Reefs* 23: 423-432.

Matsumoto, A., 2004. Heterogeneous and compensatory growth in *Melithaea flabellifera* (Octocorallia: Melithaeidae) in Japan. *Hydrobiologia* 530: 389-397.

Matsumoto, A. K., 2007. Effects of low water temperature on growth and magnesium carbonate concentrations in the cold-water gorgonian *Primnoa pacifica*. *Bulletin of Marine Science* 81: 423-435.

McFadden, C. S., 1991. A Comparative demographic analysis of clonal reproduction in a temperate soft coral. *Ecology* 72: 1849-1866.

McFadden, C. S. & L. P. Van Ofwegen, 2012. Stoloniferous octocorals (Anthozoa, Octocorallia) from South Africa, with descriptions of a new family of Alcyonacea, a new genus of Clavulariidae, and a new species of *Cornularia* (Cornulariidae). *Invertebrate Systematics* 26: 331-356.

McFadden, C. S. & L. Van Ofwegen P., 2013. Molecular phylogenetic evidence supports a new family of octocorals and a new genus of Alcyoniidae (Octocorallia, Alcyonacea). *ZooKeys*: 59-83.

Mercier, A. & J. Hamel, 2014. Lunar periods in the annual reproductive cycles of marine invertebrates from cold subtidal and deep-sea environments. In Numata, H. & B. Helm (eds), *Annual, Lunar, and Tidal Clocks*. Springer Japan: 99-120.

Mistri, M., 1995a. Population structure and secondary production of the Mediterranean octocoral *Lophogorgia ceratophyta* (L. 1758). *Marine Ecology* 16: 181-188.

Mistri, M., 1995b. Gross morphometric relationships and growth in the Mediterranean gorgonian *Paramuricea clavata*. *Bolletino Di Zoologia* 62: 5-8.

Mistri, M. & V. U. Ceccherelli, 1993. Growth of the Mediterranean gorgonian *Lophogorgia ceratophyta* (L., 1758). *Marine Ecology* 14: 329-340.

Mortensen, P. B. & L. Buhl-Mortensen, 2005. Morphology and growth of the deep-water gorgonians *Primnoa resedaeformis* and *Paragorgia arborea*. *Marine Biology* 147: 775-788.

Mosher, C. V. & L. Watling, 2009. Partners for life: a brittle star and its octocoral host. *Marine Ecology Progress Series* 397: 81-88.

Munari, C., G. Serafin & M. Mistri, 2013. Structure, growth and secondary production of two Tyrrhenian populations of the white gorgonian *Eunicella singularis* (Esper 1791). *Estuarine, Coastal and Shelf Science* 119: 162-166.

Musgrave, E. M., 1909. Experimental observations on the organs of circulation and powers of locomotion in pennatulids. *Quarterly Journal of Microscopical Science* 54: 443-482.

Noé, S. & W. -. Dullo, 2006. Skeletal morphogenesis and growth mode of modern and fossil deep-water isidid gorgonians (Octocorallia) in the West Pacific (New Zealand and Sea of Okhotsk). *Coral Reefs* 25: 303-320.

Noé, S., L. Lembke-Jene & W. -. Dullo, 2008. Varying growth rates in bamboo corals: sclerochronology and radiocarbon dating of a mid-Holocene deep-water gorgonian skeleton (*Keratoisis* sp.: Octocorallia) from Chatham Rise (New Zealand). *Facies* 54: 151-166.

Peck, L. S., 2016. A cold limit to adaptation in the sea. *Trends in Ecology & Evolution* 31: 13-26.

Peck, L. S. & S. Brockington, 2013. Growth of the Antarctic octocoral *Primnoella scotiae* and predation by the anemone *Dactylanthus antarcticus*. *Deep Sea Research Part II: Topical Studies in Oceanography* 92: 73-78.

Prouty, N. G., C. R. Fisher, A. W. Demopoulos & E. R. Druffel, 2014. Growth rates and ages of deep-sea corals impacted by the Deepwater Horizon oil spill. *Deep Sea Research Part II: Topical Studies in Oceanography*: in press.

Prouty, N. G., E. B. Roark, N. A. Buster & S. W. Ross, 2011. Growth rate and age distribution of deep-sea black corals in the Gulf of Mexico. *Marine Ecology Progress Series* 423: 101-115.

Rees, J. T., 1972. The effect of current on growth form in an octocoral. *Journal of Experimental Marine Biology and Ecology* 10: 115-123.

Risk, M. J., J. M. Heikoop, M. G. Snow & R. Beukens, 2002. Lifespans and growth patterns of two deep-sea corals: *Primnoa resedaeformis* and *Desmophyllum cristagalli*. *Hydrobiologia* 471: 125-131.

Roark, E. B., T. P. Guilderson, S. Flood-Page, R. B. Dunbar, B. L. Ingram, S. J. Fallon & M. McCulloch, 2005. Radiocarbon-based ages and growth rates of bamboo corals from the Gulf of Alaska. *Geophysical Research Letters* 32: L04606.

Roark, E. B., T. P. Guilderson, R. B. Dunbar, S. J. Fallon & D. A. Mucciarone, 2009. Extreme longevity in proteinaceous deep-sea corals. *Proceedings of the National Academy of Sciences* 106: 5204-5208.

Roberts, J. M., A. Wheeler, A. Freiwald & S. Cairns, 2009. Cold-water corals: the biology and geology of deep-sea coral habitats. Cambridge University Press, Cambridge, UK; New York.

Robinson, L. F., J. F. Adkins, N. Frank, A. C. Gagnon, N. G. Prouty, E. Brendan Roark & T. v. de Flierdt, 2014. The geochemistry of deep-sea coral skeletons: A review of vital effects and applications for palaeoceanography. *Deep Sea Research Part II: Topical Studies in Oceanography* 99: 184-198.

Rooper, C. N., M. E. Wilkins, C. S. Rose & C. Coon, 2011. Modeling the impacts of bottom trawling and the subsequent recovery rates of sponges and corals in the Aleutian Islands, Alaska. *Continental Shelf Research* 31: 1827-1834.

Rossi, S., J. Gili & X. Garrofé, 2011. Net negative growth detected in a population of *Leptogorgia sarmentosa*: quantifying the biomass loss in a benthic soft bottom-gravel gorgonian. *Marine Biology* 158: 1631-1643.

Sánchez, J. A., H. R. Lasker, E. G. Nepomuceno, J. D. Sánchez & M. J. Woldenberg, 2004. Branching and self-organization in marine modular colonial organisms: a model. *The American Naturalist* 163: E24-E39.

Sartoretto, S. & P. Francour, 2012. Bathymetric distribution and growth rates of *Eunicella verrucosa* (Cnidaria: Gorgoniidae) populations along the Marseilles coast (France). *Scientia Marina* 76: 349-355.

Sebens, K. P., 1983. The larval and juvenile ecology of the temperate octocoral *Acyonium siderium* Verrill. II. Fecundity, survival, and juvenile growth. *Journal of Experimental Marine Biology and Ecology* 72: 263-285.

Sherwood, O. A. & E. N. Edinger, 2009. Ages and growth rates of some deep-sea gorgonian and antipatharian corals of Newfoundland and Labrador. *Canadian Journal of Fisheries and Aquatic Sciences* 66: 142-152.

Sherwood, O. A., E. N. Edinger, T. P. Guilderson, B. Ghaleb, M. J. Risk & D. B. Scott, 2008. Late Holocene radiocarbon variability in Northwest Atlantic slope waters. *Earth and Planetary Science Letters* 275: 146-153.

Sherwood, O. A., D. B. Scott, M. J. Risk & T. P. Guilderson, 2005. Radiocarbon evidence for annual growth rings in the deep-sea octocoral *Primnoa resedaeformis*. Marine Ecology Progress Series 301: 129-134.

Soong, K., 2005. Reproduction and colony integration of the sea pen *Virgularia juncea*. Marine Biology 146: 1103-1109.

Sorauf, J. & J. Jell, 1977. Structure and incremental growth in the ahermatypic coral *Desmophyllum cristagalli* from the North Atlantic. Palaeontology 20: 1-19.

Squires, D. F., 1960. Scleractinian corals from the Norfolk Island cable. Records of the Auckland Institute and Museum 5: 195-201.

Sun, Z., J. Hamel & A. Mercier, 2011. Planulation, larval biology, and early growth of the deep-sea soft corals *Gersemia fruticosa* and *Duva florida* (Octocorallia: Alcyonacea). Invertebrate Biology 130: 91-99.

Sun, Z., J. Hamel & A. Mercier, 2010. Planulation periodicity, settlement preferences and growth of two deep-sea octocorals from the northwest Atlantic. Marine Ecology Progress Series 410: 71-87.

Szmant-Froelich, A., 1974. Structure, iodination and growth of the axial skeletons of *Muricea californica* and *M. fruticosa* (Coelenterata: Gorgonacea). Marine Biology 27: 299-306.

Taylor, R. E. & O. Bar-Yosef, 2014. Radiocarbon dating: an archaeological perspective. Left Coast Press, Albuquerque.

Thresher, R. E., 2009. Environmental and compositional correlates of growth rate in deep-water bamboo corals (Gorgonacea; Isididae). Marine Ecology Progress Series 397: 187-196.

Thrush, S. F. & P. K. Dayton, 2002. Disturbance to marine benthic habitats by trawling and dredging: implications for marine biodiversity. *Annual Review of Ecology and Systematics* 33: 449-473.

Tracey, D. M., H. Neil, P. Marriott, A. H. Andrews, G. M. Cailliet & J. A. Sánchez, 2007. Age and growth of two genera of deep-sea bamboo corals (family Isididae) in New Zealand waters. *Bulletin of Marine Science* 81: 393-408.

Troffe, P. M., C. D. Levings, G. E. Piercey & V. Keong, 2005. Fishing gear effects and ecology of the sea whip *Halipteris willemoesi* (Cnidaria: Octocorallia: Pennatulacea) in British Columbia, Canada: preliminary observations. *Aquatic Conservation: Marine and Freshwater Ecosystems* 15: 523-533.

Tunncliffe, V. & J. P. M. Syvitski, 1983. Corals move boulders: an unusual mechanism of sediment transport. *Limnology and Oceanography* 28: 564-568.

Van Ofwegen, L. P. v. & C. S. McFadden, 2009. A new family of octocorals (Anthozoa: Octocorallia) from Cameroon waters. *Journal of Natural History* 44: 23-29.

Von Bertalanffy, L., 1938. A quantitative theory of organic growth (inquiries on growth laws. II). *Human Biology* 10: 181-213.

Wainwright, S. A. & J. R. Dillon, 1969. On the orientation of sea fans (genus *Gorgonia*). *The Biological Bulletin* 136: 130-139.

Wareham, V. E. & E. N. Edinger, 2007. Distribution of deep-sea corals in the Newfoundland and Labrador region, Northwest Atlantic Ocean. *Bulletin of Marine Science* 81: 289-313.

Wassenberg, T. J., G. Dews & S. D. Cook, 2002. The impact of fish trawls on megabenthos (sponges) on the north-west shelf of Australia. *Fisheries Research* 58: 141-151.

Watanabe, S., A. Metaxas, J. Sameoto & P. Lawton, 2009. Patterns in abundance and size of two deep-water gorgonian octocorals, in relation to depth and substrate features off Nova Scotia. *Deep Sea Research Part I: Oceanographic Research Papers* 56: 2235-2248.

Watling, L., S. C. France, E. Pante & A. Simpson, 2011. Chapter Two - Biology of Deep-Water Octocorals. In Michael Lesser (ed), *Advances in Marine Biology*. Academic Press: 41.

White, H. K., P. Y. Hsing, W. Cho, T. M. Shank, E. E. Cordes, A. M. Quattrini, R. K. Nelson, R. Camilli, A. W. Demopoulos, C. R. German, J. M. Brooks, H. H. Roberts, W. Shedd, C. M. Reddy & C. R. Fisher, 2012. Impact of the Deepwater Horizon oil spill on a deep-water coral community in the Gulf of Mexico. *Proceedings of the National Academy of Sciences of the United States of America* 109: 20303-20308.

Willemoes-Suhm, R., 1875. Notes on some young stages of Umbellularia, and on its geographical distribution. *Journal of Natural History* 15: 312-315.

Williams, G. C., 1995. Living genera of sea pens (Coelenterata: Octocorallia: Pennatulacea): illustrated key and synopses. *Zoological Journal of the Linnean Society* 113: 93-140.

Williams, G. C., 2011. The global diversity of sea pens (Cnidaria: Octocorallia: Pennatulacea). *PLoS ONE* 6: 1-11.

Williams, B. & A. G. Grottoli, 2008. Attempts to culture and monitor growth rates in deep-water antipatharians and gorgonians. In Sulak, K. J., M. T. Randall, K. E. Luke, A. D. Norem & J. M. Miller (eds), *Characterization of Northern Gulf of Mexico Deepwater Hard Bottom Communities with Emphasis on *Lophelia* Coral - *Lophelia* Reef Megafaunal Community Structure, Biotopes, Genetics, Microbial Ecology, and Geology*. USGS Open-File Report 2008-1148; OCS Study MMS 2008-015, 15 April 2008, 8 Chapters, pp., 8 Master Appendices (incl. Interactive Dive Track DVD): Master Appendix F.

Williams, G. C. & P. Alderslade, 2011. Three new species of pennatulacean octocorals with the ability to attach to rocky substrata (Cnidaria: Anthozoa: Pennatulacea). *Zootaxa*: 33-48.

Williams, G. C., B. W. Hoeksema & L. P. Van Ofwegen, 2012. A fifth morphological polyp in Pennatulacean octocorals, with a review of polyp polymorphism in the genera *Pennatula* and *Pteroeides* (Anthozoa: Pennatulidae). *Zoological Studies* 51: 1006-1017.

Wilson, M. T., A. H. Andrews, A. L. Brown & E. E. Cordes, 2002. Axial rod growth and age estimation of the sea pen *Halipteris willemoesi* Kölliker. *Hydrobiologia* 471: 133-142.

Wyeth, R. C. & A. O. D. Willows, 2006. Field behavior of the nudibranch mollusc *Tritonia diomedea*. *The Biological Bulletin* 210: 81-96.

Yesson, C., M. L. Taylor, D. P. Tittensor, A. J. Davies, J. Guinotte, A. Baco, J. Black, J. M. Hall-Spencer & A. D. Rogers, 2012. Global habitat suitability of cold-water octocorals. *Journal of Biogeography* 39: 1278-1292.

Yoshioka, P. M. & B. B. Yoshioka, 1991. A comparison of the survivorship and growth of shallow-water gorgonian species of Puerto Rico. *Marine Ecology Progress Series* 69: 253-260.

2. Decadal longevity and slow growth rates in the deep-water sea pen *Halipteris finmarchica* (Sars, 1851) (Octocorallia: Pennatulacea): Implications for vulnerability and recovery from anthropogenic disturbance¹

Abstract

Growth rates and longevity are key factors in assessing the vulnerability of many invertebrates to anthropogenic disturbance. Sea pens are benthic invertebrates frequently entrained as fisheries bycatch, but whose growth (recovery) rates are poorly known. Here, longevity and growth rates were estimated for the deep-water sea pen *Halipteris finmarchica* from the Northwest Atlantic and compared to those published for *Halipteris willemoesi* from the Bering Sea. Axes were cross-sectioned to visualize growth rings and estimate longevity and growth rates. Chronology of growth rings was examined with trace element microanalysis of Sr/Ca, Mg/Ca, Ba/Ca and Na/Ca in the axis using Secondary Ion Mass Spectrometry. The relationship between growth rates and environmental variables was investigated. The number of rings ranged 13-22 among 26 colonies. Trace element microanalysis yielded a number of elemental ratio peaks comparable to the number of rings visually determined. Diametric growth rates were

¹ Neves, B.M., Edinger, E., Layne, G., Wareham, V. (2015) Decadal longevity and slow growth rates in the deep-water sea pen *Halipteris finmarchica* (Sars, 1851) (Octocorallia: Pennatulacea): Implications for vulnerability and recovery from anthropogenic disturbance. *Hydrobiologia*. 759(1):147-170.

significantly smaller than those published for *H. willemoesi*, while linear growth rates (extension in height) were not different. No significant relationships were detected between growth rates and environmental variables for *H. finmarchica*. Our data suggest that *H. finmarchica* is a slow-growing, relatively long-lived organism whose recovery from damage can take over 20 years.

2.1 Introduction

Concerns regarding the vulnerability, conservation and management of deep-sea corals have been raised in recent years (Roberts & Hirshfield, 2004). Deep-sea corals comprise a variety of higher taxa of cnidarians, many of which have been recognized as slow-growing, with high longevities commonly recorded in their skeletons as growth bands/rings (Roberts et al., 2009). While growth rates and longevity in several species of deep-sea scleractinians and gorgonians have been estimated (Risk et al., 2002, Roark et al., 2005, Gass & Roberts, 2006, Brooke & Young, 2009, Sherwood & Edinger, 2009), almost nothing is known about growth rates and longevity in sea pens (order Pennatulacea).

Sea pens are colonial octocorals of worldwide distribution, usually found inhabiting soft sediments. They are composed of a proximal peduncle used for anchorage in the soft substrate, and of a distal rachis where autozooids are found. Most genera possess an internal skeleton (i.e. axis) that gives support to the colony (Williams, 1995). The axis in sea pens is usually made of a combination of carbonate and organic material (Franc et al., 1975, 1985, Wilson et al., 2002, Chapters 2-5).

The presence of growth rings in the axis of some sea pens suggests that age and growth rates in these animals can be estimated from these structures. Considering that deep-water sea pens constitute important habitat for other species (Brodeur, 2001, Baillon et al., 2012), and that they are vulnerable to anthropogenic activities (e.g. commercial fisheries) (Troffe et al., 2005, Malecha & Stone, 2009), knowledge of their growth rates and age are important to the management and conservation of these organisms.

Halipteris finmarchica (Sars, 1851) is one of the most conspicuous species of pennatulaceans in the Northwest (NW) Atlantic (Wareham & Edinger, 2007, Murillo et al., 2011, Baker et al., 2012), where it has been recorded at depths up to 2000 m (Baker et al., 2012). As other species in the genus, *H. finmarchica* has an elongated and slender, whip-like shape (Williams, 1995). It can reach heights of >100 cm and colonies reach sexual maturity at around 18 cm (Baillon et al., 2014). Like several other sea pens, *H. finmarchica* possesses an internal axis (Williams, 1995) that in cross section reveals the presence of alternating dark and light growth bands (this study). However, band periodicity in this sea pen has not yet been determined.

Wilson et al. (2002) estimated growth rates and age in *Halipteris willemoesi* Kölliker, 1870, a co-generic species from Pacific waters. Ages of up to 48 years (i.e. 48 rings) were estimated in this species (Wilson et al., 2002), and colonies might be even older considering that they can reach heights over 2 m (Brodeur, 2001). Validation of ring formation periodicity could not be achieved for *H. willemoesi* (see Wilson et al., 2002), but there is indication that, as in other corals, growth rings in sea pens do have an annual periodicity. Formation of growth rings in young colonies of the shallow water sea pen *Ptilosarcus gurneyi* (Gray, 1860) is known to be annual, with dark bands believed to be formed during summer, and light bands during winter time (Birkeland, 1974).

The radiometric ageing techniques most commonly used to validate ring periodicity in other types of corals are difficult to apply in sea pens for several reasons. First, the axes of sea pens usually have very small diameters (e.g. 1-6 mm; Wilson et al., 2002, this study), limiting the use of ^{210}Pb , which requires larger sample sizes (Roberts et al., 2009). Secondly, the longevities of sea pens determined so far suggest they might not

reach great ages (Birkeland, 1974, Wilson et al., 2002), limiting the use of bomb-radiocarbon (bomb- ^{14}C) dating, which is more suitable for organisms that were alive during the onset and peak of bomb- ^{14}C , between the late 1950s and early 1970s (e.g. Campana, 1997, Sherwood et al., 2005); and U/Th dating works best for aragonitic carbonates at least 1000 years old (Jull, 2006). Finally, some sea pens are known to have collagen as part of their axes (e.g. Ledger & Franc, 1978, Franc et al., 1985, Wilson et al., 2002), which restricts the use of the amino-acid racemization dating technique (see Collins et al., 1999). Furthermore, the logistical challenges associated with *in situ* studies of deep-sea organisms constrains the use of marking/tagging techniques (Brooke & Young, 2009).

Parallel to the aforementioned techniques, elemental ratios of Metal/Calcium (Me/Ca) in coral skeletons have been widely used as proxies for environmental changes (Rosenberg, 1980), and to a smaller extent to determine growth rates and longevity (Weinbauer et al., 2000, Roark et al., 2005). For example, cycles in the ratio Strontium/Calcium (Sr/Ca) in the carbonate section of some corals has been interpreted as an indicator of growth rates (Weinbauer et al., 2000, Roark et al., 2005).

In addition to the lack of information on growth rates and longevity, not much is known about environmental growth control in cold-water corals - although depth, temperature and food input are generally recognized as important factors influencing growth (Roberts et al., 2009). Temperature, surface primary productivity, salinity and calcite saturation seem to be some of the most influential environmental factors in determining the distribution of cold-water sea pens (Yesson et al., 2012).

Here we used Secondary Ion Mass Spectrometry (SIMS) to investigate patterns in the distribution of trace elements (Mg/Ca, Sr/Ca, Ba/Ca, and Na/Ca) across the axis of *H. finmarchica* from the NW Atlantic, and estimate longevity and growth rates. Our specific objectives were: (1) to investigate the existence of cyclicity in the distribution of trace elements in the axis of *H. finmarchica*; (2) to estimate longevity and growth rates in *H. finmarchica* and to compare them with those published for *H. willemoesi* from the Bering Sea (from Wilson et al., 2002); and (3) to investigate relationships between growth rates, age and environmental variables (i.e. temperature, depth, latitude, chlorophyll a, particulate organic carbon, and particulate inorganic carbon) in *H. finmarchica*.

2.2 Materials and Methods

2.2.1 Study area and sampling

Colonies of *H. finmarchica* were obtained during multispecies trawl surveys conducted by Fisheries and Oceans Canada (DFO) in the NW Atlantic using a Campellen 1800 shrimp trawl for ~ 15 minutes at a speed of 3 knots, with a 55m door sweep area. The surveys occurred from 2004-2011 at depths ranging 347-1210 m (Fig. 2-1). Samples have been kept frozen at -20 °C since collection. A total of 26 colonies were included in this study (Table 2-1).

2.2.2 Ring counting and growth rate estimation

Colonies were measured and photographed before axis extraction for transverse sectioning (57.5-129.5 cm). The axes were extracted from the tissue and sectioned at a

distance ranging from 5-10% of colony height, where axis diameter is the widest (as observed in *H. willemoesi*; Wilson et al., 2002). These sections were embedded in epoxy (Epofix™) for a second sectioning using a Buehler ISOMET low speed saw, in order to obtain better quality cross sections. The cross sections were polished using BUEHLER silicon carbide grinding paper (grit 600/P 1200) and/or a Struers TegraPol 31 lapping wheel, then visualized and photographed on stereomicroscope under ultraviolet (UV) light, which greatly improves the visualization of growth rings. To further improve ring visualization, the photos color levels were adjusted using the image software GIMP 2.8.8.

The photos were analyzed using the image software imageJ (Schneider et al., 2012) and both the diameter and number of rings were determined. Rings were assumed to represent years, and were counted at three non-consecutive times, with the average value being considered the definitive number of rings for each colony. Diametric and linear growth rates were estimated as axis diameter and colony height, respectively, divided by the number of rings (i.e. years). Growth rates were compared to those published for *H. willemoesi* from Northeast Pacific waters (Wilson et al., 2002), and our calculated (observed) age in *H. finmarchica* was compared to the age predicted from the regression equation produced by these authors, where age in years can be estimated as a function of axis diameter:

$$(1) \text{ Estimated age (years)} = 7X (\text{maximum axis diameter}) - 0.2$$

This estimated (expected) age based on axis diameter is abbreviated as Exp1. We also used the knowledge of size at maturity in *H. finmarchica* (i.e. 18 cm; Baillon et al.,

2014) and our estimation of linear growth rates to determine the age at maturity for the species.

Then diametric growth rates for the years up to maturity (N) were estimated by measuring the axis diameter of the first N rings, divided by N. Furthermore, we used age and size at maturity to estimate the number of rings expected for a colony based in its height (Exp2). For instance, a colony 18 cm in height is estimated to be N years old, thus assuming a directly proportional relationship colony age can be estimated based on colony height.

Linear growth rates in Pacific *H. willemoesi* showed a trend of medium sized colonies growing faster than small and large colonies (cf. Wilson et al., 2002). Therefore, we also plotted linear and diametric growth rates in relation to colony height to investigate growth patterns in *H. finmarchica*.

Table 2-1. Sampling information, colony measurements, age, and growth rates for *Halipteris finmarchica* from the Northwest Atlantic.

Sample	Year	Sampling and colony information					Number of rings			Growth rates		
		Latitude	Longitude	Depth	Height	Diameter	Obs \pm SD	Exp1	Exp2	Dgrowth	Lgrowth	Dgrowth4 th
007	2004	56.4	-57.817	509	27.5 ^b	1.61	15 \pm 0.82	11.07	n/a	0.107	n/a	0.105
009	2005	42.95	-49.595	1210	75 ^b	3.10	22 \pm 1.25	21.5	n/a	0.143	n/a	0.080
010	2006	43.98	-52.967	878	99	3.10	21 \pm 1.25	21.5	20	0.145	4.641	0.115
012	2006	44.22	-53.000	814	82 ^b	3.04	21 \pm 2.62	21.08	n/a	0.147	n/a	0.117
013	2005	44.07	-52.917	1028	68	3.36	22 \pm 0.94	23.32	14	0.150	3.045	0.129
014	2005	42.97	-49.582	950	65	1.56 ^d	13 \pm 0.47	10.72	13	0.117	4.875	0.099
015	2004	43.92	-52.615	518	74.31	2.14	16 \pm 0.47	14.78	15	0.131	4.550	0.120
016	2004	44.10	-52.918	440	72	2.56	18 \pm 1.25	17.72	15	0.140	3.927	0.112
024	2005	43.70	-52.333	622	44.5 ^b	2.26	19 \pm 0.82	15.62	n/a	0.119	n/a	0.132
031A	2010	43.09	-51.368	598	95.5	2.13	17 \pm 0.00	14.71	20	0.125	5.618	0.137
031B	2010	43.09	-51.368	598	57.5	2.07	16 \pm 0.94	14.29	12	0.127	3.520	0.095
031C	2010	43.09	-51.368	598	68	1.72	15 \pm 0.47	11.84	14	0.112	4.435	0.082
032A	2010	45.53	-56.664	347	80.5 ^b	2.38	20 \pm 0.94	16.46	n/a	0.121	n/a	0.081
032B	2010	45.53	-56.664	347	78.3 ^b	2.37	18 \pm 1.25	16.39	n/a	0.134	n/a	0.120
032C	2010	45.53	-56.664	347	116	2.45	16 \pm 1.25	16.95	24	0.150	7.102	0.132
033	2011	43.43	-51.914	618	72.1 ^b	2.65	20 \pm 0.47	18.35	n/a	0.135	n/a	0.107
034A	2005	43.60	-52.220	785	129.5	2.99	21 \pm 0.47	20.73	27	0.145	6.266	0.117
034B	2005	43.60	-52.220	785	80.7 ^b	2.14	18 \pm 1.63	14.78	n/a	0.119	n/a	0.083
035A	2007	43.33	-51.779	761	92	2.62	19 \pm 0.47	18.14	19	0.136	4.759	0.107
035B	2007	43.33	-51.779	761	86.5 ^b	2.89	21 \pm 0.94	20.03	n/a	0.147	n/a	0.103
035C	2007	43.33	-51.779	761	77	2.07	18 \pm 0.47	14.29	16	0.117	4.358	0.098
036A	2005	43.31	-51.728	798	95.65	2.55	20 \pm 1.25	17.23	20	0.122	4.704	0.123
036B	2005	43.31	-51.728	798	111.7	2.64	17 \pm 0.47	18.28	23	0.152	6.444	0.130
036C	2005	43.31	-51.728	798	75	2.30	20 \pm 0.82	16.25	15	0.118	3.750	0.093
036D	2005	43.31	-51.728	798	100	2.64	19 \pm 0.94	18.28	21	0.141	5.357	0.144
038	2006	47.39	-46.383	756	86.03	2.22	17 \pm 0.82	15.34	18	0.131	5.061	0.105

The units are as follow: latitude and longitude (decimal degrees), depth (m), height (cm), axis diameter (mm). Obs is mean observed number of rings (\pm SD), Exp1 is the expected number of rings based on axis diameter calculated using the regression equation by Wilson et al. (2002) for *Halipteris willemoesi*, Exp2 is the expected number of rings based on colony height, Dgrowth is diametric growth rates ($\text{mm}\cdot\text{yr}^{-1}$), Lgrowth is linear growth rates ($\text{cm}\cdot\text{yr}^{-1}$), and Dgrowth^{4th} is diametric growth rates for the first four years of life. ^bColonies incomplete in height, ^cdoes not represent maximum diameter size, n/a: not available. Table on previous page.

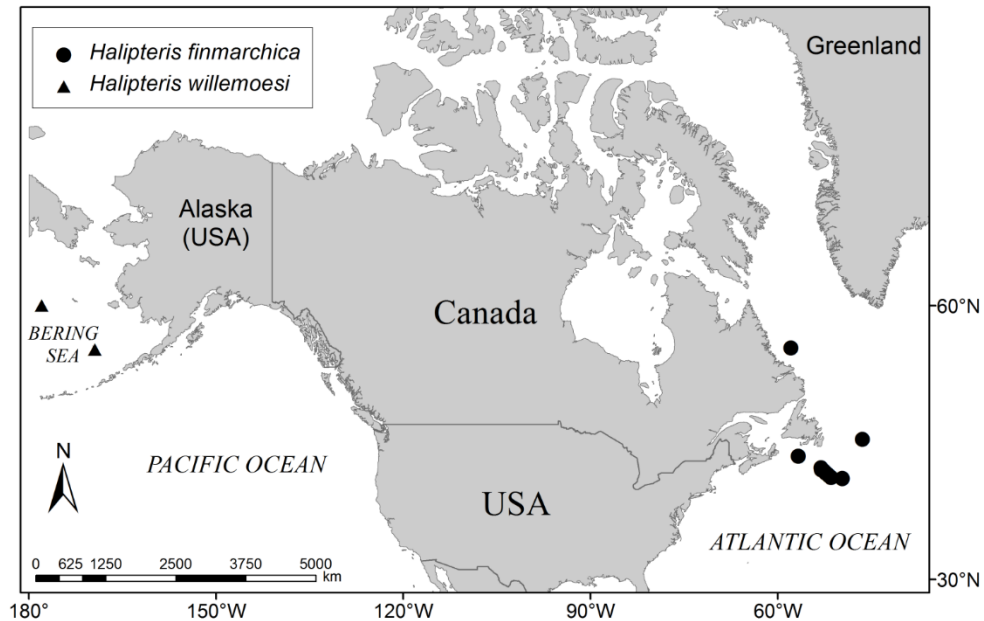


Figure 2-1. Map showing the locations included in this study. Circles are the locations of *Halipteris finmarchica* samples from the Northwest Atlantic, and triangles are locations of *H. willemoesi* from the Bering Sea (from Wilson et al., 2002).

2.2.3 Environmental data

Relationships between environmental variables (i.e. depth, latitude, temperature, chlorophyll a, surface particulate organic carbon, and surface particulate inorganic carbon) and growth rates and age in *H. finmarchica* were investigated. Latitude, longitude and depth were obtained during the surveys and they represent the average of a survey set. Bottom temperature for the locations of *H. finmarchica* was retrieved from the World Ocean Database 2009 (Boyer et al., 2009), using the available data on similar depths and areas surrounding the sampled localities (Table 2-1), and viewed in Ocean Data View 4.6.0 (Schlitzer, 2014). For *H. willemoesi* we used the local temperature published by

Wilson et al. (2002). Data on particulate organic carbon (POC), particulate inorganic carbon (PIC) and chlorophyll a (a proxy for phytoplankton biomass) were downloaded from <http://oceancolor.gsfc.nasa.gov/> and extracted in ArcGIS 10.0 using Marine Ecology Geospatial Tools (Roberts et al., 2010). Annual POC and PIC for the period of 2002-2013 were obtained from the Aqua Moderate Resolution Imaging Spectroradiometer Sensor (MODIS) L3 product database. Annual chlorophyll a concentration for the period of 1998–2010 was obtained from the Sea-viewing Wide Field-of-view Sensor (SeaWiFS) L3 product database. The years of 2008-2009 were excluded from the chlorophyll a analysis since little or no data were available for certain months of these years. Therefore, average annual chlorophyll a concentration for the period of 1998-2010 (excluding 2008-2009) were used to characterize the local surface phytoplankton biomass for each location from where colonies of *H. finmarchica* have been collected, as well as for the locations of *H. willemoesi*. The spatial resolution of chlorophyll a, POC, and PIC was 9 km (cell size of 1/12 geographic degree).

2.2.4 Axis composition

In order to determine the carbonate structure and composition of the axis in *H. finmarchica*, an X-ray diffraction (XRD) analysis was performed at the Earth Resources Research and Analysis (TERRA) facility, Memorial University of Newfoundland using a Rigaku Ultima-IV with a Cu source used in Bragg-Brentano configuration. One axis was crushed into a powder using a ceramic mortar and pestle, and a total of 1 g of sample was used for the analysis.

2.2.5 Trace element analysis

A high spatial resolution analysis of Mg/Ca, Sr/Ca, Ba/Ca and Na/Ca was performed across the axis of three colonies of *H. finmarchica* (009, 034A, 035B) using a Cameca IMS 4f Secondary Ion Mass Spectrometer (SIMS) (CREAIT, Memorial University of Newfoundland). Trace element analysis of colonies 034A and 035B was performed in different cross sections from those used to estimate age and growth rates. Therefore, in the sections used for the trace element analysis age was also estimated but does not correspond to the age estimated for the section of widest diameter. The cross sections mounted in epoxy were gold coated (300Å) prior to SIMS analysis. Transects started from the core in the direction of the outermost region of the cross section. Transect lengths varied with the radius length, ranging from 1.75-1.98 mm. The individual spots were spaced 25 µm apart.

Prior to each analysis the spot was pre-sputtered for 120 s in order to eliminate contamination from the gold coat and to penetrate the shallowly damaged surface of the polished sample. The samples were bombarded with primary $^{16}\text{O}^-$ ions accelerated through a 10.0 kV nominal potential. A primary ion current of 3.0-8.0 nA was critically focused on the sample over a spot diameter of 20-25 µm. The secondary ions were accelerated into the mass spectrometer through a 4500 V nominal potential and energy filtered to suppress isobaric interferences using a sample offset voltage of -80 V and energy window of 60eV.

Each analysis involved 15 cycles of peak counting on $^{23}\text{Na}^+$ (2s), $^{24}\text{Mg}^+$ (6 s), $^{42}\text{Ca}^+$ (1s), $^{88}\text{Sr}^+$ (4s), $^{138}\text{Ba}^+$ (10s). Background position (22.69 Da; 1s) was also counted to monitor detection noise. The reference standard used was a calcite from the Oka

Carbonatite Complex, Québec (OKA-C). A calcite from Franklin (NJ – USA) was used as a secondary standard. Standards were used to convert measured Metal/Ca count ratios to mmol/mol quantities.

Internal precisions for individual spot analyses are shown as error bars in figure 3.12. Reproducibility (1σ) of elemental ratio determinations between analytical sessions, based on replicate analyses of the OKA-C standard during each session, were better than 0.50% for Na, 0.50% for Mg, 0.25% for Sr and 0.40% for Ba.

2.2.6 Data analysis

Data analysis was performed using General Linear Models (GLM) to investigate relationships between (1) colony height, axis diameter, and age, (2) growth rates between the two species of *Halipterus* and (3) growth rates and age in relation to environmental variables. Ten colonies were excluded from the analysis on colony size because they were clearly incomplete in height, with both axis and tissue tips missing (Table 2-1). Another sample (014) was excluded from the analyses using age and diameter because the axis was not primarily sectioned at the region of maximum diameter and later became unavailable.

Assumptions of linearity, homogeneity, normality and independence of residuals were evaluated by producing residual diagnostic plots for linear models (Kabacoff, 2011). If diagnostics of normality were not clearly satisfactory we performed permutation (randomization) tests using the lmPerm package of RStudio version 0.97.551 (Team, 2008), with addition of a perm=Prob parameter, which samples from all possible

permutations (Kabacoff, 2011). Permutation tests can be used where the data is sampled from unknown distributions and where sample sizes are small (Kabacoff, 2011).

Spearman's correlation was performed to test for relationships between colony height and axis diameter. For the analysis on colony age in relation to colony height we performed a simple linear regression as well as a regression through the origin with the objective of including age at first maturity, which was not present in our dataset since all analyzed colonies were > 18 cm. A Wilcoxon-Signed-Rank test, a non-parametric version of a paired t-test (Quinn & Keough, 2002), was performed to test the hypothesis that observed and predicted ages (based on axis diameter and colony height) for *H. finmarchica* are not significantly different. A paired t-test was used to test for differences in diametric growth rates for the whole colony versus growth rates before reaching maturity.

A Kruskal-Wallis test was performed to test for differences in the trace element ratios among colonies (variances were heteroscedastic) and a Mann-Whitney U test was used to determine which samples differ from each other. Significance level for all analyzes was set at 0.05. The error was estimated using standard deviation (SD).

2.3 Results

2.3.1 Axis composition

The X-ray diffraction analysis showed that the carbonate fraction of the axis in *H. finmarchica* is composed of magnesian calcite (Ca, Mg) CO₃ (Appendix 2-1).

2.3.2 Growth rates and age

The axis of *H. finmarchica* is generally round, and growth rings are readily visible in cross section (Fig. 2-2C). In the analyzed specimens, rings were seen as dark and light couplets. In some cross sections intermediate rings were seen between wide rings, and they might be formed on smaller temporal scales than the wide rings (e.g. sub annual). Rings are more easily distinguishable when seen under UV light, particularly because the UV light significantly increases the visibility of white materials, including calcite. In some colonies the axis is somewhat squared at the thickest part of the axis, becoming round towards the tip. The average number of growth rings ranged from 13-22, with diametric growth rates averaging $0.13 \text{ mm}\cdot\text{yr}^{-1} \pm 0.01 \text{ SD}$, and linear growth rates averaging $4.9 \text{ cm}\cdot\text{yr}^{-1} \pm 1.03 \text{ SD}$ (Table 2-1).

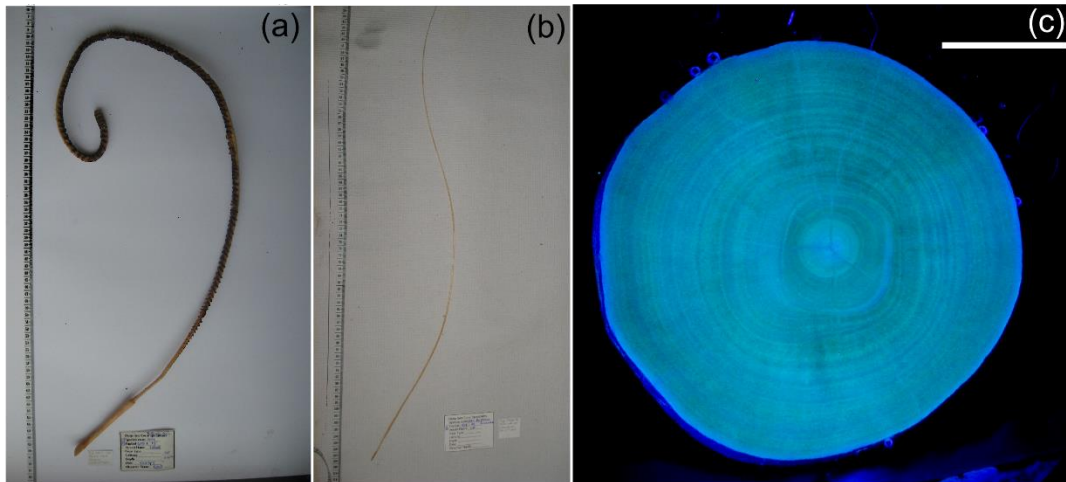


Figure 2-2. *Halipteris finmarchica* showing: whole colony (A), whole axis only (B), cross section under ultraviolet (UV) light (C). Scale bar = 1 mm.

Considering our estimated linear growth rates of $4.9 \text{ cm}\cdot\text{yr}^{-1}$, a colony of *H. finmarchica* would take *ca.* 4 years to reach sexual maturity (at 18 cm; cf. Baillon et al. 2014). Based on this information, diametric growth rates for the first four years of life were also estimated, yielding an average rate of $0.11 \text{ mm}\cdot\text{yr}^{-1} \pm 0.02 \text{ SD}$ for this period of life (Table 2-1), which is significantly slower than diametric growth rates for the whole colony life span ($t=6.49$, $df=1, 25$, $p<0.05$).

Diametric growth rates in Pacific *H. willemoesi* were significantly greater than those in *H. finmarchica* ($F=7.84$; $df=1, 35$, $p<0.05$; Fig. 2-3A), but linear growth rates were statistically indistinguishable ($F=0.46$; $df=1, 26$, $p=0.5$; Fig. 2-3B). Furthermore, the observed ages for colonies of *H. finmarchica* were significantly different from the ages predicted when using the regression equation generated for *H. willemoesi* (cf. Wilson et al., 2002) ($Z=3.43$, $df=1, 24$, $p<0.05$; Fig. 2-4), although the specimens of *H. finmarchica* were on average only 1.5 years older than the age predicted by the equation (Table 2-1; Fig. 2-4). On the other hand, estimated ages using colony height were not significantly different from the observed ages for *H. finmarchica* ($Z=0.36$, $df=1, 16$, $p=0.75$, Fig. 2-4).

A positive correlation was observed between colony height and axis diameter in *H. finmarchica*, although only close to significance ($r=0.47$, $df=1, 14$, $p=0.06$, Fig. 2-5A) and the number of growth rings significantly increased with axis diameter ($R^2=0.76$, $df=1, 24$, $p<0.05$, Fig. 2-5B). There was no significant relationship between colony height and age ($R^2=0.05$, $df=1, 14$, $p=0.4$, Fig. 2-5C), although when running the regression through the origin the relationship was significant (Fig. 2-5C).

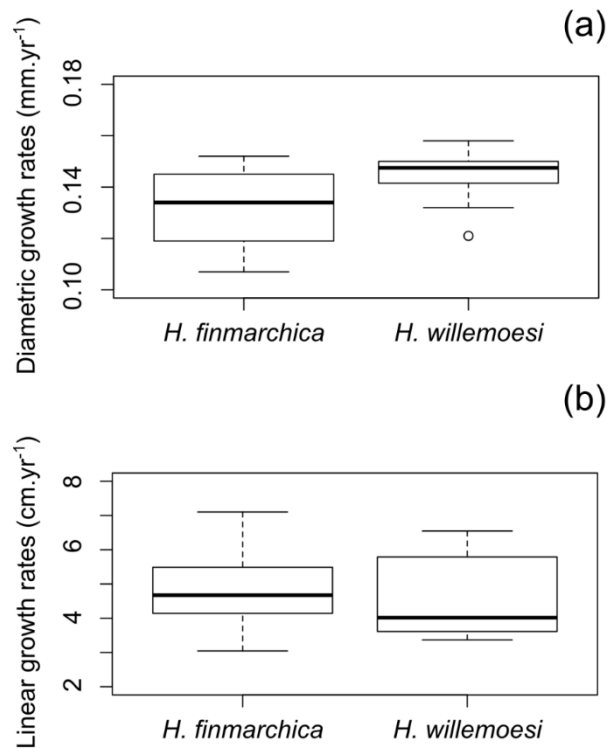


Figure 2-3. Box-plots showing: diametric (A) and linear growth rates (B) in *Halipteris finmarchica* from the Northwest Atlantic and *H. willemoesi* from the Bering Sea (cf. Wilson et al., 2002).

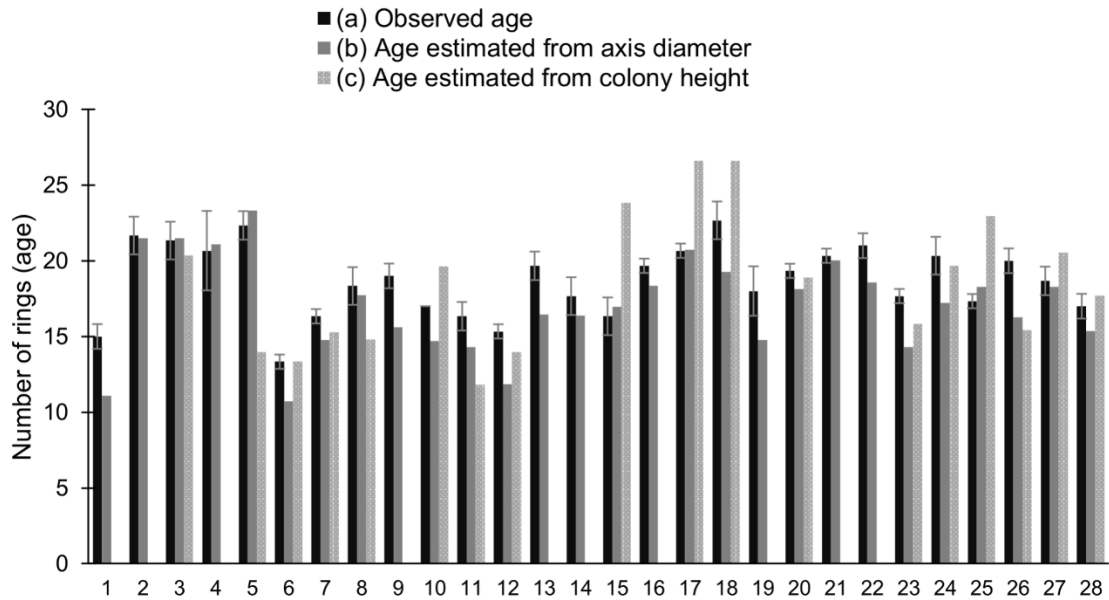


Figure 2-4. Observed and estimated number of rings in *Halipteris finmarchica* per colony: average number of rings (observed, A), estimated number of rings based on axis diameter (using the regression equation produced by Wilson et al. (2002) for *H. willemoesi*, B), estimated number of rings based on colony height (based on the relationship between size at maturity for *H. finmarchica* from Baillon et al. (2014), our estimated linear growth rates and age at maturity, C). The number of rings based on height was not estimated for colonies of incomplete size.

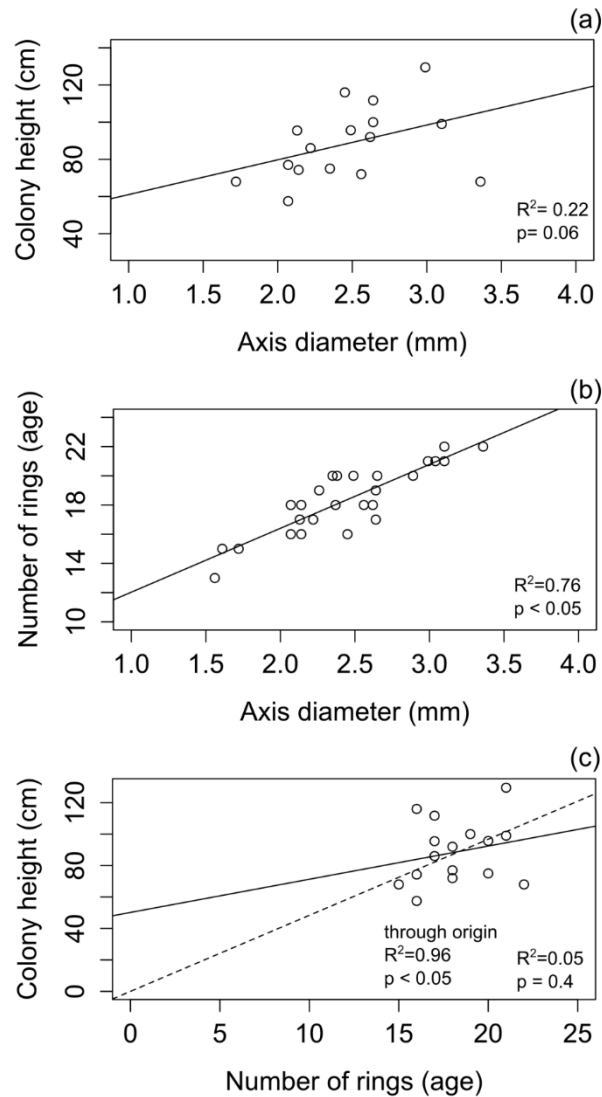


Figure 2-5. Relationships between: colony height and axis diameter (A), number of rings and axis diameter (B), colony height and number of rings (C), where the dashed line represents the regression through the origin.

Linear growth rates in *H. finmarchica* increased with colony height ($R^2 = 0.66$, $df = 1, 15$, $p < 0.05$), although this trend was not significant for diametric growth rates ($R^2 =$

0.33, $df = 1, 15$, $p < 0.05$) (Fig. 2-6A). When plotting linear growth rates in relation to height for both *H. finmarchica* and *H. willemoesi*, linear growth rates for the Atlantic species were in the range of the medium size colonies of *H. willemoesi* (Fig. 2-6B).

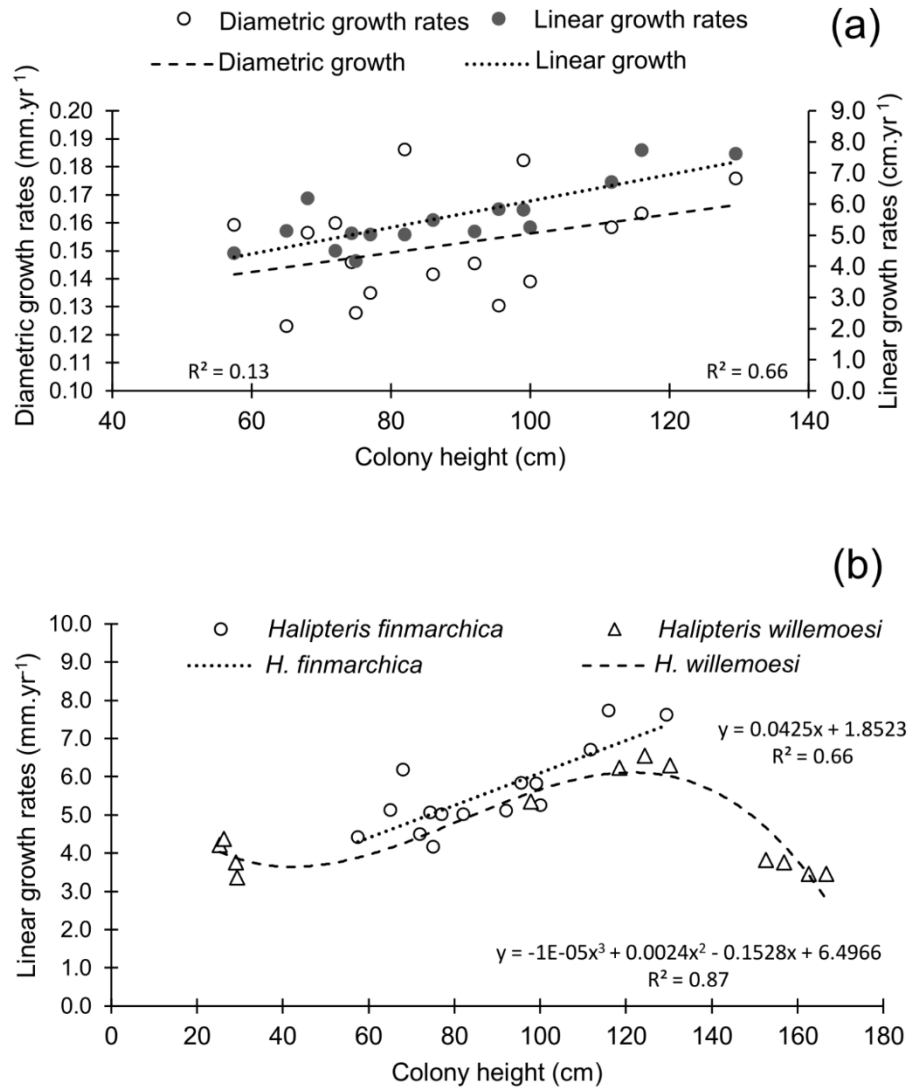


Figure 2-6. Diametric and linear growth rates in *Halipteris finmarchica* in relation to colony height (A), linear growth rates in relation to colony height in *H. finmarchica* (circles, B) and in *H. willemoesi* (triangles; data from Wilson et al., 2002). In b *H. willemoesi* showed the best fit when adding a cubic term to the regression.

2.3.3 Environmental variables

There were no significant relationships between diametric growth rates and environmental variables for *H. finmarchica* (Table 2-2; Fig. 2-7). However, when pooling the two species together significant relationships were detected, with diametric growth rates being statistically related to latitude, temperature, chlorophyll a concentration and POC, although in all cases the relationship was very weak ($R^2 < 0.2$; Table 2-2; Fig. 2-7B-E). Chlorophyll a and POC were different between the localities of the two species, but PIC was not (Fig. 2-8). No relationships were observed between diametric growth rates and depth or PIC for *H. finmarchica* nor when pooling the data on the two species (Fig. 2-7A, F). No significant relationships were detected between linear growth rates and environmental variables (Table 2-2; Fig. 2-9A to F).

When looking at relationships between number of rings (age) and environmental variables for *H. finmarchica*, a significant positive relationship between number of rings and depth was identified (Fig. 2-10A, $R^2=0.37$, $df= 1, 23$, $p = 0.001$), but no relationships were observed with other environmental variables (Table 2-2; Fig. 2-10B to F).

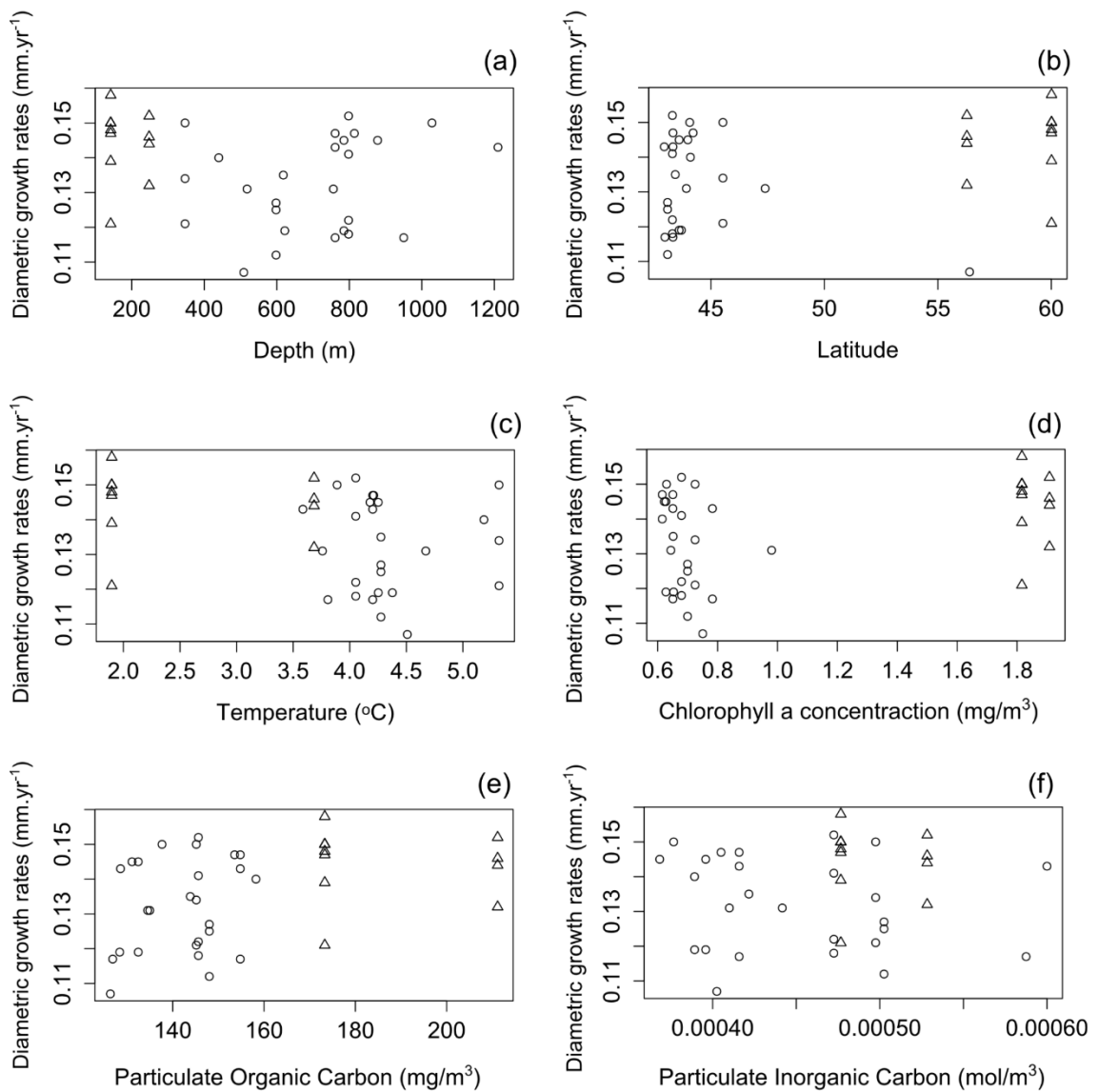


Figure 2-7. Relationships between diametric growth rates and: depth (A), latitude (B), temperature (C), chlorophyll a concentration (D), particulate organic carbon (POC, E), and particulate inorganic carbon (PIC, F) for *Halipteris finmarchica* (circles) and *H. willemoesi* (cf. Wilson et al., 2002; triangles).

Table 2-2. Results of linear regression analyzes using permutation techniques on growth rates and number of rings (age) for *Halipteris finmarchica* only, and for both species pooled (*H. finmarchica* and *H. willemoesi*) in relation to environmental variables.

Variables	<i>Halipteris finmarchica</i>				Both species					
	Dgrowth		Lgrowth		Number of rings		Dgrowth		Lgrowth	
	R ²	p value	R ²	p value	R ²	p value	R ²	p value	R ²	p value
Depth (m)	0.05	0.24	0.07	0.23	0.56	0.001	0.06	0.15	2.008 ⁻⁰⁵	0.98
Temperature (°C)	0.0002	0.96	0.06	0.34	0.20	0.12	0.14	0.02	0.001	0.88
Latitude	0.09	0.08	0.04	0.62	0.01	0.66	0.11	0.02	0.004	0.80
Chlorophyll a (mg/m ³)	0.05	0.71	0.03	0.58	0.13	0.12	0.16	0.02	0.02	0.42
POC (mg/m ³)	0.05	0.19	0.01	0.56	0.13	0.18	0.17	0.01	0.10	0.08
PIC (mol/m ³)	0.03	0.37	0.05	0.28	0.36	0.01	0.001	0.86	0.001	0.94

Dgrowth represents diametric growth rates (mm·yr⁻¹) and Lgrowth represents linear growth rates (cm·yr⁻¹). Values in bold are statistically significant at $\alpha=0.05$.

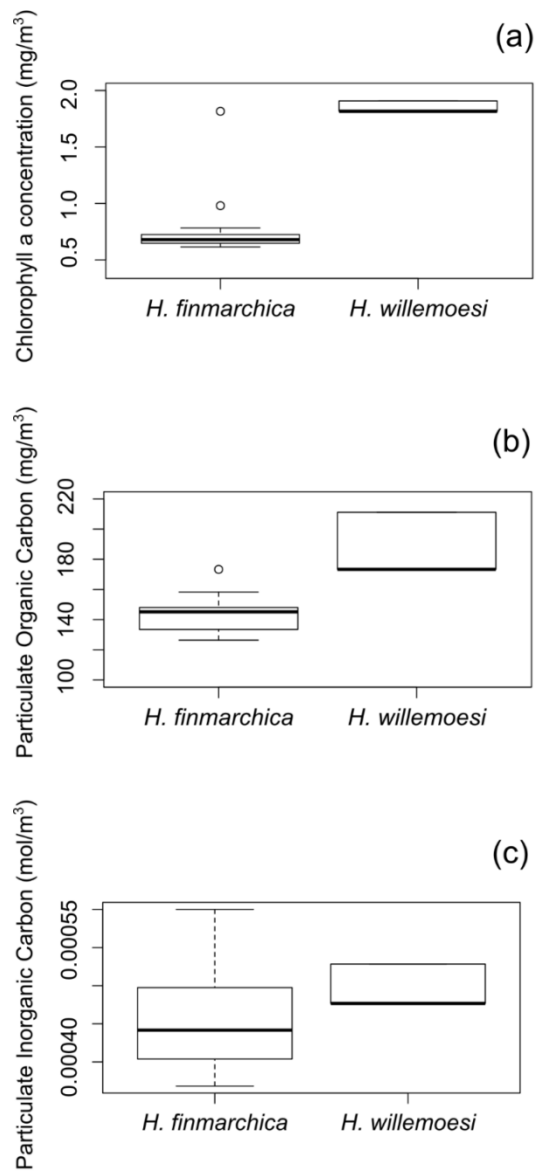


Figure 2-8. Environmental data from the locations of *Halopteris finmarchica* (Northwest Atlantic) and *H. willemoesi* (Bering Sea; from Wilson et al., 2002): mean annual chlorophyll a concentration (A), particulate organic carbon (POC, B), and particulate inorganic carbon (PIC, C) from the periods ranging 1997-2010 (chlorophyll a; excluding 2008-2009) and 2002-2013 (POC and PIC).

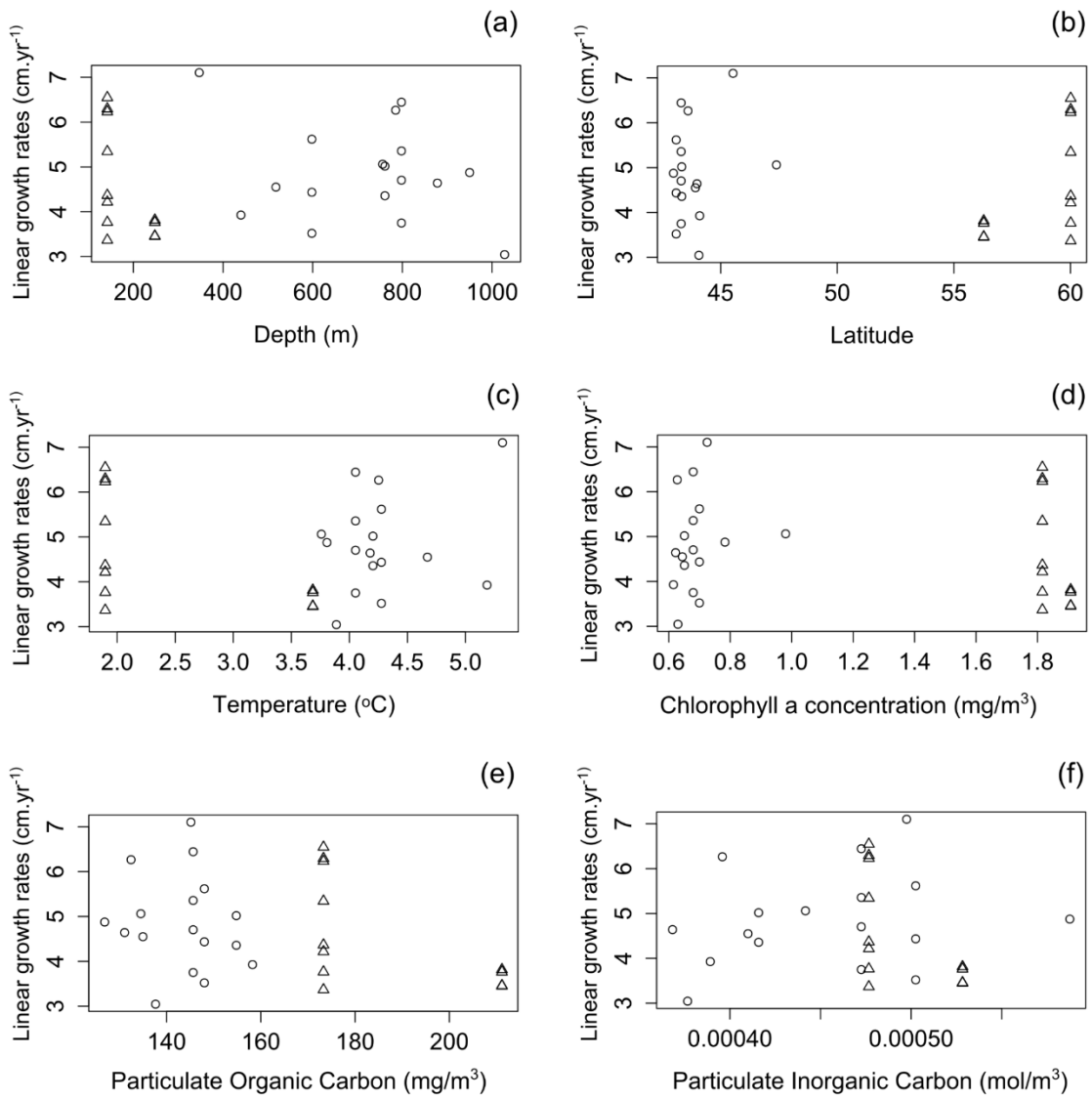


Figure 2-9. Relationships between linear growth rates and: depth (A), latitude (B), temperature (C), chlorophyll a concentration (D), particulate organic carbon (POC, E), and particulate inorganic carbon (PIC, F) for *Halopteris finmarchica* (circles) and *H. willemoesi* (cf. Wilson et al., 2002; triangles).

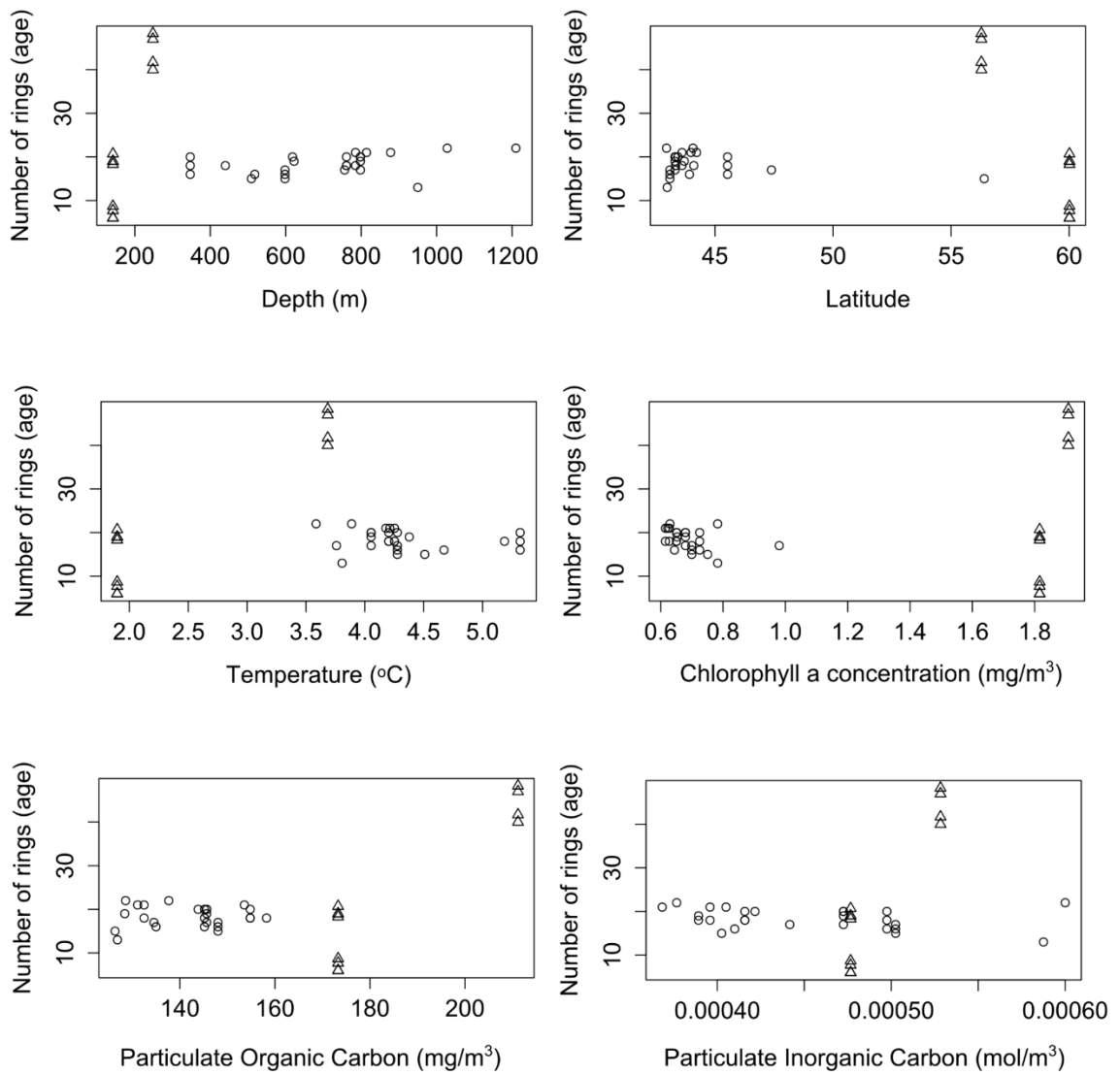


Figure 2-10. Number of rings (age) in *Halipteris finmarchica* in relation to: depth (A), latitude (B), temperature (C), chlorophyll a concentration (D), particulate organic carbon (POC, E), and particulate inorganic carbon (PIC, F).

2.3.4 Trace element analysis

In *H. finmarchica* Sr/Ca ratios ranged 1.59-2.17 mmol·mol⁻¹, Mg/Ca ratios ranged 61.4-97.2 mmol·mol⁻¹, Ba/Ca ranged 0.005-0.070 mmol·mol⁻¹, and Na/Ca ranged 15.9-39.7 mmol·mol⁻¹ (Table 2-3). Ratios were the highest in sample 035B, followed by 034A and 009, except for Mg/Ca, where the highest values were found in sample 034A, followed by 009 and 035B (Table 2-3; Fig. 2-11). Metal/Ca ratios were significantly different between colonies 035B and 034A, 035B and 009 for all four trace element ratios, between 034A and 009 for Sr/Ca, but not between 034A and 009 for the other three trace element ratios (Table 2-4; Fig. 2-11).

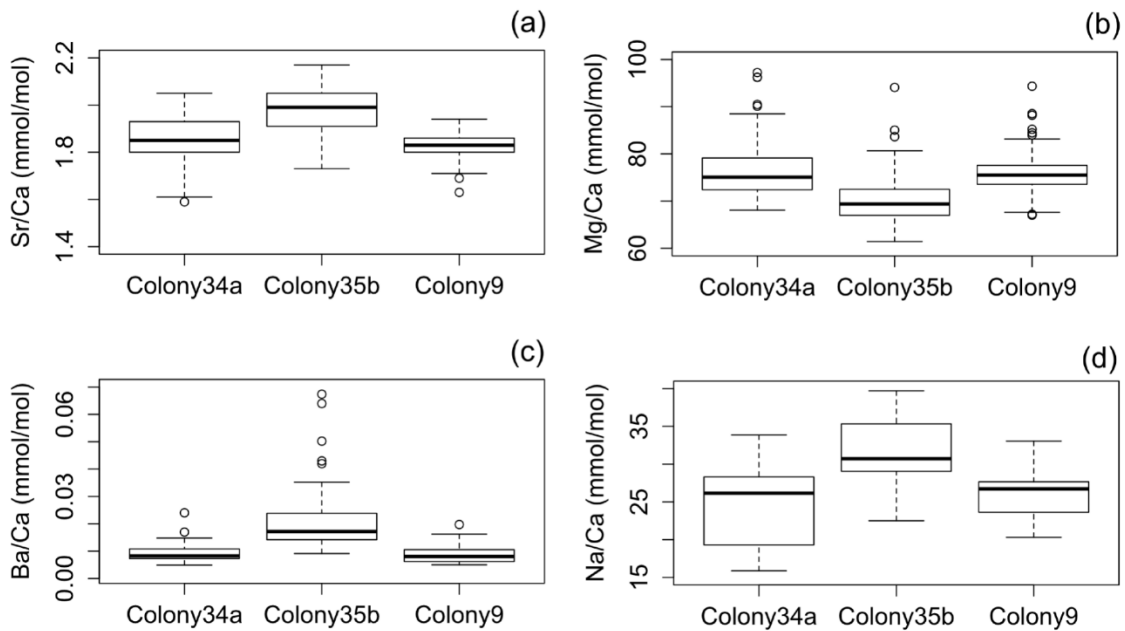


Figure 2-11. Trace element ratios (Mg/Ca, Sr/Ca, Ba/Ca, and Na/Ca) in the axis of three colonies of *Halipteris finmarchica* (one transect per axis/colony).

A significant negative correlation between Sr/Ca and Mg/Ca was observed for samples 009 and 035B (Fig. 2-12A-B), and a tendency of negative relationship was also observed for sample 034A (Table 2-3). However, this relationship was weak, with R^2 values ranging 0.03-0.29 in the three samples. Sr/Ca and Ba/Ca showed a tendency to increase with distance from core (i.e. age), while Mg/Ca and Na/Ca tended to decrease with distance from core (Fig. 2-12A, C). Ba/Ca shows sharp peaks in all three colonies, particularly in 035B (Fig. 2-12C). These peaks do not correspond to unusual peaks in the other three elements and peaks appear in both light and dark rings (Fig. 2-12C). The distribution of the analyzed Me/Ca ratios along the transects showed a pattern where the number of peaks in all four ratios is comparable to the number of rings visually determined (Table 2-3; Fig. 2-13). The elevated peaks in Mg/Ca seem to correspond to the dark bands of *H. finmarchica*'s axis (Fig. 2-13).

Table 2-3. Results from the Mann-Whitney U test on the relationship between Sr/Ca, Mg/Ca, Na/Ca and Ba/Ca (mmol/mol) ratios per sample of *Halopteris finmarchica* colonies.

Samples	Sr/Ca		Mg/Ca		Ba/Ca		Na/Ca	
	W	p	W	p	W	p	W	p
009 vs 034A	2976.5	0.03	2405	0.87	2814	0.13	2260	0.44
009 vs 035B	5054.5	<2.2e-16	1120.5	5.7e-10	5204	<2.2e-16	4606	7.81e-13
034A vs 035B	4122	4.75e-16	1002.5	6.9e-10	4703	<2.2e-16	4147	2.43e-11

Values in bold are statistically significant at $\alpha=0.05$

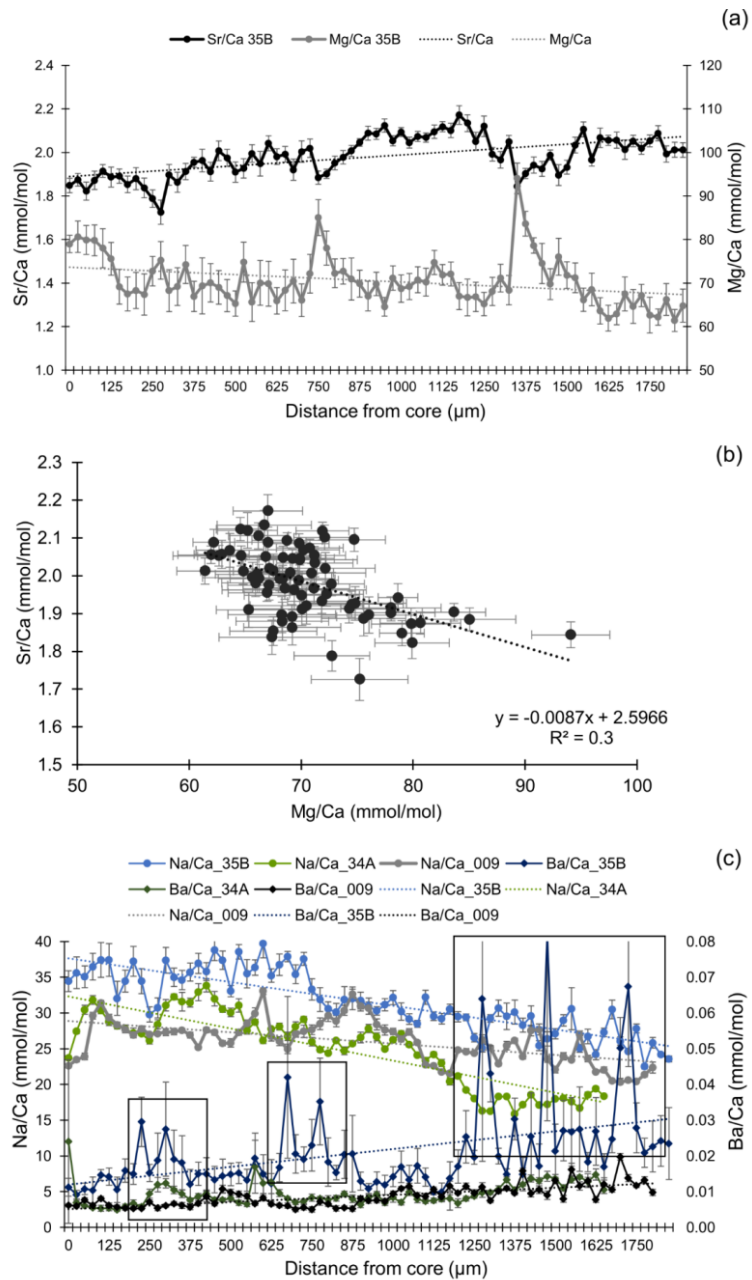


Figure 2-12. Distribution of trace element ratios across the axes radius of *Halipteris finmarchica*: Sr/Ca and Mg/Ca in relation to distance from core for sample 035B (A), correlation between Sr/Ca and Mg/Ca for sample 035B ($r=-0.54$, $p<0.05$, B), Ba/Ca and Na/Ca in relation to distance from core for all three analyzed samples (C). Error bars are $\pm 1\sigma$.

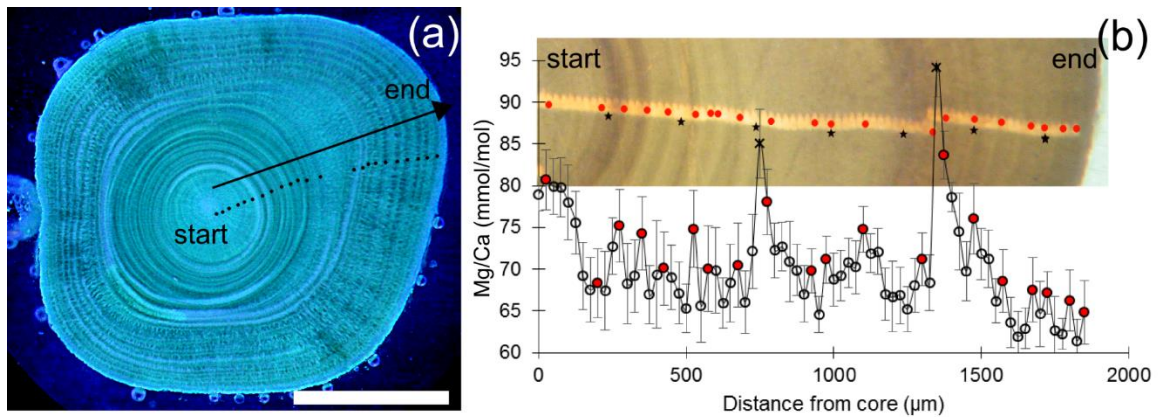


Figure 2-13. Distribution of Mg/Ca peaks along the radius of one colony of *Halipteris finmarchica* (sample 035B): cross section of axis showing rings (identified by black dots) and direction of SIMS transect (A), distribution of Mg/Ca along the SIMS transect, with filled red dots emphasizing positive peaks and x representing the first sample of a transect that has an extreme value (B). Error bars are $\pm 1\sigma$. Stars represent every 10 points. Scale bar in A = 1 mm.

2.4 Discussion

2.4.1 Growth rates and age in *Halipteris finmarchica* and comparison between the two species

In this study growth rings formation periodicity was assumed to be annual, and therefore estimated growth rates were also based on this assumption. Growth ring formation periodicity in other octocorals has been confirmed to be annual, such as in deep-water colonies of the gorgonian *Primnoa resedaeformis* (Sherwood et al., 2005), and

in young colonies of the sea pen *P. gurneyi* (Birkeland, 1974), and several other species (Marschal et al., 2004, Sherwood & Edinger, 2009). One of the factors usually considered a trigger to growth ring formation in deep-water organisms is seasonal increase in food availability, such as spring phytoplankton blooms (Gage & Tyler, 1991, Gooday, 2002). This suggests that, in locations where autumn blooms are also significant, rings would be formed twice a year if triggered by blooms. A decadal analysis of seasonal cycles of phytoplankton abundance on the South Newfoundland and Newfoundland shelves revealed that the peak in diatom abundance, dinoflagellate abundance, and phytoplankton color index (PCI) in this region usually occurs in April, and does not show a distinct and recurrent second peak during the year (Head & Pepin, 2009). This suggests that autumn blooms in the study area, if present, do not have the same magnitude as spring blooms and are probably not a major ring formation influence in the studied colonies of *H. finmarchica*.

The axis of *H. finmarchica* is composed of magnesian calcite, as is the axis of *H. willemoesi* (Wilson et al., 2002). Diametric growth rates of *H. finmarchica* and *H. willemoesi* were statistically different, as were observed ages versus ages predicted from axis diameter. Differences in diametric growth rates between these two species could be related to the differential chlorophyll a concentration and POC (as proxies for food availability) between the two areas (see Fig. 2-8). Differential growth rates between related species from Atlantic versus Pacific waters have already been observed in other coral species, such as the gorgonians *Primnoa resedaeformis* (Gunnerus, 1763) and *Primnoa pacifica* Kinoshita, 1907 whose difference in growth rates have also been suggested to be food related (Sherwood & Edinger, 2009).

Since the compared sea pens do not belong to the same species, it is also possible that intrinsic differences between the two species influence colony growth rates. The main difference between *H. finmarchica* and *H. willemoesi* is the number of feeding polyps per row, with the Atlantic species having 15 and the Pacific species having 12 (Kükenthal, 1915). The number and size of polyps can influence the amount of food ingested by an octocoral polyp (Lewis, 1982), therefore an increased number of polyps per row might allow the Atlantic colonies to compensate and get comparable net amounts of food to the Pacific colonies, which might have more access to food considering that both chlorophyll a and surface POC were higher at the *H. willemoesi* locations. However, the relative polyp size and total number of polyps per colony in the two species has not been quantitatively compared, thus this hypothesis remains to be tested.

Growth rates in the two species of *Halopteris* were very similar in magnitude (0.13 vs. 0.14 mm·yr⁻¹), despite the statistical difference. Although the statistically significant difference in rates could be a response to differential environmental conditions or to different colony morphology as discussed above, it could also be related to technical inaccuracies rather than to actual differences. For instance, we acknowledge that the visual ring counting technique for *H. finmarchica* is subject to imprecisions, most likely related to discerning between annual and sub-annual rings (i.e. intermediate bands seen along the width of a wide ring), as also observed in *H. willemoesi* (Wilson et al., 2002). Sub-annual rings have been recognized in other deep-water corals (e.g. Risk et al., 2002), but the distinction between annual and sub-annual rings in poorly studied sea pens axes is not well understood yet, and the mistaken identification of a sub-annual ring as annual would lead to an overestimation of age, and vice-versa. Our ring counts were higher than

most of the expected number of rings based on the regression equation produced for *H. willemoesi* (see Fig. 2-4). If the number of rings observed in *H. finmarchica* was overestimated, this could explain the slightly slower diametric growth rates observed for this species.

Our data show that the number of rings significantly increased with axis diameter, and that there was a positive correlation between axis diameter and colony height (although weak). This implies a corollary positive relationship between number of rings and colony height, although this relationship was not statistically distinct (Fig. 2-5C). It is possible that our size range was too restricted for this relationship to be statistically detected, or that our sample size was not sufficiently large. Since the predicted ages using size and age at maturity (which was also based in colony height), were not statistically different from the observed ages, we consider that height can be used as a predictor of age and that perhaps the reduced subset of samples available for this analysis (due to broken colonies) have had an adverse influence on the results.

The studied colonies of *H. finmarchica* showed diametric growth rates to be slower in the first four years of life, relative to rates calculated for the whole colony lifespan. This is contrary to the general view that some organisms tend to grow faster during their first years of life, because reaching larger sizes faster reduces mortality and because achieving sexual maturity earlier might allow resources to be diverted to reproduction earlier (Sebens, 1987, Arendt, 1997). Furthermore, in benthic organisms with an erect form, fast initial growth might maximize food capture (Bavestrello et al., 2012). What might be behind our result for *H. finmarchica* is that axial (i.e. skeletal) growth is not necessarily coupled with tissue growth, as observed in other invertebrates;

including scleractinian corals (Anthony et al., 2002), octocoral sclerites (Tentori et al., 2004), bivalves (Palmer, 1981), and fish otoliths (Mosegaard et al., 1988). Chang et al. (2007) showed that the sea whip *Junceella fragilis* (Ridley, 1884) switches from sclerites to axial skeleton as the main support system during colony growth, as a way of coping with an increased height and exposure to hydrodynamic forces. In *H. finmarchica* axial growth rates might be reduced in the first years of life to allow a higher allocation of resources to tissue growth; but as the colony grows, there is a need to improve skeletal support, as observed in *J. fragilis* (Chang et al., 2007). This could explain the subsequent changes in axial increment in the following years of life. Our technique did not allow for an estimation of linear extension in the first years of life.

Average linear growth rates in *H. finmarchica* ($4.9 \text{ cm}\cdot\text{yr}^{-1}$) were not statistically different for those calculated for *H. willemoesi* ($4.5 \text{ cm}\cdot\text{yr}^{-1}$; Wilson et al., 2002), but were faster than those published for other cold-water whip-shaped corals, although there is not much information available on growth in these types of coral. In the shallow-water sea pen *P. gurneyi* linear growth rates of three-year old colonies were $2.52 \text{ cm}\cdot\text{yr}^{-1}$ (based on an increment of 2.37 cm in 11 months) (Birkeland, 1974). Black corals from deep New Zealand waters showed linear growth rates of $2.9 \text{ cm}\cdot\text{yr}^{-1}$ (Grange, 1985), and the deep-water gorgonian *Chrysogorgia agassizii* (Verrill, 1883) showed a linear growth rate of $1 \text{ cm}\cdot\text{yr}^{-1}$ (Vinogradov, 2000). On the other hand, tropical, shallow water sea whips appear to show faster growth rates than deep-water counterparts. For instance, the tropical whip black corals *Cirrhipathes* cf. *anguina* and *Stichopathes* cf. *maldivensis* showed linear growth rates of $13.25 \text{ cm}\cdot\text{month}^{-1}$ and $1.3 \text{ cm}\cdot\text{month}^{-1}$, respectively, reaching up to 3 m in

height (Bo et al., 2009), while the tropical whip gorgonian *J. fragilis* showed linear growth rates of 6.1 cm.month⁻¹ (1.4 cm.week⁻¹) (Walker & Bull, 1983).

Possible uncoupled skeletal and tissue growth might also help to explain why diametric growth rates were significantly different in the two species, but linear growth rates were not. For example, the data showed by Wilson et al. (2002) suggest linear growth rates to be faster in medium size colonies of *H. willemoesi* than in small and large colonies; while diametric growth rates were similar in all size ranges. Therefore, it is possible that these two types of growth are not entirely synchronized.

When plotting linear growth rates of the two species together (See Fig. 2-6B), this pattern of faster linear growth in intermediate size colonies can be recognized for *H. willemoesi*, while in the studied colonies of *H. finmarchica* linear growth rates appear to increase with colony size, based on the size range available in our study. In corals as diverse as gorgonians and solitary scleractinians, growth patterns have been considered to follow the Von Bertalanffy growth curve (Mistri & Ceccherelli, 1993, 1994, Mistri, 1995, Hamel et al., 2010, Goffredo et al., 2010), in which growth rates decrease with increasing size, with an asymptote being reached (Kaufmann, 1981). Other corals, such as the soft coral *Anthomastus ritteri* Nutting, 1909, seem to show initial slow growth followed by faster growth and reaching of an asymptote, thus following the Gompertz growth curve (Cordes et al., 2001). *H. willemoesi* also seems to follow the Gompertz growth pattern (Wilson et al., 2002). Here we showed that linear growth rates in *H. finmarchica* increase with colony height, but due to our limited colony size range we could not detect patterns of initial versus later linear growth rates. Therefore, the analysis of colonies from a wider size range seems to be necessary before patterns of linear growth rates can be drawn for

this species. On the other hand, we did find that in *H. finmarchica* diametric growth rates were slower in the first four years of life, which suggests that skeletal growth rates in this species might also follow the Gompertz pattern.

Since size at first maturity in *H. finmarchica* was estimated to be at 18 cm (Baillon et al., 2014), all the studied colonies can be assumed to be mature. In *H. willemoesi* the average linear growth rates of $4.5 \text{ cm}\cdot\text{yr}^{-1}$ indicate that estimated age at maturity would be at four years, assuming size at maturity in these two species to be the same. Our estimated age of maturity of ca. four years is similar to that estimated for shallow water sea pens such as *P. gurneyi*, where sexual maturity is reached at the age of five years, at ca. 24 cm (Birkeland, 1974). Similarly, *Virgularia juncea* (Pallas, 1766) colonies 16 cm in height already had gonads (Soong, 2005). Thus, our study indicates that *H. finmarchica* will reach ca. 4 years before reproductive activities begin.

2.4.2 Growth rates and age in relation to environmental variables

The absence of significant relationships between growth rates in *H. finmarchica* and the individual environmental variables analyzed might suggest that small scale differences in these variables might not be enough to influence growth in this species or to be statistically detected. However, when pooling the data from the two species, both temperature, latitude, chlorophyll a and POC were significantly related to diametric growth rates. Temperature was negatively related to diametric growth rates, which is contrary to the typical view of a positive relationship between these two variables (Sebens, 1987). This disagreement suggests that this statistical relationship could have been influenced by the limited data points available, particularly for the Pacific species,

and by the different growth rates between the two species, rather than to an actual biological relationship. On the other hand, as discussed above, chlorophyll a and POC are related to food availability and are expected to have an influence on growth rates in this type of organism (Sebens, 1987).

Colony age was positively related to depth, which could be associated to a smaller exposure to fishing disturbance, considering that most bottom trawling in Atlantic Canada occurs at <350 m (between 1980-2000) (Wallace & David Suzuki Foundation, 2007). This has also been discussed for gorgonians in the NW Atlantic where colony size in *Paragorgia arborea* (Linnaeus, 1758) increased with depth, although *Primnoa resedaeformis* showed the opposite pattern (Watanabe et al., 2009). In the NW Atlantic *H. finmarchica* has been observed at depths up to >2000 m (Baker et al., 2012). With bottom fisheries increasingly shifting to deeper waters (Morato et al., 2006), colonies from a wider depth range will become more exposed and vulnerable to fishing gear, perhaps affecting populations' age structure.

2.4.3 Trace element ratios and environmental significance

The average trace element ratios in *H. finmarchica* were very similar to the ratios observed in the gorgonian *P. pacifica*, which showed slightly increased ranges for all four elements (Aranha et al., 2014). This gorgonian also showed an inverse correlation between Sr/Ca and Mg/Ca ratios. In Gulf of Alaska bamboo corals, Sr/Ca ratios ranged 5.1-5.9 mmol·mol⁻¹ (Roark et al., 2005), being *ca.* three times higher than the observed in *H. finmarchica*.

Trace element ratios in colony 035B were different from ratios in the other two colonies, but ratios in colonies 034A and 009 were not significantly different from each other, with exception of Sr/Ca ratios. Colony 035B was collected from a similar depth and latitude as colony 034A; therefore these variables do not explain why trace element ratios in this colony were different from those of the other two colonies.

The similarity between the number of rings and the number of peaks in the trace element ratios suggests that the physical and chemical characteristics of growth rings in *H. finmarchica* are related. Samples 009 and 035B showed very similar estimated number of rings and peaks in the trace elements, which were less comparable in sample 034A. This sample also did not show a significant relationship between Sr/Ca and Mg/Ca, showing that it diverged from the other samples in the distribution of trace elements along the axis. Roark et al. (2005) used Sr/Ca cycles to verify growth rate estimates and coral ages using the calcite of bamboo corals. These authors observed that the number of Sr/Ca cycles (i.e. 84) was consistent with the age determined by radiocarbon dating, confirming that the observed Sr/Ca cycles in the studied specimen were annual. Similarly, Cardoso et al. (2013) showed that Sr/Ca cycles corresponded to seasonality in the growth lines of the bivalve *Macoma balthica* (Linnaeus, 1758), validating an annual periodicity in ring formation (Cardoso et al., 2013).

Elevated peaks in Mg/Ca ratios could be related to increased water temperature (Lutz & Rhoads, 1980) and could be seen as an indicator of summer growth. However, annual temperature variations are small to insignificant in the deep sea (Gage & Tyler, 1991); therefore significant fluctuations in Me/Ca ratios must be related to other reasons, such as physiological factors, considering the influence of vital effects in the metal/Ca

distribution of coral skeletons (de Villiers et al., 1995, Robinson et al., 2014) and food availability (Roark et al., 2005). Hart and Cohen (1996) showed that Sr/Ca variations in two deep-water scleractinians were related to vital or kinetic effects, instead of purely to temperature variations. In certain marine fish otoliths water chemistry has recently been suggested to be the main control on Sr and Ba uptake (Walther & Thorrold, 2006), although temperature (Elsdon & Gillanders, 2004), and physiology (Kalish, 1989, 1992, Walther et al., 2010) have also been correlated with changes in Sr/Ca composition in these structures. Similarly, environmental factors have also been suggested to play only an indirect role in shallow-water scleractinian coral Sr/Ca ratios (Weber, 1973), with some corals showing a strong internal control of their biomineralization activity (Meibom et al., 2007, Brahmi et al., 2012).

Intrinsic biological processes affect deep-water corals growth since, as in other invertebrates, colonies might reduce or increase resource allocation to the skeleton during periods related to reproduction (e.g. production of gametes, spawning) (Kozłowski, 1992, Arendt, 1997, Heino & Kaitala, 1999). In *H. finmarchica* reproduction is seasonal, with an annual spawning that follows spring phytoplankton blooms (Baillon et al., 2014). The observed peaks in Mg/Ca could reflect an increase in magnesium intake during the pre-spawning period, since magnesium seems to play a role in ovule maturation, sperm viability and fecundation in invertebrates (Stolkowski, 1977). However, reproduction does not explain the overall formation of growth rings, especially in the years preceding sexual maturation. Therefore, it is possible that the observed fluctuations in the trace element ratios were influenced by other factors, such as seasonal rises in food availability (i.e. phytoplankton blooms), as previously discussed in terms of possible temporal

influences on ring formation. For instance, a higher nutrient flux might lead to a higher skeletal accretion rate and higher Mg/Ca ratios.

Sr/Ca showed a tendency to increase with distance from core (i.e. age), which is in accordance with variations observed for other invertebrates such as bivalves - although both increasing and decreasing Sr/Ca with age have been observed in these animals (Rosenberg, 1980). Considering that diametric growth rates tended to be slower in the first four years of life, it seems that here Sr/Ca ratios tended to increase with diametric growth rates, which is contrary to the pattern observed in other corals, such as the scleractinian *Pavona clavus* (Dana, 1846) (de Villiers et al., 1995) and the octocoral *Corallium rubrum* (Linnaeus, 1758) (Weinbauer et al., 2000), where Sr/Ca cycles have been shown to be inversely related to growth rates. On the other hand, Thresher (2009) found no correlation between Sr/Ca and growth rates for 16 bamboo coral colonies (from different genera) Thresher (2009) and Sinclair et al. (2011) questioned the relationship between growth rates and Sr/Ca in bamboo corals. Therefore, patterns of Sr/Ca increasing or decreasing with age and growth rates might be species-specific and there is no consensus on this relationship yet.

Peaks in Ba/Ca were observed in both light and dark rings. Like Sr/Ca, Ba/Ca showed a slight tendency to increase with colony age. Sporadic sharp spikes in Ba/Ca in some of the SIMS spots might be related to the presence of assimilated particles such as a sediment particle, which would alter the Ba/Ca ratio by contribution of lithogenic barium (Edinger et al., 2008). However, in many cases peaks in the Ba/Ca ratios were not accompanied by peaks in Na/Ca, with Mg/Ca and Sr/Ca still showed opposing patterns, indicating that the observed spikes seem to represent Ba incorporated directly into the

skeleton. Ba/Ca has been used as a proxy for primary productivity, and these spikes could be related to spikes in the environment. However, annual chlorophyll a did not show increased values for these corresponding years of Ba/Ca spikes.

Although in other calcareous organisms/structures both environmental and physiological factors have been shown to have an influence on their trace element composition, as discussed above, this is the first study to look at trace element composition in the axis of a sea pen, and at this moment we cannot determine which factors might have the most influence on the observed variations. Studies under laboratory conditions, examining the direct influence of environmental factors on trace element composition in an attempt to resolve the source (s) of trace element fluctuations in the axis of sea pens would be valuable.

2.5 Conclusions

Measured growth rates were statistically different between the two species of *Halipteris*, but average rates were very similar. Technical issues can have influenced the statistical detection of such differences, which might thus not be biologically meaningful. The absence of individual relationships between environmental variables and growth rates in *H. finmarchica* - but the presence of relationships when pooling the two species - might imply that the influence of environmental factors on growth rates in *H. finmarchica* may only be identified when variations in environmental factors are large enough in magnitude. Growth rates might be influenced by increased inputs of food, particularly those reflected by seasonal variations in chlorophyll a and POC. The positive influence of

depth on colony age could be related to a smaller exposure of deeper colonies to fishing disturbance.

The comparable number of cycles in the trace elements and the number of growth rings suggests a correspondence between these two variables. The presence of cycles in the distribution of the trace elements along the axis of *H. finmarchica* suggest that sea pens might have potential as proxies for short-term environmental changes. Considering the annual rise in food input due to phytoplankton blooms and seasonal reproduction of *H. finmarchica*, we think it's plausible to assume that rings in this species are formed annually, although we acknowledge that additional studies are needed to corroborate this assumption. Further studies on potential sources of trace element variation in the axis of sea pens might also help to clarify the temporal scale of ring formation in this group of corals.

2.6 References

Anthony, K. R. N., S. R. Connolly & B. L. Willis, 2002. Comparative analysis of energy allocation to tissue and skeletal growth in corals. *Limnology and Oceanography* 47: 1417-1429.

Aranha, R., E. Edinger, G. Layne & G. Piercey, 2014. Growth rate variation and potential paleoceanographic proxies in *Primnoa pacifica*: Insights from high-resolution trace element microanalysis. *Deep Sea Research Part II: Topical Studies in Oceanography* 99: 213-226.

Arendt, J., 1997. Adaptive intrinsic growth rates: An integration across taxa. *Quarterly Review of Biology* 72: 149-177.

Baillon, S., J. Hamel & A. Mercier, 2014. Protracted oogenesis and annual reproductive periodicity in the deep-sea pennatulacean *Halipteris finmarchica* (Anthozoa, Octocorallia). *Marine Ecology* 36: 1364-1378.

Baillon, S., J. Hamel, V. E. Wareham & A. Mercier, 2012. Deep cold-water corals as nurseries for fish larvae. *Frontiers in Ecology and the Environment* 10: 351-356.

Baker, K. D., V. E. Wareham, P. V. R. Snelgrove, R. L. Haedrich, D. A. Fifield, E. N. Edinger & K. D. Gilkinson, 2012. Distributional patterns of deep-sea coral assemblages in three submarine canyons off Newfoundland, Canada. *Marine Ecology Progress Series* 445: 235-249.

Bavestrello, G., R. Cattaneo-Vietti, C. G. Di Camillo & M. Bo, 2012. Helicospiral growth in the whip black coral *Cirrhopathes* sp. (Antipatharia, Antipathidae). *The Biological Bulletin* 222: 17-25.

- Birkeland, C., 1974. Interactions between a sea pen and seven of its predators. *Ecological Monographs* 44: 211-232.
- Bo, M., C. G. Di Camillo, A. M. Addamo, L. Valisano & G. Bavestrello, 2009. Growth strategies of whip black corals (Cnidaria: Antipatharia) in the Bunaken Marine Park (Celebes Sea, Indonesia). *Marine Biodiversity Records* 2.
- Boyer, T. P., J. I. Antonov, O. K. Baranova, H. E. Garcia, D. R. Johnson, R. A. Locarnini, A. V. Mishonov, D. Seidov, I. V. Smolyar & M. M. Zweng, 2009. World Ocean Database 2009, Chapter 1: Introduction, NOAA Atlas NESDIS 66. U.S. Gov. Printing Office, Washington, D.C.
- Brahmi, C., C. Kopp, I. Domart-Coulon, J. Stolarski & A. Meibom, 2012. Skeletal growth dynamics linked to trace-element composition in the scleractinian coral *Pocillopora damicornis*. *Geochimica et Cosmochimica Acta* 99: 146-158.
- Brodeur, R. D., 2001. Habitat-specific distribution of Pacific ocean perch (*Sebastes alutus*) in Pribilof Canyon, Bering Sea. *Continental Shelf Research* 21: 207-224.
- Brooke, S. & C. Young, 2009. In situ measurement of survival and growth of *Lophelia pertusa* in the northern Gulf of Mexico. *Marine Ecology Progress Series* 397: 153-161.
- Campana, S. E., 1997. Use of radiocarbon from nuclear fallout as a dated marker in the otoliths of Haddock *Melanogrammus aeglefinus*. *Marine Ecology Progress Series* 150: 49-56.
- Cardoso, J. F. M. F., S. Santos, J. I. Witte, R. Witbaard, H. W. van der Veer & J. P. Machado, 2013. Validation of the seasonality in growth lines in the shell of *Macoma balthica* using stable isotopes and trace elements. *Journal of Sea Research* 82: 93-102.

Chang, W., K. Chi, T. Fan & C. Dai, 2007. Skeletal modification in response to flow during growth in colonies of the sea whip, *Junceella fragilis*. *Journal of experimental marine biology and ecology* 347: 97-108.

Collins, M. J., E. R. Waite & A. C. T. van Duin, 1999. Predicting protein decomposition: the case of aspartic-acid racemization kinetics. *Philosophical Transactions of the Royal Society of London. Series B: Biological Sciences* 354: 51-64.

Cordes, E. E., J. W. Nybakken & G. VanDykhuisen, 2001. Reproduction and growth of *Anthomastus ritteri* (Octocorallia: Alcyonacea) from Monterey Bay, California, USA. *Marine Biology* 138: 491-501.

de Villiers, S., B. K. Nelson & A. R. Chivas, 1995. Biological controls on coral Sr/Ca and $\delta^{18}\text{O}$ reconstructions of sea surface temperatures. *Science* 269: 1247-1249.

Edinger, E. N., K. Azmy, W. Diegor & P. R. Siregar, 2008. Heavy metal contamination from gold mining recorded in *Porites lobata* skeletons, Buyat-Ratototok district, North Sulawesi, Indonesia. *Marine Pollution Bulletin* 56: 1553-1569.

Elsdon, T. S. & B. M. Gillanders, 2004. Fish otolith chemistry influenced by exposure to multiple environmental variables. *Journal of Experimental Marine Biology and Ecology* 313: 269-284.

Franc, S., P. W. Ledger & R. Garrone, 1985. Structural variability of collagen fibers in the calcareous axial rod of a sea pen. *Journal of Morphology* 184: 75-84.

Gage, J. D. & P. A. Tyler, 1991. *Deep-sea biology: a natural history of organisms at the deep-sea floor*. Cambridge University Press, Cambridge England; New York, NY, USA.

Gass, S. E. & J. M. Roberts, 2006. The occurrence of the cold-water coral *Lophelia pertusa* (Scleractinia) on oil and gas platforms in the North Sea: Colony growth, recruitment and environmental controls on distribution. *Marine Pollution Bulletin* 52: 549-559.

Goffredo, S., E. Caroselli, G. Mattioli & F. Zaccanti, 2010. Growth and population dynamic model for the non-zooxanthellate temperate solitary coral *Leptopsammia pruvoti* (Scleractinia, Dendrophylliidae). *Marine Biology* 157: 2603-2612.

Gooday, A., 2002. Biological responses to seasonally varying fluxes of organic matter to the ocean floor: A review. *Journal of Oceanography* 58: 305-332.

Grange, K. R., 1985. Distribution, standing crop, population structure, and growth rates of black coral in the southern fiords of New Zealand. *New Zealand Journal of Marine and Freshwater Research* 19: 467-475.

Hamel, J., Z. Sun & A. Mercier, 2010. Influence of size and seasonal factors on the growth of the deep-sea coral *Flabellum alabastrum* in mesocosm. *Coral Reefs* 29: 521-525.

Hart, S. R. & A. L. Cohen, 1996. An ion probe study of annual cycles of Sr/Ca and other trace elements in corals. *Geochimica et Cosmochimica Acta* 60: 3075-3084.

Head, E. & P. Pepin, 2009. Long-term variability in phytoplankton and zooplankton abundance in the Northwest Atlantic in Continuous Plankton Recorder (CPR) samples. DFO Can. Sci. Advis. Sec. Res. Doc. 2009/063. vi + 29 p.

Heino, M. & V. Kaitala, 1999. Evolution of resource allocation between growth and reproduction in animals with indeterminate growth. *Journal of Evolutionary Biology* 12: 423-429.

- Jull, A. J. T., 2006. Dating techniques. In Elias, S. A. (ed), Encyclopedia of Quaternary science. Elsevier, Amsterdam: 454-459.
- Kabacoff, R., 2011. R in action: data analysis and graphics with R. Manning, Shelter Island, NY.
- Kalish, J. M., 1989. Otolith microchemistry: validation of the effects of physiology, age and environment on otolith composition. *Journal of Experimental Marine Biology and Ecology* 132: 151-178.
- Kalish, J. M., 1992. Formation of a stress-induced chemical check in fish otoliths. *Journal of Experimental Marine Biology and Ecology* 162: 265-277.
- Kaufmann, K., 1981. Fitting and using growth curves. *Oecologia* 49: 293-299.
- Kozłowski, J., 1992. Optimal allocation of resources to growth and reproduction: Implications for age and size at maturity. *Trends in Ecology & Evolution* 7: 15-19.
- Kükenthal, W., 1915. Pennatularia. Das Tierreich. Verlag von R. Friedlander und Sohn, Berlin.
- Ledger, P. W. & S. Franc, 1978. Calcification of collagenous axial skeleton of *Veretillum cynomorium* Pall (Cnidaria Pennatulacea). *Cell and Tissue Research* 192: 249-266.
- Lewis, J. B., 1982. Feeding behaviour and feeding ecology of the Octocorallia (Coelenterata: Anthozoa). *Journal of Zoology* 196: 371-384.
- Lutz, R. A. & D. C. Rhoads, 1980. Growth patterns within the molluscan shell: an overview. In Rhoads, D. C. & R. A. Lutz (eds), *Skeletal growth of aquatic organisms: biological records of environmental change*. Plenum Press, New York: 203-248.

Malecha, P. W. & R. P. Stone, 2009. Response of the sea whip *Halipteris willemoesi* to simulated trawl disturbance and its vulnerability to subsequent predation. *Marine Ecology Progress Series* 388: 197-206.

Marschal, C., J. Garrabou, J. Harmelin & M. Pichon, 2004. A new method for measuring growth and age in the precious red coral *Corallium rubrum* (L.). *Coral Reefs* 23: 423-432.

Meibom, A., S. Mostefaoui, J. Cuif, Y. Dauphin, F. Houlbreque, R. Dunbar & B. Constantz, 2007. Biological forcing controls the chemistry of reef-building coral skeleton. *Geophysical Research Letters* 34(2): L02601.

Mistri, M., 1995. Gross morphometric relationships and growth in the Mediterranean gorgonian *Paramuricea clavata*. *Bolletino Di Zoologia* 62: 5-8.

Mistri, M. & V. U. Ceccherelli, 1993. Growth of the Mediterranean gorgonian *Lophogorgia ceratophyta* (L., 1758). *Marine Ecology* 14: 329-340.

Mistri, M. & V. Ceccherelli, 1994. Growth and secondary production of the Mediterranean gorgonian *Paramuricea clavata*. *Marine Ecology Progress Series* 103: 291-296.

Morato, T., R. Watson, T. J. Pitcher & D. Pauly, 2006. Fishing down the deep. *Fish and Fisheries* 7: 24-34.

Mosegaard, H., H. Svedäng & K. Taberman, 1988. Uncoupling of somatic and otolith growth rates in Arctic Char (*Salvelinus alpinus*) as an effect of differences in temperature response. *Canadian Journal of Fisheries and Aquatic Sciences* 45: 1514-1524.

Murillo, F. J., M. P. Durán, A. Altuna & A. Serrano, 2011. Distribution of deep-water corals of the Flemish Cap, Flemish Pass, and the Grand Banks of Newfoundland

(Northwest Atlantic Ocean): interaction with fishing activities. ICES Journal of Marine Science: Journal du Conseil 68: 319-332.

Palmer, A. R., 1981. Do carbonate skeletons limit the rate of body growth? Nature 292: 150-152.

Quinn, G. P. & M. J. Keough, 2002. Experimental design and data analysis for biologists. Cambridge University Press, Cambridge, UK; New York.

Risk, M. J., J. M. Heikoop, M. G. Snow & R. Beukens, 2002. Lifespans and growth patterns of two deep-sea corals: *Primnoa resedaeformis* and *Desmophyllum cristagalli*. Hydrobiologia 471: 125-131.

Roark, E. B., T. P. Guilderson, S. Flood-Page, R. B. Dunbar, B. L. Ingram, S. J. Fallon & M. McCulloch, 2005. Radiocarbon-based ages and growth rates of bamboo corals from the Gulf of Alaska. Geophysical Research Letters 32: L04606.

Roberts, J. J., B. D. Best, D. C. Dunn, E. A. Treml & P. N. Halpin, 2010. Marine Geospatial Ecology Tools: An integrated framework for ecological geoprocessing with ArcGIS, Python, R, MATLAB, and C++. Environmental Modelling & Software 25: 1197-1207.

Roberts, J. M., A. Wheeler, A. Freiwald & S. Cairns, 2009. Cold-water corals: the biology and geology of deep-sea coral habitats. Cambridge University Press, Cambridge, UK; New York.

Roberts, S. & M. Hirshfield, 2004. Deep-sea corals: out of sight, but no longer out of mind. Frontiers in Ecology and the Environment 2: 123-130.

Robinson, L. F., J. F. Adkins, N. Frank, A. C. Gagnon, N. G. Prouty, E. Brendan Roark & T. v. de Flieddt, 2014. The geochemistry of deep-sea coral skeletons: A review of

vital effects and applications for palaeoceanography. *Deep Sea Research Part II: Topical Studies in Oceanography* 99: 184-198.

Rosenberg, G. D., 1980. An ontogenetic approach to the environmental significance of bivalve shell chemistry. In Rhoads, D. C. & R. A. Lutz (eds), *Skeletal growth of aquatic organisms: biological records of environmental change*. Plenum Press, New York: 133-168.

Schlitzer, R., 2014. *Ocean Data View*.

Schneider, C. A., W. S. Rasband & K. W. Eliceiri, 2012. NIH Image to ImageJ: 25 years of image analysis. *Nature Methods* 9: 671-675.

Sebens, K. P., 1987. The ecology of indeterminate growth in animals. *Annual Review of Ecology and Systematics* 18: 371-407.

Sherwood, O. A. & E. N. Edinger, 2009. Ages and growth rates of some deep-sea gorgonian and antipatharian corals of Newfoundland and Labrador. *Canadian Journal of Fisheries and Aquatic Sciences* 66: 142-152.

Sherwood, O. A., D. B. Scott, M. J. Risk & T. P. Guilderson, 2005. Radiocarbon evidence for annual growth rings in the deep-sea octocoral *Primnoa resedaeformis*. *Marine Ecology Progress Series* 301: 129-134.

Sinclair, D. J., B. Williams, G. Allard, B. Ghaleb, S. Fallon, S. W. Ross & M. Risk, 2011. Reproducibility of trace element profiles in a specimen of the deep-water bamboo coral *Keratoisis* sp. *Geochimica et Cosmochimica Acta* 75: 5101-5121.

Soong, K., 2005. Reproduction and colony integration of the sea pen *Virgularia juncea*. *Marine Biology* 146: 1103-1109.

Stolkowski, J., 1977. Magnesium in animal and human reproduction. *Revue Canadienne de Biologie* 36: 135-177.

Team, R. D. C., 2008. R: A language and environment for statistical computing. R Foundation for Statistical Computing, Vienna, Austria.

Tentori, E., D. Allemand & R. Shepherd, 2004. Cell growth and calcification result from uncoupled physiological processes in the soft coral *Litophyton arboreum*. *Marine Ecology Progress Series* 276: 85-92.

Thresher, R. E., 2009. Environmental and compositional correlates of growth rate in deep-water bamboo corals (Gorgonacea; Isididae). *Marine Ecology Progress Series* 397: 187-196.

Troffe, P. M., C. D. Levings, G. E. Piercey & V. Keong, 2005. Fishing gear effects and ecology of the sea whip *Halipterus willemoesi* (Cnidaria: Octocorallia: Pennatulacea) in British Columbia, Canada: preliminary observations. *Aquatic Conservation: Marine and Freshwater Ecosystems* 15: 523-533.

Vinogradov, G. M., 2000. Growth rate of the colony of a deep-water gorgonian *Chrysogorgia agassizi*: In situ observations. *Ophelia* 53: 101-103.

Walker, T. & G. Bull, 1983. A newly discovered method of reproduction in gorgonian coral. *Marine Ecology Progress Series* 12: 137-143.

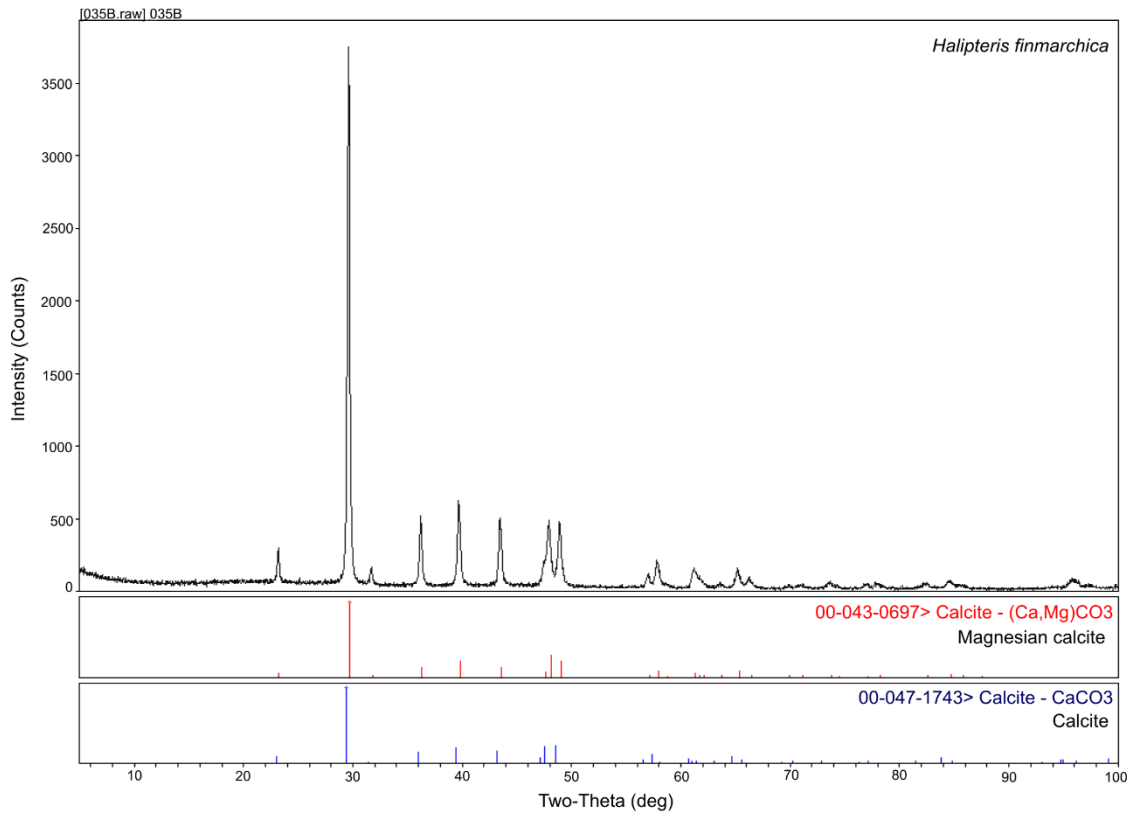
Wallace, S. & David Suzuki Foundation, 2007. Dragging our assets: toward an ecosystem approach to bottom trawling in Canada. David Suzuki Foundation, Vancouver, B.C.

- Walther, B. D., M. J. Kingsford, M. D. O'Callaghan & M. T. McCulloch, 2010. Interactive effects of ontogeny, food ration and temperature on elemental incorporation in otoliths of a coral reef fish. *Environmental Biology of Fishes* 89: 441-451.
- Walther, B. D. & S. R. Thorrold, 2006. Water, not food, contributes the majority of strontium and barium deposited in the otoliths of a marine fish. *Marine Ecology Progress Series* 311: 125-130.
- Wareham, V. E. & E. N. Edinger, 2007. Distribution of deep-sea corals in the Newfoundland and Labrador region, Northwest Atlantic Ocean. *Bulletin of Marine Science* 81: 289-313.
- Watanabe, S., A. Metaxas, J. Sameoto & P. Lawton, 2009. Patterns in abundance and size of two deep-water gorgonian octocorals, in relation to depth and substrate features off Nova Scotia. *Deep Sea Research Part I: Oceanographic Research Papers* 56: 2235-2248.
- Weber, J. N., 1973. Incorporation of strontium into reef coral skeletal carbonate. *Geochimica et Cosmochimica Acta* 37: 2173-2190.
- Weinbauer, M. G., F. Brandstätter & B. Velimirov, 2000. On the potential use of magnesium and strontium concentrations as ecological indicators in the calcite skeleton of the red coral (*Corallium rubrum*). *Marine Biology* 137: 801-809.
- Williams, G. C., 1995. Living genera of sea pens (Coelenterata: Octocorallia: Pennatulacea): illustrated key and synopses. *Zoological Journal of the Linnean Society* 113: 93-140.

Wilson, M. T., A. H. Andrews, A. L. Brown & E. E. Cordes, 2002. Axial rod growth and age estimation of the sea pen, *Halipteris willemoesi* Kölliker. *Hydrobiologia* 471: 133-142.

Yesson, C., M. L. Taylor, D. P. Tittensor, A. J. Davies, J. Guinotte, A. Baco, J. Black, J. M. Hall-Spencer & A. D. Rogers, 2012. Global habitat suitability of cold-water octocorals. *Journal of Biogeography* 39: 1278-1292.

Appendix 2-1 X-Ray Diffraction analysis for the carbonate portion of the axis in *Halipterus finmarchica*. Overlap between the axis in *H. finmarchica* axis (black), magnesian calcite (red), and calcite (blue). Note that the axis of *H. finmarchica* follows the same pattern as magnesian calcite.



3. Size metrics, and estimates of age and growth rates in one of the tallest known sea pens: *Umbellula encrinus* (Cnidaria: Pennatulacea) from Baffin Bay²

Abstract

Umbellula encrinus is a deep-water sea pen commonly found in Baffin Bay (between Greenland and Canada). It can reach tall sizes (~2 m) and in this region it has often been caught as fisheries bycatch. In this study our main objectives were to estimate longevity and growth rates in this species, and to investigate relationships between estimated growth rates and environmental variables in colonies from Baffin Bay. Additionally, video-surveys, and fisheries and scientific bycatch data were used to estimate the size structure and abundance of *U. encrinus* in the region. Longevity was determined by visually counting the number of growth rings seen in the internal skeleton (axis) of *U. encrinus*, and radial and linear growth rates were calculated based on the estimated longevities and on axis radius (radial growth) and colony height (linear growth). ¹⁴C analyses and trace element microanalysis were performed aiming to identify patterns that could indicate growth ring formation periodicity. *U. encrinus* had the highest relative abundance at Scott Inlet (~22 colonies/km), and its size structure did not show any strong patterns, probably due to a limited sample size for most areas (N_{range}= 3-16). The ¹⁴C analysis suggests that *U. encrinus* performs similarly to other deep-water octocorals in the

²To be submitted to the Canadian Journal of Fisheries and Aquatic Sciences.

Northwest Atlantic, which lay down rings annually. Average number of rings ranged from 2 to 68. Growth rates averaged $0.067 \text{ mm}\cdot\text{yr}^{-1}$ (radial rates) and $4.53 \text{ cm}\cdot\text{yr}^{-1}$ (linear rates). The analysis of growth rates in relation to environmental factors revealed significant relationships between radial growth rates and temperature, depth, and surface salinity. *U. encrinus* is a long-lived vulnerable sea pen. A better understanding of its ecology and distribution patterns in Baffin Bay is vital for the survival and appropriate management of this species in the region.

3.1 Introduction

Umbellula Gray, 1870 is a genus of deep-water sea pens of worldwide distribution. They have an elongated stalk, a crown of polyps restricted to the distal extremity of the colony, and a proximal peduncle that anchors the colony in soft substrates (Williams, 1995). Some species in the genus can reach large sizes (e.g. ~2 m in height) (Jørgensen et al., 2015, this study) supported by an internal calcified skeleton (axis) where growth rings can be identified (Ellis, 1753, this study).

Umbellula encrinus Linnaeus, 1758 is a species of boreal/polar distribution (Broch, 1956). In the Northwest (NW) Atlantic, it is the sea pen species showing the northernmost distribution, having been recorded up to northern Baffin Bay (Broch, 1956, 1958). It has been recorded in the Newfoundland region (Wareham, 2009), and at the Mid-Atlantic ridge (Molodtsova et al., 2008, Mortensen et al., 2008). It is also abundant in Norwegian waters (Buhl-Mortensen et al., 2012, 2014), and in the Barents Sea, where it is considered highly vulnerable to bottom trawling (Jørgensen et al., 2015).

As with other deep-sea corals, these sea pens are frequently caught as fisheries bycatch (Wareham & Edinger, 2007, Jørgensen et al., 2015). At least since the 18th century, colonies of *U. encrinus* inhabiting great depths at remote regions have been exposed to fishing gear. In fact, the first known mention of *Umbellula* dates from 1753, based on samples collected near Greenland (74° N, ~430 m), during a whaling operation that recovered colonies (Ellis, 1753).

In certain areas of Baffin Bay (between Greenland and the Canadian Archipelago), *U. encrinus* might be present in high densities. The Danish Ingolf Expedition documented

dense occurrences of *Umbellula lindahli* K lliker, 1875 when trawling in the Umanak Fjord (West Greenland) (Mortensen, 1912). More recent reports also show that *U. encrinus* is commonly caught as fishing bycatch from trawling in both East (J rgensen et al., 2013) and West Baffin Bay (Wareham, 2009). During another recent exploratory fishery survey in Jones Sound and Qikiqtarjuaq (Baffin Bay) several colonies of *U. encrinus* were caught as longline bycatch (this study), again indicating that colonies in this area might be abundant.

Baffin Bay is partially covered with ice during almost the entire year, except for the months of August and September (Tang et al., 2004). Although the presence of ice limits fishing in the west side of the Bay, it still occurs in all months of the year on the Greenland side (NAFO division 1A), with the target species being Greenland Halibut *Reinhardtius hippoglossoides* and shrimp (<http://www.nafo.int/data/frames/data.html>).

The conspicuous presence of *U. encrinus* in soft bottom communities in Baffin Bay, and their wide bathymetric distribution, added to their vulnerability to different types of fishing gear in an increasingly fished area (e.g. Christiansen et al., 2014), raise concerns regarding their overall susceptibility to damage. Recently, J rgensen et al. (2015) considered *U. encrinus* in the Barents Sea as a highly vulnerable species that needs more awareness.

Their attainable large sizes suggests that they might be long-lived, and as other cold-water corals they might be slow-growing (Wilson et al., 2002, Sherwood & Edinger, 2009, Chapter 2). Furthermore, the possibility of being found in high densities highlights their potential as vulnerable marine ecosystems (VMEs) and habitat for other species (e.g.

Baillon et al., 2012), as some sea pens are known to form large fields (Brodeur, 2001, Baker et al., 2012, Davies et al., 2014, Porporato et al., 2014).

In this study our objectives were to describe the size structure, and estimate age and growth rates for *U. encrinus* from West Baffin Bay by using samples obtained as bycatch from scientific trawl surveys, experimental fishing bycatch, as well as video data sampled using a remotely operated vehicle (ROV). Furthermore, relationships between growth rates and environmental variables were also investigated. Because growth ring formation periodicity has never been assessed in this species, we also assessed frequency of ring formation. Knowledge of their size-frequency distribution combined with data on longevity and growth rates can be used to assess population structure that can help to guide the appropriate management of the species, particularly in response to fisheries bycatch.

3.2. Material and methods

3.2.1 Sampling

The study area comprises eight sites in Baffin Bay: Northeast Baffin Bay, Jones Sound, Lancaster Sound mouth, Scott Inlet, Home Bay (head and mouth), Qikiqtarjuaq, Cape Dyer, and Cumberland Sound (Fig. 3-1, Table 3-1). Samples from Cape Dyer (N = 16), Home Bay (N = 4), and Lancaster Sound (N = 8) were obtained during multispecies trawl surveys conducted by Fisheries and Oceans Canada (DFO) from 2004-2012. Several of these colonies were incomplete in size, and therefore these were not included in the size structure portion of the study. In these surveys a Campellen 1800 shrimp trawl

with a 55 m door sweep area was employed. The trawls occurred at depths ranging 188-620 m, for ~15 minutes at a speed of 3 knots.

At Cumberland Sound four colonies (60.5-80 cm) were obtained during the multispecies trawl surveys described above, and another 18 colonies (53.5-102 cm) were obtained as longline bycatch during surveys conducted by DFO in August 2013 aboard the *Nuliajuk*, at average depths ranging 711-1203 m. Each longline set consisted of 800 hooks (size 14), spaced 3.66 m, deployed along 1.6 km.

Three additional colonies (75.5-96 cm) were collected in Cumberland Sound at 600 m, during a scientific trawl survey aboard the CCGS vessel *Amundsen*, in July 2013. An Agassiz trawl with a 1.5 m opening and a 40 mm net mesh size, with a 5 mm cod end liner was used in this survey. It was deployed for 3 minutes on average, at a speed of 1.5-1.7 knots. Colonies from Northeast Baffin Bay (N= 6, 87-158.5 cm) were also collected aboard the *Amundsen* in October 2015, using a beam trawl with an opening of 3 m², and a 0.95 cm cod end mesh for 20 minutes, at an average speed of 2.4 knots.

Samples from Jones Sound (N= 95, 11-230 cm) and Qikiqtarjuaq (N= 23, 97-210) were obtained as longline bycatch during an exploratory turbot fishery. Surveys were conducted aboard the Arctic Fisheries Alliance (AFA) vessel *Kiviug I*, in September and October 2014 at each site, respectively. Each longline string consisted of ~1050 hooks (mixed sizes 12, 14, and 16), spaced ~1.8 m, along ~4 km in Jones Sound, and ~8 km in Qikiqtarjuaq. Average depths (start and end of a set) were 567-764 m in Jones Sound, and 582 m in Qikiqtarjuaq. Two additional samples (113.5-122.5 cm) from Qikiqtarjuaq were obtained in October 2015 aboard the *Amundsen*, using the same Agassiz trawl specified in the previous paragraph.

Video data were obtained at Scott Inlet (N= 16), Home Bay (N= 5), Qikiqtarjuaq (N= 4), and Cape Dyer (N= 3). A Super-Mohawk (SuMo) ROV was deployed in July 2014 and in October 2015 aboard the CCGS *Amundsen*. The SuMo ROV has a high-definition camera (1Cam Alpha, Sub C Imaging, 24.1 megapixels) and it projects a pair of lasers 6 cm apart for size estimation. Colonies were opportunistically video-recorded along transects 0.94-2.7 km long, at depths ranging 475-750 m (Table 3-2). Camera average field of view (width) was 3.3 m.

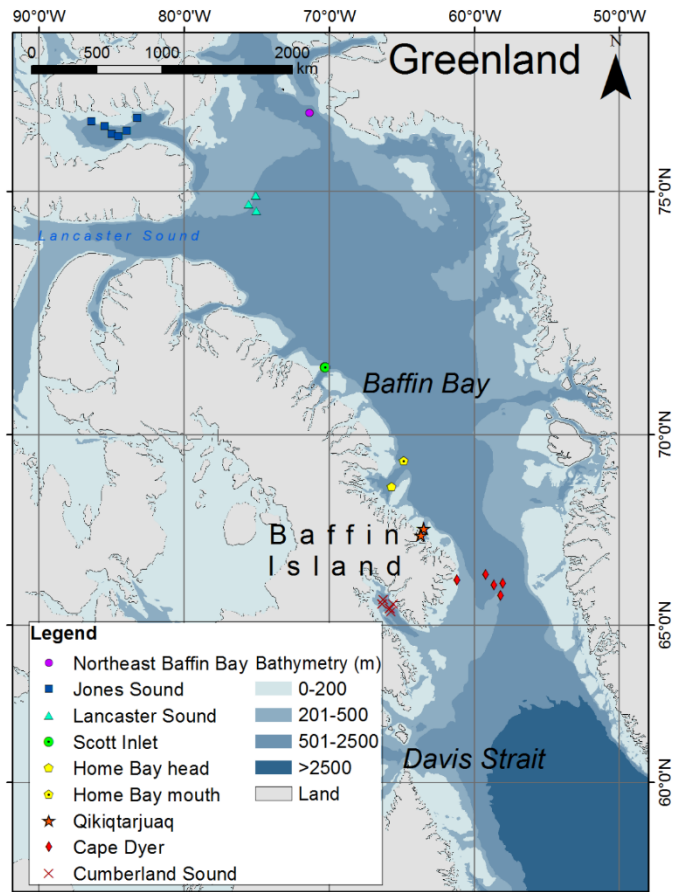


Figure 3-1. Map of study area.

Table 3-1. General sample information for colonies of *Umbellula encrinus* included in this study.

Sample	N growth	N size	N catch	Depth (m)	Latitude (N)	Longitude (W)	Location	Sampling method
127-132	6	6	6	670.5	76.3334	-71.3454	NE Baffin Bay	Beam trawl
JS0010 ¹	na	1	1	675.5	75.9370	-86.1857	Jones Sound	Longline
JS0011 ¹	na	5	5	579	76.0635	-86.1681	Jones Sound	Longline
JS0013_1	1	1	1	567.5	76.2041	-86.3950	Jones Sound	Longline
JS0015_1-9 ²	9	37	37	764	76.1180	-85.4886	Jones Sound	Longline
JS0017 ¹	na	3	3	678	76.0409	-85.414	Jones Sound	Longline
JS0021_1-2 ²	2	5	5	671	75.9942	-84.9828	Jones Sound	Longline
JS0023_1-5 ²	5	6	6	629	75.9515	-84.5241	Jones Sound	Longline
JS0025_1-13 ²	13	28	28	689	76.0469	-83.9489	Jones Sound	Longline
JS0027 ¹	na	2	2	834.5	76.1252	-83.0362	Jones Sound	Longline
JS0029_1-3 ²	3	7	7	622.5	76.2564	-83.2425	Jones Sound	Longline
028	1	1	3	505	74.7685	-75.5495	Lancaster Sound	Campelen trawl
029, 045, 047-048, 053	5	5	8	533	74.9332	-75.0570	Lancaster Sound	Campelen trawl
044	1	1	16	559	74.6559	-75.0045	Lancaster Sound	Campelen trawl
Extra_4 ¹	na	1	na	559	74.6559	-75.0045	Lancaster Sound	Campelen trawl
Video_SI ¹	na	16	na	475-600	71.5148	-70.2800	Scott Inlet	ROV survey
027, 042, 050, 052	4	4	8	468	68.7229	-65.7077	Home Bay	Campelen trawl
Video_HB ¹	na	5	na	700-750	69.3634	-64.8512	Home Bay	ROV survey
Qik0009_1_11 ²	11	23	23	582	67.6494	-63.4933	Qikiqtarjuaq	Longline
133-134	2	2	2	665	67.4693	-63.7143	Qikiqtarjuaq	Agassiz trawl
Video_QIK ¹	na	4	na	620-680	67.4742	-63.6929	Qikiqtarjuaq	ROV survey
030A-I, 037	10	3	10	188	66.2648	-61.1890	Cape Dyer	Campelen trawl
049A-B ¹	1	2	2	511	66.1308	-58.6533	Cape Dyer	Campelen trawl
051A-B ¹	1	2	2	551	65.8358	-58.2150	Cape Dyer	Campelen trawl
054	1	1	4	620	66.1692	-58.0342	Cape Dyer	Campelen trawl

Sample	N growth	N size	N catch	Depth (m)	Latitude (N)	Longitude (W)	Location	Sampling method
056 ¹	na	1	1	212	65.8110	-61.3600	Cape Dyer	Campelen trawl
Video_CD ¹	na	3	na	746-750	66.4133	-59.2185	Cape Dyer	ROV survey
041A ¹ , B ¹ , C	1	3	3	628	65.5915	-66.3235	Cumberland Sound	Agassiz trawl
055A ¹ , B ¹ , C, D ¹	1	4	6	488	65.5967	-65.5967	Cumberland Sound	Campelen trawl
081-087, 089	8	8	na	na	na	na	Cumberland Sound	Longline
088, 090, 092-094	5	5	na	1203	65.4707	-65.8133	Cumberland Sound	Longline
091	1	1	na	711	65.7273	-66.2723	Cumberland Sound	Longline
095 ¹	na	1	na	1095	65.3684	-65.7254	Cumberland Sound	Longline
Extra_1-3 ¹	na	3	na	na	na	na	Cumberland Sound	Longline
Total	92	200						

Latitude, longitude, and depth from samples obtained from trawling and longline are the average of a survey set (beginning and end).¹Not included in the growth study. ²Additional colonies from same station included in the size structure study.

Table 3-2. Specifications of ROV video-transects.

Site	Year	Depth (m)	Transect length (km)	Speed (knots)
Scott Inlet	2014	475-600	2.7	0.5
Home Bay	2014	700-750	2.2	0.5
Qikiqtarjuaq	2015	620-680	0.95	0.5
Cape Dyer	2015	746-750	0.94	0.5

3.2.2 Remark on species identification

Two species of *Umbellula* have been reported for the Northwest Atlantic: *U. encrinus* and *U. lindahli*, whose similarity has been discussed by some authors. Broch (1958) considered the Arctic *U. encrinus* an ecologically distinct geographical form of *U. lindahli*. Dolan (2008) suggested that *U. lindahli* is a junior synonym of *U. encrinus*. For the purposes of this study, our samples have been tentatively identified as *U. encrinus* based on the presence of a quadrangular axis, absence of sclerites in the polyps, stoutness, and geographical location. However, a revision of *Umbellula* species without sclerites is necessary in order to confirm species identity (Dr. G. Williams, personal communication).

3.2.3 Abundance and size-frequency distribution

A total of 200 colony height measurements were included in the size-frequency distribution study (Table 3-1), including data obtained from the video analysis (N= 28). Relative abundance was calculated by dividing the number of colonies (total catch from trawls, longlines, and video surveys) by surveyed distance (based on ship/ROV speed and survey duration). Density was calculated as the number of colonies per m² (area determined based on surveyed distance, speed, and opening width of trawls, and average

video field of view width). Abundance and density were only determined for samples of known catch (trawls and longline, Table 3-1).

Size frequency-distribution was determined by measuring specimens brought onboard and from video observations. Colonies were measured in their whole length, from the proximal tip to the tip of the polyparium (cluster of polyps) (Fig. 3-2), except in colonies where the polyparium was missing. Peduncle and rachis (stalk plus polyparium) size were also individually determined. A total of 95 colonies were measured for colony height *versus* peduncle height relationships, although only 85 were included in the statistical analysis due to missing information on depth (used as covariate). For the video analysis, colonies were only measured when the scaling lasers touched the colony or were touching the bottom immediately near the colony.

Because the peduncle of sea pens remains buried in the sediment, peduncle size could not be visualized in the videos. Therefore, it was estimated using a regression equation based on the relationship between rachis length and peduncle length calculated for the collected colonies in Baffin Bay ($R^2 = 0.76$, $N = 95$, this study). Thus, peduncle length was estimated from the following equation:

$$\text{Plength} = 0.1598 * (\text{rachis length}) + 4.3742$$

Final colony size for the specimens observed in video could then be determined by summing the measured rachis length to the estimated peduncle length.

We also investigated relationships between hook size and colony height for samples collected as longline bycatch.

3.2.4 Longevity and growth patterns

The internal axis of *U. encrinus* is a stiff but flexible stem whose carbonate portion is composed of magnesian calcite (Chapter 5). It was the structure used to estimate longevity and growth rates in the studied species. The axis was extracted from each colony and primarily cross-sectioned at the thickest portion (just above the peduncle) using a rock saw or a manual drill. This section was embedded in epoxy (Epofix™) for a second sectioning using an IsoMet® low speed saw (Buehler). Cross sections were polished either manually using a Buehler carbide grinding paper (grit 600/P1200) or a polishing machine (Struers TegraForce-5, to produce the high quality lapidary finish required for samples analyzed for trace elements), then visualized and photographed under UV light using a stereomicroscope. The UV light improves the visibility of growth rings by increasing the contrast between pale and dark rings. Ring visibility could be further improved by digitally adjusting photo color levels, using the software GIMP 2.8.8.

Because the axis of *U. encrinus* is squared and four-lobed, rings from each of the four lobes were counted and averaged. The software imageJ (Schneider et al., 2012) was used to measure axis radius and area. Radial growth rates for *U. encrinus* were determined as the radius of the four lobes averaged, divided by the average number of rings. Radial rates were determined rather than diametric growth rates (e.g. Wilson et al., 2001, Chapters 2 and 4) because of the four-fold symmetry of the axis in this species. Linear growth rates (increment in vertical extension) were calculated as colony height divided by the average number of rings. Most colonies from Cape Dyer were incomplete in size, and these were not included in the analyses involving colony size.

A total of 92 colonies were used for the growth rates estimates (Table 3-1). In some colonies the axes had darker areas that make rings more difficult to visualize. For these colonies, although the number of rings was not estimated, radius and area could still be measured for relationships with colony height (N= 95).

Growth ring formation periodicity was assessed by using two different approaches. First we used the bomb-¹⁴C method, as an attempt to identify a peak in the ¹⁴C concentration, which corresponded to the peak in the oceanic ¹⁴C formed in the late 1960s and early 1970s in the Northwest Atlantic as a result of atomic bomb testing (Campana, 1997). Our second approach involved a trace element analysis that addressed the identification of patterns that could indicate cyclicity in the trace elements, which could be suggestive of ring formation periodicity.

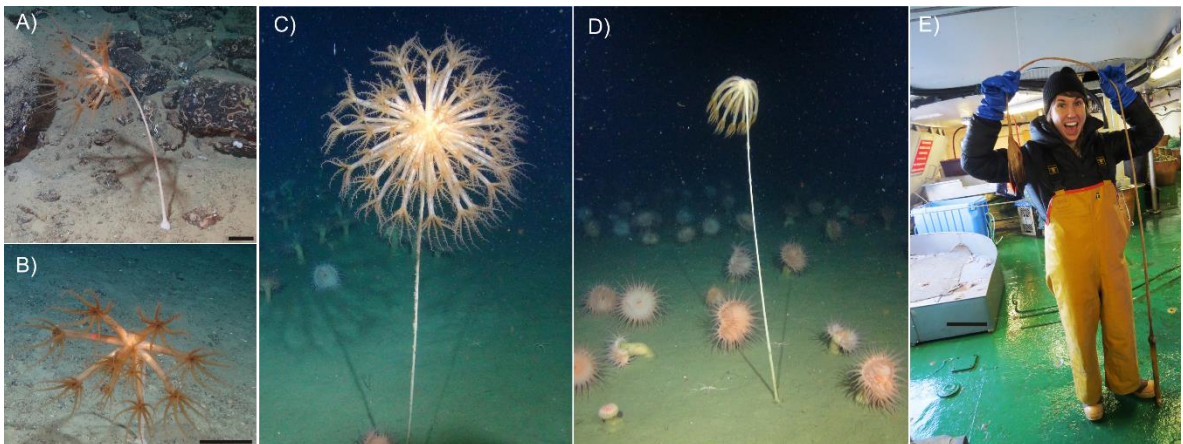


Figure 3-2. Colonies of *Umbellula encrinus*: *in situ* at Scott Inlet (A-B), at Qikiqtarjuaq (C-D), freshly caught sample from Jones Sound (E). Scale bars = 6 cm. Credits: ArcticNet-CSSF-DFO (A-D) and Laura Wheeland (E).

3.2.5 Bomb-¹⁴C analysis

Bomb-¹⁴C analysis was performed in the axis of one colony from Jones Sound (sample JS0013_1), whose number of growth rings (i.e. longevity) suggested that it was alive before and during the peak in oceanic ¹⁴C in the early 1970s (see Results section). The axis of a single colony was analyzed because it was the only available sample estimated to be alive in the 1970s. Because of the thin axis diameter of sea pens in general, subsamples for ¹⁴C analysis were obtained from a longitudinal section of the axis. A piece of axis ~2.5 cm long was glued to a glass slide and longitudinally sectioned using an Isomet® Low Speed Saw. To avoid contamination between the sample and the glue, the axis was adhered with labelling tape, then glued to the slide using Krazy Glue™.

Subsamples from the core, middle, and outer regions of the axis were obtained mainly by milling the sample to a powder using an automated micromilling machine (New Wave Research MicroMill, CREAT, Memorial University of Newfoundland). The edge was more challenging for automated micromilling, therefore it was manually scraped using a blade. For the micromilling we used a drill bit diameter of 350 μm, milling at a depth of 45-50 μm, at a traverse speed of 900 μm/second. A minimum of ~3 mg per subsample was collected for this analysis.

Subsamples for ¹⁴C analysis were sent to the Center for Accelerator Mass Spectrometry at the Lawrence Livermore National Laboratory (California, USA). δ¹³C values are the assumed values according to Stuiver and Polach (1977). Radiocarbon concentration is given as Δ¹⁴C following the conventions of Stuiver and Polach (1977).

3.2.6 Trace elements analysis

A high spatial resolution analysis of Sr/Ca, Mg/Ca, Ba/Ca and Na/Ca was also performed across the axis of three colonies of *U. encrinus* (samples 028, 029, 030F) using a Cameca IMS 4f Secondary Ion Mass Spectrometer (SIMS) (CREAIT, Memorial University of Newfoundland). The polished cross sections mounted in epoxy were gold coated (300Å) prior to SIMS analysis. Transects started from the core, in the direction of the outermost region of the cross section. Transect lengths varied with the radius length, ranging 1.67-1.88 mm, with individual spots spaced 25 µm apart. Detailed procedures for the trace elements analysis are described in Aranha et al. (2014) and in Chapter 2.

It was difficult to visualize the sample core for colony 030F and the SIMS transect started in part of another lobe. For the comparison between number of rings and number of trace element ratios peaks we only show the data starting from the core, so we skipped the first 14 observations.

3.2.7 Environmental data

Relationships between environmental variables and growth rates and number of rings in *U. encrinus* were investigated. Latitude and depth were obtained during the surveys and represent the average of a survey set. Bottom temperature was retrieved from the World Ocean Database 2009 (Boyer et al., 2009), using the available data from similar depths and areas surrounding the sampled localities. Bottom temperature data for the northernmost stations was obtained from the Polar Data Catalogue (<https://www.polardata.ca/>), and additional data were obtained from the World Ocean

Atlas 2013 version 2 (Locarnini et al., 2013). Some samples had bottom temperature data for the day of collection, and these were added to the dataset.

Data on annual surface chlorophyll a, particulate organic carbon (POC) (a proxy for phytoplankton biomass) and sea surface temperature (SST) were downloaded from <http://oceancolor.gsfc.nasa.gov/> and extracted in ArcGIS 10.1 using Marine Geospatial Ecology Tools (Roberts et al., 2010). Chlorophyll a, POC and SST for the period of 2002-2014 were obtained from the Aqua Moderate Resolution Imaging Spectroradiometer Sensor (MODIS) L3 product database. Since chlorophyll a and POC are highly correlated, we limited the statistical analysis to chlorophyll a, and POC is only graphically shown to illustrate its relationship to growth rates. Because of the influence of ice in Baffin Bay, we also extracted chlorophyll a data for summer periods (21 June-20 September of the same year; 2003-2014). Spatial resolution was 9 km, with cell sizes of 1/12 geographic degree.

Surface salinity was obtained from the Simple Ocean Data Assimilation (SODA) database 2.2.4 for the years 1990-2010 (Carton & Giese, 2008). We used salinity for the month of July only, instead of annual data because of the influence of ice in Baffin Bay (partially covered with ice during almost the entire year, Tang et al., 2004). Data were downloaded from the National Center for Atmospheric Research website and extracted in ArcMap using Multidimension Tools. These data had a pixel resolution of 0.25° x 0.4°.

Ocean surface velocity data were obtained from the Ocean Surface Currents Analyses (OSCAR) project. Data were directly imported and extracted in ArcMap using the NOAA OSCAR tool in the Marine Geospatial Ecology Tools extension. These data

were used as an average of measurements taken every five days from the years 1992-2004, with a spatial resolution of 1/3 of a degree.

Depth, temperature, proxies of primary productivity, and current velocity were chosen because of the known overall importance of these variables to cold-water coral distribution (Roberts et al., 2009). Salinity was included as an opportunistic variable, without a specific hypothesis on its relationship to growth rates.

3.2.8 Data analysis

Descriptive statistics were used to characterize the size structure of the studied populations. Skewness (g_1) and kurtosis (g_2) were calculated to determine whether there was a dominant size class among the studied populations (e.g. Gori et al., 2011). Skewness, kurtosis, and their standard errors (SE) were determined using SPSS 23. Skewness and kurtosis are significant if g_1 and g_2 divided by their standard errors are > 2 . Significant skewness and kurtosis indicate the prevalence of a particular size class in the population (Sokal & Rohlf, 2012).

Relationships between peduncle length, percentage of peduncle, axis radius, axis area, and colony height were investigated through general linear models (GLMs) in RStudio version 0.99.484, by controlling depth using the R function *aov* (Type I sum of squares). For the analysis of axis area vs. colony height a quadratic polynomial regression was fitted, as this relationship is not linear. When investigating these relationships we pooled the data from all locations and only controlled for depth. The reason for that is that the influence of location on colony height might not be real, but rather an effect of

different sampling effort, gear, different year of collection, etc., across the sampling sites.

Depth was kept as a co-variate because it had no influence on the sample size.

In order to investigate relationships between growth rates and environmental variables, we first assessed whether there were significant relationships between growth rates and colony height. If a significant relationship was identified, we opted for performing simple regressions between growth rates and each environmental variable, while controlling for height using the *aov* function in R. This approach was chosen instead of analyzing the data by size classes in a multiple regression because of the reduced number of samples when including all environmental variables, as not all observations had all environmental data available. Interactions between bottom temperature and depth were included in the model having bottom temperature as the predictor variable.

To assess how well colony size and axis radius predict axis number of rings (i.e. age), we performed a cross-validation by generating a regression equation using only 75% of the data (training sample), with the other 25% being randomly isolated (hold-out sample) (cf. Kabacoff, 2015). A power equation was then applied to the 25% hold-out sample to estimate number of rings from colony height and axis radius. To test for significant differences between the number of observed and predicted rings in the hold-out dataset, a paired *t*-test was performed in R.

To compare trace element ratios between colonies, a Mann-Whitney test was performed, as residuals were clearly heteroscedastic. The relationship between Mg/Ca and Sr/Ca was assessed through a Pearson correlation.

Assumptions of linearity, homogeneity, normality, and independence of residuals were evaluated through the visual analysis of residual diagnostic plots for linear models in R (Kabacoff, 2015). Significance levels for all analyses were set at $\alpha = 0.05$. Error is shown as standard deviations, unless specified.

3.3. Results

3.3.1 Abundance and size-frequency distribution

Colony height based on measurements of 200 colonies ranged 10-248 cm, including those measured from specimens and video (Table 3-3, Fig. 3-3). At Northeast Baffin Bay a total of six colonies ranging between 87-159 cm in height were caught in the beam trawl, with a relative abundance of 3.3 colonies·km⁻¹, and a density of 0.0014 colonies·m⁻² (Fig. 3-4).

At Jones Sound, a total of 21 longline fishing sets were completed at average depths ranging 80-840 m, with colonies being caught in 10 sets, at depths ranging between 579-840 m. At this location, 95 colonies were caught in the longline hooks, yielding an abundance of 2.4 colonies·km⁻¹ (95 colonies in 40 km surveyed), and a density of 0.02 colonies·m⁻², with colony size ranging between 11-230 cm (Table 3-3). This abundance is inflated by a single set where 37 colonies were caught in 4 km of longlining (9.25 colonies·km⁻¹; Fig. 3-4). At Lancaster Sound a relative abundance of 11.5 colonies·m⁻² was estimated (Fig. 3-4), and a density of 0.0002 colonies·m⁻², with colony sizes ranging between 125-224 cm (Table 3-3).



Figure 3-3. Colonies of *Umbellula encrinus* in situ. Size cannot be indicated in all photos because the scaling lasers are not visible at these distances. Scale bars = 6 cm. Top-left photo shows a colony estimated to measure ~2 m. Credits: ArcticNet-CSSF-DFO.

At Qikiqtarjuaq a total of 25 colonies were caught in a single longline fishing set (~8 km long) at an average depth of 582 m, yielding a relative abundance of 3.1 colonies·km⁻¹, and a density of 0.003 colonies·m⁻² (Fig. 3-4). At this site, colony height ranged between 97-210 cm (Table 3-3).

Abundance and colony height were also estimated from the video surveys. At Home Bay, 17 colonies were observed along 2.2 km of video (Fig. 3-4). From these, only five colonies could be measured because the scaling lasers were not close enough to all observed colonies. These colonies were estimated to measure between 16-94 cm. Three of these colonies did not have polyps accounted for because it was not possible to measure them and in one colony the polyparium was missing (and assumed to be from *U. encrinus*, as no other similar sea pens are found in the region). Colonies obtained from trawling at Home Bay showed a relative abundance of 3.6 colonies·km⁻¹, and a density of 0.002 colonies·m⁻².

At Scott Inlet, 59 colonies were observed in ~2.7 km of video (~22 colonies·km⁻¹, 0.007 colonies·m⁻²; Fig. 3-4). From these, 16 colonies could be measured, with sizes estimated to range 21-103 cm (Table 3-3). At Qikiqtarjuaq, eight colonies were observed along 954 m of video transect, yielding a density of 0.003 colonies·m⁻² (Fig. 3-4). Only four colonies could be measured, with colony height estimates ranging 83-193 cm. At Cape Dyer, ten colonies were observed along 935 m of video transect, yielding a density of 0.003 colonies·m⁻² (Fig. 3-4), but only three colonies could be measured, whose heights ranged between 165-292 cm.

At Cumberland Sound colony height ranged 54-201 cm, with relative abundances of 3.8 and 4.3 colonies·km⁻¹ (Campelen and Agassiz trawl, respectively). Densities were

0.0001 and 0.013 colonies·m⁻², respectively. No sea pen fields were observed in the video-surveyed sites.

The descriptive statistics showed that colonies from Cape Dyer had significant positive skewness and kurtosis, while samples from Jones Sound were close to significance, but with negative values (Table 3-3, Fig. 3-5).

3.3.2 Hook size versus colony size

There were no trends between hook size and size of colonies caught in Qikiqtarjuaq and Jones Sound, with all three hook sizes (12, 14, and 16) catching both short and tall sea pens (Fig. 3-6). At Cumberland Sound hook size was 14, and colonies 53.5-102 cm long were caught in the hooks. However, the bycatch obtained in the Cumberland Sound surveys was not limited to the samples included in this study, such that we cannot exclude the possibility of smaller and larger sized colonies being also caught with this hook size at this site.

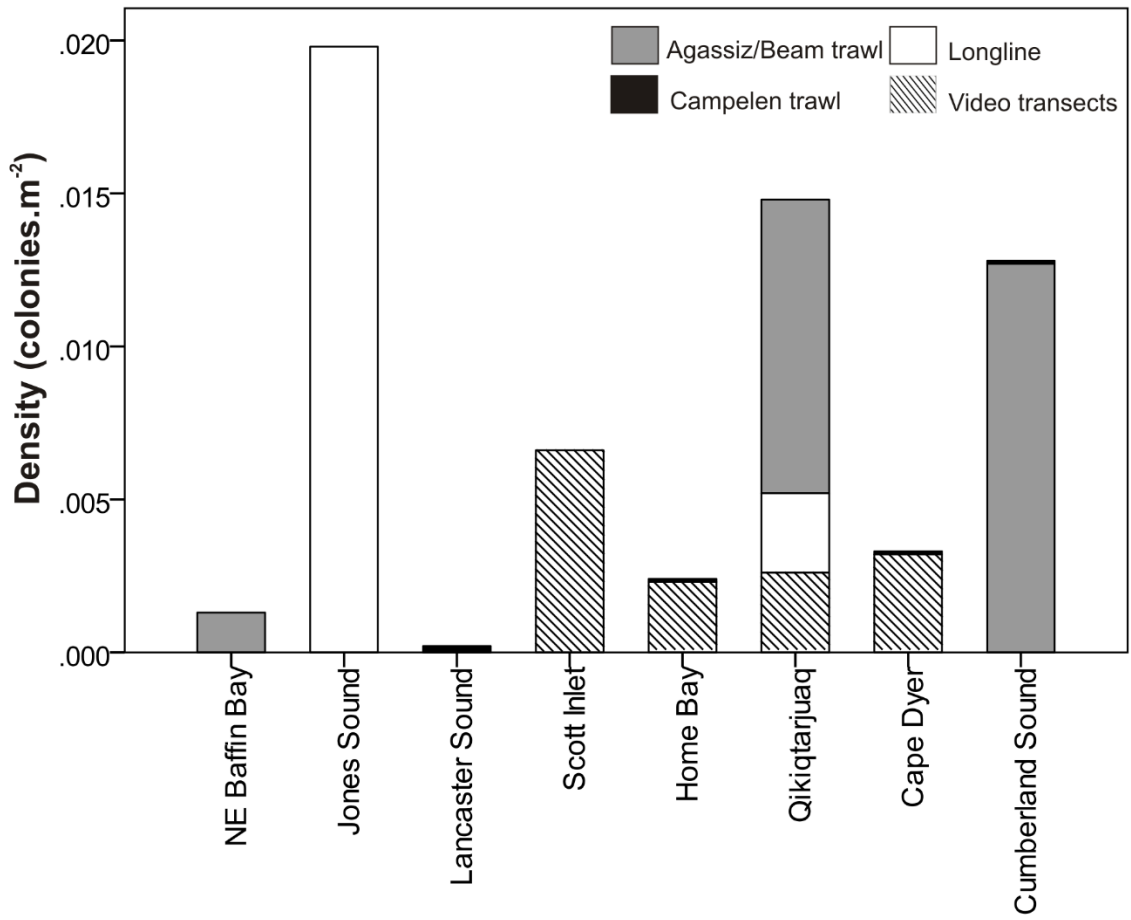


Figure 3-4. Density of *Umbellula encrinus* colonies from trawl, longline and video surveys by site in Baffin Bay (Left to right: north-south).

Table 3-3. Descriptive statistics for the size structure of *Umbellula encrinus* from Baffin Bay.

Location	N	Video	Total measured	Size range (cm)		Skewness		Kurtosis			
				Min	Max	g1	SE g1	Sig g1 (>2)	g2	SE g2	Sig g2 (>2)
NE Baffin Bay	6	na	6	87	158.5	-0.01	0.85	-0.01	-2.29	1.74	-1.32
Jones Sound	95	na	95	11	230	-0.43	0.25	-1.72	-0.95	0.49	-1.95
Lancaster	8	na	8	124.5	223.5	0.46	0.75	0.61	-0.38	1.48	-0.26
Scott Inlet	na	59(16)	16	20.4	108	0.22	0.56	0.39	-1.08	1.09	-0.99
Home Bay	4	17(5)	9	16.4	248	0.15	0.72	0.22	-2.34	1.40	-1.67
Qikiqtarjuaq	25	8(4)	29	83	210	0.32	0.43	0.73	-0.44	0.85	-0.52
Cape Dyer	16(9)*	10(3)	12	81	177	1.94	0.64	3.04	4.13	1.23	3.36
Cumberland	25	na	25	53.5	102	0.27	0.46	0.57	-0.91	0.90	-1.01
Total	170	28	200								

Numbers in parentheses represent measured specimens. Not all colonies were used in the growth study.*7 colonies incomplete in size (not measured). Significant kurtosis and skewness shown in bold.

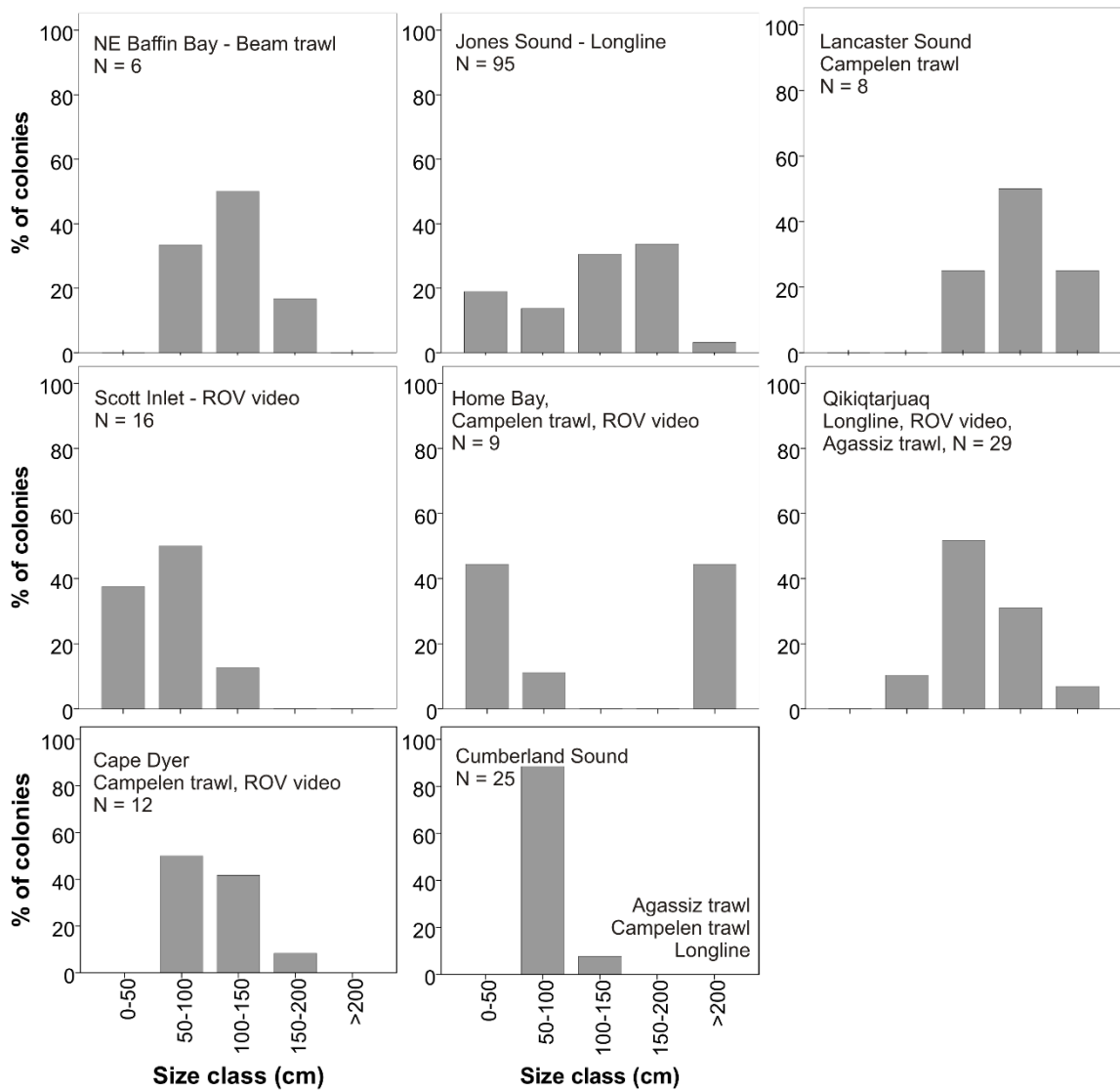


Figure 3-5. Size frequency distribution of *Umbellula encrinus* from Baffin Bay.

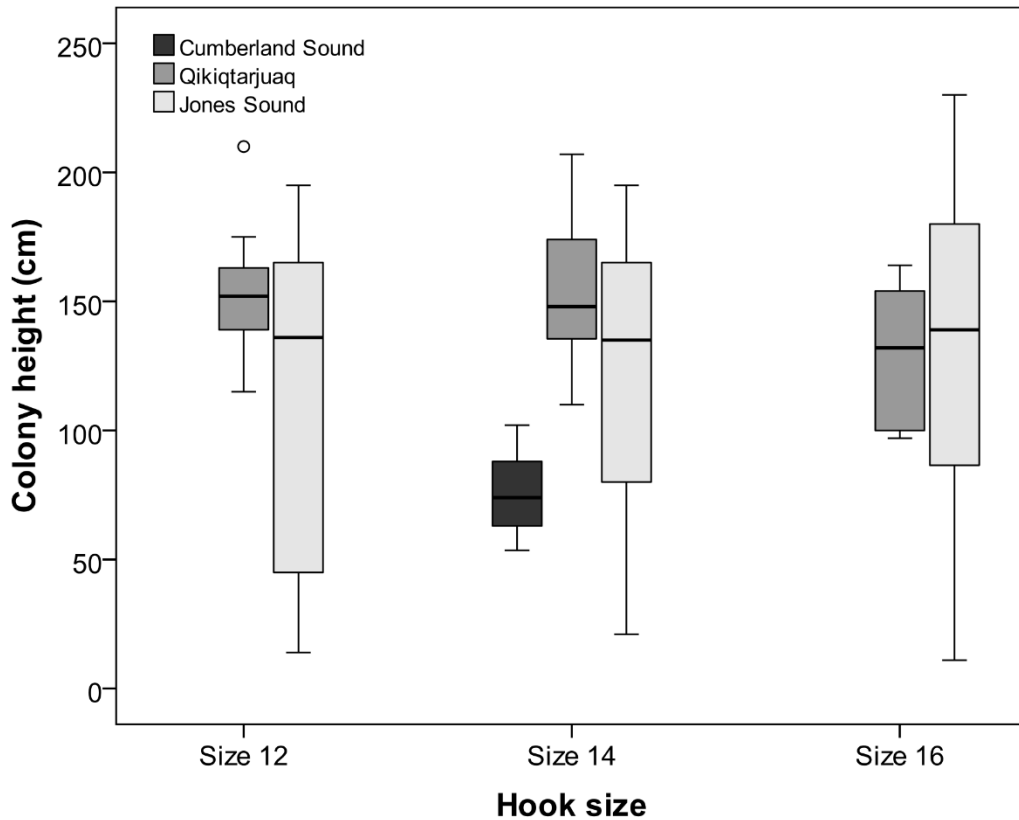


Figure 3-6. Colony height in relation to hook size for samples of *Umbellula encrinus* caught as longline bycatch at Cumberland Sound, Qikiqtarjuaq, and Jones Sound (Baffin Bay). In Cumberland Sound only hook size 14 was used. Black horizontal bars inside the boxes represent the median, boxes are limited by minimum and maximum values, and circles are outliers.

3.3.3 Colony and axis metrics in relation to colony size

There was a strong positive relationship between peduncle length and total colony height (Fig. 3-7A, $F= 381.1$, $p< 2e-16$, $N = 85$), but a negative relationship was observed between percentage of peduncle and colony height (Fig. 3-7B, $F= 15.52$, $p< 0.0002$, $N = 85$). There were no significant interactions between colony height and water depth.

When investigating the relationship between axis radius and colony height there was a positive trend (Fig. 3-7C), but a significant interaction between colony height and depth was identified (F= 4.388, p= 0.04, N= 88). The same was observed for the relationship between axis area and colony height (Fig. 3-7D, F= 4.991, p= 0.03, N= 88).

3.3.4 Bomb-¹⁴C analysis

The average number of rings for the colony analyzed for ¹⁴C was 68 (average of four lobes). The results from the bomb-¹⁴C analysis showed that in all subsamples from the single analysed colony $\Delta^{14}\text{C}$ values were pre-bomb (negative values), showing an increase from the core to the edge of the sample (Fig. 3-8, Table 3-4). The ¹⁴C curve for *U. encrinus* follows a similar pattern to the observed in the calcite of the bamboo coral *Keratoisis grayi* (Wright, 1869) (published as *K. ornata*) from the SW Grand Banks (NW Atlantic), but differs from the gorgonin portion of *K. grayi* and the gorgonian *Primnoa resedaeformis* (Gunnerus, 1763) (Fig. 3-8).

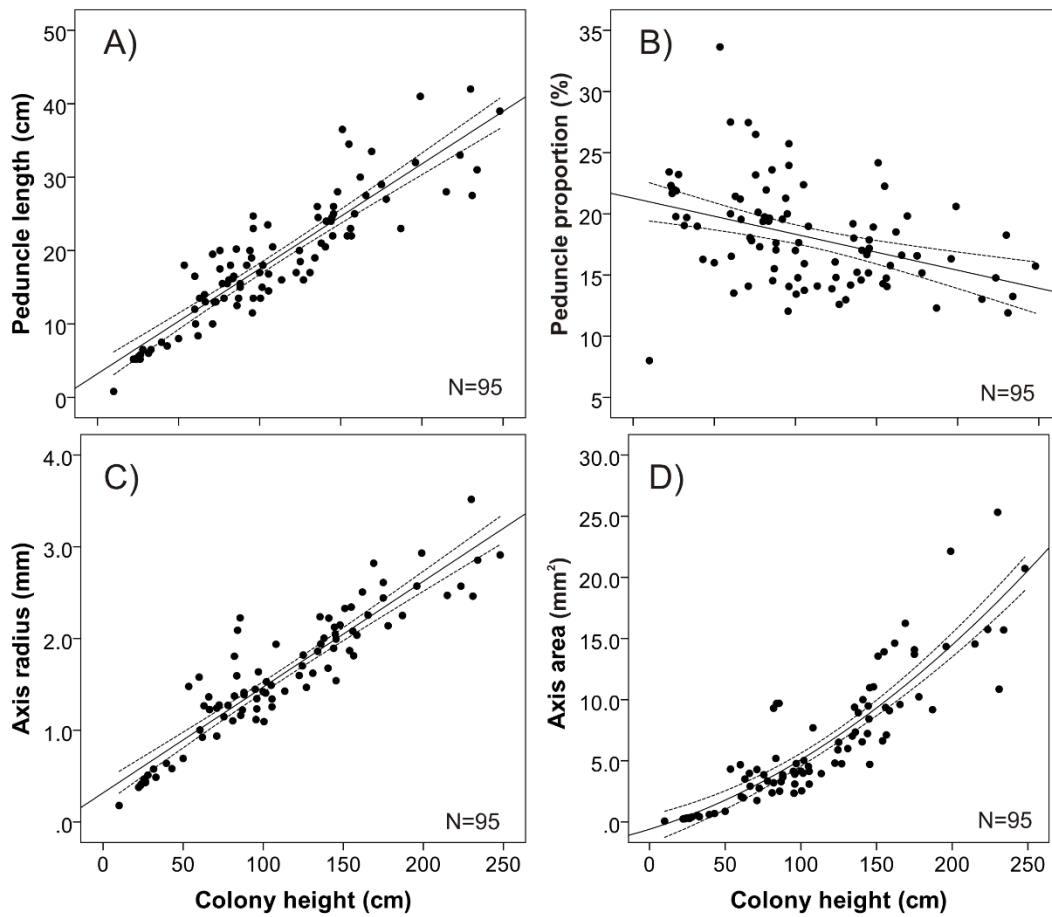


Figure 3-7. Peduncle and axis metrics in relation to colony size in *Umbellula encrinus* from Baffin Bay: A) peduncle length, B) peduncle proportion, C) axis radius, D) axis area. Fit lines and confidence intervals (dashed lines) are for reference only, as the regression equation also included depth as a covariate. All observations shown, including the ones not included in the statistical analysis due to missing depth information.

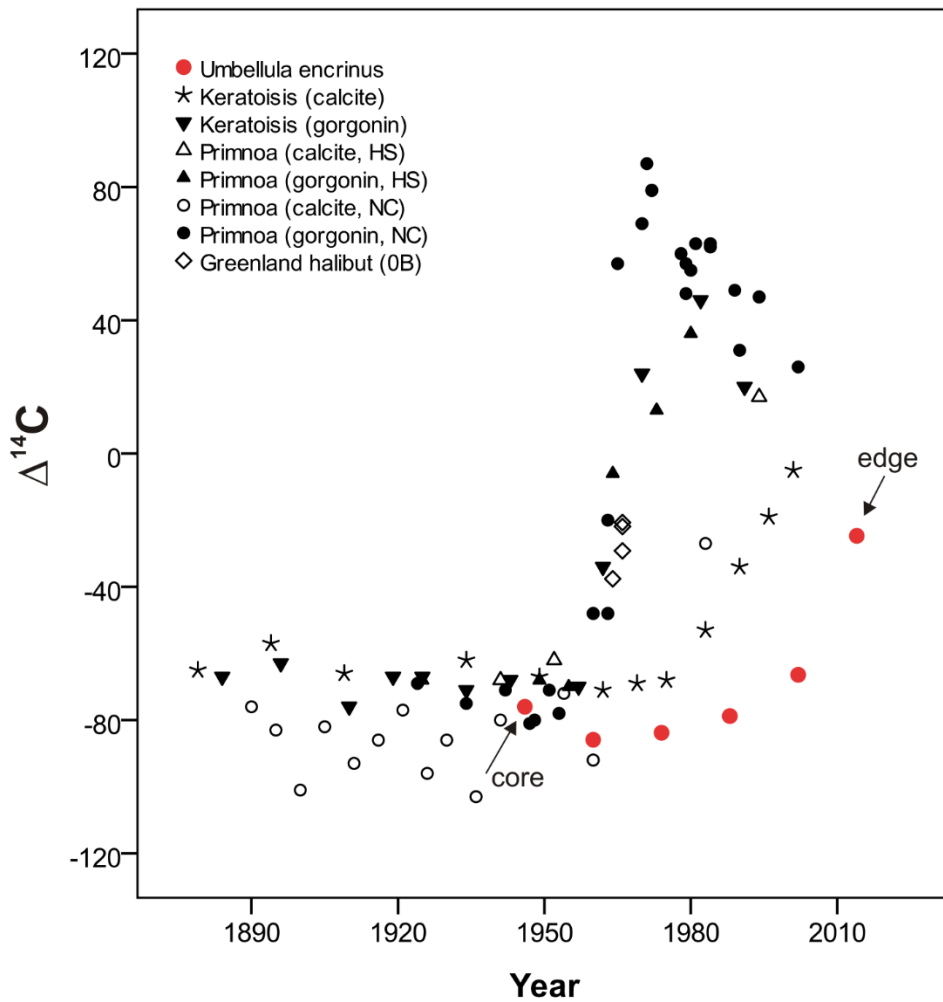


Figure 3-8. $\Delta^{14}\text{C}$ for the axis of a live-collected colony of *Umbellula encrinus* sampled in 2014 at Jones Sound (red circles) in relation to year. The data is overlaid with $\Delta^{14}\text{C}$ data from the calcite and gorgonin from *Keratoisis grayi* from the SW Grand Banks (Sherwood et al., 2008), calcite and gorgonin from *Primnoa resedaeformis* from the Hudson Strait (HS) and NE Channel (NC) (Sherwood et al., 2008), and calcite from the otoliths of the Greenland halibut *Reinhardtius hippoglossoides* (Walbaum, 1792) from NAFO zone 0B (Treble et al., 2008).

Table 3-4. $\Delta^{14}\text{C}$ values from the axis of a live-collected colony of *Umbellula encrinus* sampled in 2014. The year associated to the core region was determined as the average number of rings visually counted (N= 68) subtracted from 2014. The years for the intermediate regions were estimated as the number of rings between core and edge, divided by the number of regions.

Sample id	Region	Year	CAMS #	$\Delta^{14}\text{C}$	\pm
umbel_13_1_core	Core	1946	171230	-76.0	3.5
umbel_13_1_2	Middle	1960	171231	-85.9	3.8
umbel_13_1_3	Middle	1974	171232	-83.8	3.7
umbel_13_1_4	Middle	1988	171233	-78.8	3.7
umbel_13_1_5	Middle	2002	171234	-66.4	3.6
umbel_13_1_edge	Edge	2014	171235	-24.7	3.8

3.3.5 Trace element analysis

The trace element analysis performed in the axes of three *U. encrinus* colonies showed that the number of peaks in all four element ratios is comparable to the number of rings visually determined (Table 3-5, Fig. 3-9). Average trace element ratios ranged 0.013 mmol·mol⁻¹ for Ba/Ca to 89.95 mmol·mol⁻¹ for Mg/Ca (Table 3-5).

Table 3-5. Trace elements distribution in the axes of three *Umbellula encrinus* colonies.

Sample	Sr/Ca	Mg/Ca	Ba/Ca	Na/Ca	Mg/Ca vs Sr/Ca	Rings	Peaks (Mg/Ca)	Peaks (Sr/Ca)
028	1.37-1.85	84.2-122.8	0.006-0.05	21.3-88.4	-0.72	28	24	25
029	1.47-1.95	78.5-126.9	0.007-0.06	31.2-71.9	-0.72	23	21	23
030F	1.62-2.59	59.6-96.4	0.006-0.02	28.8-53.1	-0.50	31	24	25
Average	1.79	90	0.013	36.8	-	-	-	-
SD	0.09	9.59	0.03	2.69	-	-	-	-

Ratios are in mmol·mol⁻¹. Values in bold are statistically significant at $\alpha=0.05$.

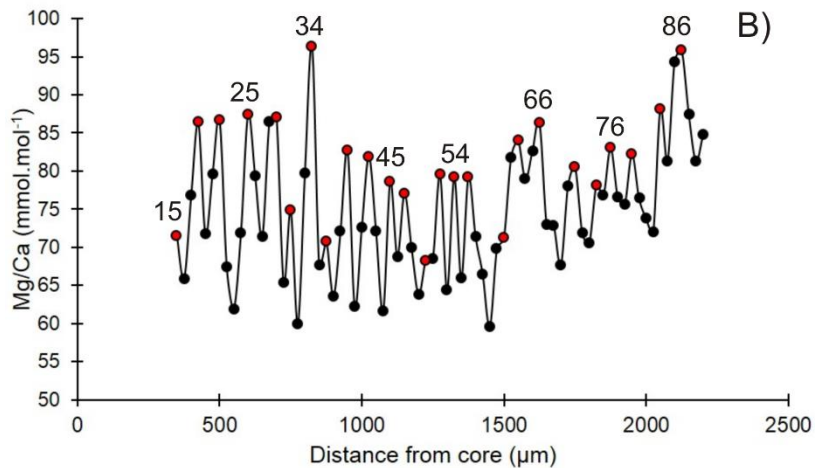
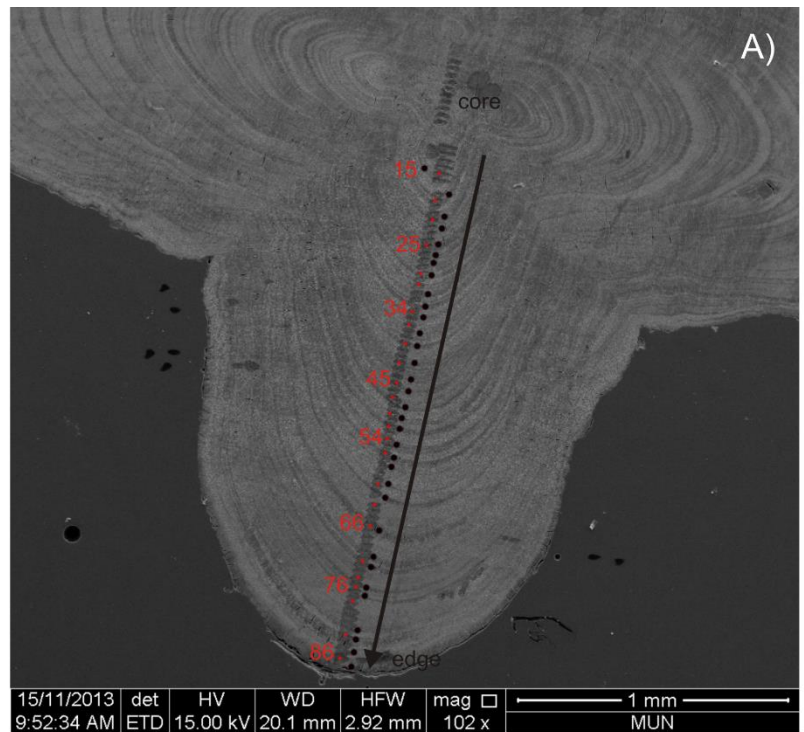


Figure 3-9. Growth rings and Mg/Ca profile in the axis of *Umbellula encrinus*: A) Cross section of the axis seen under Scanning Electron Microscope (SEM) showing SIMS transect, growth rings (indicated by black dots), and Mg/Ca peaks (red dots); B) Mg/Ca peaks with distance from core, with red dots corresponding to red dots shown in A.

Trace element/Ca ratios did not show any strong trends in relation to distance from core (Fig. 3-10).

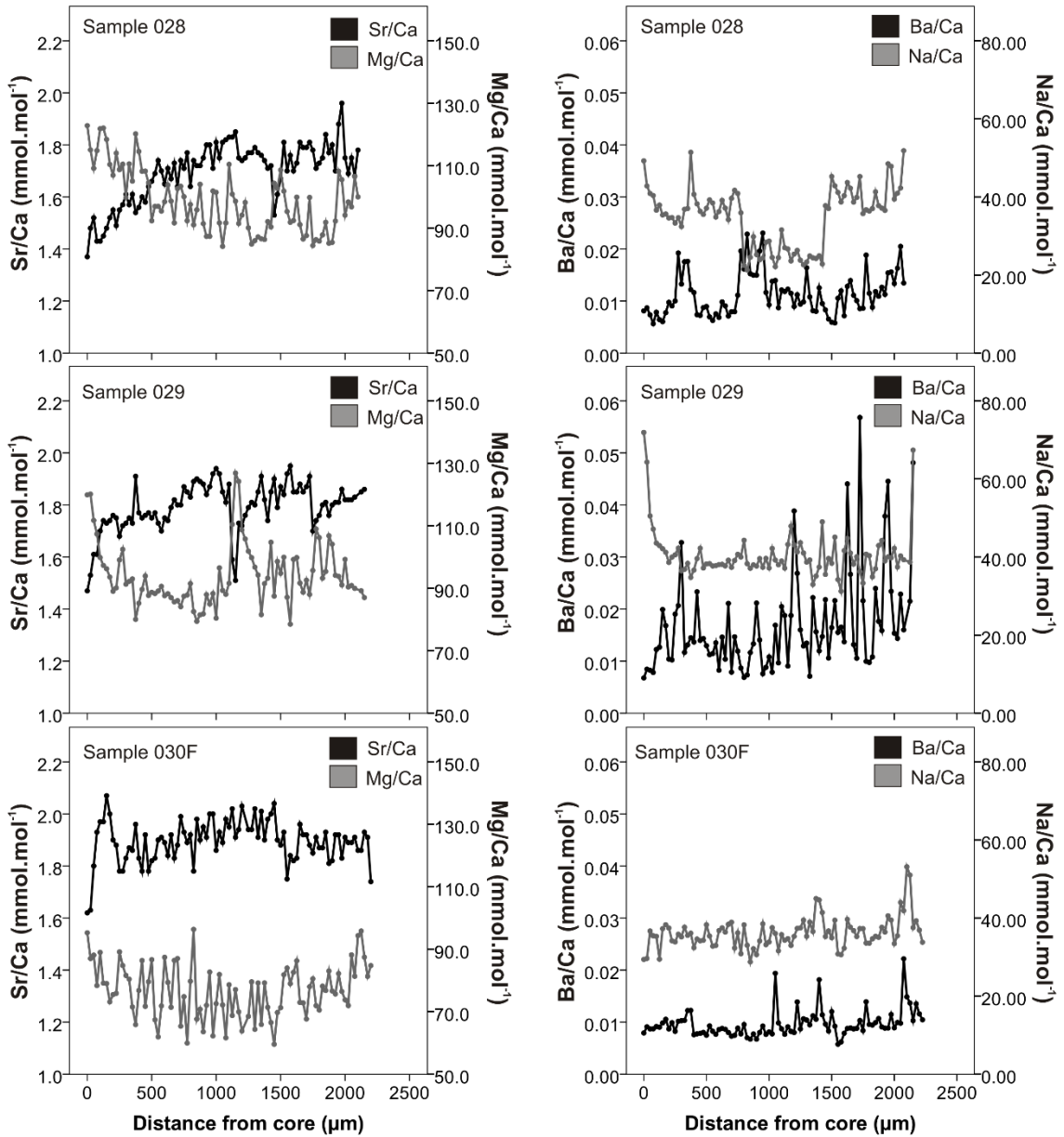


Figure 3-10. Trace elements distribution with distance from core along the axis radius of three *Umbellula encrinus* colonies (samples 028, 029, and 030F).

Mg/Ca and Sr/Ca were negatively correlated in all three samples (sample 028, $r = -0.72$, $N = 85$; sample 029, $r = -0.72$, $N = 86$; sample 030, $r = -0.5$, $N = 89$; Fig. 3-11). The results from the Mann-Whitney test showed that ratios were significantly different between colonies for all four elements, except for Na/Ca between samples 028 and 030F (Table 3-6).

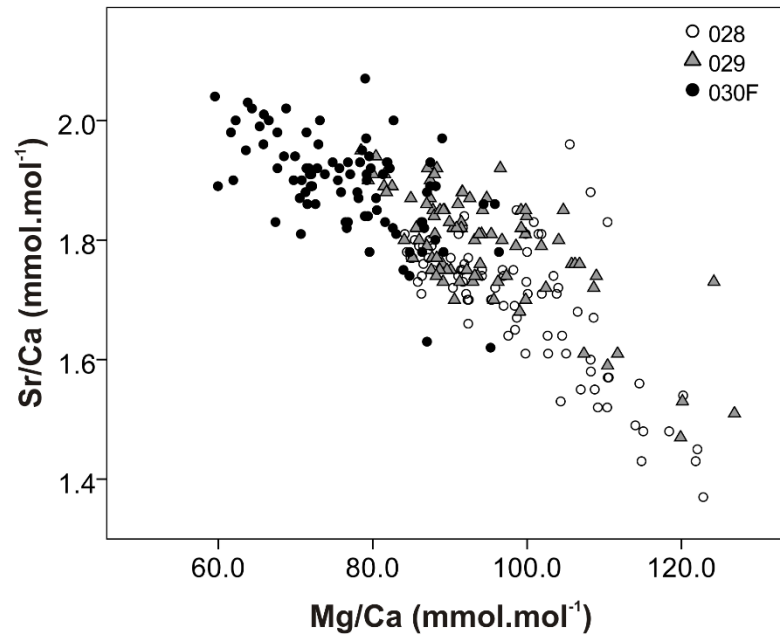


Figure 3-11. Relationship between Mg/Ca and Sr/Ca ratios in the axis of *Umbellula encrinus* for all three analyzed samples.

Table 3-6. Results from the Mann-Whitney test on the comparison of trace element ratios between colonies of *Umbellula encrinus*.

Samples	Sr/Ca		Mg/Ca		Ba/Ca		Na/Ca	
	W	p	W	p	W	p	W	p
028 vs 029	1730.5	2.7e-09	4709	1.14e-03	2185	5.6e-06	2189.5	6.0e-06
028 vs 030F	438.5	< 2.2e-16	7355	< 2.2e-16	4718	7.7e-03	3910	0.80
029 vs 030F	1432	5.2e-13	7182.5	< 2.2e-16	6297	6.9e-13	6183	7.7e-12

Values in bold are statistically significant at $\alpha=0.05$

3.3.6 Longevity and growth rates

The axis of *U. encrinus* is squared, with a four-fold symmetry where rings can be observed in cross section (Fig. 3-12).

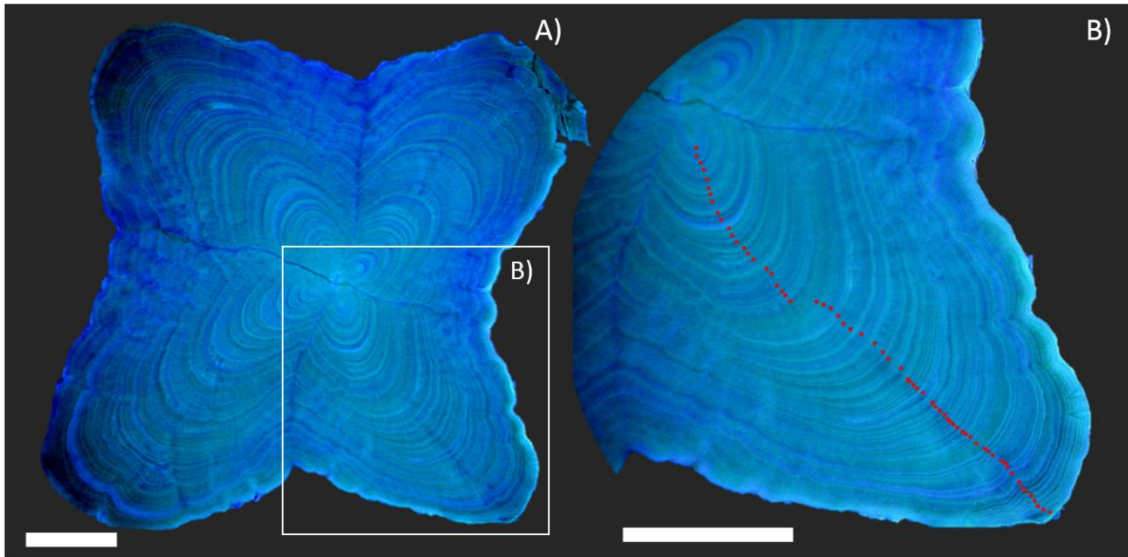


Figure 3-12. Cross section of the internal axis of *Umbellula encrinus* seen under UV light (stereomicroscope). Red dots indicate growth rings. Scale bars = 1 mm.

The average number of growth rings for all analyzed colonies ranged 2-68. Based on our ^{14}C analysis we consider rings to represent years; therefore radial growth rates for *U. encrinus* averaged $0.067 \pm 0.015 \text{ mm}\cdot\text{yr}^{-1}$, with linear growth rates averaging $4.5 \pm 1.2 \text{ cm}\cdot\text{yr}^{-1}$.

No trends regarding growth rates or number of rings in relation to location were observed, with most sites showing both old/young as well as slower/faster growing colonies (Fig. 3-13).

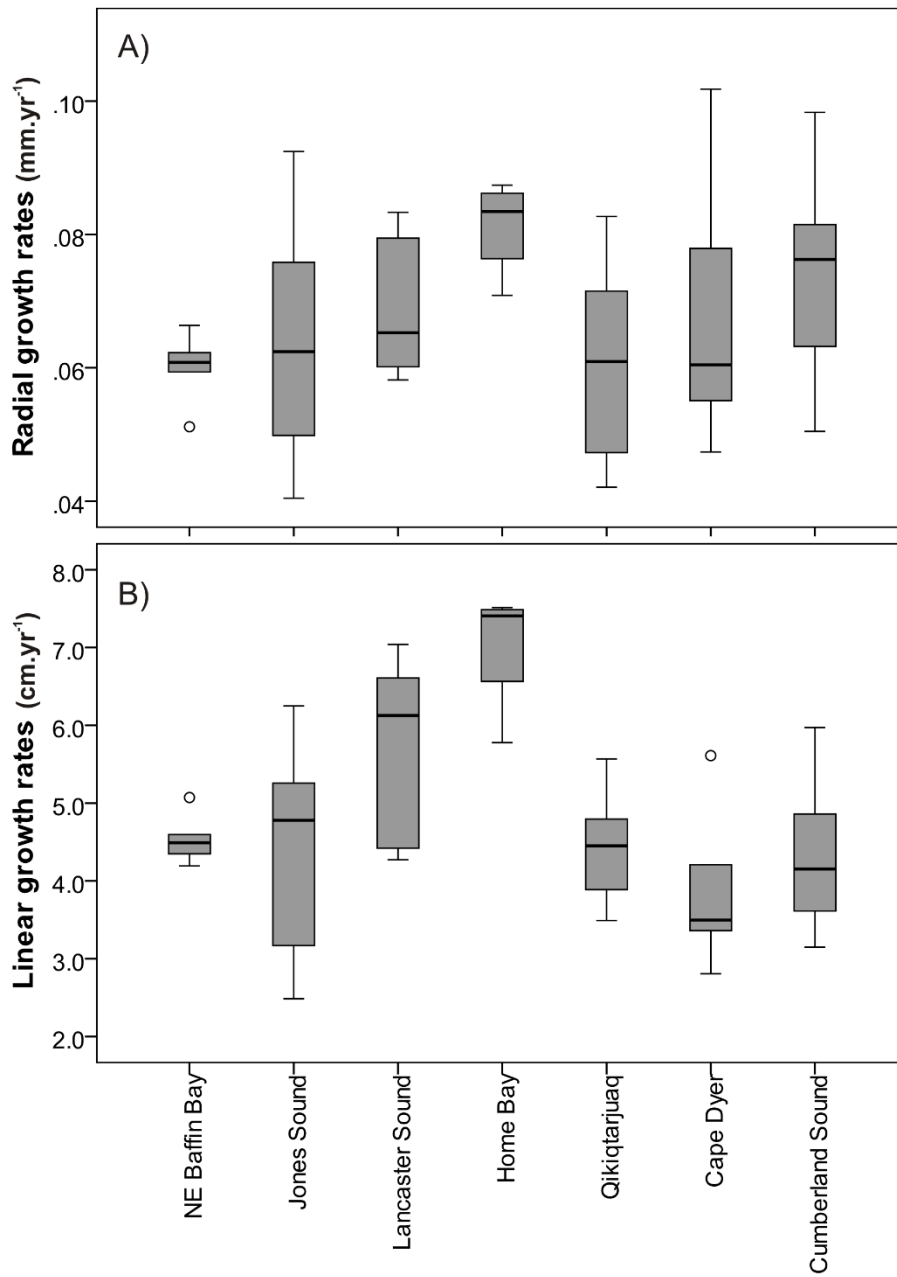


Figure 3-13. Growth rates in *Umbelulla encrinus* per site. Black horizontal bars inside the boxes represent the median, boxes are limited by minimum and maximum values, and circles are outliers. Left to right: north-south.

Radial growth rates significantly increased with colony height (Fig. 3-14A, $F=24.88$, $p=4e-06$, $N=77$), as did linear growth (Fig. 3-14B, $F=133.59$, $p=2e-16$, $df=77$).

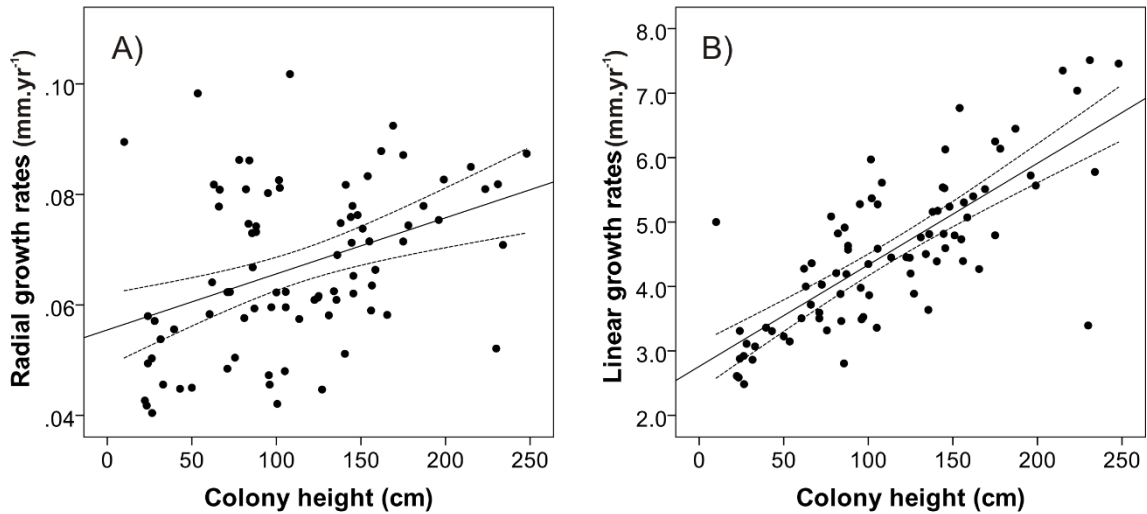


Figure 3-14. Growth rates in relation to colony height in *Umbellula encrinus* from Baffin Bay: A) Radial growth rates, and B) linear growth rates. Fit lines and confidence intervals (dashed lines) are for reference only, as the regression equation also included depth as a covariate.

There was a positive trend between average number of rings and colony height (Fig. 3-15A), but a significant interaction between height and depth was also found ($F=5.805$, $p=0.019$, $N=77$), indicating that the relationship number of rings-height varies with depth. There was also a positive significant relationship between number of rings and axis radius (Fig. 3-15B, $F=249.07$, $p<2e-16$, $N=84$). A power equation had the highest R^2 in both relationships.

There was no significant difference between average number of observed rings and number of rings predicted from colony height when using ~25% of the dataset ($t = -0.024$, $p = 0.98$, $N = 21$). Despite the non-statistical difference, agreements were quite variable between samples, with the absolute difference between observed and predicted number of rings ranging 0-27 rings, and the tallest colonies showing the highest disagreement (Table 3-7). There was also no significant difference between average number of observed rings and number of rings expected from axis radius when using ~25% of the dataset ($t = 0.11$, $p = 0.92$, $N = 21$). Similarly to when using height to estimate number of rings, agreements were variable (0-23 rings), but were better for tall colonies in comparison to the estimates from height (Table 3-7).

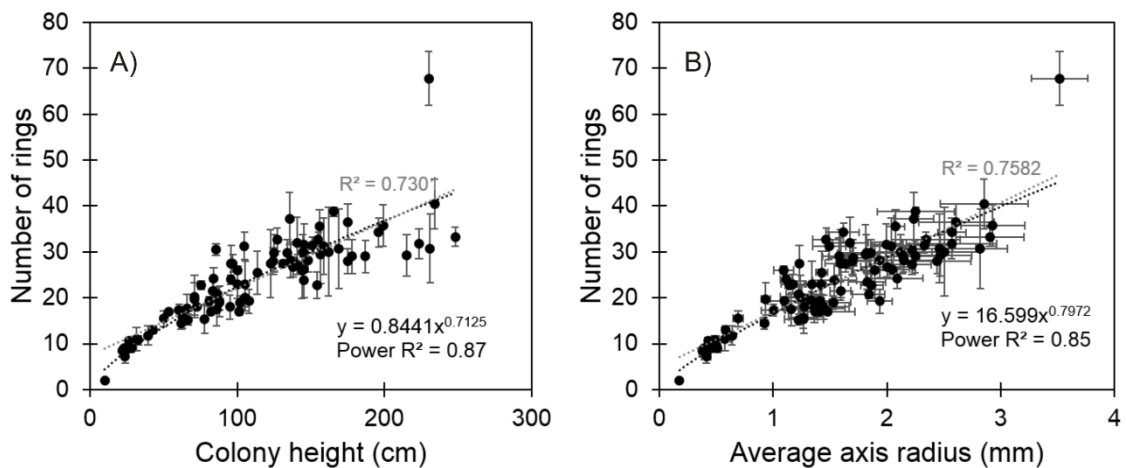


Figure 3-15. Number of rings in relation to A) colony height, and B) axis radius in *Umbellula encrinus* from Baffin Bay. Error bars = standard deviations of average number of rings and average radius. R^2 is shown for both linear (gray) and power equations.

Table 3-7. Comparison between observed (Obs) number of rings in *Umbellula encrinus* from visual counting and number of rings estimated from equations on the relationship between number of rings and colony size ($EstH = 0.8094 * height^{0.7228}$), and axis radius ($EstR = 16.646 * radius^{0.7887}$) when using 25% of the data (hold-out sample).

Sample id	Height	Radius	Obs	Number of rings from height		Number of rings from radius	
				EstH	Absolute Obs-EstH	EstR	Absolute Obs-EstR
027_2nd	231	2.46	30.8	41	11	34	3
030F	85.6	2.22	30.5	20	10	31	1
044	223.5	2.57	31.8	40	9	35	3
045	187	2.25	29.0	36	7	32	3
047	145.5	1.54	23.8	30	6	23	0
048	156	2.15	33.5	31	2	30	3
050	234	2.85	40.5	42	1	38	2
081	63	1.27	15.8	16	0	20	4
082	66.5	1.23	15.3	17	2	20	4
090	88	1.41	19.3	21	1	22	3
092	102	1.53	19.0	23	4	23	4
093	95	1.45	18.0	22	4	22	4
JS0013_1	230	3.52	67.8	41	27	45	23
JS0015_9	136	1.94	28.3	28	0	28	0
JS0023_5	86	1.16	17.5	20	3	19	1
JS0025_7	23.3	0.40	9.0	8	1	8	1
JS0029_3	148	2.15	28.3	30	2	30	2
QIK2014_9_1	151	2.33	31.5	30	1	32	1
QIK2014_9_3	144	1.89	26.0	29	3	28	2
QIK2014_9_5	135.5	2.24	37.3	28	9	31	6
129	158.5	2.04	31.3	32	0	29	3

3.3.7 Growth rates in relation to environmental factors

Because of the very strong relationship between linear growth rates and colony height, we restricted the analysis on environmental factors to radial growth rates in order to control for colony height (interactions with height were always significant when trying

to use linear growth rates). When examining the relationships between radial growth rates and environmental factors, there was a significant positive relationship with bottom temperature ($F= 6.534$, $p= 0.046$, $N =77$), surface salinity ($F= 13.25$, $p= 0.0005$, $N=84$), and depth ($F= 4.001$, $p= 0.049$, $N =77$), but not with latitude ($F= 1.947$, $p= 0.167$, $N= 77$), chlorophyll a summer ($F= 1.214$, $p= 0.27$, $N= 84$), or surface currents velocity ($F= 2.02$, $p= 0.16$, $N= 77$) (Fig. 3-16). There was a significant interaction between colony height and SST ($F= 5.704$, $p= 0.02$, $N= 84$), so that the relationship between radial growth rates and this factor varies with colony height (Fig. 3-17).

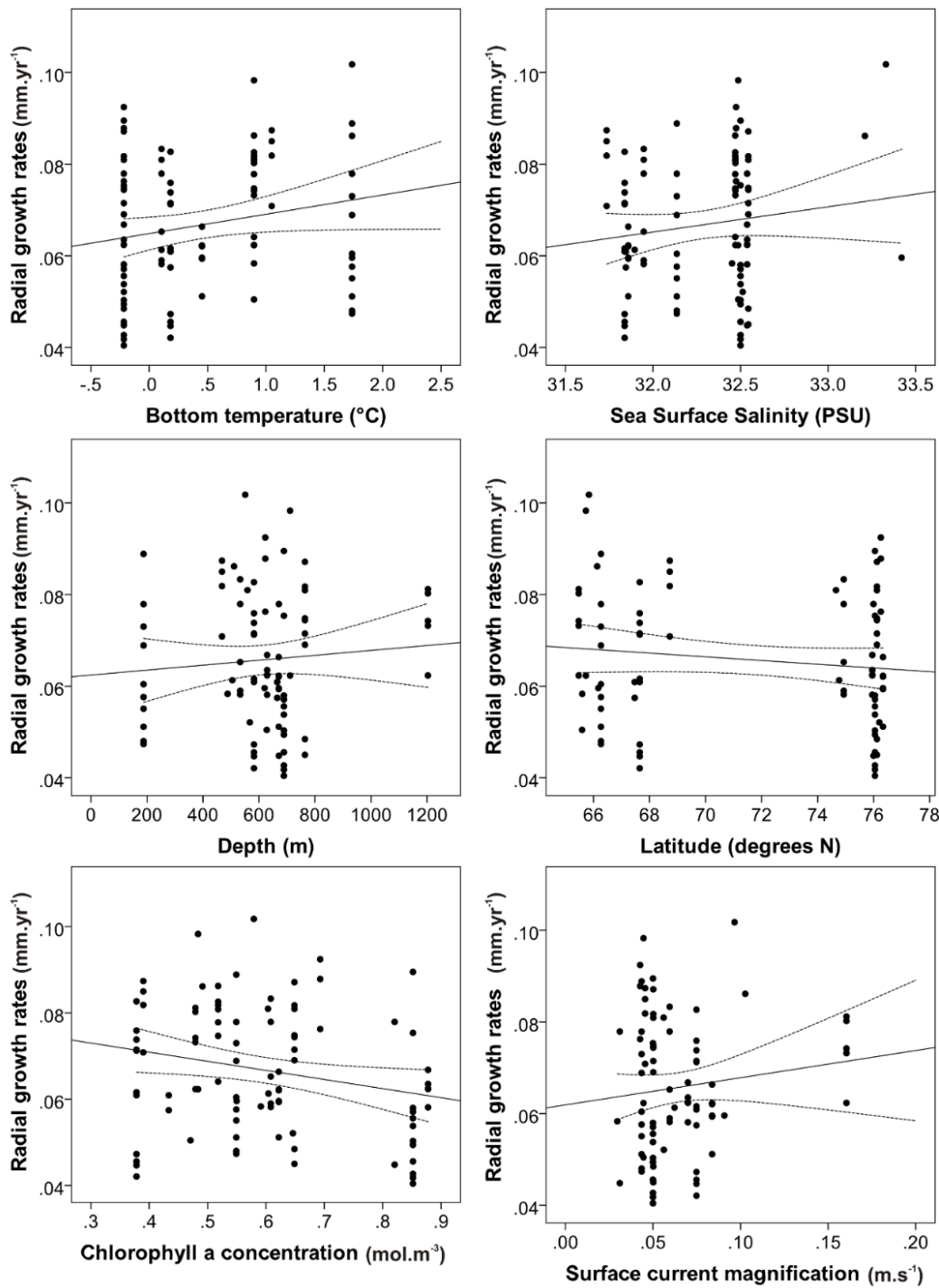


Figure 3-16. Radial growth rates in *Umbellula encrinus* in relation to environmental variables. Fit lines and confidence intervals (dashed lines) are for reference only, as the regression equation also included depth as a covariate.

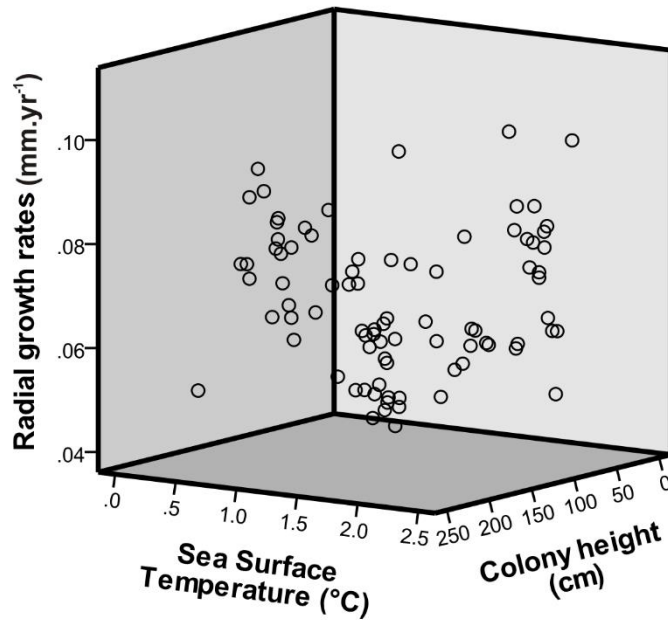


Figure 3-17. 3D-plot of the relationship between radial growth rates in *Umbellula encrinus*, colony height, and sea surface temperature (SST).

3.4. Discussion

3.4.1 Abundance and size-frequency distribution

A total of 94 colonies were observed during the video analysis at the four surveyed sites (Home Bay, Scott Inlet, Qikiqtarjuaq, and Cape Dyer), of which Scott Inlet had the highest abundance (22 colonies·km⁻¹). Previous accounts of *U. encrinus* near Greenland have shown the potential for dense aggregations to occur. In fact, colonies of *U. encrinus* have been commonly caught as bycatch in the Greenland side of Baffin Bay, at depths ranging 131-1354 m (Jørgensen et al., 2013). Furthermore, a video from a baited

camera obtained in 2015 in Lancaster Sound (unpublished data) indicates that colonies are densely distributed there (~50 colonies over ~0.6 km of bottom), as they were seen at a higher frequency than at the video-surveyed sites included in this study.

In the Barents Sea, >5000 colonies of *U. encrinus* have been trawled during a 15 minute trawling operation (Jørgensen et al., 2015). Based on vessel speeds of 3.7-9.3 km.hour⁻¹ reported by these authors, this indicates very high relative abundances of ~2150-5405 colonies·km⁻¹.

In the Hardanger fjord (Norway), other sea pens have been found in average densities of 1.75 colonies·m⁻² (Buhl-Mortensen & Buhl-Mortensen, 2014). *Pteroeides spinosum* (Ellis, 1764) can reach densities up to >7 colonies·m⁻² in the Mediterranean Sea (Porporato et al., 2014), and *Pennatula aculeata* Danielssen, 1860 had densities up to >8 colonies·m⁻² in the Gulf of Maine (NW Atlantic) (Langton et al., 1990). Sea pens can also be very densely distributed in Newfoundland, where they have been seen forming fields over 1 km long with maximum densities of 33 colonies·m⁻² (Baker et al., 2012).

Therefore, the fact that sea pens are often found forming dense fields, plus the evidence of high densities of *U. encrinus* in the Barents Sea, and the indication of their dense presence in the Umanak Fjord and Lancaster Sound suggest that this sea pen has the potential to form large fields as well. The identification of sites of high density of *U. encrinus* colonies (e.g. fields) in Baffin Bay is urged before trawling activities broaden and deepen in the Arctic (c.f. Christiansen et al., 2014).

In terms of their size-frequency distribution, the significant and positive skewness for the Cape Dyer colonies indicates that based on the available sample size this populations is dominated by small size classes (e.g. Gori et al., 2011). Samples from

Jones Sound had negative $g1/SE$ and $g2/SE$ values close to 2, which could indicate a trend of large size colonies. However, our sample sizes were small for most sites (e.g. Lancaster Sound, $N = 8$), which could have resulted in the non-observation of dominant size classes at these sites.

3.4.2 Colony and axis metrics in relation to colony size

The relationship between colony height and peduncle length in *U. encrinus* was strong and significant. Although larger colonies do have larger peduncles, percentage of peduncle tended to decrease with colony height. This negative relationship between peduncle percentage and colony height was already reported for other sea pens (Baillon et al., 2016). From a growth perspective, it suggests that as a colony becomes larger over time, peduncle growth rates seem to be reduced.

The peduncle in sea pens plays a very important support role by allowing the colony to anchor in the soft substrate. It needs to be robust and it is supported by a series of strong muscles (Musgrave, 1909). However, it remains buried in the sediment, playing no direct role in food capture or reproduction. It seems that there is an optimal peduncle size, which is capable of supporting very large colonies, without the need to keep increasing in length.

The significant interactions between axis metrics (radius and area) and depth, indicates that depth has an influence in the relationship between axis metrics and colony height. Since the axis is an essential part of the colony, it is expected that it thickens with time, which allows growth rings to be deposited. Radial growth rates (thickening of the axis over time) were shown to be strongly related to colony height. So that the influence

of depth on axis metrics might simply be a response of the influence of depth on colony height. We did find a trend of colony height decreasing with depth, but this relationship was not statistically significant when controlling for location (data not shown). On the other hand, *U. encrinus* tends to be smaller at greater depths (Molodtsova et al., 2008), and this pattern has also been observed in other sea pen species (Baillon et al., 2016). Whether changes with depth also have a direct influence on axis metrics is still to be determined. But it is likely that changes in depth and sediment grain size can influence both colony and axis metrics (Hickson, 1916).

3.4.3 Bomb-¹⁴C and trace element analysis

The results from the bomb-¹⁴C analysis showed an increase in ¹⁴C with distance from the core and all subsamples showed pre-bomb values (negative values). The analyzed sample was collected in 2014 and it was estimated to be ~68 years in age. Our analysis indicates a great delay in the ¹⁴C intake by the colony, in relation to ¹⁴C values obtained from the skeletons of other deep-water corals in the NW Atlantic (Sherwood et al., 2008). The ¹⁴C ventilation in deep waters of Jones Sound is not well understood yet, as to our knowledge this is the first study to report ¹⁴C data from deep water in this site. Further ¹⁴C analysis of additional *U. encrinus* skeletons along a latitudinal gradient in Baffin Bay might further elucidate patterns in the ¹⁴C ventilation in the region.

The ¹⁴C curve for our data is comparable to that shown by Sherwood et al. (2008) for the calcite of the bamboo coral *K. grayi*, in which growth rings were confirmed to be formed annually. Although not an unequivocal evidence for annual ring formation, this result suggests that *U. encrinus* might perform similarly to *K. grayi*, and probably also lay

down rings annually. A similar pattern was obtained for the sea pen *Pennatula grandis* Ehrenberg, 1834 (Chapter 4). We recognize that sea pens and gorgonians are different organisms, and that additional studies on sea pens are necessary before further conclusions can be made in terms of ^{14}C composition of these organisms, and correspondent interpretations.

In terms of the trace elements analysis, this is the second study to determine the trace element composition of a sea pen axis (Chapter 2). In both studies, the trace element analysis was applied to detect patterns that could indicate cyclicity in the axis chemical composition. This could shed a light on ring formation periodicity, considering the challenges involved in validating frequency of ring formation in sea pens (Chapter 2). In *U. encrinus* the number of trace element ratio peaks was comparable to the number of rings visually determined in most samples, as observed for *Halipteris finmarchica* (Sars, 1851) (Chapter 2). While this does not prove ring formation periodicity (cf. Chapter 2), it confirms an association between rings and axis geochemistry. As suggested for *H. finmarchica*, annual spring phytoplankton blooms could be a trigger for ring formation, which is reflected in the axis geochemistry.

The trace element ratios for *U. encrinus* showed ranges very similar to those found in the axis of *H. finmarchica* (Chapter 2), despite the fact that the *H. finmarchica* samples were from the Grand Banks area (Newfoundland), and the *U. encrinus* samples from northernmost waters. Sr/Ca and Ba/Ca ratios for these two species were the most similar, with averages differing by only 0.04 and $<0.001 \text{ mmol}\cdot\text{mol}^{-1}$, respectively. Mg/Ca and Na/Ca ratios were about $10 \text{ mmol}\cdot\text{mol}^{-1}$ higher in *U. encrinus* than in *H. finmarchica*. The similarity in the trace element ratios between the two species reflects the similarity of

their axis composition, with both species having Mg-Calcite skeleta (Chapters 2, 5), and indicates that the axis carbonate component in these sea pens is a conservative trait.

The two samples collected from comparable depths (028 and 029) were similar while a third sample (030) from shallower depth was strikingly different. The significant negative correlation between Mg/Ca and Sr/Ca was expected, and it was also found in *H. finmarchica* (Chapter 2).

3.4.4 Longevity and growth rates

As suggested by our ^{14}C analysis, we believe that the number of rings probably represents age in years in *U. encrinus*. In this study colonies of *U. encrinus* showed a maximum average number of rings of 68, with an average of 23.6 ± 9.3 . Average number of rings and radial growth rates ($0.068 \text{ mm}\cdot\text{yr}^{-1}$) were comparable to those estimated for other species of sea pens (Birkeland, 1974, Wilson et al., 2002, Chapter 2), but to our knowledge the colony showing 68 rings represents the oldest sea pen recorded so far.

Using size to estimate the number of rings (i.e. age) might be useful for colonies of intermediate size; while for very large colonies it might be useful to give an estimate of minimum age only. For instance, the predicted number of rings was similar to the observed number of rings in most cases (refer to table 3-7), except for the extremely large colonies (e.g. colony JS0013_1), in which the absolute difference between number of observed and predicted rings was very large (e.g. 27 rings). If we apply the equation on the relationship between colony height and number of rings for the tallest sample observed in the video transect in Qikiqtarjuaq (2.1 m), we obtain an estimated number of rings of 50. Based on the number of rings counted for the 2.3 m tall colony from Jones

Sound (68 rings), it is possible that this relationship is underestimating the age of this very tall colony from Qikiqtarjuaq.

Furthermore, the observation of short colonies bearing large peduncles and polypariums in Cumberland Sound, having similar estimated ages to tall colonies of similar polyparium sizes, suggests that for this species colony height might not be the single most precise age indicator, since in some cases short colonies might be as old as larger colonies. Axis radius was also a good indicator of estimated number of rings, as observed in other sea pens (e.g. diameter in the sea whip *Halipteris willemoesi* Kölliker, 1870; Wilson et al., 2002). In this context, tall colonies are usually older than short colonies, but examining colony height only might lead to an underestimation of colony age. Axis radius might be a better metric to predict colony age in *U. encrinus*.

Although there was a significant relationship between growth rates and bottom temperature and surface salinity, no significant relationships were identified with latitude, chlorophyll a, or surface currents velocity. The significant interaction between colony height and SST prevented a more detailed analysis of radial growth rates in relation to this variable. *U. encrinus* is a boreal-Arctic species, and as such it inhabits environments too cold to most cold-water corals, which are usually found in waters between 4-12 °C (Roberts et al., 2006). However, to live in such cold environments comes with limitations, and slower growth rates are among the possible metabolic consequences suffered by animals living in these environments (Peck, 2015).

The absence of significant relationships with surface chlorophyll a might be the result of using surface data, instead of bottom data. However, obtaining bottom data for all studied sites over a considerable temporal range is very difficult. Polynyas - areas of

open water where ice is thin or reduced, where spring primary production is high - are found near four of the studied areas: Jones Sound, NE Baffin Bay, Lancaster Sound, and Cumberland Sound (Barber & Massom, 2007). It is not clear yet whether in the studied areas the high surface primary productivity is reflected at similar levels in the deep-water benthos below the surface, particularly at the temporal scales analyzed in this study (i.e. summer).

In certain polar systems, particulate organic carbon is rapidly exported to the benthos during the spring bloom, but during summer and fall zooplankton expands and the system retains more carbon than it exports (Grebmeier & Barry, 2007). Furthermore, there is a greater degradation of particulate organic matter (POM) with depth in the Arctic (Roy et al., 2015). These authors found that direct assimilation of pelagic and sedimentary POM was not likely the main carbon assimilation pathway for benthic invertebrates in Arctic waters. In fact, ice algae was shown to be a component of the diet of certain benthic organisms in these environments (Roy et al., 2015).

We analyzed summer data due to the limitation of satellite data for the spring season at most of the studied areas. Therefore, the increase in primary productivity during summer months (in relation to winter) might not be directly associated to an increased productivity at the benthos level. On the other hand, summer values should give an indication of the levels of productivity of the area during spring (e.g. high, low).

In this sense, there are different possible explanations for the non-significant relationships between growth rates and surface chlorophyll a in *U. encrinus*: 1) productivity is not a direct factor driving growth rates in this species; 2) surface productivity does not fully represent bottom patterns at those depths and locations; 3)

other sources of food such as ice algae or zooplankton are part of the diet of this species; and/or 4) the temporal scale analyzed is not the most appropriate, with spring being more suitable.

Relationships between growth rates and environmental factors in *U. encrinus* might also be secondary, as relationships between growth rates and colony height were strong and statistically significant. Therefore, intrinsic factors might be more influential than environmental factors in the growth rates of this species. This pattern of colony growth rates changing with colony size has been observed in several other invertebrates including corals.

In many cases, growth rates tend to be faster in the first years of life, decreasing with age (Grigg, 1974, Mistri & Ceccherelli, 1993, Matsumoto, 2004, Sartoretto & Francour, 2012). In *U. encrinus* our data showed an increase in growth rates with colony height. This was also observed for *H. finmarchica* (Chapter 2) and in the soft coral *Anthomastus ritteri* Nutting, 1909 (Cordes et al., 2001). It might be that a more limited number of feeding polyps in the first years of life limits growth rates, which become faster as the organism grows and more polyps become available. This reasoning could also explain why chlorophyll a does not seem to have an influence in the growth rates in *U. encrinus*. Even if more food is available, intake rates will depend on the access to this food, which will also depend on how many functional polyps are available for feeding.

U. encrinus might also feed on zooplankton, as already found for other deep-water sea pens (Baillon et al., 2016), or even deposit feed (e.g. the soft coral *Gersemia antarctica* (Kükenthal, 1902), Slattery et al., 1997), as a great amount of muddy material

can be found in their gastrovascular cavities (BMN, personal observation). In these cases, other proxies for food availability would be more appropriate than surface chlorophyll a.

In *Funiculina quadrangularis* (Pallas, 1766) colony size increased exponentially in the first three years of age (40 cm in three years), yielding linear growth rates of $\sim 13 \text{ cm}\cdot\text{yr}^{-1}$ (Berg, 1941). This rate is considerably faster than the estimated rates for small colonies in our study and even faster than our maximum average linear growth rates. These are also much faster than those estimated for *Ptilosarcus gurneyi* (Gray, 1860) (Birkeland, 1974), *H. willemoesi* (Wilson et al., 2002), and *H. finmarchica* (Chapter 2).

Colonies studied by Berg (1941) were from shallow-water environments, but so were the colonies studied by Birkeland (1974), so depth does not explain observed variations in growth rates. Berg (1941) indicates that when the colony reaches maturity, growth rates slow down. Growth rates in *H. finmarchica* were estimated based on mature colonies (Baillon et al., 2014, Chapter 2) and if *H. willemoesi* has the same maturity size as *H. finmarchica*, then growth rates in these colonies were also estimated based on mature colonies.

In this sense, it is possible that the difference between mature and juvenile colonies has an important influence in colony growth rates, which could perhaps explain these differential growth rates, although size of maturity has not yet been determined for *U. encrinus*. Our smallest colony was 10 cm tall (single colony), and it had estimated linear growth rates of $5 \text{ cm}\cdot\text{yr}^{-1}$, which are faster than most colonies $< 100 \text{ cm}$ tall. This might indicate exceptionally fast growth rates in juvenile colonies, which were not covered in this study.

3.4.5 Vulnerability and conservation

The slow radial growth rates and great longevity of *U. encrinus* in Baffin Bay indicate a long recovery rate for populations exposed to physical damage. In this study, most of the sea pen colonies have been obtained as trawl bycatch, but the samples from Jones Sound, Qikiqtarjuaq, and Cape Dyer were obtained as longline bycatch, showing the vulnerability of the species to different types of fishing gear.

At Jones Sound, colonies of all size ranges were caught in longline hooks of varied sizes, suggesting that both young and old colonies are vulnerable to this type of gear. Although other studies have started to examine the impacts of longline gear on deep-water coral communities (e.g. Durán Muñoz et al., 2011, Sampaio et al., 2012), sea pens have seldom been considered (e.g. Edinger et al., 2007, Mytilineous et al., 2014).

Fisheries surveys using longline gear are an important source of coral bycatch in the Newfoundland and Labrador region, as longlines can be deployed in deep and rough-bottom areas of difficult access to trawls, which are also considered good habitat for corals (Edinger et al., 2007). From our video analysis, we identified *U. encrinus* living in both dominantly soft and hard bottom environments, indicating that it is not exclusive to entirely flat and soft bottom areas.

Although longline fisheries can have a smaller impact than bottom trawling (Pham et al., 2014), knowledge on the distribution and ecology of *U. encrinus* in Arctic environments is still limited, and further studies are necessary before the vulnerability of these sea pens can be fully assessed. Further video surveys in the area are therefore very important and recommended to assist a better understanding of the distributional patterns

of *U. encrinus* in Baffin Bay, so that conservation strategies to protect this long-lived, iconic Arctic animal can be delineated.

Acknowledgements

We thank CCGS *Amundsen* and the Arctic Fishery Alliance vessel *Kiviuq I*, and *Nuliajuk* captains and crew, *Amundsen* chief scientists Dr. Maurice Levasseur and Dr. Philippe Archambault. We also thank the ROV pilots Ian Murdock, Peter Lockhart, and Vincent Auger. Glenn Piercey, Michael Shaffer, David Grant and Brian Loveridge (CREAIT, Memorial University) assisted with sectioning, polishing, trace element analysis, and micromilling for ^{14}C analysis (GP). Dr. Kent Gilkinson (Fisheries and Oceans Canada) for making samples available. Cindy Grant, Anni Mäkelä, and Alexis Burnt for samples collected aboard the *Amundsen*. Tom Guilderson (Lawrence Livermore National Laboratory) for the ^{14}C analysis. Research is funded by the Natural Sciences and Engineering Research Council of Canada (NSERC) (doctoral scholarship to BMN) and Canadian Healthy Oceans Network (CHONe).

3.5 References

Aranha, R., E. Edinger, G. Layne & G. Piercey, 2014. Growth rate variation and potential paleoceanographic proxies in *Primnoa pacifica*: Insights from high-resolution trace element microanalysis. *Deep Sea Research Part II: Topical Studies in Oceanography* 99: 213-226.

Baillon, S., J. Hamel & A. Mercier, 2014. Protracted oogenesis and annual reproductive periodicity in the deep-sea pennatulacean *Halipteris finmarchica* (Anthozoa, Octocorallia). *Marine Ecology* 36: 1364-1378.

Baillon, S., M. English, J. Hamel & A. Mercier, 2016. Comparative biometry and isotopy of three dominant pennatulacean corals in the Northwest Atlantic. *Acta Zoologica*: in press.

Baillon, S., J. Hamel, V. E. Wareham & A. Mercier, 2012. Deep cold-water corals as nurseries for fish larvae. *Frontiers in Ecology and the Environment* 10: 351-356.

Baker, K. D., V. E. Wareham, P. V. R. Snelgrove, R. L. Haedrich, D. A. Fifield, E. N. Edinger & K. D. Gilkinson, 2012. Distributional patterns of deep-sea coral assemblages in three submarine canyons off Newfoundland, Canada. *Marine Ecology Progress Series* 445: 235-249.

Barber, D. G. & R. A. Massom, 2007. Chapter 1 The role of sea ice in Arctic and Antarctic Polynyas. In W.O. Smith & D.G. Barber (eds), *Polynyas: Windows to the World*. Elsevier: 1-54.

Berg, S. E., 1941. Die Entwicklung und Koloniebildung bei *Funiculina quadrangularis* (Pallas). *Zoologiska bidrag fran Uppsala* 20: 1-100.

- Birkeland, C., 1974. Interactions between a sea pen and seven of its predators. *Ecological Monographs* 44: 211-232.
- Boyer, T. P., J. I. Antonov, O. K. Baranova, H. E. Garcia, D. R. Johnson, R. A. Locarnini, A. V. Mishonov, D. Seidov, I. V. Smolyar & M. M. Zweng, 2009. World Ocean Database 2009, Chapter 1: Introduction, NOAA Atlas NESDIS 66. U.S. Gov. Printing Office, Washington, D.C.
- Broch, H., 1956. Oktokorallen russischer Expeditionen im Polarmeer während der Jahre 1929-1935. I Kommisjon Hos H. Ascehoug and Co. (W. Nygaard), Oslo.
- Broch, H., 1958. Octocorals. Part I: Pennatularians. University Press, Cambridge.
- Brodeur, R. D., 2001. Habitat-specific distribution of Pacific ocean perch (*Sebastes alutus*) in Pribilof Canyon, Bering Sea. *Continental Shelf Research* 21: 207-224.
- Buhl-Mortensen, P. & L. Buhl-Mortensen, 2014. Diverse and vulnerable deep-water biotopes in the Hardangerfjord. *Marine Biology Research* 10: 253-267.
- Buhl-Mortensen, L., P. Buhl-Mortensen, M. F. J. Dolan, J. Dannheim, V. Bellec & B. Holte, 2012. Habitat complexity and bottom fauna composition at different scales on the continental shelf and slope of northern Norway. *Hydrobiologia* 685: 191-219.
- Campana, S. E., 1997. Use of radiocarbon from nuclear fallout as a dated marker in the otoliths of Haddock *Melanogrammus aeglefinus*. *Marine Ecology Progress Series* 150: 49-56.
- Carton, J. A. & B. S. Giese, 2008. A reanalysis of ocean climate using Simple Ocean Data Assimilation (SODA). *Monthly Weather Review* 136: 2999-3017.
- Christiansen, J. S., C. W. Mecklenburg & O. V. Karamushko, 2014. Arctic marine fishes and their fisheries in light of global change. *Global Change Biology* 20: 352-359.

Cordes, E. E., J. W. Nybakken & G. VanDykhuisen, 2001. Reproduction and growth of *Anthomastus ritteri* (Octocorallia: Alcyonacea) from Monterey Bay, California, USA. *Marine Biology* 138: 491-501.

Davies, J. S., K. L. Howell, H. A. Stewart, J. Guinan & N. Golding, 2014. Defining biological assemblages (biotopes) of conservation interest in the submarine canyons of the South West Approaches (offshore United Kingdom) for use in marine habitat mapping. *Deep Sea Research Part II: Topical Studies in Oceanography* 104: 208-229.

Dolan, E., 2008. Phylogenetics, systematics and biogeography of deep-sea Pennatulacea (Anthozoa: Octocorallia): evidence from molecules and morphology. PhD thesis. University of Southampton, England.

Durán Muñoz, P., F. J. Murillo, M. Sayago-Gil, A. Serrano, M. Laporta, I. Otero & C. Gómez, 2011. Effects of deep-sea bottom longlining on the Hatton Bank fish communities and benthic ecosystem, north-east Atlantic. *Journal of the Marine Biological Association of the United Kingdom* 91: 939-952.

Edinger, E., K. Baker, R. Devillers & V. Wareham, 2007. Coldwater corals off Newfoundland and Labrador: Distribution and Fisheries Impacts. World Wildlife Fund Canada, Toronto.

Ellis, J., 1753. A letter from Mr. John Ellis to Mr. Peter Collinson, FRS concerning a cluster-polype, found in the sea near the coast of Greenland. *Philosophical Transactions* 48: 305-308.

Gori, A., S. Rossi, C. Linares, E. Berganzo, C. Orejas, M. Dale & J. Gili, 2011. Size and spatial structure in deep versus shallow populations of the Mediterranean gorgonian

Eunicella singularis (Cap de Creus, northwestern Mediterranean Sea). *Marine Biology* 158: 1721-1732.

Grebmeier, J. M. & J. P. Barry, 2007. Chapter 11 Benthic processes in Polynyas. In W.O. Smith & D.G. Barber (eds), *Polynyas: Windows to the World*. Elsevier: 363-390.

Grigg, R. W., 1974. Growth rings: annual periodicity in two gorgonian corals. *Ecology* 55: 876-881.

Hickson, S. J., 1916. *The Pennatulacea of the Siboga Expedition: with a general survey of the order*. Late EJ Brill.

Jørgensen, L. L., B. Planque, T. H. Thangstad & G. Certain, 2015. Vulnerability of megabenthic species to trawling in the Barents Sea. *ICES Journal of Marine Science: Journal du Conseil* 73: i84-i97.

Jørgensen, O.A., O.S. Tendal & N. Hammeken Arboe, 2013. Preliminary mapping of the distribution of corals observed off West Greenland as inferred from bottom trawl surveys 2010-2012. Northwest Atlantic Fisheries Association. Scientific Council Meeting. NAFO SCR Doc. 13/007. Serial No. N6156.

Kabacoff, R., 2015. *R in action: data analysis and graphics with R*. Manning, Shelter Island.

Langton, R., E. Langton, R. Theroux & J. Uzmans, 1990. Distribution, behavior and abundance of sea pens, *Pennatula aculeata*, in the Gulf of Maine. *Marine Biology* 107: 463-469.

Locarnini, R. A., A. V. Mishonov, J. I., T. P. Antonov, H. E. Boyer, O. K. Garcia, M. M. Baranova, C. R. Zweng, J. R. Paver, D. R. Reagan, H. Johnson M. & D. Seidov, 2013.

World Ocean Atlas 2013, Volume 1: Temperature. S. Levitus, Ed., A. Mishonov Technical Ed.; NOAA Atlas NESDIS 73, 40 pp.

Matsumoto, A., 2004. Heterogeneous and compensatory growth in *Melithaea flabellifera* (Octocorallia: Melithaeidae) in Japan. *Hydrobiologia* 530: 389-397.

Mistri, M. & V. U. Ceccherelli, 1993. Growth of the Mediterranean gorgonian *Lophogorgia ceratophyta* (L., 1758). *Marine Ecology* 14: 329-340.

Molodtsova, T. N., N. P. Sanamyan & N. B. Keller, 2008. Anthozoa from the northern Mid-Atlantic Ridge and Charlie-Gibbs Fracture Zone. *Marine Biology Research* 4: 112-130.

Mortensen, T., 1912. The Danish Ingolf Expedition 5, part 2. Copenhagen: H. Hagerup, Copenhagen.

Mortensen, P. B., L. Buhl-Mortensen, A. V. Gebruk & E. M. Krylova, 2008. Occurrence of deep-water corals on the Mid-Atlantic Ridge based on MAR-ECO data. *Deep Sea Research Part II: Topical Studies in Oceanography* 55: 142-152.

Musgrave, E. M., 1909. Experimental observations on the organs of circulation and powers of locomotion in pennatulids. *Quarterly Journal of Microscopical Science* 54: 443-482.

Mytilineou, C., C. J. Smith, A. Anastasopoulou, K. N. Papadopoulou, G. Christidis, P. Bekas, S. Kavadas & J. Dokos, 2014. New cold-water coral occurrences in the Eastern Ionian Sea: Results from experimental long line fishing. *Deep Sea Research Part II: Topical Studies in Oceanography* 99: 146-157.

Peck, L. S., 2016. A cold limit to adaptation in the sea. *Trends in Ecology & Evolution* 31: 13-26.

Pham, C. K., H. Diogo, G. Menezes, F. Porteiro, A. Braga-Henriques, F. Vandeperre & T. Morato, 2014. Deep-water longline fishing has reduced impact on Vulnerable Marine Ecosystems. *Scientific Reports* 4.

Porporato, E. D., M. C. Mangano, F. De Domenico, S. Giacobbe & N. Spanò, 2014. First observation of *Pteroeides spinosum* (Anthozoa: Octocorallia) fields in a Sicilian coastal zone (Central Mediterranean Sea). *Marine Biodiversity* 44: 589-592.

Roberts, J. J., B. D. Best, D. C. Dunn, E. A. Treml & P. N. Halpin, 2010. Marine Geospatial Ecology Tools: An integrated framework for ecological geoprocessing with ArcGIS, Python, R, MATLAB, and C++. *Environmental Modelling & Software* 25: 1197-1207.

Roberts, J. M., A. J. Wheeler & A. Freiwald, 2006. Reefs of the deep: the biology and geology of cold-water coral ecosystems. *Science* 312: 543-547.

Roberts, J. M., A. Wheeler, A. Freiwald & S. Cairns, 2009. Cold-water corals: the biology and geology of deep-sea coral habitats. Cambridge University Press, Cambridge, UK; New York.

Roy, V., K. Iken, M. Gosselin, J. Tremblay, S. Bélanger & P. Archambault, 2015. Benthic faunal assimilation pathways and depth-related changes in food-web structure across the Canadian Arctic. *Deep Sea Research Part I: Oceanographic Research Papers* 102: 55-71.

Sampaio, Í, A. Braga-Henriques, C. Pham, O. Ocaña, V. de Matos, T. Morato & F. M. Porteiro, 2012. Cold-water corals landed by bottom longline fisheries in the Azores (north-eastern Atlantic). *Journal of the Marine Biological Association of the United Kingdom* 92: 1547-1555.

Sartoretto, S. & P. Francour, 2012. Bathymetric distribution and growth rates of *Eunicella verrucosa* (Cnidaria: Gorgoniidae) populations along the Marseilles coast (France). *Scientia Marina* 76: 349-355.

Schneider, C. A., W. S. Rasband & K. W. Eliceiri, 2012. NIH Image to ImageJ: 25 years of image analysis. *Nature Methods* 9: 671-675.

Sherwood, O. A. & E. N. Edinger, 2009. Ages and growth rates of some deep-sea gorgonian and antipatharian corals of Newfoundland and Labrador. *Canadian Journal of Fisheries and Aquatic Sciences* 66: 142-152.

Sherwood, O. A., E. N. Edinger, T. P. Guilderson, B. Ghaleb, M. J. Risk & D. B. Scott, 2008. Late Holocene radiocarbon variability in Northwest Atlantic slope waters. *Earth and Planetary Science Letters* 275: 146-153.

Slattery, M., J. B. McClintock & S. S. Bowser, 1997. Deposit feeding: a novel mode of nutrition in the Antarctic colonial soft coral *Gersemia antarctica*. *Mar Ecol Prog Ser* 149: 299-304.

Sokal, R. R. & F. J. Rohlf, 2012. *Biometry: the principles and practice of statistics in biological research*. W.H. Freeman, New York.

Stuiver, M. & H. A. Polach, 1977. Discussion: reporting of ^{14}C data. *Radiocarbon* 19: 355-363.

Tang, C. C. L., C. K. Ross, T. Yao, B. Petrie, B. M. DeTracey & E. Dunlap, 2004. The circulation, water masses and sea-ice of Baffin Bay. *Progress in Oceanography* 63: 183-228.

Treble, M. A., S. E. Campana, R. J. Wastle, C. M. Jones & J. Boje, 2008. Growth analysis and age validation of a deepwater Arctic fish, the Greenland halibut

(*Reinhardtius hippoglossoides*). Canadian Journal of Fisheries and Aquatic Sciences 65: 1047-1059.

Wareham, V. E., 2009. Updates on deep-sea coral distributions in the Newfoundland and Labrador and Arctic Regions, Northwest Atlantic. In Gilkinson, K. & E. Edinger (eds), The ecology of deep-sea corals of Newfoundland and Labrador waters: biogeography, life history, biogeochemistry, and relation to fishes. Canadian Technical Report on Fisheries Aquatic Sciences. 2830: vi + 136 p.

Wareham, V. E. & E. N. Edinger, 2007. Distribution of deep-sea corals in the Newfoundland and Labrador region, Northwest Atlantic Ocean. Bulletin of Marine Science 81: 289-313.

Williams, G. C., 1995. Living genera of sea pens (Coelenterata: Octocorallia: Pennatulacea): illustrated key and synopses. Zoological Journal of the Linnean Society 113: 93-140.

Wilson, M. T., A. H. Andrews, A. L. Brown & E. E. Cordes, 2002. Axial rod growth and age estimation of the sea pen, *Halipteris willemoesi* Kölliker. Hydrobiologia 471: 133-142.

4. Growth patterns in the deep-water sea pen *Pennatula grandis* Ehrenberg, 1834 (Cnidaria: Octocorallia) inferred from growth rings and colony metrics³

Abstract

Pennatula grandis is one of the most conspicuous species of sea pens observed in the Northwest (NW) Atlantic. As other deep-water corals, it is vulnerable to bottom contact fishing gear and other anthropogenic threats. Here we estimated longevity, growth rates and patterns, and determined the internal skeleton (axis) composition in colonies of *P. grandis* from the NW Atlantic. Longevity was determined by counting the number of growth rings in the axis, and a ¹⁴C analysis was performed in an effort to validate frequency of ring formation for the species. Growth rates were investigated in relation to colony height and environmental variables, and growth patterns were determined by investigating metrics of different colony parts. The carbonate portion of the axis is composed of magnesian calcite, and average 85% of axis weight. The average number of growth rings ranged 4-31. The results from the ¹⁴C analysis indicate that ¹⁴C assimilation in the skeleton of the studied colonies is comparable to that of other corals in the region, whose frequency of ring formation is annual. Based on this, diametric growth rates averaged 0.13 mm·yr⁻¹ while linear growth rates averaged 1.8 cm·yr⁻¹. There were significant negative relationships between diametric growth rates and chlorophyll a, POC

³For submission to Acta Zoologica.

and PIC for large size colonies (30.5-54.5 cm). The investigation of relationships between different parts of the colonies indicated a negative allometric growth, where peduncle and polyp leaves grow slower than the whole colony. This study showed that *P. grandis* can reach longevities of decades, with slow growth rates similar to those estimated for other sea pen species.

4.1 Introduction

Sea pens are colonial octocorals commonly associated with a life on soft bottoms (Williams, 1995). Most sea pens possess an inner supporting structure - the axis (also called style or rod) (Bayer et al., 1983), which is usually composed of calcite and of an organic component such as collagen (Marks et al., 1949, Ledger & Franc, 1978, Franc et al., 1975, 1985). In some species the axis is known to have growth rings (Birkeland, 1974, Wilson et al., 2002, Chapter 2), but little is known about growth and longevity in sea pens.

In a study on predator-prey relationships in the shallow-water sea pen *Ptilosarcus gurneyi* (Gray, 1860), Birkeland (1974) determined longevity and growth rates based on ring counting specimens of known age. Growth rates and age were also estimated in the sea-whip *Halipteris willemoesi* Kölliker, 1870 from the Bering Sea (Wilson et al., 2002), in *Halipteris finmarchica* (Sars, 1851) (Chapter 2), and in *Umbellula encrinus* Linnaeus, 1758 (Chapter 3) from the Northwest (NW) Atlantic. These studies showed that sea pens can live for decades and have slow linear growth rates ranging 2-6 cm·yr⁻¹ (vertical extension).

Since there are so few published studies on growth of sea pens, our knowledge on these organisms' growth remains at best superficial. Growth patterns in terms of changes in colony morphology, and relationships between colony and axis also remain sparsely understood. Soong (2005) studied a shallow-water population of *Virgularia juncea* (Pallas, 1766), and made observations on the relationship between axis and colony metrics. Baillon et al. (2016) studied changes in the morphometry of sea pens in the NW

Atlantic including *Pennatula aculeata* Danielssen, 1860, and determined relationships between axis and colony size.

In the Northwest (NW) Atlantic, deep-water sea pens are abundant and frequently caught as fisheries bycatch (Wareham and Edinger, 2007). *Pennatula* Linnaeus, 1758 (Family Pennatulidae) is one of the most abundant and diverse genera of sea pens observed in this region, sometimes seen forming dense fields up to 1 km long (Baker et al., 2012). Species of *Pennatula* are feather-shaped sea pens with polyps inserted in polyp leaves (Williams, 1995), and they bear an internal axis usually cylindrical in shape (Hickson, 1916, Williams, 1995).

Considering the vulnerability and exposure of sea pens to fishing gear in the NW Atlantic, and the general lack of knowledge on sea pen growth rates, age and axis biology, the objectives of this study were: (1) to characterize the axis of *Pennatula grandis* Ehrenberg, 1834 from the NW Atlantic in terms of axis metrics (i.e. diameter, area, and weight) and composition; (2) to investigate relationships between axis metrics and other parts of the colony (rachis and peduncle); (3) to validate frequency of ring formation; (4) to estimate age and growth rates, and (5) to investigate relationships between growth rates and environmental variables. Other colony characteristics were analyzed in order to discuss growth in terms of addition of polyp leaves, changes in axis weight, colony height, and axis diameter.

4.2 Material and methods

4.2.1 Sampling and identification

Colonies were collected from six regions in the NW Atlantic: Davis Strait, Labrador, East Newfoundland, Grand Banks, Laurentian Channel, and Gulf of St-Lawrence (Fig. 4-1, Appendix 4-1), between the years 2004-2011 during multi-species trawl surveys conducted by Fisheries and Oceans Canada (DFO), using a Campelen 1800 shrimp trawl. Each trawl was 15 minutes long, covering a distance of ~0.8 nautical miles, at a speed of 3 knots. Samples were collected at average depths ranging between 52-1451 m, and kept frozen at -20 °C.

Species identification was performed using Kükenthal (1915), Hickson (1916), and other specialized bibliography. Specimens of *Pennatula* from the British Museum of Natural History collection were accessed for observation of specific taxonomic characters. Additionally, samples from seven colonies were sent to Ms. Raissa Hogan (University of Ireland at Galway) for a molecular study. The analysis of the mitochondrial protein-coding gene *mtMutS* (*msh1*) performed on these specimens also indicated the presence of a single species among the studied colonies based on a small genetic distance between clades (Hogan et al., 2015). Despite attempts to precisely identify the studied species, identification as *P. grandis* will be considered tentative, as the genus still requires revision (Dr. G. Williams, personal communication).

4.2.2 Colony metrics

Colony height, peduncle length, proportion of peduncle, and total number of pairs of polyp leaves were determined for each colony. Colony height is defined as the total distance between the distal and the proximal tips of the colony. Rachis is the distal portion of the colony, which contains autozooids. Peduncle is the proximal region of the colony, which remains embedded in the sediment (Fig. 4-7).

In order to determine how far the axis extends in the colony, an incision of the ventral side of the upper rachis was performed to locate where the axis ends. The distance from the distal tip of axis to the tip of rachis was measured (axis free space length), and the number of pairs of polyp leaves in this axis-free space was also determined.

Total colony wet weight and colony dry weight was determined for 10 colonies of varied sizes (7-20 cm, ids 1-10). Whole colonies were set to oven-dry at 60 °C for 48 hours. The percentage of axis in relation to total colony dry weight was determined for these 10 colonies.

A maximum of 120 colonies of *P. grandis* had height and peduncle length determined, but not all metrics were available for all of these, as 10 of these colonies were only used for the axis carbonate portion of the study (section 4.2.3). Therefore, 110 colonies had most of the metrics determined, except for axis-free space which was only determined for 102 colonies (space in polyp leaves), and 98 colonies (space in length).

Colonies were classified as small, medium and large using descriptive statistics for each species. From the minimum value up to the 25% percentile: small; from 26%-

75%: medium, and from 76% to the maximum value: large. Classes were the following: 3.7-15.5 cm (small, N=36), 16-30 cm (medium, N=54), and 30.5-54.5 (large, N=30).

A power equation ($y = Ax^b$) was used to determine the direction into which colony is growing faster, assuming an allometric growth. If b (coefficient of growth/allometry) > 1 , the allometry is considered positive and it indicates that y is increasing faster than x (Gould, 1966). For this, the pooled observations for the relationships between peduncle length and number of polyp leaves (y) in relation to colony height (x) were used.

4.2.3 Axis characteristics

In order to determine the carbonate composition of the axis in *P. grandis* an X-ray diffraction (XRD) analysis was conducted at the Earth Resources Research and Analysis (TERRA) facility, Memorial University of Newfoundland, using a Rigaku Ultima-IV with a Cu source used in Bragg-Brentano configuration. The whole axis of one colony was crushed into a powder using a ceramic mortar and pestle. A total of 1 g of sample was used for this analysis.

An Energy Dispersive X-rays (EDX) analysis was also performed to further explore the relative elemental composition of the axis in *P. grandis*. For this analysis, a cross section of one axis was embedded in epoxy (EpofixTM - Electron Microscopy Sciences) for cross sectioning using an Isomet[®] Low Speed Saw. The section was polished using a Struers TegraPol 31 lapping wheel, and carbon coated. Three random transects 394 to ~1337 μm long were performed along the radius of the axis using a FEI MLA 650F equipped with dual Bruker 5th generation XFlash SDD X-ray detectors (CREAIT, Memorial University of Newfoundland). The targeted elements for this

analysis were C, N, O, Ca, P, and Mg, and they are given as counts (number of X-rays).

We also determined the Mg/Ca ratio using the results from the EDX analysis.

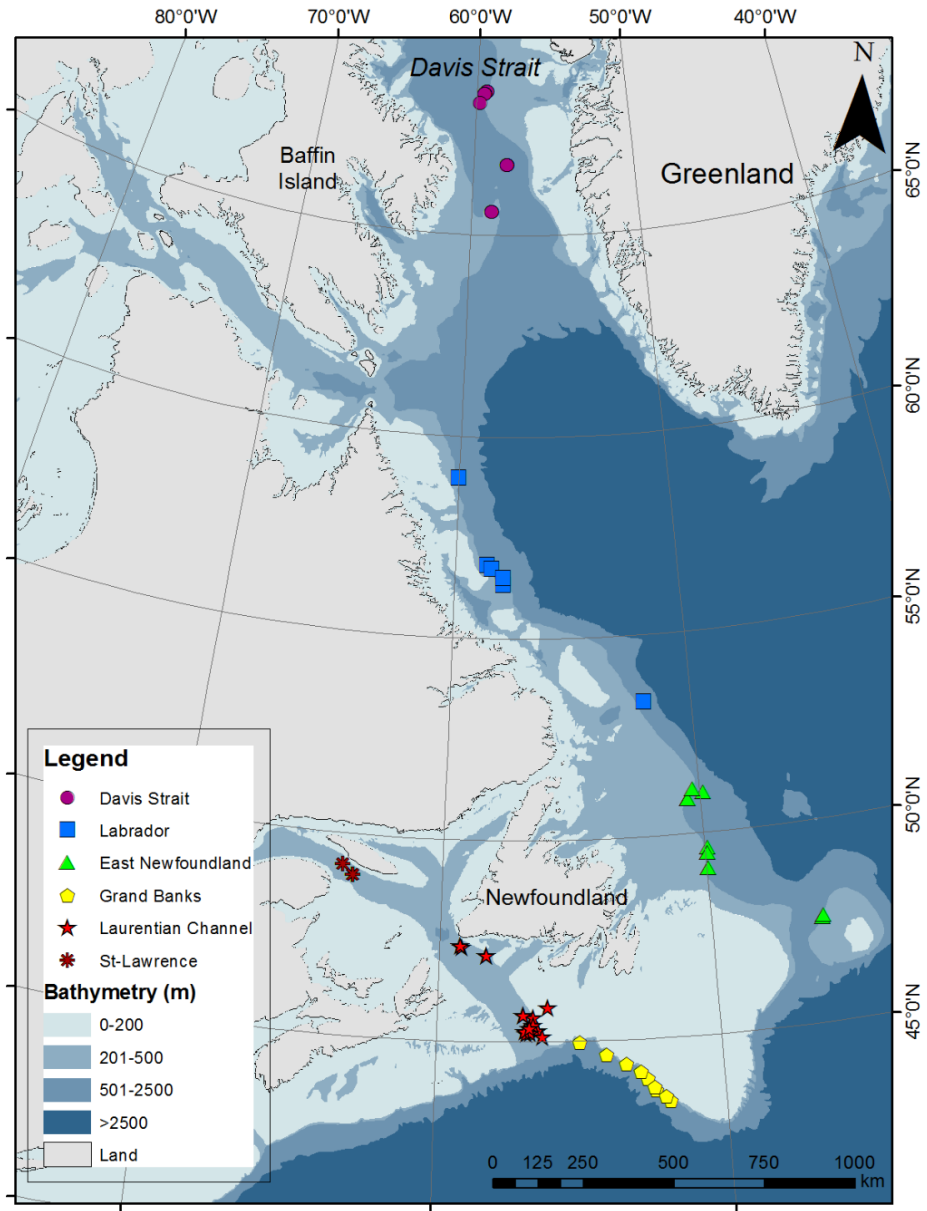


Figure 4-1. Map of study area.

Because the EDX analysis had a more qualitative focus, we used another approach to estimate the percentage of carbonate in relation to organic material in the axis. To this end, ten colonies of *P. grandis* from the same location and depth were used (ids 1-10). Axes were extracted from the colonies, and all adherent material was removed. They were set to air dry, and weighed (W_1). These samples were then placed in an oven (Thermo Scientific Lindberg) at 105°C overnight (> 12 hours) to eliminate residual moisture (c.f. Wang et al., 2011), and their dry weight was determined (W_2) (see below on issue regarding the use of heat to treat the axes). These samples were topped with 5% HCl for ~24 hours, which was enough to dissolve the carbonate. The samples were set to air dry for several hours and re-weighted repeatedly until there was no weight change (W_3). The final weight (W_3) corresponded to the organic portion of the axis, and the difference between the initial post-dehydration (W_2) and final (W_3) weights corresponded to the carbonate portion. The percentage of each material (including water) in the axes could then be estimated.

We found that there was a considerable shrinkage of the axes after treatment in HCl (47-60% of axis original length, Appendix 4-2). This shrinkage associated to exposure to HCl has already been reported for the axis of the sea pen *H. finmarchica* (published as *Balticina finmarchica*) (Marks et al., 1949), and it was also noticed in the sea pens *U. encrinus* and *A. grandiflorum* (Chapter 5). It is probably the result of the heat produced by the reaction with HCl, and not a product of the thermal treatment to which samples were submitted for dehydration, as non-heated axes also shrank when embedded in HCl (personal observation, BMN). Furthermore, Marks et al. (1949) observed a

shrinkage without mentioning any heat treatment. The likely explanation for this phenomenon is that the heat produced by the reaction modified the arrangement of the collagen molecules, and when the carbonate portion of the axis was released, the collagen fibers were no longer supported, and the axis shrank (c.f. Marks et al., 1949). For the purposes of this study, shrunken axes were still viable, as the shrinkage is due to changes in the molecular structure (e.g. breakage of hydrogen bonds), not changes in sample weight.

We also examined the axis carbonate proportion using hydrogen peroxide (H₂O₂) to obtain the inverse result, dissolving the organic matter instead of the carbonate. To this end one sample of *P. grandis* was measured, weighed, embedded in H₂O₂ 30% for 48 hours, and weighted again following the same procedure explained above. The aim of this procedure was merely informative, to determine if both techniques would yield comparable results.

4.2.4 Bomb-radiocarbon (¹⁴C) analysis

As an attempt to validate frequency of ring formation in *P. grandis*, a bomb-radiocarbon (bomb-¹⁴C) analysis was performed in subsamples of the axis from two colonies (39.5 and 42.5 cm). We analyzed the axes of two *P. grandis* colonies collected in 1983 in the Gulf of St-Lawrence (NW Atlantic), which have been hosted at the Canadian Museum of Nature (CMN). These samples have been kept in ethanol 70% since collection. Based on year of collection and estimated age, we believed that these colonies were alive during the peak in ocean ¹⁴C resulting from atomic bomb tests in the early 1950s and late 60s. Only two colonies were available for the study.

To maximize sampling, subsamples for ^{14}C analysis were obtained by longitudinally drilling the axis. A piece of axis ~5 cm long was removed from each colony, involved with Fisherbrand™ labelling tape, and glued to a glass slide using Crazy Glue™. The labelling tape was used to avoid contamination between the sample and the glue. The sample was then longitudinally sectioned using an Isomet® Low Speed Saw. The axis half glued to the glass slide was then longitudinally subsampled to a powder using an automated Micromilling device (New Wave Research MicroMill, CREAT, Memorial University of Newfoundland). The axis was subsampled from the core, middle, and edge regions in one colony (CMN#1), and from five regions from the core to the edge of the axis of the other available colony (CMN#2, larger colony) (Fig. 4-2). Subsamples from the edge area were also obtained by manually scratching the outer region of the section with a razor blade, as not much material could be obtained when drilling the edge with the micromill. Transect width was 350 μm , corresponding to the drill bit width. A drilling depth of 20-30 μm , with the drilling being conducted as three passes along the section was enough to collect sufficient material for the ^{14}C analysis (at least 3 mg per subsample).

Powdered axis samples were sent for ^{14}C analysis at the Centre for Accelerator Mass Spectrometry (AMS), Lawrence Livermore National Laboratory (USA). Results are reported as $\Delta^{14}\text{C} \pm 1\text{s}$ error following the conventions of Stuiver and Polach (1977).

4.2.5 Longevity and growth rates

For the study of longevity and growth rates, we assessed growth rings present in the axis of *P. grandis*. The axes were extracted from the tissue and set to air dry for at

least a day before proceeding with the analysis. Weighing the axes was not in the initial conception of the project and most colonies had their axes sectioned and embedded in epoxy before weighing. Therefore, the axes of only 58 colonies were weighed, to the nearest 0.001 g. The axes of the ten colonies used in the HCl experiment (ids 1-10) were also weighed, and this information was used in the final estimation of carbonate composition of a whole sea pen.

In order to visualize growth rings, sections of the axis were primarily cut at defined locations using a rock saw. Cross sections were made at the zone just above the muscular bulb. If rings were difficult to visualize, an additional cross section was made in the peduncle area, where the axis has a squared shape.

Following the same procedures used in the EDX analysis, these primary sections were embedded in epoxy and then transversely sectioned using an Isomet® Low Speed Saw. Cross sections were manually polished using a Buehler silicon carbide grinding paper (grit 600/P1200) to reduce saw marks. Cross sections were then observed in stereomicroscope under ultraviolet (UV) light, and photographed. The image software GIMP 2.8.8 was used to enhance rings distinction by adjusting the photo color levels. The use of UV light and color level adjustment greatly improve the visibility of growth rings in these organisms (e.g. Chapters 2-3). Growth rings were counted from the photographs at three non-consecutive times and averaged. Axis widest diameter and area were measured from the photographs of cross sections using ImageJ (Schneider et al., 2012). Additionally, we measured axis diameter every ~2 cm using a digital caliper in order to obtain more measurements.

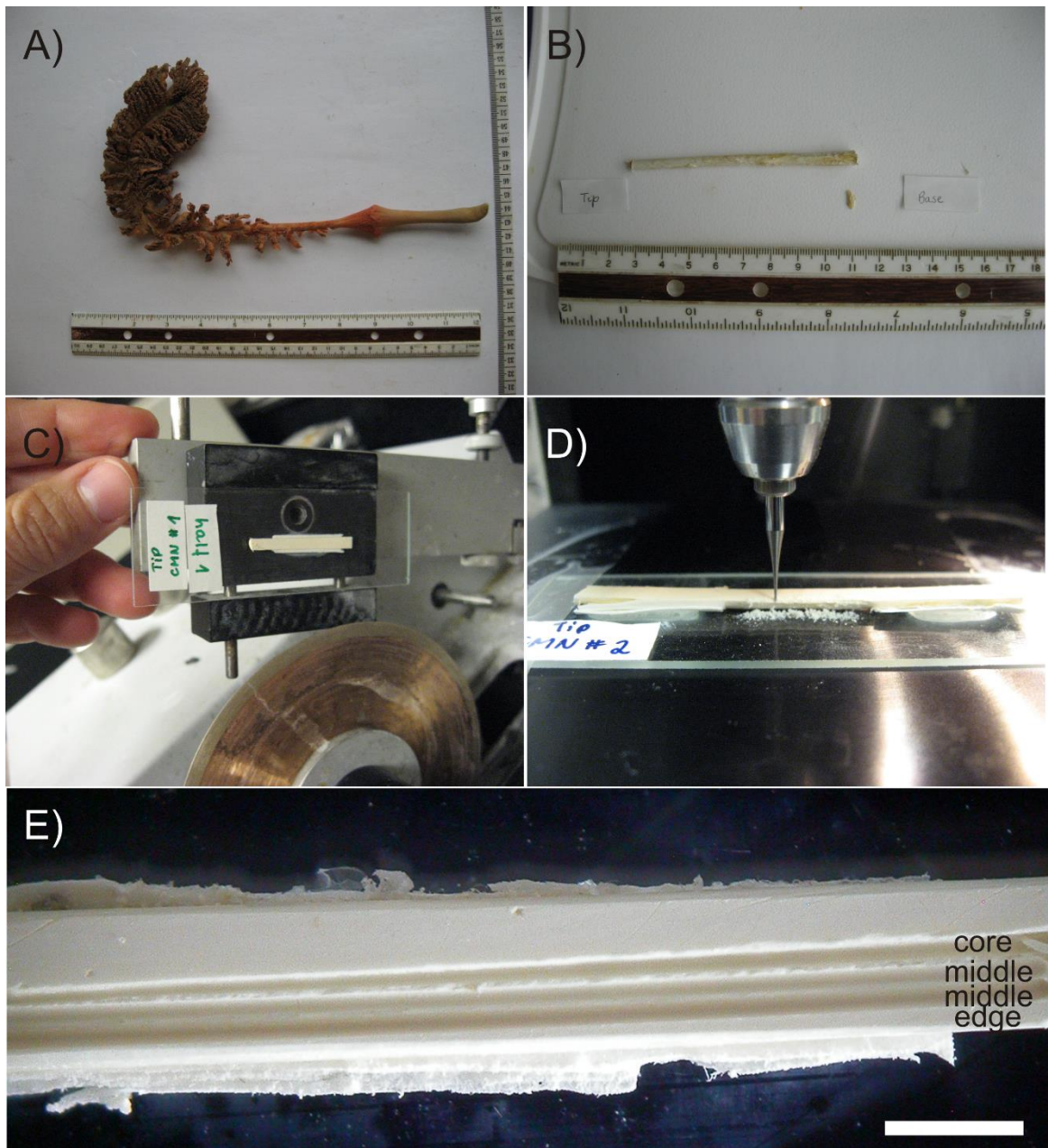


Figure 4-2. A) *Pennatula grandis* colony, B) piece of axis subsampled for ^{14}C analysis, C) longitudinal section of the axis, D) axis being micromilled for ^{14}C analysis, E) resulting drilled axis. Scale bar = 2 mm.

Because the number of growth rings was not necessarily determined from the largest diameter areas (single measurement from cross section), it was also estimated from the largest diameters measured using the caliper, if different. For that we applied the equation on the relationship diameter-age obtained from the cross sections. In this way maximum expected age could be calculated to avoid underestimation.

Growth rates were determined as axis diameter and colony height divided by the number of growth rings (i.e. age) for diametric, and linear growth rates respectively. These growth rates estimates were made based on the number of rings, diameters, and areas obtained from the cross sections.

4.2.6 Environmental data

Relationships between environmental variables (i.e. depth, latitude, temperature, chlorophyll a, surface particulate organic carbon, and surface particulate inorganic carbon) and growth rates and number of rings in *P. grandis* were investigated. Latitude, longitude and depth were obtained during the trawl surveys and they represent the average of a survey set.

Bottom temperature and salinity were retrieved from the World Ocean Database 2013 (Boyer et al., 2013) and viewed in Ocean Data View 4.7.4 (Schlitzer, 2015). Bottom temperature data were also obtained from the Ocean Data Inventory (Bedford Institute of Oceanography database) for the Gulf of St-Lawrence and Newfoundland and Labrador shelves. We averaged the available bottom temperature of the ten CTD casts closest to each sea pen sample.

Data on surface particulate organic carbon (POC), particulate inorganic carbon (PIC), chlorophyll a (a proxy for phytoplankton biomass), and sea surface temperature (SST) were downloaded from <http://oceancolor.gsfc.nasa.gov/> and extracted in ArcGIS 10.1 using Marine Geospatial Ecology Tools (Roberts et al., 2010). Annual data for the period of 2002-2014 were obtained from the Aqua Moderate Resolution Imaging Spectroradiometer Sensor (MODIS) L3 product database. The spatial resolution was 4 km (cell size of 1/24 geographic degree).

Average data on annual surface salinity was obtained from the Simple Ocean Data Assimilation (SODA) database 2.2.4 for the years 1990-2010 (Carton & Giese, 2008). Data were downloaded from the National Center for Atmospheric Research website and extracted in ArcMap using Multidimension Tools. These data had a pixel resolution of 0.25° x 0.4°.

Ocean surface velocity data were obtained from the Ocean Surface Currents Analyses (OSCAR) project. Data were directly imported and extracted in ArcMap using the NOAA OSCAR tool in the Marine Geospatial Ecology Tools extension. These data were used as an average of measurements taken every five days from 1992-2004, with a spatial resolution of 1/3 of a degree.

As for chapter 2 and 3, most environmental variables were chosen because of their known overall importance to cold-water coral distribution (Roberts et al., 2009). The exception was salinity, which was included as an opportunistic variable, without a specific hypothesis on its relationship to growth rates.

4.2.7 Data analysis

General Linear Models (GLMs) were used to assess relationships between colony/axis metrics (peduncle length, proportion of peduncle, density of polyp leaves, axis diameter, area, and weight), number of rings (i.e. colony age), and growth rates in relation to colony height. Because colonies were collected from different locations and depths, we performed GLMs including location and depth as covariates using the function *aov* (type I sum of squares) in RStudio (Kabacoff, 2015). If interactions with location were significant, we repeated the models by location. Nonsignificant interactions were maintained in the models, based on theoretical expectations regarding the interaction (Aiken & West, 1991), as both location and depth have been shown to explain colony size in NW Atlantic sea pens (c.f. Baillon et al., 2016). The Labrador site only had six observations, and for this reason results on any of the analysis performed specifically for this location should be taken cautiously, especially if the outcome differed from that of the other sites.

When investigating relationships between colony growth rates and environmental factors we opted for performing simple regressions instead of a single multiple regression in order to control for colony height. If there were interactions between the colony height and location in these models, models were performed by size class, with locations pooled and height being controlled again. Because there was no significant relationship between colony height and depth when controlling for location, depth was added to the models as a covariate, and an interaction was added only to assess the assumption of homogeneity of slopes. If the interaction was non-significant, it was excluded and the model was run again without the interaction term.

The investigation on the relationship between number of polyp leaves and colony height was investigated through a generalized linear model using a Poisson regression (glm function), since this variable represents counts. The R package *qqc* was used to test for significant overdispersion. If a significant overdispersion was identified, then a quasipoisson regression was used (Kabacoff, 2015).

Cook's distance plots were used to identify possible influential observations (Kabacoff, 2015). In the case of Cook's distance ≥ 1 , the observation was considered influential and removed from the model if noticed to be influencing the assumptions of linearity, homogeneity, normality, and independence of residuals, which were evaluated through residuals versus fits plots in RStudio (Kabacoff, 2015). Significance level (α) for all tests was set at 5%. Error is reported as the standard deviation (SD). All analyses were performed in RStudio version 0.99.484.

4.3. Results

4.3.1 Colony height versus location and depth

There was a significant relationship between colony height and location ($F=22.91$, $p < 2e-16$, $N=110$), but not with depth ($F=1.38$, $p=0.24$, $N=110$). For this reason, further analyses involving colony height were performed by location, but not controlling for depth unless stated. Colonies from the Laurentian Channel area were taller than at the other sites (Fig. 4-3).

4.3.2 Peduncle metrics and polyp leaves versus colony height

When pooling the data on the relationship between peduncle length and colony height, there was a positive trend (Fig. 4-4A), whose statistical significance was assessed by examining each location separately. There were significant positive relationships between peduncle length and colony height at all sites (Appendix 4-3). Conversely, the peduncle became proportionally smaller as the colony increased in height (Fig. 4-4B); although this relationship was not statistically significant for colonies from the Davis Strait and Labrador regions (Appendix 4-3). Number of pairs of polyp leaves significantly increased with colony size at all locations (Fig. 4-4C, Appendix 4-3), but polyp leaves density showed the opposite pattern of density decreasing as colony size increased (Fig. 4-4D, Appendix 4-3).

By fitting colony metrics to the allometric equation ($y = Ax^b$), the relationships between peduncle length (plength) and colony height ($\text{plength} = 0.5237 * \text{cheight}^{0.8281}$) as well as number of pairs of polyp leaves (PL) and colony height ($\text{PL} = 2.9576 * \text{cheight}^{0.691}$) had coefficients of allometry < 1 , indicating a negative allometry. This shows that both peduncle and number of polyp leaves grow at slower rates than the overall colony.

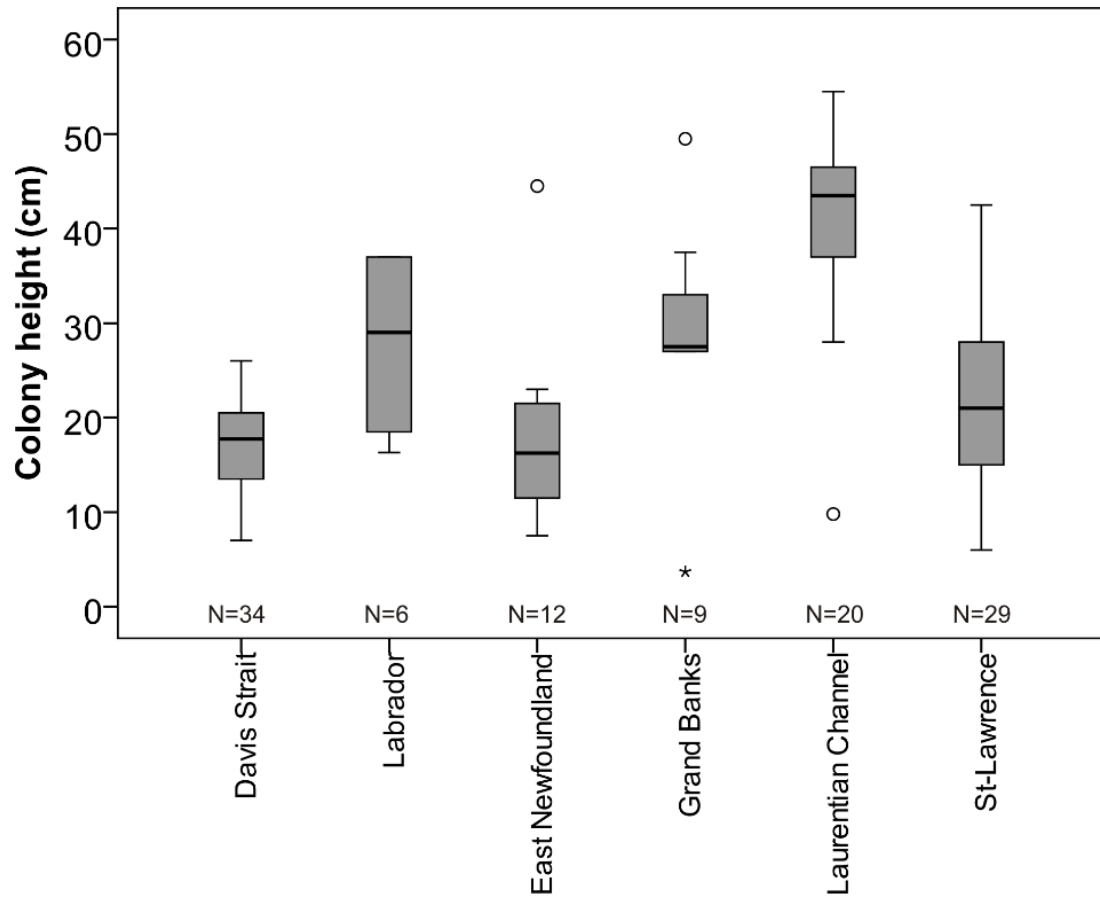


Figure 4-3. Colony height in *Pennatula grandis* from the Northwest Atlantic by location.

Black horizontal bars inside the boxes represent the median, boxes are limited by minimum and maximum values, and circles are outliers. Left to right: north-south.

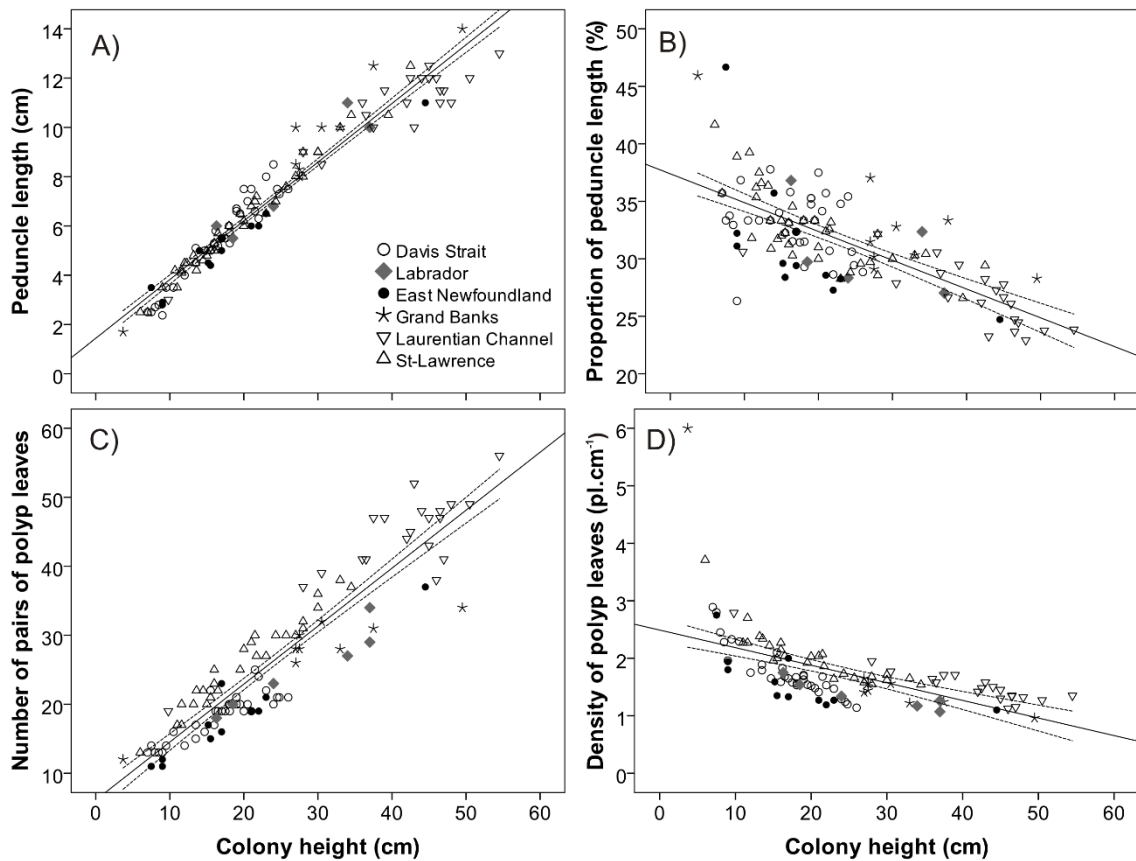


Figure 4-4. Colony metrics in relation to colony height in *Pennatula grandis*: A) peduncle length, B) proportion of peduncle length, C) number of pairs of polyp leaves, and D) density of pairs of polyp leaves. Fit lines and confidence intervals (dashed lines) are for reference only, as the regression equation also included depth as a covariate.

4.3.3 Axis characteristics

The XRD analysis showed that the carbonate portion of the axis in *P. grandis* is composed of magnesian calcite $(\text{Ca,Mg})\text{CO}_3$ (Appendix 4-4). The EDX analysis showed Ca as the element with the highest relative frequency ($77.31\% \pm 0.39$), followed by C

(6.58% ± 0.15), O (6.41% ± 0.12), Mg (4.85% ± 0.07), P (2.96% ± 0.09), and N (1.88% ± 0.02). No specific trends were observed in terms of distance from the center, but the number of main peaks in the distribution of calcium was comparable to the number of rings visually counted (average = 19) (Fig. 4-5). The Mg/Ca ratio in the axis ranged 0.04-0.08.

Using the HCl method, the carbonate material for the whole axis corresponded in average to 85% of axis weight in the ten analyzed samples (Table 4-1, Fig. 4-6). The non-carbonate portion of the axis was composed of 13% of organic material and 2% of water (Table 4-1, Fig. 4-6). There was a trend of axis carbonate proportion decreasing with colony size in *P. grandis* (Fig. 4-6).

When using the technique of H₂O₂ to determine axis carbonate proportion the results were comparable, with the carbonate portion of the axis representing 86% of axis weight. After treatment with H₂O₂ the proximal extremity of the axis was completely dissolved, leaving only a cluster of CaCO₃ sclerites.

Axis' surface was mainly smooth, with no bumps or substantial ridges observed (Fig. 4-7). It was beige in color, sometimes showing a superficial reddish tone right after extraction from the colony. It became of an amber color after dissolution of the carbonate portion in HCl and of a bright white color after treatment with H₂O₂ (Fig. 4-7). The axis had an asymmetric to round shape in the first cm, becoming relatively squared, and switching back to round above the peduncle (Fig. 4-7).

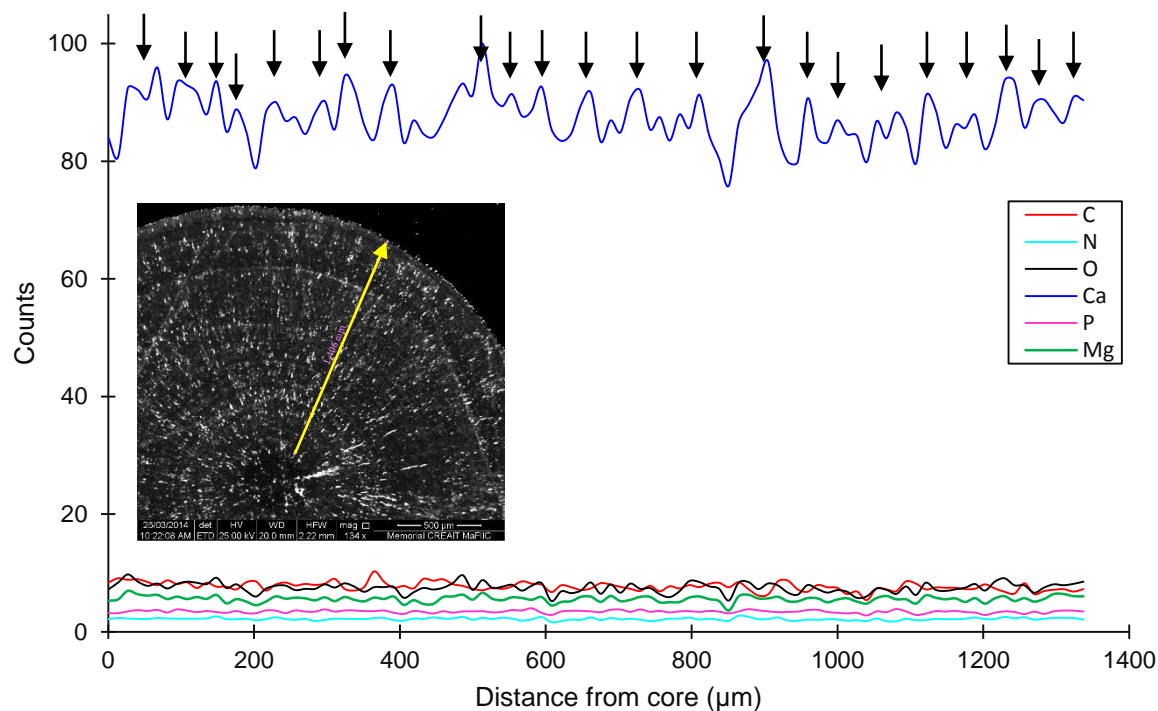


Figure 4-5. Results on the EDX analysis on a transect from the center (near the core) to the edge in a cross section of the axis of *Pennatula grandis* (sample 074, inset). Black arrows point to main peaks (N = 23) in the distribution of Ca.

Table 4-1. Summary of axis composition in *Pennatula grandis* (N=10).

	Weight (g)			Percentage		
	Water	Organic	CaCO ₃	%water	%organic	%CaCO ₃
Min	0.001	0.003	0.04	1.49	7.73	80.0
Max	0.011	0.095	0.42	2.94	17.9	90.0
Average	0.005	0.034	0.21	1.91	12.9	85.2
SD	0.003	0.024	0.12	0.42	2.63	2.64

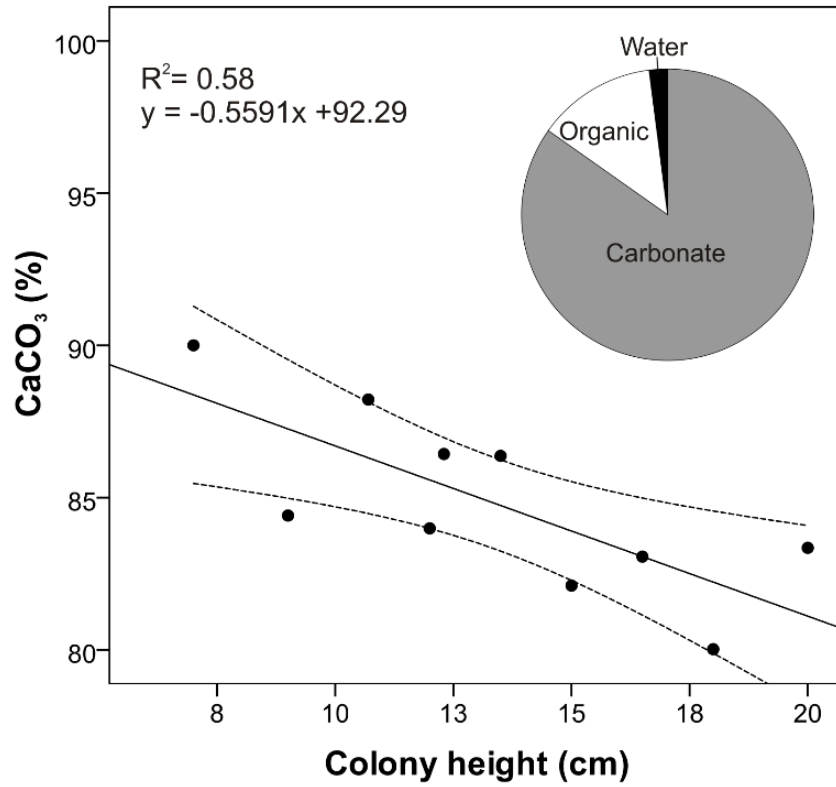


Figure 4-6. Axis composition and carbonate proportion in relation the colony height in colonies of the sea pen *Pennatula grandis* from the NW Atlantic.

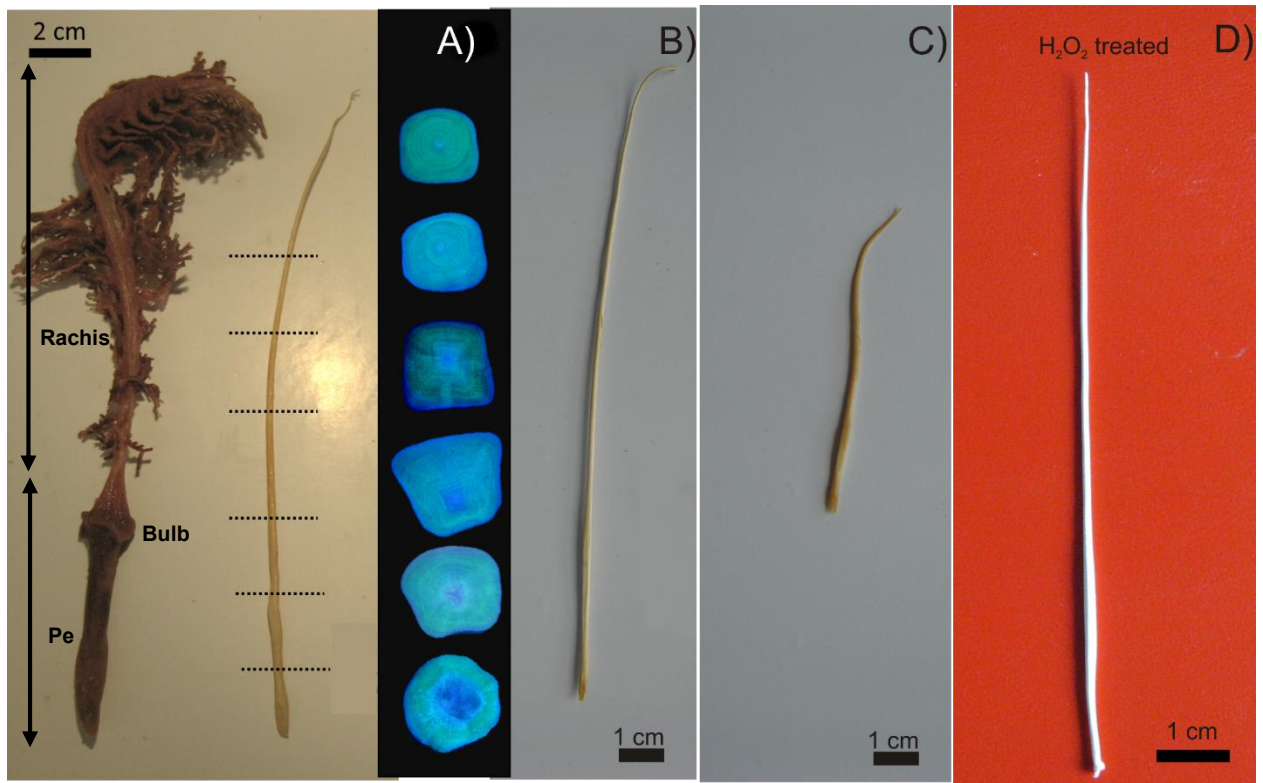


Figure 4-7. Axis of the sea pen *Pennatulula grandis* after extraction from the colony, showing A) cross sections along its length, B) before, and C) after treatment with HCl, and D) another axis after treatment with H₂O₂. Pe: peduncle.

The axis was shorter than the whole colony height, with a portion of the rachis remaining axis-free (Fig. 4-8A inset). At its distal tip, the axis assumes the form of a delicate spiral (or hook), and even when uncoiling the axis, it does not extend throughout the whole rachis. There was a trend of the axis-free space increasing with colony height (Fig. 4-8). The axis-free space length ranged 0.5-7.5 cm (Fig. 4-8A), and the number of pairs of polyp leaves in the axis-free space ranged 2-16 (Fig. 4-8B). This trend was statistically significant both in terms of axis-free space length and in number of pairs of

polyp leaves in the axis-free space, except for the Labrador and Laurentian Channel colonies, and Grand Banks (gap in cm) (Appendix 4-3).

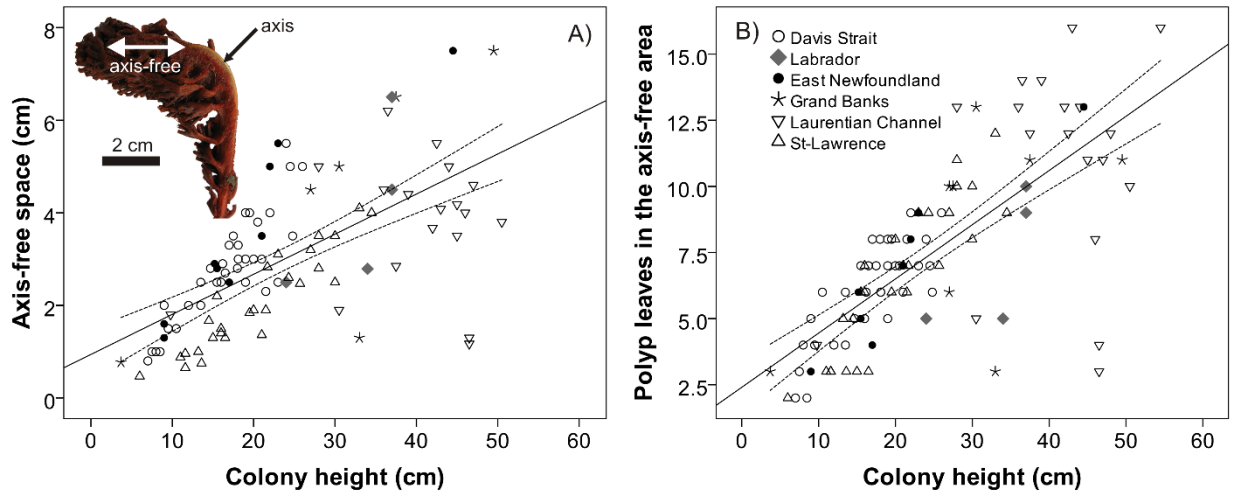


Figure 4-8. Axis-free space in *Pennatulula grandis* in relation to colony height in terms of A) space length (A) and B) number of pairs of polyp leaves. Inset in A shows extension of axis visible through the tissue.

4.3.4 Axis metrics versus colony height

There were significant positive relationships between axis metrics (i.e. axis diameter, area, and weight) and colony height for almost all locations (Appendix 4-3, Fig. 4-9A-C). The axes used in the HCl experiment represented between 21 and 29% of the colony dry weight ($24\% \pm 2.2$, $N=10$), and there were no trends on axis proportion in relation to colony height for the size classes available (Fig. 4-9D).

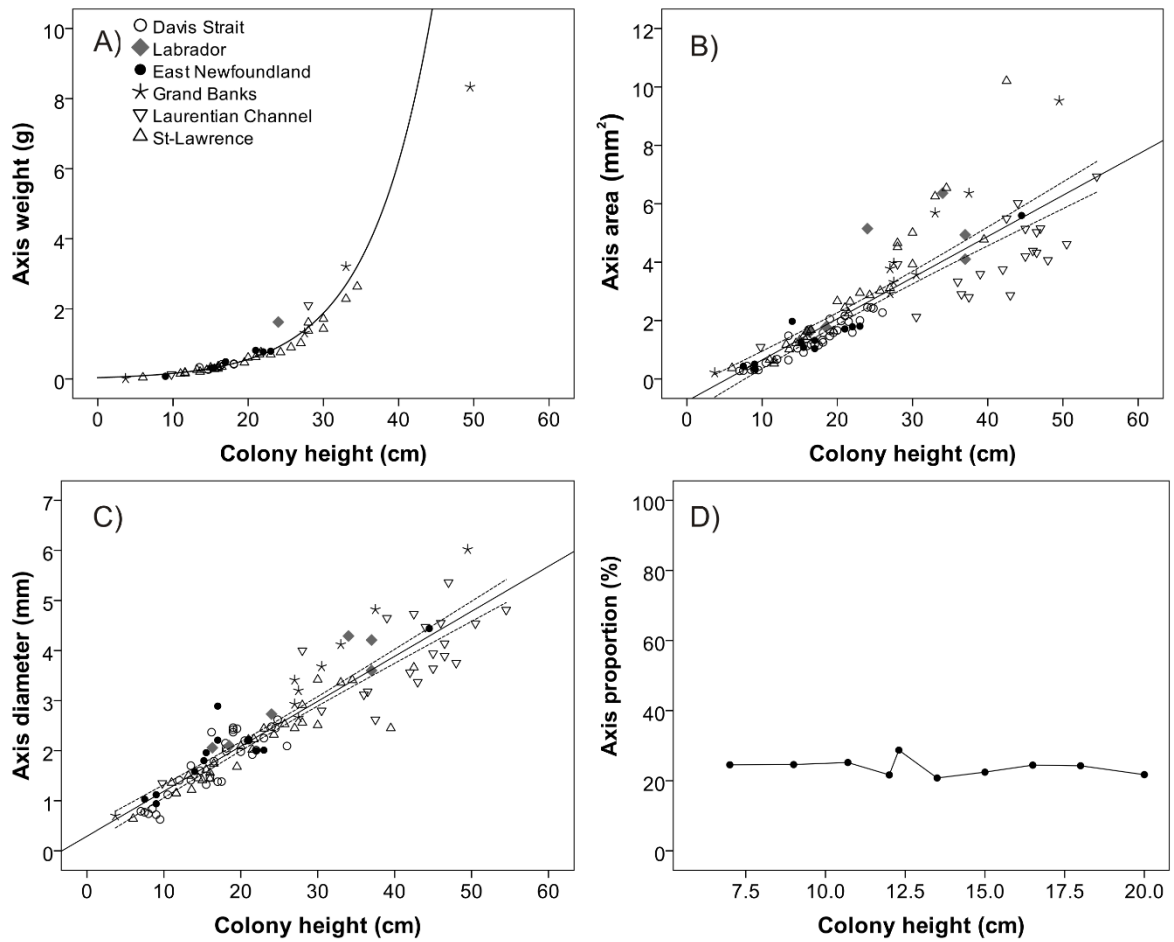


Figure 4-9. Axis metrics in relation to colony height in *Pennatula grandis*: A) axis weight, B) axis area, C) axis diameter, and D) axis proportion (in weight, N= 10).

When applying the allometric equation to the relationship between axis diameter and colony height, a slope very close to 1 was obtained, which indicates a certain inclination towards isometry for this morphological trait ($\text{Diameter} = 0.1217 \cdot \text{height}^{0.9442}$).

4.3.5 Bomb-radiocarbon (^{14}C) analysis

An average of 31 rings were counted in the largest *P. grandis* sample from the Canadian Museum of Nature (CMN#2, 42.5 cm), and 27 rings from the smallest colony (CMN#1, 39.5 cm). The radiocarbon analysis yielded pre-bomb $\Delta^{14}\text{C}$ values for both colonies, with maximum values of -14.6 and -30.6 in the samples from the edge of the axes (Table 4-2, Fig. 4-10). In both colonies there was a clear increase in the $\Delta^{14}\text{C}$ values from the core to the edge of the axes (Fig. 4-10).

Table 4-2. Results of ^{14}C analysis in the axis of two *Pennatula grandis* colonies. Samples were collected in 1983 (edge region). The year for the core region equals 1983 minus the number of rings visually counted. The years for the middle regions were estimated as the number of rings between core and edge, divided by the number of regions. CAMS is the Center for Accelerator Mass Spectrometry analytical identifier.

Sample	Region	Year	CAMS #	$\Delta^{14}\text{C}$	\pm	^{14}C age	\pm SE
CMN#1_1	core	1956	171220	-60.6	3.69	500	35
CMN#1_2	middle	1963	171221	-53.9	4.30	445	40
CMN#1_3	middle	1970	171223	-28.1	3.37	230	30
CMN#1_4	edge	1983	171224	-14.6	3.68	120	35
CMN#2_1	core	1952	171225	-76.4	3.51	640	35
CMN#2_2	middle	1958	171226	-74.0	3.40	620	30
CMN#2_3	middle	1964	171227	-76.8	3.41	640	30
CMN#2_4	middle	1971	171228	-72.4	4.06	605	40
CMN#2_6	edge	1983	171229	-30.6	3.94	250	35

These values were quite distinct from those previously reported for the proteinaceous part of the skeleton in the gorgonians *Primnoa resedaeformis* (Gunnerus, 1763) and *Keratoisis grayi* (Wright, 1869) (published as *K. ornata*), but very similar to

values from the calcite portion of the skeleton in *K. grayi*, in which rings are formed annually (Sherwood et al., 2008, Fig. 4-10).

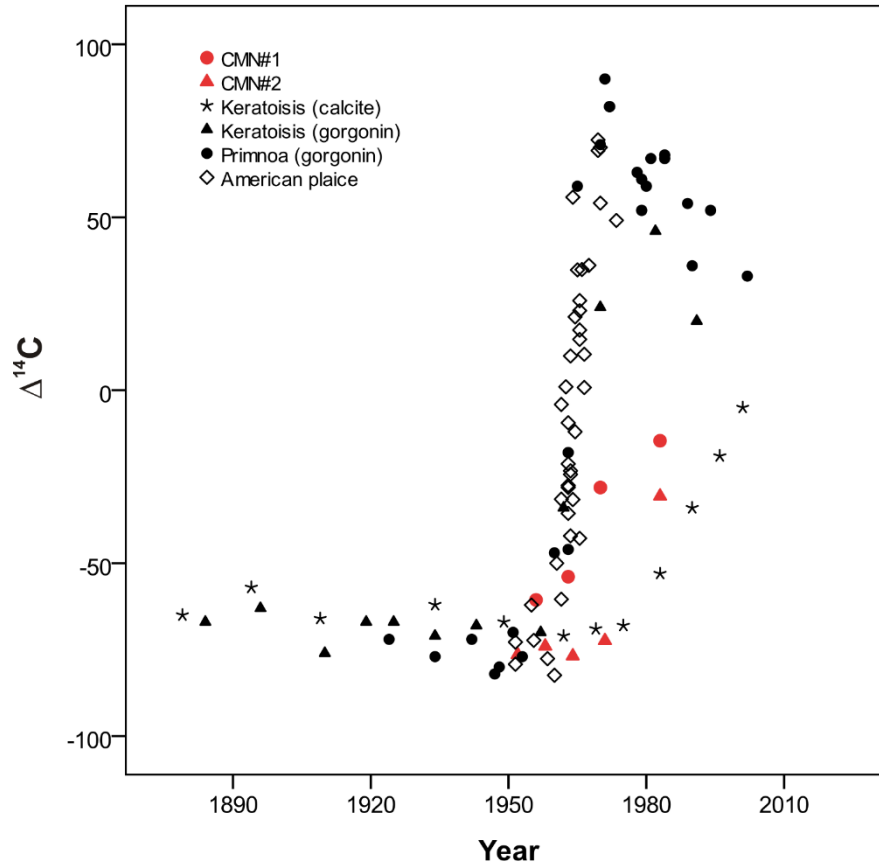


Figure 4-10. $\Delta^{14}\text{C}$ for axis of two *Pennatulula grandis* colonies from the Gulf of St-Lawrence (red symbols) in relation to year, overlaid with $\Delta^{14}\text{C}$ data from calcite and gorgonin in *Keratoisis grayi* from the SW Grand Banks (Sherwood et al., 2008), gorgonin in *Primnoa resedaeformis* from the Northeast Channel – Nova Scotia (Sherwood et al., 2005), and otolith from American plaice *Hippoglossoides platessoides* (Fabricius, 1780) from the Southern Gulf of St. Lawrence for reference (Morin et al., 2013).

4.3.6 Estimated longevity and growth rates

Growth rings were not clearly seen in the first 2 cm of axis where it is porous and composed by minute calcareous corpuscles (Fig. 4-11A), but they could be readily seen across the axis when illuminated with UV light, at least from above the peduncle (Fig. 4-11B). In small colonies, the visualization of growth rings was more challenging.

The average number of rings for all analyzed colonies ranged 4-31. The number of counted rings increased with colony height (Fig. 4-12A), and this relationship was significant for colonies from all regions except Labrador (Appendix 4-3). Because there were no significant interactions between axis diameter and location we pooled the data on the analysis on number of rings in relation to axis diameter, which yielded a significant positive relationship between these two variables ($F= 40.95$, $p= 4.33e-09$, $N= 110$) while controlling for colony height (no significant interaction) (Fig. 4-12B). When estimating number of rings from the largest diameter (measured with the caliper), the maximum average number of rings was ~ 32 (Number of rings = $8.8993 \cdot \text{diameter}^{0.7107}$).

Considering ring to be formed annually, diametric growth rates ranged between $0.06\text{-}0.21 \text{ mm}\cdot\text{yr}^{-1}$, averaging $0.13 \text{ mm}\cdot\text{yr}^{-1} \pm 0.03$. Linear growth rates ranged between $0.58\text{-}3.79$, averaging $1.81 \text{ cm}\cdot\text{yr}^{-1} \pm 0.6$. There was a positive trend between growth rates and colony height when pooling all observations (Fig. 4-13). In the GLM analysis there were no significant relationships between diametric growth rates and location (Fig. 4-14A), depth or their interactions, but there was a significant relationship with colony height ($F= 6.6$, $p= 0.012$). Similarly, there were significant relationships between linear growth rates and height ($F= 45.64$, $p= 1.6e-09$) and also with location ($F= 4.10$, $p= 0.001$, Fig. 4-14B), but no significant interactions were identified.

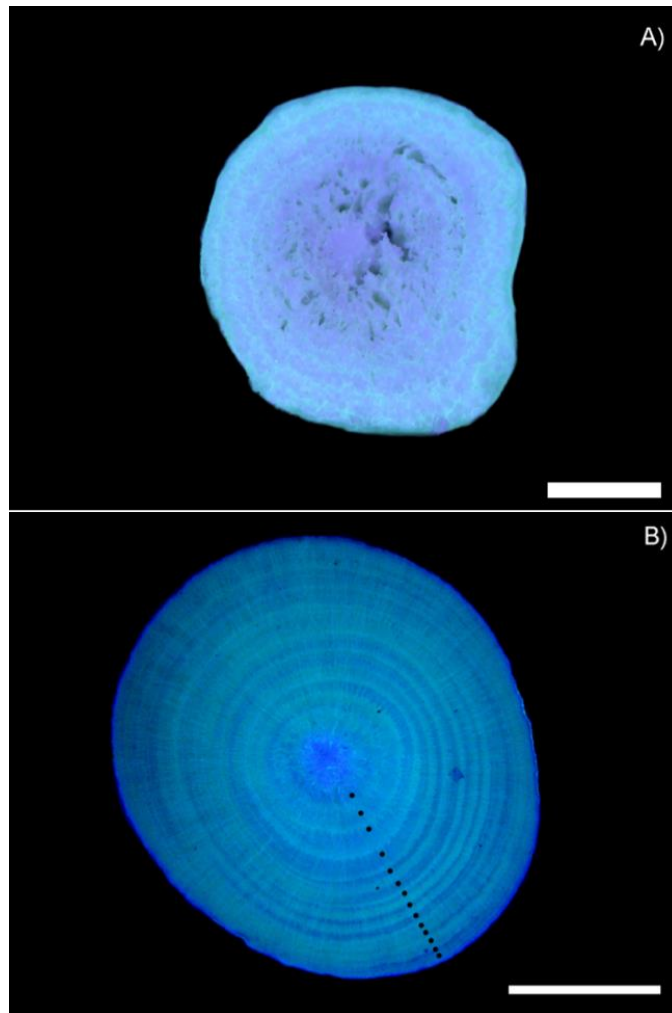


Figure 4-11. Cross sections of the axis in *Pennatula grandis* under UV light at the base (A, specimen 011) showing a porous aspect, and above the peduncle area (B, specimen 075) showing growth rings depicted by 14 black dots. Photos were not taken from the same colony. Scale bars = 1 mm.

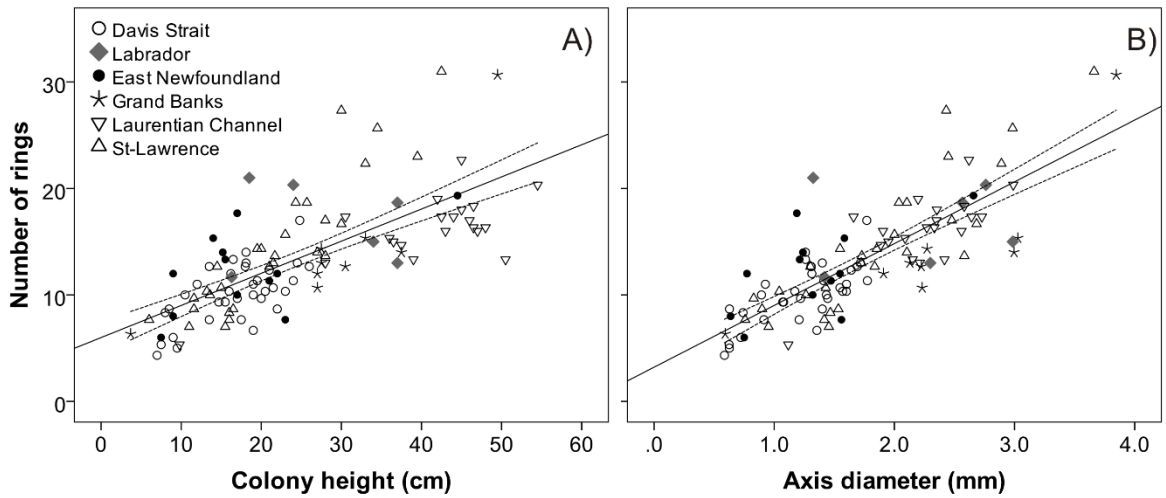


Figure 4-12. Number of rings in relation to A) colony height, and B) axis diameter in *Pennatula grandis*. Fit lines and confidence intervals (dashed lines) are for reference only, as the regression equation also included depth as a covariate.

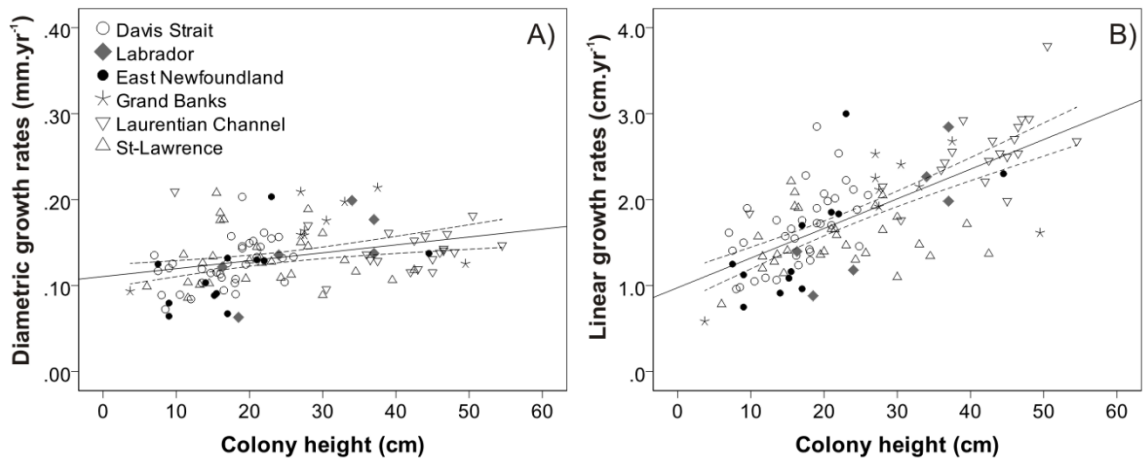


Figure 4-13. Growth rates in relation to colony height in *Pennatula grandis*. A) Diametric growth rates ($\text{mm}\cdot\text{yr}^{-1}$), and B) Linear growth rates ($\text{cm}\cdot\text{yr}^{-1}$). Fit lines and confidence intervals (dashed lines) are for reference only, as the regression equation also included depth as a covariate.

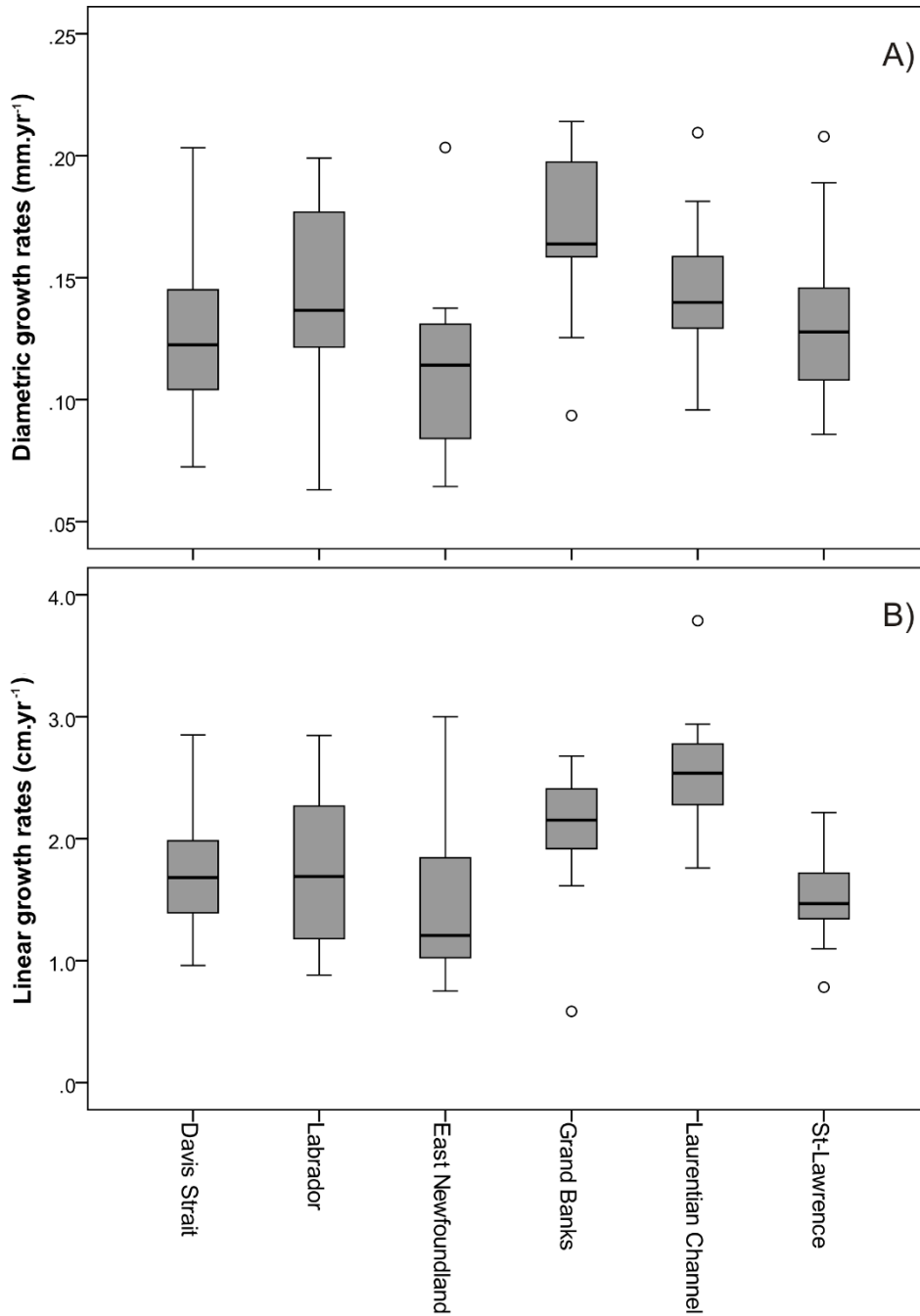


Figure 4-14. Diametric and linear growth rates in *Pennatula grandis* from the NW Atlantic by site (left to right: north-south). Black horizontal bars inside the boxes represent the median, boxes are limited by minimum and maximum values, and circles are outliers.

4.3.7 Growth rates in relation to environmental factors

Because there were no significant relationships between diametric growth rates and locations or depth, but with height, the analysis between diametric growth rates and environmental factors was performed by pooling locations, but by size classes (i.e. small, medium, and large). In order to control for colony height, simple regressions were performed between growth rates and each environmental factor. Because the relationship between linear growth rates and location was statistically significant, the analysis on growth rates in relation to environmental factors was only performed using diametric growth rates.

From this analysis there were no significant relationships between diametric growth rates and any of the environmental variables for the small and medium size classes, but there were significant negative relationships with chlorophyll a, POC, and PIC for the large size class (Table 4-3, Fig. 4-15).

Table 4-3. Results of the GLM analysis between diametric growth rates and environmental factors in *Pennatula grandis* by size class (small, medium, and large), with colony height as a co-variable. Interaction indicates a significant interaction between the environmental variable and colony height.

	Small			Medium			Large		
	F	p-value	N	F	p-value	N	F	p-value	N
Chlorophyll a	0.723	0.403	29	Interaction		51	5.097	0.033	30
POC	1.209	0.282	29	Interaction		51	5.415	0.028	30
PIC	2.023	0.167	29	Interaction		51	6.053	0.021	30
SST	0.365	0.551	29	1.11	0.298	51	0.007	0.932	30
Surface currents	Interaction		29	Interaction		51	0.859	0.363	30
Surface salinity	3.49	0.074	29	Interaction		51	Interaction		30
Bottom temperature	1.143	0.295	29	2.384	0.132	36	0.042	0.840	30
Bottom salinity	0.063	0.804	29	0.019	0.890	35	0.713	0.406	30

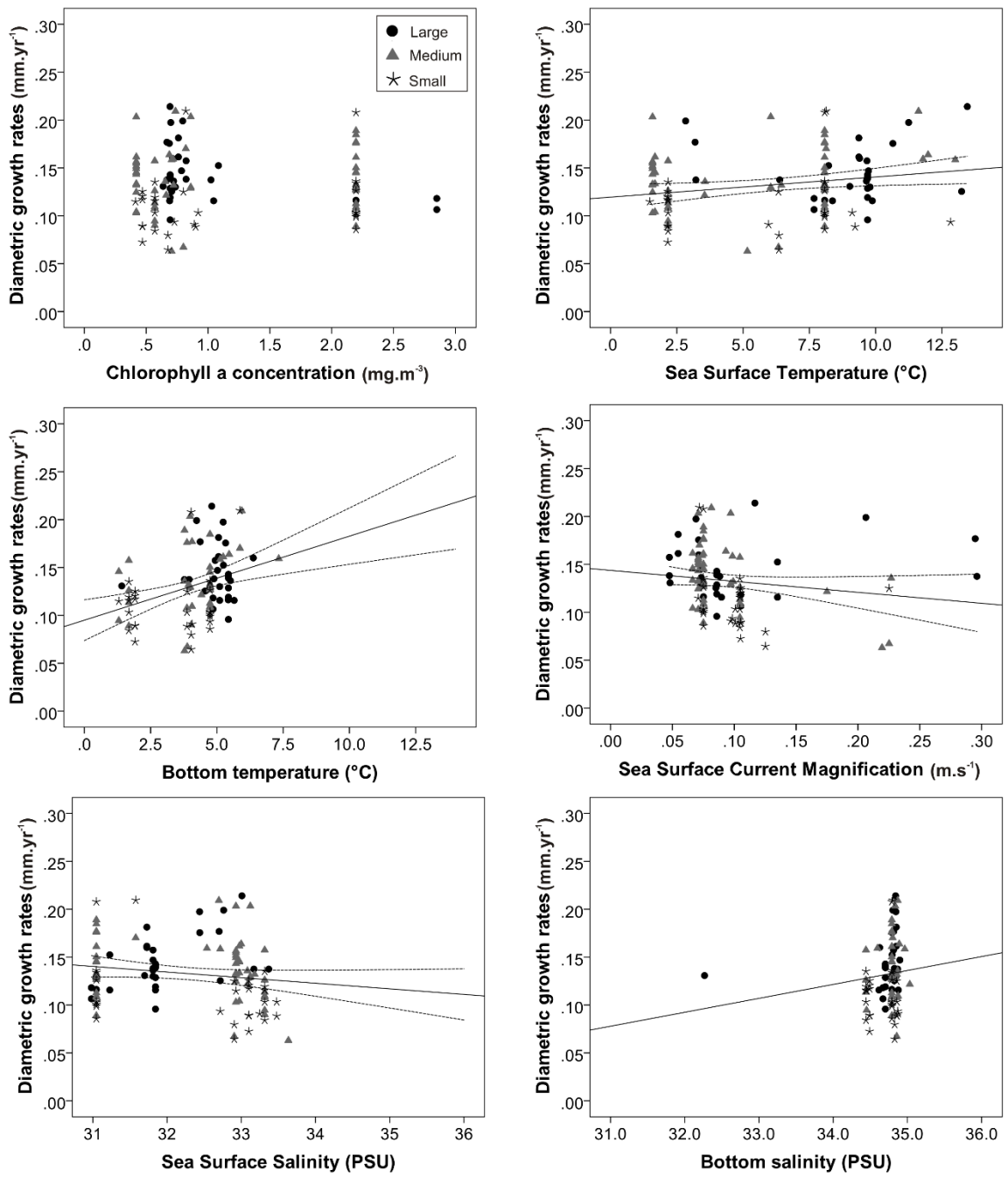


Figure 4-15. Diametric growth rates in the sea pen *Pennatula grandis* from the NW Atlantic in relation to environmental variables by size class. Fit lines and confidence intervals (dashed lines) are for reference only, as the regression equation also included height as a covariate. POC and PIC had the same patterns as chlorophyll a, with

chlorophyll a and POC strongly correlated (Pearson's $r = 0.98$, $N=42$, unique values only including data on all size classes).

4.4. Discussion

4.4.1 Relationship between peduncle and colony height

The strong relationship between peduncle length and colony height in sea pens was already reported in previous studies (e.g. Hickson, 1916, Baillon et al., 2016, Chapter 3), and it is intuitive since the peduncle anchors the whole colony into the sediment (Williams, 1995). In the sea pansy *Renilla koellikeri* Pfeffer, 1886 peduncle length increased with flow velocity (Kastendiek, 1976). Although the rachis is usually longer than the peduncle, in *Gyrophyllum* spp. the peduncle is longer than the rachis (Williams, 1995).

The negative relationship between peduncle proportion and colony height was also found in the deep-water sea pens *Umbellula encrinus* Linnaeus, 1758 (Chapter 3), *Halipterus finmarchica*, and *Anthoptilum grandiflorum* (Verrill, 1879), but not in *Pennatula aculeata* (Baillon et al., 2016). The negative relationship between proportion of peduncle and colony height suggests that at some point during colony life, rachis and peduncle grow at different rates, with the peduncle growing at a slower rate than the rachis. Polyp leaves (and autozooids) are only present in the rachis. By not being directly involved in feeding and reproduction, the peduncle might grow slower once its size is large enough to support the colony, and then growth slows down. This was also showed by the allometric equation and negative allometric growth. The observation by Baillon et

al. (2016) that a related species (*P. aculeata*) shows a different pattern, indicates that this relationship is not generalized, but rather species-specific.

Hickson (1916) mentioned that in *Pennatula* spp., *Gyrophyllum* spp., and *Scytalium* spp. from a same location, the ratio rachis length/stalk (peduncle) length is practically constant. He suggested that this relationship should change with depth and nature of bottom, and that in deep-sea species the peduncle is longer in proportion to the rachis. Peduncle proportion decreased with depth in *A. grandiflorum*, but not in *H. finmarchica* and *P. aculeata* (Baillon et al., 2016). Grain size should have an influence on peduncle metrics, and the relationship between peduncle (size and proportion) and colony height might change with bottom type, as different granulometries can have important consequences to burrowing organisms (Huz et al., 2002), but this is still to be investigated in the context of sea pens.

4.4.2 Number and density of polyp leaves

The total number of pairs of polyp leaves increased with colony height, but smaller colonies had more polyp leaves per cm of rachis than large colonies. Because in the genus *Pennatula* polyp leaves support and host the autozooids, it makes sense that when the colony is young it primarily grows by adding new polyp leaves, which are required to support the autozooids. The colony keeps adding new autozooids in formed polyp leaves, and simultaneously creating new polyp leaves.

On the other hand, the observation that density of polyp leaves decreased with colony height might indicate that the speed at which new polyp leaves are created decreases with time, as the colony probably invests more on autozooid addition than on

the creation of new polyp leaves. This is partially corroborated by the observation that in *P. aculeata* the density of polyps increased with colony height (Baillon et al., 2016).

Similarly, polyp leaves might become less dense and crowded over time because there is new rachis space being created. In *P. grandis* the distance between polyp leaves is higher at the distal portion of the rachis (Sars, 1846). This was also showed by the allometric equation and negative allometric growth.

In *P. aculeata* polyp density was also shown to increase in colonies inhabiting waters >1000 m (Baillon et al., 2016), which might help colonies to cope with food availability limitations at those depths. This suggests that the addition rate of autozooids might be plastic and adjustable depending on environmental conditions. However, since we did not find significant relationships between colony height and depth, we think that for the specimens included in this study density of polyp leaves depends on colony height, with a pattern of slower polyp leaf growth (addition) over time.

4.4.3 Axis-free space

Larger colonies have a larger axis-free space than smaller colonies (in space length and in number of pairs of polyp leaves), indicating that this gap increases as the colony grows. Musgrave (1909) indicated that the axis of certain sea pens can coil and uncoil, suggesting that part of the axis-free space might not be permanent. Baillon et al. (2016) also noticed that in *P. aculeata* the axis does not follow the whole colony height, while it does in *A. grandiflorum* and *H. finmarchica*. The authors suggested that having this gap might be related to colony withdrawal in the sediment, a behavior observed in *P. aculeata* (Langton et al., 1990). It is clear that the oblique musculature associated to the

axis of sea pens has an important role in colony movement, and it has been suggested that the coiled axis could act as a spring, helping to propel the colony (Musgrave, 1909).

Another reason for the existence of a gap between the tips of axis and rachis has been suggested by Jungersen (1904). In the original description of *Pennatula prolifera* Jungersen, 1904, this gap has been suggested to be related to reproduction by transversal fission (Jungersen, 1904). Jungersen argued that the region in the rachis seeming to suffer transversal fission is found just above the region where the axis ends. To this author, the absence of axis in this area could be related to the fact that this portion is going to be separated from the colony. But to our knowledge, transversal fission has not been reported in *P. aculeata* or *P. grandis*, both of which have an axis-rachis gap.

At least for *P. grandis* the gap between axis and rachis length increases in larger colonies and it is possible that it is not related to reproduction, as very small and young colonies also had this gap. The larger gap in larger colonies might simply indicate that the rachis grows faster than the axis, but perhaps it also indicates the existence of different roles for the axis-rachis gap during ontogeny.

4.4.4 Axis composition

In *P. grandis* the carbonate portion of the axis was composed of magnesian calcite (CaMgCO_3), which has also been reported in the axis of the sea pens *H. willemoesi* (Wilson et al., 2002), *U. encrinus*, *A. grandiflorum* (Chapter 5), *H. finmarchica* (Chapter 2), *P. aculeata* (data not shown), and *Virgularia* sp. (Dalyell, 1848). Besides calcium carbonate, calcium phosphate (phosphate de chaux) has been identified in the axis of *Pennatula phosphorea* Linnaeus, 1758 (Dalyell, 1848, Pelouze & Fremy, 1865).

The results from the EDX analysis did not show any trends on the distribution of the tested elements along the radius of the axis, but the comparable number of Ca peaks and number of rings visually determined indicates that EDX analysis might be considered as a tool for cross-validation when determining the number of rings in a sample. By examining the trace element composition in the axis of *H. finmarchica* (Chapter 2) and *U. encrinus* (Chapter 3) using Secondary Ion Mass Spectrometry (SIMS) a similar pattern was observed, indicating a potential geochemical signature of the rings. However, SIMS is a precise, relatively expensive technique while EDX is cheaper and faster, although less precise. A refining of the EDX technique in the context of the axis of sea pens might therefore be useful, when the objective is simply a cross-validation or elemental characterization of the sample.

We found that *ca.* 85% of the whole axis was composed of carbonate material. This is comparable to the previously reported for *V. mirabilis* (also 85%, Dalyell, 1848), and it is higher than the found in *P. phosphorea*, in which ~70% of the axis was composed of carbonate material (calcium carbonate and calcium phosphate) (Pelouze & Fremy, 1865). It is also higher than in *A. grandiflorum* (65%) and *U. encrinus* (71%) (Chapter 5). The mineral content of mollusk shells can be over 95% of the shell composition (Currey, 1999), but in the case of sea pens, colony flexibility (allowed due to the axis flexibility) helps to reduce drag and increase filtering efficiency (Best, 1988). Therefore, the organic component of the axis is of major importance to the skeleton of a sea pen. Differences in the carbonate proportion of the axis between taxa might be related to colony size, particular needs for more flexibility or rigidity, and even environmental factors including regional carbonate-ion concentration (Marubini et al., 2003).

The need for flexibility also seems to be identified in the observed trend of axis carbonate proportion decreasing with colony height in *P. grandis*. As colonies grow, they will probably need a stronger skeleton, but that is flexible enough to avoid breakage. This decrease in the amount of carbonate material related to flexibility has already been reported for other organisms. In stalked crinoids, longer stalks exhibit more flexibility than shorter ones (Baumiller & Ausich, 1996). Chang et al. (2007) showed an increase in axis weight and decrease in calcareous sclerites weight with colony height for the sea whip *Juncella fragilis* (Ridley, 1884).

The dissolution of the proximal extremity of the axis after treatment with H₂O₂ suggests that this area is not heavily calcified, but only composed of sclerites embedded in the axis tissue. In the sea pen *Veretillum cynomorium* (Pallas, 1766) this portion of the axis is of organic nature (Ledger & Franc, 1978), and it might not have an important role in colony support. It has been suggested to play a role in colony withdrawal in *Virgularia juncea* (Soong, 2005).

The Mg/Ca ratio in the axis of *P. grandis* ranged 0.04-0.08, which is much lower than that determined for the sclerites of *P. aculeata* and *H. finmarchica* (in average 0.13 and 0.17, respectively) (Baillon et al., 2016). This might suggest that the calcium content relative to magnesium is much higher in the axis than in the sclerites.

No other recent studies have shown the percentage of organic and inorganic material in the axes of sea pens. But our finding that *ca.* 85% of the axis is composed of carbonate material, and that the axis can make in average 24% of total colony dry weight, summed to the fact that sclerites can represent >60% of tissue dry weight in *P. aculeata* (English, 2012) suggest that >65% of a whole sea pen colony can be composed of

carbonate material. In the context of ocean acidification (e.g. Orr, 2005, Maier, 2012, Bostock et al., 2015) it would be important to investigate the existence of phylogenetic, geographic, and bathymetric natural variation in the carbonate composition of the axis of other sea pen species, as more acidic waters might have important consequences to the structure and support of these organisms.

4.4.5 Axis metrics versus colony height

As it would be expected, axis metrics (i.e. diameter, area, and weight) increased with colony height, although their patterns differed, with diameter showing a linear pattern and weight showing a near exponential pattern. Weight-length relationships in several marine invertebrates are often presented as power equations (e.g. Towers et al., 1994, McKinney et al., 2004, Kilada et al., 2009), where growth is faster over time but with a variable rate (Kaufmann, 1981). In other cases, this relationship has been considered using log-transformed variables in a linear equation (Chang et al., 2007, Robinson et al., 2010).

The coefficient of allometry (~ 1) in the relationship between axis diameter and colony height indicates that the increase in axis diameter is almost proportional to the increase in colony height. Widening of the axis as the colonies grow might therefore have a different importance than peduncle growth or addition of polyp leaves, as these seem to be growing slower than the rest of the colony.

4.4.6 Bomb radiocarbon (^{14}C) analysis

In both colonies the ^{14}C analysis yielded pre-bomb (negative) values, with a clear increase from the core to the edge of the axis. Sherwood et al. (2008) found that $\Delta^{14}\text{C}$ values from the calcite of the deep-water gorgonians *P. resedaeformis* and *K. grayi* in the NW Atlantic were delayed in relation to gorgonin $\Delta^{14}\text{C}$ values from the same colonies. In these corals, gorgonin is formed from fresh particulate organic matter from surface waters, while calcite is formed from dissolved inorganic carbon at depth.

Sherwood et al. (2008) identified a lag of at least 20 years in the bomb- ^{14}C signal between surface and deeper waters in the Labrador Slope Water that goes through the SW Grand Banks region. A branch of the Labrador Slope Water enters the Gulf of St. Lawrence (Townsend et al., 2006), from where our samples analyzed for ^{14}C were collected (Anticosti channel, at ~500 m). This indicates that the depleted ^{14}C values found in our samples from the Gulf of St. Lawrence might also be reflecting the ^{14}C delay between surface and deeper waters seen in the gorgonians collected in the Grand Banks region by Sherwood et al. (2008).

The similarity in the $\Delta^{14}\text{C}$ values and corresponding years between the sea pens and these gorgonians (refer to fig. 4-10) indicates that calcite in the sea pens might come from the same source as in the gorgonians (i.e. dissolved inorganic carbon at depth). Because sea pens do not have individual proteinaceous rings like gorgonians, in this study it was not possible to determine specific $\Delta^{14}\text{C}$ values for protein and calcite. Nevertheless, since in *P. resedaeformis* and in *K. grayi* growth rings are known to be formed annually (Sherwood et al., 2005, Sherwood & Edinger, 2009), the comparability of ^{14}C values in *P. grandis* and in these gorgonians, besides the trend of $\Delta^{14}\text{C}$ values increasing with distance

from the core, can be interpreted as an indication that growth rings in these sea pens are also formed annually. A similar pattern was found for the sea pen *U. encrinus* from Jones Sound (Chapter 3).

4.4.7 Estimated growth rates

Diametric growth rates for *P. grandis* were in the same range of those estimated in other studied sea pens. Average diametric growth rates in this species were $0.13 \text{ mm}\cdot\text{yr}^{-1}$, the same for the deep-water sea whip *H. finmarchica* (Chapter 2), and comparable to those of *H. willemoesi* ($0.14 \text{ mm}\cdot\text{yr}^{-1}$, Wilson et al., 2002), and *U. encrinus*, in which radial growth rates (roughly half of diametric rates) averaged $0.07 \text{ mm}\cdot\text{yr}^{-1}$ (Chapter 3).

On the other hand, linear growth rates in *P. grandis* were in average $1.8 \text{ cm}\cdot\text{yr}^{-1}$, which are slower than those estimated for *H. willemoesi* ($4.5 \text{ cm}\cdot\text{yr}^{-1}$) (Wilson et al., 2002) and *H. finmarchica* ($4.9 \text{ cm}\cdot\text{yr}^{-1}$) (Chapter 2). Conversely, they were similar to those observed in the more related species *Ptilosarcus gurneyi*, a shallow-water sea pen also belonging to the family Pennatulidae. *P. gurneyi* showed linear increments of 2.3 and 2.4 cm in 11 months (i.e. $\sim 2.5\text{-}2.65 \text{ cm}\cdot\text{yr}^{-1}$) (Birkeland, 1974). However, the colonies studied by Birkeland were only 2 years-old in age. The similarity in growth rates between these two species might be related to the similar colony morphological traits such as the presence of polyp leaves and a strong bulb in the peduncle area, and even the presence of mesozooids, not found in most sea pens (Williams, 1995, Williams et al., 2012).

Growth rates increased with colony height, which might be related to a more limited number of polyps in the early life of these organisms. Having few polyps might denote less means of gathering food, which could limit growth. This growth pattern

(slower at the beginning) has also been observed in the soft coral *Anthomastus ritteri* Nutting, 1909 (Cordes et al., 2001), and in the sea pens *H. finmarchica* (Chapter 2) and *U. encrinus* (Chapter 3).

We found no statistically significant relationships between growth rates and most environmental variables tested, with chlorophyll a/POC/PIC being the only variables that had significant negative relationships with diametric growth rates for colonies in the large size class only. In the gorgonians *Primnoa* spp. a significant positive relationship between growth rates and surface chlorophyll a was identified (Chapter 6), and considering that phytodetritus is among the main food items consumed by the related species *P. aculeata* (Baillon et al., 2016), we would expect to see a positive relationship between these two variables. Therefore, it is possible that this relationship in *P. grandis* is not cause-effect, and that other factors make these colonies to grow slower in regions where chlorophyll a concentration is higher, and vice-versa. The observation that linear growth rates increase with colony height, as observed in other sea pens (Chapters 2-4) might indicate that in these animals, intrinsic and ontogenetic factors might have a more important role controlling growth rates than environmental factors. Therefore, although environmental factors do have an influence on the distribution of cold-water sea pens (Yesson et al., 2012, Greathead et al., 2014), it seems that most of the tested factors do not directly influence growth rates in *P. grandis*.

4.4.8 Summary of growth patterns inferred from colony metrics and growth rings

In this study we showed that number of polyp leaves, peduncle size, all axis metrics, and growth rates increased with colony height. Colony height and axis metrics

increased with number of rings (i.e. colony age). On the other hand, density of polyp leaves, proportion of peduncle, and axis carbonate proportion decreased with colony height.

As individually addressed in the previous sections, these data seem to suggest that different parts of the colony grow at different rhythms, illustrating their allometric growth. As peduncle length increases with colony height, but its percentage decreases, the colony seems to put less effort into peduncle growth over time and more effort into rachis growth. The same pattern was observed in relation to polyp leaves, as their total abundance increases with colony size, but their density decreases, indicating a reduction in the speed of addition of new polyp leaves over time.

The positive relationship between axis metrics and colony size, with axis weight increasing exponentially with colony height, helps to highlight the importance of the axial skeleton in these organisms. Furthermore, axis proportion (differently from proportion of peduncle) did not change with colony height in the analyzed specimens, indicating a certain consistency of this character throughout colony life (among the size classes analyzed). There was an indication of axis carbonate proportion decreasing with colony height, which suggests a need for more flexibility as the colony grows taller.

Growth rates calculated from the number of rings and axis measurements point to an increase in growth rates over time, which might be related to the importance of intrinsic factors in growth. Finally, the slow growth rates and decadal longevity (~30 years) estimated for *P. grandis* have important implications for the conservation of these vulnerable organisms.

Acknowledgments

We would like to thank Glenn Piercey, Michael Shaffer, David Grant and Brian Loveridge (CREAIT, Memorial University) for assistance with sectioning, polishing, EDX analysis (MS, DG), micromilling (GP), and Wanda Aylward (CREAIT, Memorial University) for the X-ray diffraction analysis. We also thank Kent Gilkinson (Fisheries and Oceans Canada) for the access to samples. Dr. Jean-Marc Gagnon (Canadian Museum of Nature) kindly allowed the use of the *P. grandis* samples for the ^{14}C analysis. We thank Tom Guilderson for the ^{14}C analysis. Raissa Hogan and Dr. Louise Allcock (National University of Ireland) for providing details on the molecular analysis. Research is funded by the Natural Sciences and Engineering Research Council of Canada (NSERC) (doctoral scholarship to BMN) and the Canadian Healthy Oceans Network (CHONe).

4.5 References

Aiken, L. S. & S. G. West, 1991. Multiple regression: testing and interpreting interactions. SAGE Publications, Newbury Park, California.

Baillon, S., M. English, J. Hamel & A. Mercier, 2016. Comparative biometry and isotopy of three dominant pennatulacean corals in the Northwest Atlantic. *Acta Zoologica*: in press.

Baker, K. D., V. E. Wareham, P. V. R. Snelgrove, R. L. Haedrich, D. A. Fifield, E. N. Edinger & K. D. Gilkinson, 2012. Distributional patterns of deep-sea coral assemblages in three submarine canyons off Newfoundland, Canada. *Marine Ecology Progress Series* 445: 235-249.

Baumiller, T. K. & W. I. Ausich, 1996. Crinoid stalk flexibility: theoretical predictions and fossil stalk postures. *Lethaia* 29: 47-59.

Bayer, F. M., M. Grasshoff & J. Verseveldt, 1983. Illustrated trilingual glossary of morphological and anatomical terms applied to Octocorallia: 75.

Best, B. A., 1988. Passive suspension feeding in a sea pen: effects of ambient flow on volume flow rate and filtering efficiency. *The Biological Bulletin* 175: 332-342.

Birkeland, C., 1974. Interactions between a sea pen and seven of its predators. *Ecological Monographs* 44: 211-232.

Bostock, H. C., D. M. Tracey, K. I. Currie, G. B. Dunbar, M. R. Handler, S. E. M. Fletcher, A. M. Smith & M. J. M. Williams, 2015. The carbonate mineralogy and distribution of habitat-forming deep-sea corals in the southwest pacific region. *Deep Sea Research Part I: Oceanographic Research Papers* 100: 88-104.

Boyer, T. P., J. I. Antonov, O. K. Baranova, C. Coleman, H. E. Garcia, A. Grodsky, D. R. Johnson, R. A. Locarnini, A. V. Mishonov, T. D. O'Brien, C. R. Paver, J. R. Reagan, D. Seidov, I. V. Smolyar & M. M. Zweng, 2013. World Ocean Database 2013, NOAA Atlas NESDIS 72, Silver Spring, MD.

Campana, S. E., 1997. Use of radiocarbon from nuclear fallout as a dated marker in the otoliths of Haddock *Melanogrammus aeglefinus*. Marine Ecology Progress Series 150: 49-56.

Carton, J. A. & B. S. Giese, 2008. A reanalysis of ocean climate using Simple Ocean Data Assimilation (SODA). Monthly Weather Review 136: 2999-3017.

Chang, W., K. Chi, T. Fan & C. Dai, 2007. Skeletal modification in response to flow during growth in colonies of the sea whip, *Junceella fragilis*. Journal of experimental marine biology and ecology 347: 97-108.

Cordes, E. E., J. W. Nybakken & G. VanDykhuisen, 2001. Reproduction and growth of *Anthomastus ritteri* (Octocorallia: Alcyonacea) from Monterey Bay, California, USA. Marine Biology 138: 491-501.

Currey, J. D., 1999. The design of mineralised hard tissues for their mechanical functions. Journal of Experimental Biology 202: 3285-3294.

Dalyell, J. G., 1848. Rare and remarkable animals of Scotland, represented from living subjects: with practical observation on their nature. John Van Voorst, London.

English, M., 2012. A comparative analysis of the sclerites from three common species of the sea pens (Octocorallia: Pennatulacea) from Newfoundland and Labrador. Honours dissertation. 46 pages.

Franc, S., A. Huc & G. Chassagne, 1975. Calcite and collagen in the skeleton of the Cnidaria *Veretillum cynomorium* Pall. (Anthozoa. Pennatulidae): 65-69.

Franc, S., P. W. Ledger & R. Garrone, 1985. Structural variability of collagen fibers in the calcareous axial rod of a sea pen. *Journal of Morphology* 184: 75-84.

Gould, S. J., 1966. Allometry and size in ontogeny and phylogeny. *Biological Reviews* 41: 587-638.

Greathead, C., J. M. González-Irusta, J. Clarke, P. Boulcott, L. Blackadder, A. Weetman & P. J. Wright, 2014. Environmental requirements for three sea pen species: relevance to distribution and conservation. *ICES Journal of Marine Science: Journal du Conseil* 72: 576-586.

Hickson, S. J., 1916. The Pennatulacea of the Siboga Expedition: with a general survey of the order. Late EJ Brill.

Hogan, R. I., S. Heesch, A. Oppelt & A. L. Allcock, 2015. Northeast Atlantic deep-sea corals. Abstracts of the 14th Deep-Sea Biology Symposium. Aveiro, Portugal: 266.

Huz, R. d. I., M. Lastra & J. López, 2002. The influence of sediment grain size on burrowing, growth and metabolism of *Donax trunculus* L. (Bivalvia: Donacidae). *Journal of Sea Research* 47: 85-95.

Jungersen, H. F. E., 1904. The Danish Ingolf-Expedition. 1. Pennatulida. H. Hagerup, Copenhagen.

Kabacoff, R., 2015. R in action: data analysis and graphics with R. Manning, Shelter Island.

- Kastendiek, J., 1976. Behavior of the sea pansy *Renilla kollikeri* Pfeffer (Coelenterata: Pennatulacea) and its influence on the distribution and biological interactions of the species. *Biological Bulletin* 151: 518-537.
- Kaufmann, K., 1981. Fitting and using growth curves. *Oecologia* 49: 293-299.
- Kilada, R. W., S. E. Campana & D. Roddick, 2009. Growth and sexual maturity of the northern propellerclam (*Cyrtodaria siliqua*) in Eastern Canada, with bomb radiocarbon age validation. *Marine Biology* 156: 1029-1037.
- Kükenthal, W., 1915. Pennatularia. Das Tierreich. Verlag von R. Friedlander und Sohn, Berlin.
- Langton, R., E. Langton, R. Theroux & J. Uzman, 1990. Distribution, behavior and abundance of sea pens, *Pennatula aculeata*, in the Gulf of Maine. *Marine Biology* 107: 463-469.
- Ledger, P. W. & S. Franc, 1978. Calcification of collagenous axial skeleton of *Veretillum cynomorium* Pall (Cnidaria Pennatulacea). *Cell and Tissue Research* 192: 249-266.
- Maier, C., 2012. Calcification rates and the effect of ocean acidification on Mediterranean cold-water corals. *Proceedings of the Royal Society B-Biological Sciences* 279: 1716-1723.
- Marks, M. H., R. S. Bear & C. H. Blake, 1949. X-ray diffraction evidence of collagen-type protein fibers in the Echinodermata, Coelenterata and Porifera. *Journal of Experimental Zoology* 111: 55-78.

Marubini, F., C. Ferrier-Pages & J. Cuif, 2003. Suppression of skeletal growth in scleractinian corals by decreasing ambient carbonate-ion concentration: a cross-family comparison. *Proceedings of the Royal Society of London B: Biological Sciences* 270: 179-184.

McKinney, R. A., S. M. Glatt & S. R. Williams, 2004. Allometric length-weight relationships for benthic prey of aquatic wildlife in coastal marine habitats. *Wildlife Biology* 10: 241-249.

Morin, R., S. G. LeBlanc & S. E. Campana, 2013. Bomb radiocarbon validates age and long-term growth declines in American Plaice in the southern Gulf of St. Lawrence. *Transactions of the American Fisheries Society* 142: 458-470.

Musgrave, E. M., 1909. Experimental observations on the organs of circulation and powers of locomotion in pennatulids. *Quarterly Journal of Microscopical Science* 54: 443-482.

Orr, J. C., 2005. Anthropogenic ocean acidification over the twenty-first century and its impact on calcifying organisms. *Nature (London)* 437: 681-686.

Pelouze, J. & E. Fremy, 1865. *Traité de chimie, générale, analytique, industrielle et agricole. Chimie organique III.* Victor Masson et fils, Paris.

Roberts, J. J., B. D. Best, D. C. Dunn, E. A. Treml & P. N. Halpin, 2010. Marine Geospatial Ecology Tools: An integrated framework for ecological geoprocessing with ArcGIS, Python, R, MATLAB, and C++. *Environmental Modelling & Software* 25: 1197-1207.

Robertson & J. Lancaster, 2010. Length-weight relationships of 216 North Sea benthic invertebrates and fish. *Journal of the Marine Biological Association of the United Kingdom* 90: 95-104.

Robinson, L. A., S. P. R. Greenstreet, H. Reiss, R. Callaway, J. Craeymeersch, I. de Boois, S. Degraer, S. Ehrich, H. M. Fraser, A. Goffin, I. Kröncke, L. L. Jorgenson, M. R.

Sars, M., 1846. Beschreibung der *Pennatula borealis*, einer neuen Seefeder. Druck und Verlag von Johann Dahl, Christiania.

Schlitzer, R., 2015. Ocean Data View, <http://odv.awi.de>.

Schneider, C. A., W. S. Rasband & K. W. Eliceiri, 2012. NIH Image to ImageJ: 25 years of image analysis. *Nature Methods* 9: 671-675.

Sherwood, O. A. & E. N. Edinger, 2009. Ages and growth rates of some deep-sea gorgonian and antipatharian corals of Newfoundland and Labrador. *Canadian Journal of Fisheries and Aquatic Sciences* 66: 142-152.

Sherwood, O. A., E. N. Edinger, T. P. Guilderson, B. Ghaleb, M. J. Risk & D. B. Scott, 2008. Late Holocene radiocarbon variability in Northwest Atlantic slope waters. *Earth and Planetary Science Letters* 275: 146-153.

Sherwood, O. A., D. B. Scott, M. J. Risk & T. P. Guilderson, 2005. Radiocarbon evidence for annual growth rings in the deep-sea octocoral *Primnoa resedaeformis*. *Marine Ecology Progress Series* 301: 129-134.

Soong, K., 2005. Reproduction and colony integration of the sea pen *Virgularia juncea*. *Marine Biology* 146: 1103-1109.

Stuiver, M. & H. A. Polach, 1977. Discussion: reporting of ^{14}C data. *Radiocarbon* 19: 355-363.

Towers, D. J., I. M. Henderson & C. J. Veltman, 1994. Predicting dry weight of New Zealand aquatic macroinvertebrates from linear dimensions. *New Zealand Journal of Marine and Freshwater Research* 28: 159-166.

Townsend, D., A. C. Thomas, L. M. Mayer, M. A. Thomas & J. A. Quinlan, 2006. Oceanography of the Northwest Atlantic continental shelf. In Robinson, A. R. & K. H. Brink (eds), *The Sea: The Global Coastal Ocean: Interdisciplinary Regional Studies and Syntheses*. Harvard University Press.

Wang, Q., Y. Li & Y. Wang, 2011. Optimizing the weight loss-on-ignition methodology to quantify organic and carbonate carbon of sediments from diverse sources. *Environmental monitoring and assessment* 174: 241-257.

Wareham, V. E. & E. N. Edinger, 2007. Distribution of deep-sea corals in the Newfoundland and Labrador region, Northwest Atlantic Ocean. *Bulletin of Marine Science* 81: 289-313.

Williams, G. C., B. W. Hoeksema & L. P. Van Ofwegen, 2012. A fifth morphological polyp in Pennatulacean octocorals, with a review of polyp polymorphism in the genera *Pennatula* and *Pteroeides* (Anthozoa: Pennatulidae). *Zoological Studies* 51: 1006-1017.

Williams, G. C., 1995. Living genera of sea pens (Coelenterata: Octocorallia: Pennatulacea): illustrated key and synopses. *Zoological Journal of the Linnean Society* 113: 93-140.

Wilson, M. T., A. H. Andrews, A. L. Brown & E. E. Cordes, 2002. Axial rod growth and age estimation of the sea pen, *Halipteris willemoesi* Kölliker. *Hydrobiologia* 471: 133-142.

Yesson, C., M. L. Taylor, D. P. Tittensor, A. J. Davies, J. Guinotte, A. Baco, J. Black, J. M. Hall-Spencer & A. D. Rogers, 2012. Global habitat suitability of cold-water octocorals. *Journal of Biogeography* 39: 1278-1292.

Appendix 4-1 List of colonies of *Pennatula grandis* and associated depth and location.

Latitude and longitude are in decimal degrees.

Sample identification	Depth (m)	Latitude (N)	Longitude (W)	Location
078A-F	488	65.5917	-58.8117	Davis
079A-G	696	66.7461	-57.9263	Davis
080A-E	567	68.5585	-59.3751	Davis
081A-J	644	68.4910	-59.5187	Davis
110A-E	696	66.7461	-57.9263	Davis
114	924	68.2667	-59.7667	Davis
003	413	47.5833	-45.9333	East Newfoundland
004A-B	785	49.1170	-49.9330	East Newfoundland
074	918	50.9880	-49.8480	East Newfoundland
099A-C	887	50.8575	-50.4775	East Newfoundland
102	801	49.6330	-49.8830	East Newfoundland
115	801	51.0917	-50.2500	East Newfoundland
116	366	47.6333	-45.9000	East Newfoundland
117A-B	802	49.5000	-49.9000	East Newfoundland
011	320	44.0000	-52.6500	Grand Banks
066	386	44.9767	-54.9558	Grand Banks
069	212	44.1808	-52.8883	Grand Banks
072	338	44.4000	-53.3667	Grand Banks
075	618	43.4283	-51.9142	Grand Banks
098	502	43.7150	-52.3942	Grand Banks
100	649	43.5470	-52.0425	Grand Banks
109	413	44.6500	-54.0330	Grand Banks
121	549	43.7833	-52.4333	Grand Banks
001	346	56.3333	-57.8333	Labrador
002	1404	53.3425	-51.9525	Labrador
060	804	56.8233	-58.5600	Labrador
065	960	56.7208	-58.3700	Labrador
067	532	58.9558	-60.0392	Labrador
108	1451	56.4992	-57.8408	Labrador
058	219	45.5975	-56.5908	Laurentian Channel
059	422	45.1925	-56.8483	Laurentian Channel
061A-B	403	45.6525	-56.9617	Laurentian Channel
062A-F	320	45.2767	-56.4317	Laurentian Channel
063	52	45.8425	-56.0950	Laurentian Channel
064	289	45.1250	-56.2950	Laurentian Channel
068	404	45.2167	-56.7125	Laurentian Channel

Sample identification	Depth (m)	Latitude (N)	Longitude (W)	Location
070	436	47.3225	-59.1833	Laurentian Channel
071	422	45.2455	-56.8900	Laurentian Channel
073	366	45.4008	-56.6050	Laurentian Channel
076	391	45.3300	-56.7333	Laurentian Channel
077	436	47.3675	-59.2558	Laurentian Channel
101A-B	283	47.1392	-58.2942	Laurentian Channel
CMN_1	350	49.2294	-63.7922	St. Lawrence
CMN_2	350	49.2294	-63.7922	St. Lawrence
1-10	381	48.9833	-63.3667	St-Lawrence
103-107	381	48.9833	-63.3667	St-Lawrence

Appendix 4-2 Carbonate composition of the axis in ten specimens of *Pennatula grandis* from the Northwest Atlantic. Samples are from the same location and depth. Red: length reduction (%), Wgt: weight, Org: organic material.

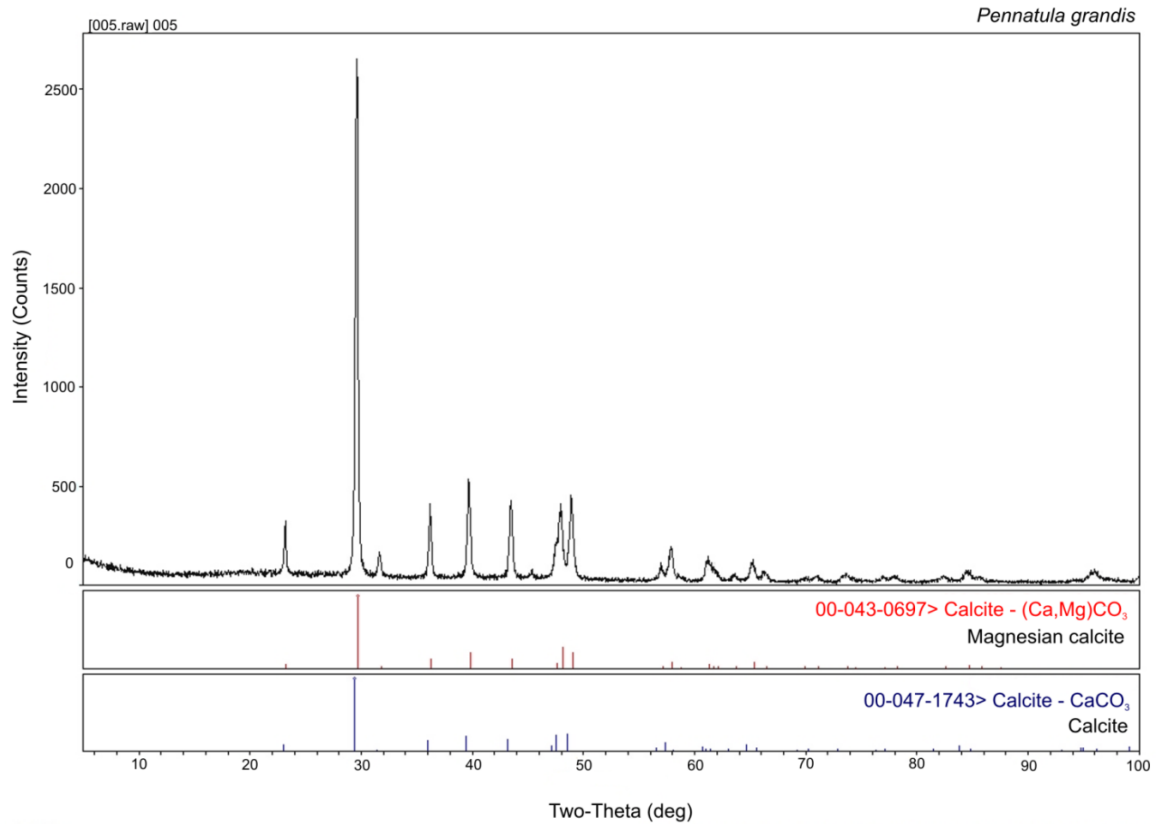
Id	Height (cm)	Axis before (cm)	Axis after (cm)	Red (%)	Wgt1	Wgt2	Wgt3	H₂O	Org	CaCO₃
1	20	17.7	8.27	53.28	0.42	0.42	0.06	1.9	15	83
2	18	17.3	7.30	57.80	0.53	0.52	0.09	2.1	18	80
3	17	13.5	5.60	58.52	0.27	0.26	0.04	1.5	15	83
4	12	11.3	5.05	55.32	0.17	0.17	0.02	2.3	14	84
5	15	13.5	5.70	57.78	0.26	0.26	0.04	1.9	16	82
6	14	12.0	6.40	46.67	0.19	0.19	0.02	1.6	12	86
7	11	9.5	3.80	60.00	0.13	0.13	0.01	1.6	10	88
8	12	11.5	5.30	53.91	0.17	0.17	0.02	2.3	11	86
9	7	6.3	3.06	51.40	0.04	0.04	0.003	2.3	8	90
10	9	8.5	3.76	55.72	0.10	0.01	0.01	2.9	13	84

Appendix 4-3 Results on the GLM analysis on the relationships between certain colony metrics and colony height for *Pennatula grandis* by locations in the Northwest Atlantic.

Versus height	Davis Strait	Labrador	East Newfoundland	Grand Banks	Laurentian Channel	St-Lawrence
Peduncle	F=410.7, p<2e-16, R ² =0.93, N=34	F=36.25, p=0.004, R ² =0.9, N=6	F=350.6, p=4.08e-9, R ² =0.97, N=12	F=130.3, p=8.89e-6, R ² =0.95, N=9	F=101.7, p=7.87e-9, R ² =0.85, N=20	F=1779, p<2e-16, R ² =0.98, N=39
% peduncle	F=1.156, p=0.29, R ² =0.03, N=34	F=2.423, p=0.19, R ² =0.38, N=6	F=6.84, p=0.026, R ² =0.41, N=12	F=13.53, p=0.008, R ² =0.66, N=9	F=23.08, p=0.0001, R ² =0.56, N=20	¹ F=52.92, p=1.22e-8, R ² =0.59, N=39
# polyp leaves	z=3.826, p=0.0001, N=34	z=2.514, p=0.012, N=6	t=8.85, p= 4.8e-6, N=12	z=3.136, p=0.002, N=9	z=4.286, p=1.82e-5, N=20	t=20.71, p<2e-16, N=29
PL density	t=-12.09, p=1.8e-13, R ² =0.82, N=34	t=-4.717, p=0.009, R ² =0.85, N=6	t=-2.648, p=0.022, R ² =0.412, N=12	t=-4.484, p=0.003, R ² =0.74, N=9	t=-11.72, p=7.42e-10, R ² =0.88, N=20	t=-6.955, p=1.79e-7, R ² =0.70, N=29
Gap in PL	z=3.389, p=0.001, N=34	z=1.236, p=0.217, N=4	t=5.685, p=0.001, N=9	z=1.999, p=0.05, N=8	z=1.498, p=0.134, N=20	z=4.945, p=7.63e-7, N=27
Gap in cm	t=9.637, p=5.5e-11, R ² =0.74, N=34	t=1.436, p=2.87, R ² =0.51, N=4	t=7.458, p=0.0001, R ² =0.89, N=9	t=2.565, p=0.06, R ² =0.62, N=8	t=0.66, p=0.52, R ² =0.03, N=16	t=2.427, p=3.38e-12, R ² =0.86, N=27
Axis diameter	F=115, p=3.97e-12, R ² =0.78, N=34	F=34.6, p=0.004, R ² = 0.896, N=6	F=56.81, p=1.98e-5, R ² = 0.85, N=12	F=157.3, p=4.73e-6, R ² = 0.96, N=8	F=25.3, p=8.76e-5, R ² = 0.58, N=20	F=163.8, p=5.62e-13, R ² = 0.86, N=29
Axis area	F=279.6, p<2e-16, R ² =0.897, N=34	F=5.273, p=0.08, R ² =0.59, N=6	F=182, p=8.74e-7, R ² = 0.96, N=10	F=21.1, p=0.004, R ² = 0.78, N=8	F=28.02, p=4.94e-5, R ² =0.61, N=20	F=287.7, p=4.56e-15, R ² =0.92, N=27
Axis weight	¹ F=6.79, p=0.06, R ² =0.63, N=6	na	F=148.1, p=1.87e-5, R ² = 0.96, N=8	na	na	F=1227, p=2e-16, R ² =0.97, N=35
Age	F=22.7, p=3.95e-5, R ² =0.415, N=34	F=0.06, p=0.82, R ² =0.015, N=6	F=4.656, p=0.056, R ² =0.32, N=12	F=19.12, p=0.003, R ² =0.73, N=9	F=21.7, p=0.0002, R ² =0.55, N=20	F=119.5, p=2.03e-11, R ² =0.82, N=29

Values in bold are significant at a 5%. Z-values for Poisson regression, and t-values for quasi-Poisson for count type of variables (#polyp leaves and gap in polyp leaves), ¹log of Y.

Appendix 4-4 X-Ray Diffraction analysis for the carbonate portion of the axis in *Pennatula grandis*. Overlap between the axis in *P. grandis* (black), magnesian calcite (red), and calcite (blue). Note that the axis of *P. grandis* follows the same pattern as magnesian calcite.



5. Morphology and composition of the internal axis in two morphologically contrasting deep-water sea pens (Cnidaria: Octocorallia)⁴

Abstract

Umbellula encrinus and *Anthoptilum grandiflorum* are two species of deep-water sea pens (Cnidaria: Octocorallia) commonly observed in the Northwest (NW) Atlantic. Here we characterized the internal skeleton (axis) of these two contrasting species, in terms of axis morphology and metrics through a vertical gradient. The axis carbonate composition was determined for both species through an X-ray diffraction analysis (XRD). The XRD analysis revealed that the carbonate portion of the axis is composed of magnesian calcite (Ca,Mg)CO₃ in both species. The axis is composed of 71% of carbonate material in *U. encrinus*, and 65% in *A. grandiflorum*. The axis of *U. encrinus* was quadrangular through its whole length, and it showed a twisting in all analyzed colonies. The axis of *A. grandiflorum* varied from elliptical near the base to cylindrical on most of the remaining length. No twisting was observed in the axis of *A. grandiflorum*. Axis metrics decreased with distance from base in both species, and showed the largest area at < 50 cm and at ~10 cm for *U. encrinus* and *A. grandiflorum*, respectively. The carbonate proportion was greatly reduced from the base to the tip of the axis in *U. encrinus*, while in *A. grandiflorum* the opposite pattern was observed. This is the first study to illustrate the

⁴ To be submitted to the Journal of Natural History.

changes along the axis of sea pens, and it might provide a baseline for future studies on the relationships between sea pens and the environment.

5.1 Introduction

Sea pens are benthic colonial cnidarians of worldwide distribution (Williams, 2011). Most sea pens have an internal skeleton (i.e. also called axis, style, or rod) that gives support to the colony. The available knowledge on the axis of sea pens is largely limited to information on axis presence/absence and general shape, as these are characters of taxonomic importance for certain taxa (Hickson, 1916).

Umbellula encrinus Linnaeus, 1758 and *Anthoptilum grandiflorum* (Verrill, 1879) are common deep-water sea pens in the Northwest (NW) Atlantic, being found at depths ~1800 m (Baker et al., 2012, Wareham and Edinger, 2007). These two taxa greatly differ in morphology. *U. encrinus* has a long stalk with a cluster of autozooids (i.e. feeding polyps) restricted to the distal extremity of the colony; and *A. grandiflorum* has the shape of a question mark, with autozooids distributed along the entire rachis length (Williams, 1995). They also differ in size, with colonies of *U. encrinus* reaching heights of approximately 2.3 m (Dolan, 2008, Chapter 3), and *A. grandiflorum* usually reaching a maximum height of 50 cm (Baillon et al., 2016).

Both species have an internal axis, which follows the entire colony length, being quadrangular in *U. encrinus* (Dolan, 2008), and sub-cylindrical in *A. grandiflorum* (Thomson & Henderson, 1906). General shape is the most common characteristic reported for the axis of most sea pens (Hickson, 1916). This information is usually found in taxonomic studies - especially early studies - as part of species descriptions/diagnoses. However, since removing the axis damages the integrity of the colony for further taxonomic studies (Hickson, 1916), it has not been described in details. Studies focusing

on the axis of sea pens are therefore sparse, including studies on axis calcification in *Veretillum cynomorium* (Pallas, 1766) (Ledger & Franc, 1978, Franc et al., 1974) and on growth rings and rates in *Ptilosarcus gurneyi* (Gray, 1860) (Birkeland, 1974), *Halipteris willemoesi* Kölliker, 1870 (Wilson et al., 2002), and *Halipteris finmarchica* (Sars, 1851) (Chapter 2), and axis metrics (Soong, 2005, Baillon et al., 2016).

Since the axis of several species of sea pens bear growth rings (Birkeland, 1974, Wilson et al., 2002, Chapters 2-5), and therefore information on colony age and growth, knowledge about the axis of sea pens is important for the general understanding of these organisms. In the NW Atlantic and in other regions of the world, sea pens are highly vulnerable to fishing gear, whose physical contact can cause dislodgement, damage, and death (Troffe et al., 2005, Malecha & Stone, 2009). Furthermore, sea pens make structure and potential habitat for other species, including both invertebrates (Baillon et al., 2014) and fish (Brodeur, 2001, Baillon et al., 2012).

Here we analyzed the axis of *U. encrinus* and *A. grandiflorum* from the NW Atlantic. Our main objective was to describe and compare how the axis changes along its length in adult colonies of these two species. We characterized the axes in terms of changes in shape, cross-sectional area, and weight along their lengths, with a tapering proportion being calculated for both species. Radial growth rates in *U. encrinus* were also determined along its height, and the axis carbonate composition for both species, as well as the proportion of carbonate and organic material in the axis were also determined. Based on our findings we propose and discuss potential hypotheses regarding the differences observed in the axes of these two species from a form and function perspective.

5.2 Methods

5.2.1 Sampling

Samples of *U. encrinus* were obtained from Baffin Bay and *A. grandiflorum* from the Davis Strait and Newfoundland waters (Fig. 5-1). Colonies were collected as bycatch during multispecies trawl surveys conducted by Fisheries and Oceans Canada (DFO) from the period of 2004-2013 (Table 5-1). Samples included here were retrieved from depths ranging 188-975 m, using a Campellen 1800 shrimp trawl for *ca.* 15 minutes at a speed of 3 knots, with a 55 m door sweep area. Samples were frozen at -20 °C following collection.

5.2.2 Axis characterization through a vertical gradient

Axes of five colonies of *U. encrinus* and eight *A. grandiflorum* were characterized through their whole length. Axes were extracted from the tissue and set to air dry for at least a day before proceeding with the analysis. The axes were cross sectioned every 5 cm for *A. grandiflorum*, and 10 cm for *U. encrinus*. Colony sizes ranged 156-248 cm in *U. encrinus* and 52.5-65 cm in *A. grandiflorum* (Table 5-1). This difference in the intervals was chosen due to the difference in colony height between these two species, and it was thought to well represent most significant changes in the axis.

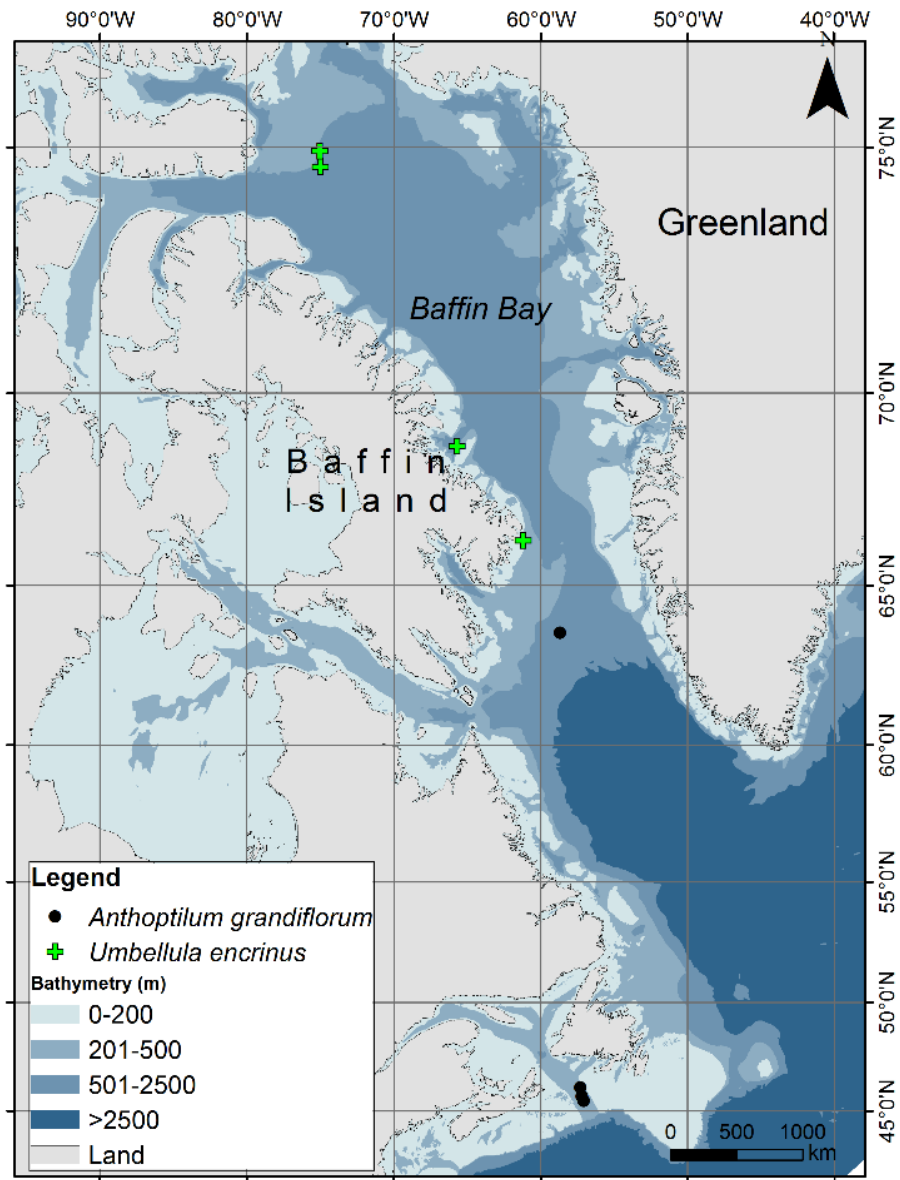


Figure 5-1. Map of study area.

Table 5-1. Sampling information on *Umbellula encrinus* and *Anthoptilum grandiflorum* from the NW Atlantic. Latitude (N) and longitude (W) are in decimal degrees. Ped = peduncle length.

Species	Id	Latitude	Longitude	Location	Depth (m)	Year	Height (cm)	Ped (cm)
<i>Umbellula encrinus</i>	042	68.7229	-65.7077	West Baffin Bay	468	2010	215	28
<i>Umbellula encrinus</i>	044	74.6559	-75.0045	Lancaster Sound	559	2010	223.5	33
<i>Umbellula encrinus</i>	045	74.9332	-75.0570	Lancaster Sound	533	2010	187	23
<i>Umbellula encrinus</i>	048	74.9332	-75.0570	Lancaster Sound	533	2010	156	23
<i>Umbellula encrinus</i>	052	68.7229	-65.7077	West Baffin Bay	468	2010	248	39
<i>Umbellula encrinus</i>	030H ¹	66.2648	-61.1890	West Baffin Bay	188.5	2008	38 ²	18.5
<i>Anthoptilum grandiflorum</i>	111A	45.6750	-57.1983	Laurentian Channel	429	2013	52.5	8.8
<i>Anthoptilum grandiflorum</i>	111B	45.6750	-57.1983	Laurentian Channel	429	2013	73.5	10.5
<i>Anthoptilum grandiflorum</i>	111C	45.6750	-57.1983	Laurentian Channel	429	2013	65	8.7
<i>Anthoptilum grandiflorum</i>	125A	46.0967	-57.2967	Laurentian Channel	357	2013	57	8.7
<i>Anthoptilum grandiflorum</i>	126A	45.4717	-57.0683	Laurentian Channel	423	2013	60.5	9
<i>Anthoptilum grandiflorum</i>	126B	45.4717	-57.0683	Laurentian Channel	423	2013	53.5	9.3
<i>Anthoptilum grandiflorum</i>	126C	45.4717	-57.0683	Laurentian Channel	423	2013	68	9
<i>Anthoptilum grandiflorum</i>	039 ¹	63.6000	-58.6833	Davis Strait	975	2012	44	6.8

¹X-ray diffraction analysis only; ²broken colony

Because *U. encrinus* has a four-lobed axis (Chapter 3), the lobes (ridges) could be individually color marked through the whole axis length using water-resistant colored pencils. For each lobe a specific color was used (Fig. 5-2). The position of each lobe at each appropriate interval (every 10 cm) was noted as one of four: top right, top left, bottom right, or bottom left. In this way it was possible to know the exact position of each lobe with distance from base. For *A. grandiflorum* the axis was single-color marked, only to differentiate ventral and dorsal parts of the axis.

The axis was first sectioned using a rock saw at the designated intervals. These sections were embedded in epoxy (Epofix™) for a second and more precise sectioning using an IsoMet® low speed saw (Buehler). Cross sections were polished using a Buehler carbide grinding paper (grit 600/ P1200), then visualized and photographed under UV light using a stereomicroscope. The software imageJ (Schneider et al., 2012) was used to measure axis radius, diameter, and area. Changes in lobe position (for *U. encrinus* only) and cross-sectional shape in relation to distance from base could then be determined. Axis degree of tapering was calculated by determining the percentage reduction in axis cross-sectional area using the following equation:

$$\text{percentage area reduction} = \left(\frac{\text{Largest area} - \text{Smallest area}}{\text{Largest area}} \right) * 100$$

Growth rings (Chapter 3) were counted in each of the four lobes in *U. encrinus* and averaged. In sections of the axis where growth rings did not occupy the whole axis, the radius was estimated only for the portion containing rings, in order to calculate radial

growth rates. In *A. grandiflorum* growth rings are not as evident, and for this reason number of rings was not determined for this species.

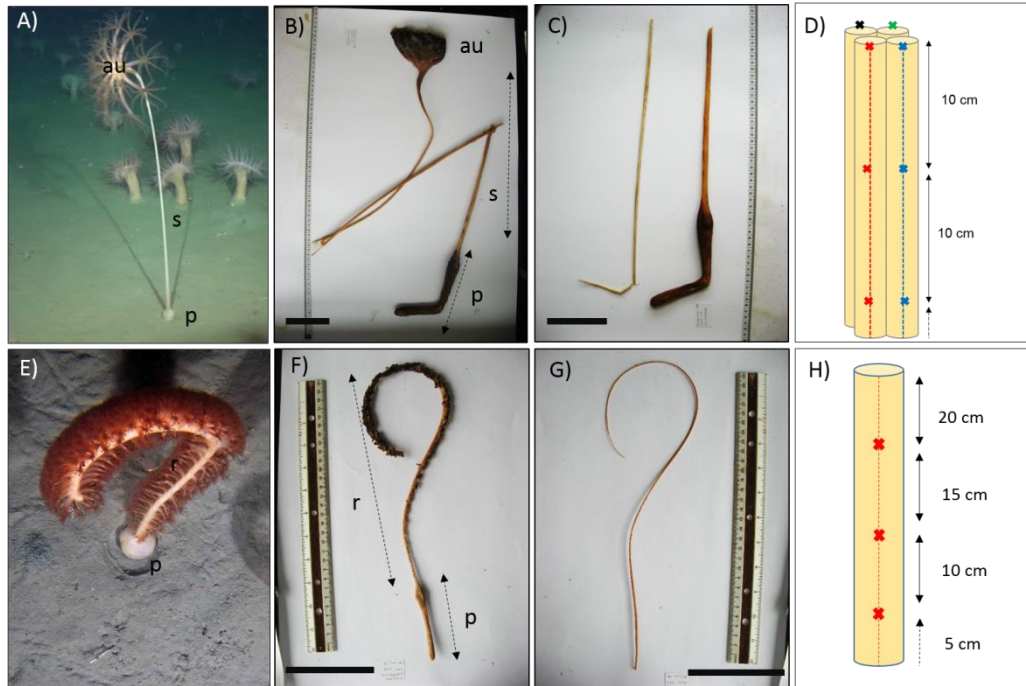


Figure 5-2. A-D) *Umbellula encrinus*: A) whole colony *in situ*, B) whole colony, C) piece of stem and corresponding extracted axis, D) axis cross sectioning scheme. E-H) *Anthoptilum grandiflorum*: E) whole colony *in situ*, F) whole colony, G) whole axis, H) axis cross sectioning scheme. au: autozooids, p: peduncle, s: stalk, r: rachis. Scale bars = 10 cm. A-B and E-F are not the same colonies. Colony in A) measures ~81 cm. Size not available for E).

5.2.3 Axis carbonate composition

An X-ray diffraction (XRD) analysis was performed to determine the carbonate composition of the axis in both species. A total of 1 g of axis from one colony of each species was crushed into a powder using a ceramic mortar and pestle. The analysis was

performed at the Earth Resources Research and Analysis (TERRA) facility, Memorial University of Newfoundland, using a Rigaku Ultima-IV with a Cu source used in Bragg-Brentano configuration.

In order to estimate the percentage of carbonate in relation to organic material in the axis, the remaining fragments of the axis from each vertical interval used for the morphologic characterization described in the previous section were sectioned and isolated. Segments ~2 cm long of *U. encrinus* and ~3 cm long of *A. grandiflorum* were used to characterize the axis carbonate proportion. These lengths were based on the available material after sections had been made for the morphological study.

The procedures used to determine the carbonate proportion in the studied colonies is detailed in Chapter 4. Briefly, sections of the axis were weighed before and after being oven-dried. Dried samples were topped with 5% HCl for 24 hours (*A. grandiflorum*) and ~72 hours for *U. encrinus*, which was enough to dissolve the carbonate. Samples were set to air dry for several hours and re-weighed repeatedly until there was no weight change. The final weight corresponded to the organic portion of the axis, and the difference between the initial post-dehydration and final weights corresponded to the carbonate portion.

Because the segments of the axis were not the exact same size, relative weight (weight/size) was used to describe weight. A paired *t*-test was used to test for differences among lobe radii in each colony of *U. encrinus*, with each possible pair being individually tested, with significance level of $\alpha = 5\%$.

5.3 Results

5.3.1 Axis morphology and metrics

5.3.1.1 *Umbellula encrinus*

The axis of *U. encrinus* has a mainly smooth surface (Fig. 5-3), except for certain areas where elevations or depressions could sometimes be seen (Fig. 5-3).

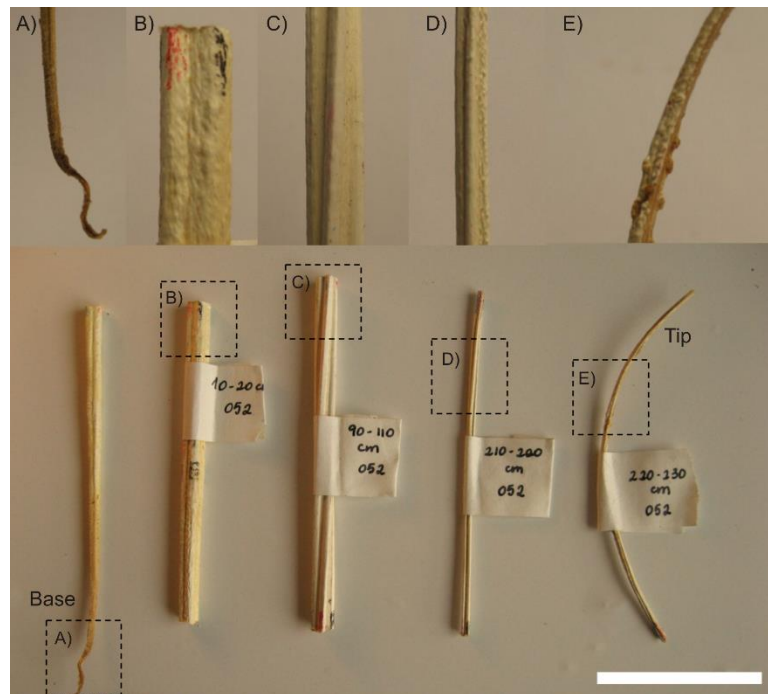


Figure 5-3. Pieces of axis showing surface at different sections of a same specimen of *Umbellula encrinus* (052). Scale bar = 5 cm (refers to bottom photos).

The axis is quadrangular in shape and it twists along its length in a very obvious fashion (Fig. 5-4A).



Figure 5-4. *Umbellula encrinus*. A) Twisting of axis, B) colony *in situ* (Scott Inlet, Baffin Bay, at 520 m) with inset showing twisting of stalk, C) colony *in situ* standing in a $\sim 90^\circ$ position (Qikiqtarjuaq, Baffin Bay, at 680 m, estimated to be ~ 2 m tall).

The quadrangular axis has distinct ridges that create a four-fold symmetry along its entire length (Fig. 5-5). In cross section, the axis is made of four lobes, which can be seen in alternating positions along its length (Fig. 5-5). The same position of lobes was observed to reoccur between 2-3 times, depending on the colony (Fig. 5-5). In most of the analyzed colonies there was no twisting in the first 40-50 cm of the axis (Fig. 5-5, Table 5-2). Twisting was observed to occur up to the distal tip of the axis, and occurred in both clockwise and counter clockwise directions in different colonies, and in a same colony (Fig. 5-5).

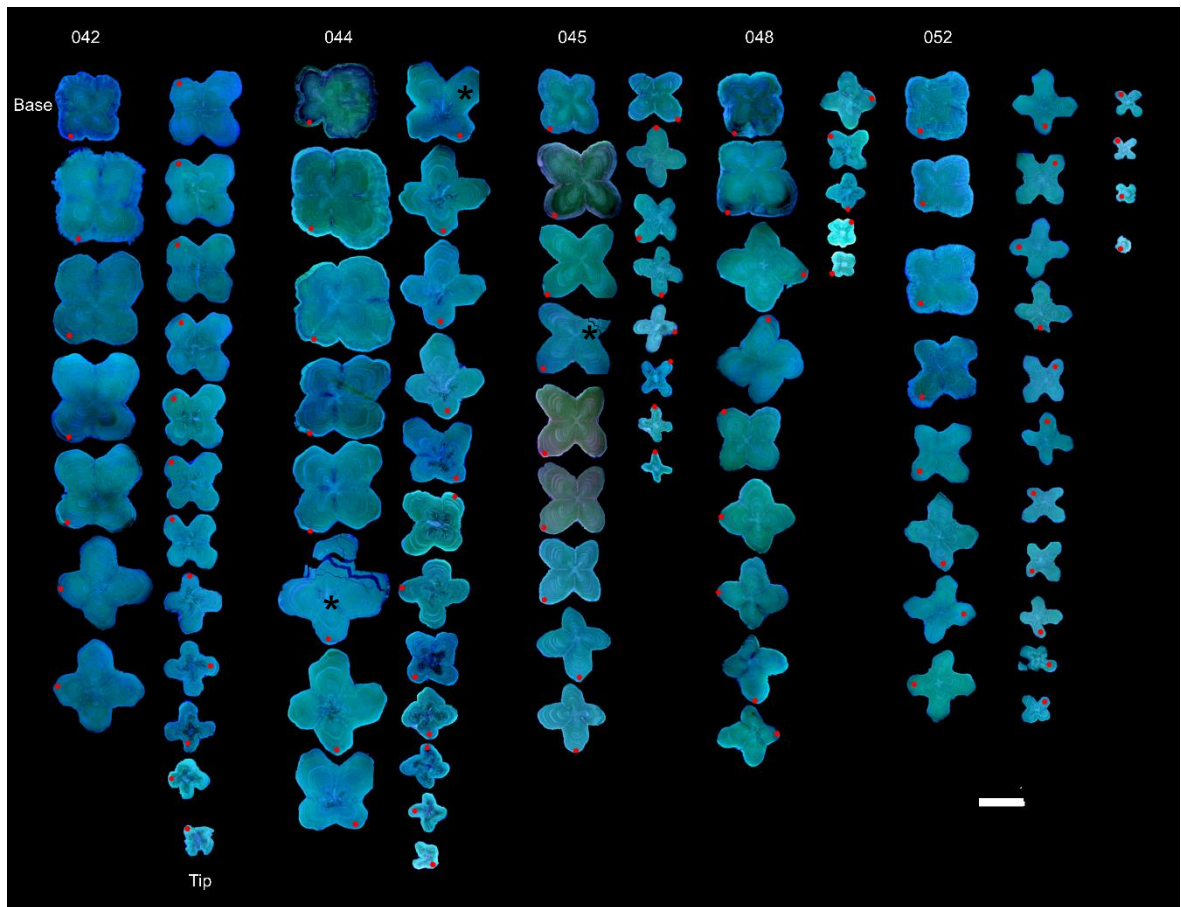


Figure 5-5. The internal axes from five *Umbellula encrinus* colonies seen as cross sections along a gradient (every 10 cm) from base to tip. Changes in the position of red dots indicate changes in lobe position due to axis twisting. *cracked samples. Cross sections were photographed under UV light. Scale bar = 2 mm.

Table 5-2. Axis cross-sectional area (mm²) per colony and start height of twisting in *Umbellula encrinus*. Cross section interval was 10 cm and twisting could have started between the previous cross section and the one where twisting was first reported.

Sample	Height (cm)	Start (cm)	Ped. (cm)	Average area	Max. area	Depth (m)
042	215	60	28	7.75 ± 4.1	15.11	468
044	223.5	60	33	9.05 ± 4.9	17.59	559
045	187	80	23	5.24 ± 3.0	10.95	533
048	156	30	23	5.42 ± 3.1	11.05	533
052	248	60	39	8.13 ± 4.8	20.72	468

The lobes are not perfectly symmetric in shape and size, with two adjacent or even opposite lobes sometimes being more similar to one another than to the two other lobes (Figs. 5-5 and 5-6). This observation was also statistically detected, with the radius of two visually similar lobes being not significantly different from each other, but different from the other two lobes (Table 5-3, Fig. 5-5).

Growth rings were observed in the four lobes. They were present in almost all cross sections along the axis length, but towards the apical region of the axis growth rings were more difficult to visualize. Furthermore, the core becomes darker with distance from base (probably organic material), occupying a larger proportion of the axis where rings were not observed.

Table 5-3. Results from the paired *t*-test on difference in lobe radii among lobes in five different colonies of *Umbellula encrinus*.

Boxes in grey highlight pairs where differences in radii were not statistically significant at $\alpha = 5\%$.

		042	044	045	048	052
Red x green		t = 6.98, df = 18, p-value = 1.62e-06	t = 5.37, df = 18, p-value = 4.24e-05	t = -5.27, df = 15, p-value = 9.36e-05	t = 0.37, df = 13, p-value = 0.71	t = 4.55, df = 21, p-value = 0.0002
Red x blue		t = -8.21, df = 18, p-value = 1.69e-07	t = -0.77, df = 19, p-value = 0.45	t = 0.5, df = 16, p-value = 0.63	t = -0.92, df = 13, p-value = 0.38	t = 0.99, df = 20, p-value = 0.33
Red x black		t = 0.61, df = 18, p-value = 0.55	t = -5.88, df = 19, p-value = 1.15e-05	t = 3.59, df = 16, p-value = 0.002	t = 0.40, df = 13, p-value = 0.70	t = -4.8, df = 20, p-value = 0.0001
Green x blue		t = 0.29, df = 18, p-value = 0.77	t = 6.05, df = 18, p-value = 1.01e-05	t = -6.18, df = 15, p-value = 1.76e-05	t = -0.92, df = 13, p-value = 0.38	t = 6.1, df = 21, p-value = 4.43e-06
Green x black		t = 9.06, df = 18, p-value = 3.99e-08	t = 1.40, df = 18, p-value = 0.18	t = -4.24, df = 15, p-value = 0.0007	t = 0.52, df = 13, p-value = 0.61	t = -0.45, df = 21, p-value = 0.66
Black x blue		t = -7.19, df = 18, p-value = 1.08e-06	t = 5.64, df = 19, p-value = 1.94e-05	t = -3.38, df = 16, p-value = 0.004	t = -0.88, df = 13, p-value = 0.40	t = 6.17, df = 21, p-value = 3.99e-06

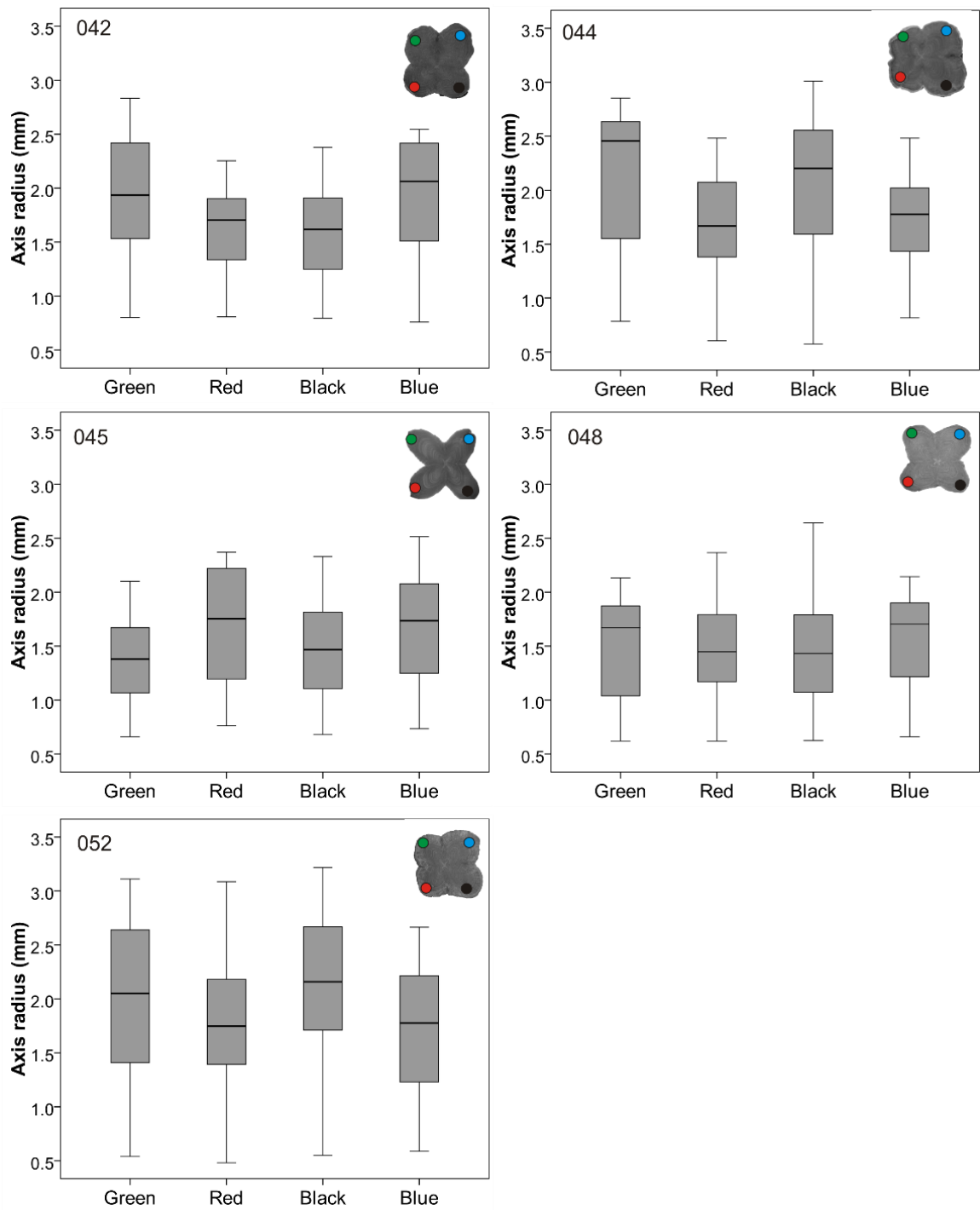


Figure 5-6. Axis radius in each of the four lobes in five colonies of *Umbellula encrinus*.

Average number of rings ranged 4-38, and assuming rings are formed annually average radial growth rates ranged 0.04-0.08 mm·yr⁻¹ in a same colony (Table 5-4).

Despite this range, no clear trends on changes in radial growth rates along the axis of the five studied colonies were observed, although in two colonies (042 and 052) there was a tendency of growth rates decreasing towards the tip of the colony, or increasing with age (Fig. 5-7).

Table 5-4. Average number of rings and radial growth rates (Rgrowth) in five colonies of *Umbellula encrinus*.

Sample	Number of rings	Average ± SD	Rgrowth (mm·yr⁻¹)	Average ± SD
042	10.3-34.5	24.8 ± 6.7	0.036-0.078	0.053 ± 0.013
044	8.3-32.3	23.0 ± 6.9	0.045-0.084	0.062 ± 0.011
045	8.0-29	18.9 ± 6.7	0.048-0.081	0.067 ± 0.009
048	7.5-37.8	24.5 ± 8.9	0.044-0.058	0.051 ± 0.004
052	4.0-33.3	22.1 ± 7.6	0.044-0.084	0.068 ± 0.011

Axis cross-sectional area was the largest at 20-30 cm (6-13% of colony height) and from then it decreased with distance from base, with the apical axis cross-sectional area representing 5-10% of the largest area measured near the base (Figs. 5-5 and 5-8A, Table 5-5). The axis was lighter near the base. A large increase was then observed at ~10 cm and from there axis weight decreased with distance from base (Fig. 5-8B).

Table 5-5. Axis cross-sectional area (mm²) in *Umbellula encrinus* and *Anthoptilum grandiflorum* near the base (largest) and near the distal tip (smallest), and percentage reduction of axis cross-sectional area (degree of tapering).

Species	Sample	Largest	Smallest	% reduction
<i>Umbellula encrinus</i>	042	15.11	1.51	89.99
	044	17.60	1.11	93.70
	045	10.95	0.85	92.28
	048	11.05	1.02	90.77
	052	20.72	0.75	96.37
Average				92.6 ± 2.3
<i>Anthoptilum grandiflorum</i>	125A	2.60	0.71	72.55
	126A	2.72	0.56	79.60
	126B	2.57	0.46	82.14
	126C	3.76	0.75	80.15
	126D	1.45	0.36	74.86
	111A	1.97	0.34	83.00
	111B	4.47	0.98	78.03
	111C	4.54	1.55	65.83
Average				77 ± 5.4

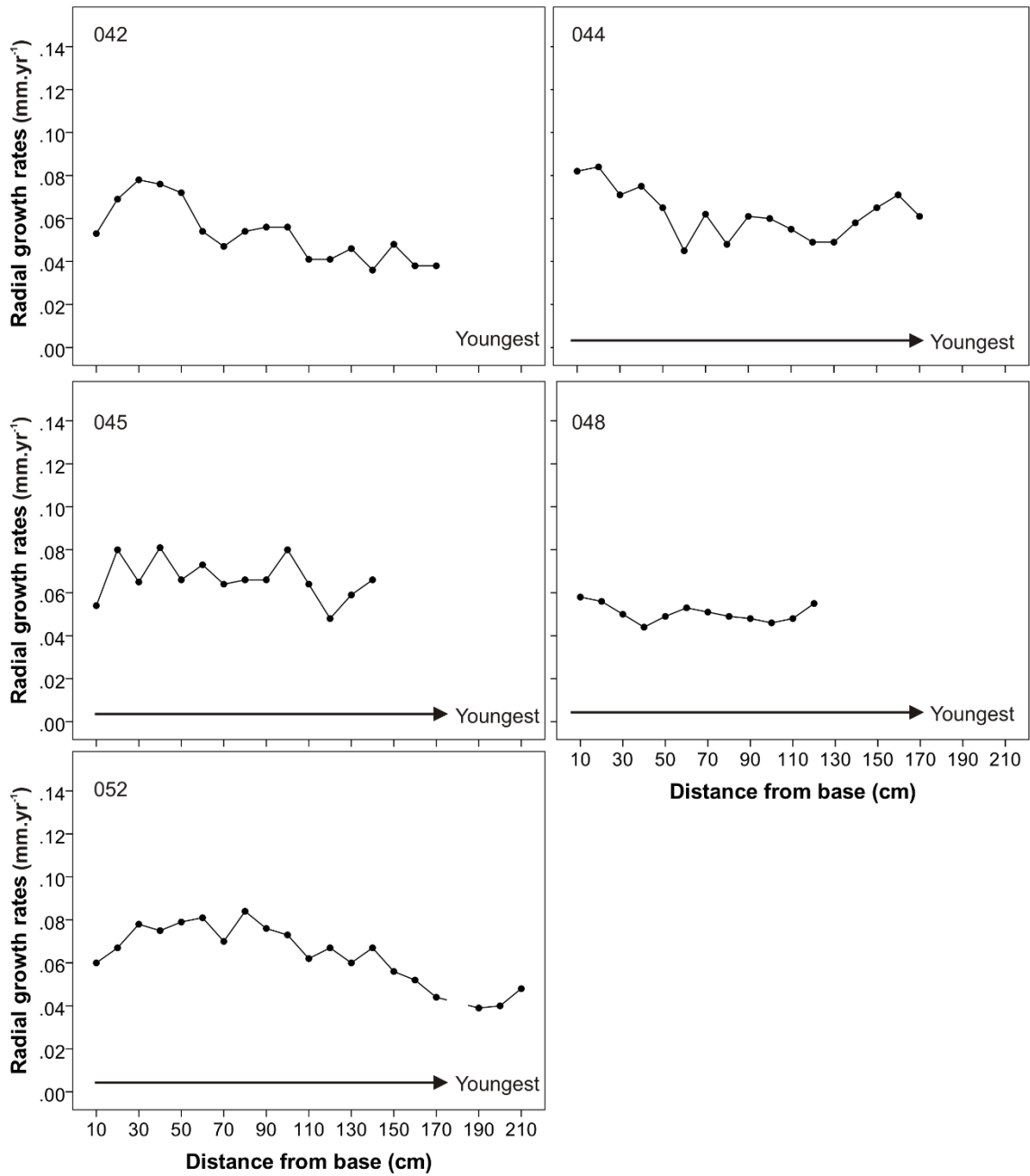


Figure 5-7. Radial growth rates in relation to distance from base in five colonies of *Umbellula encrinus*.

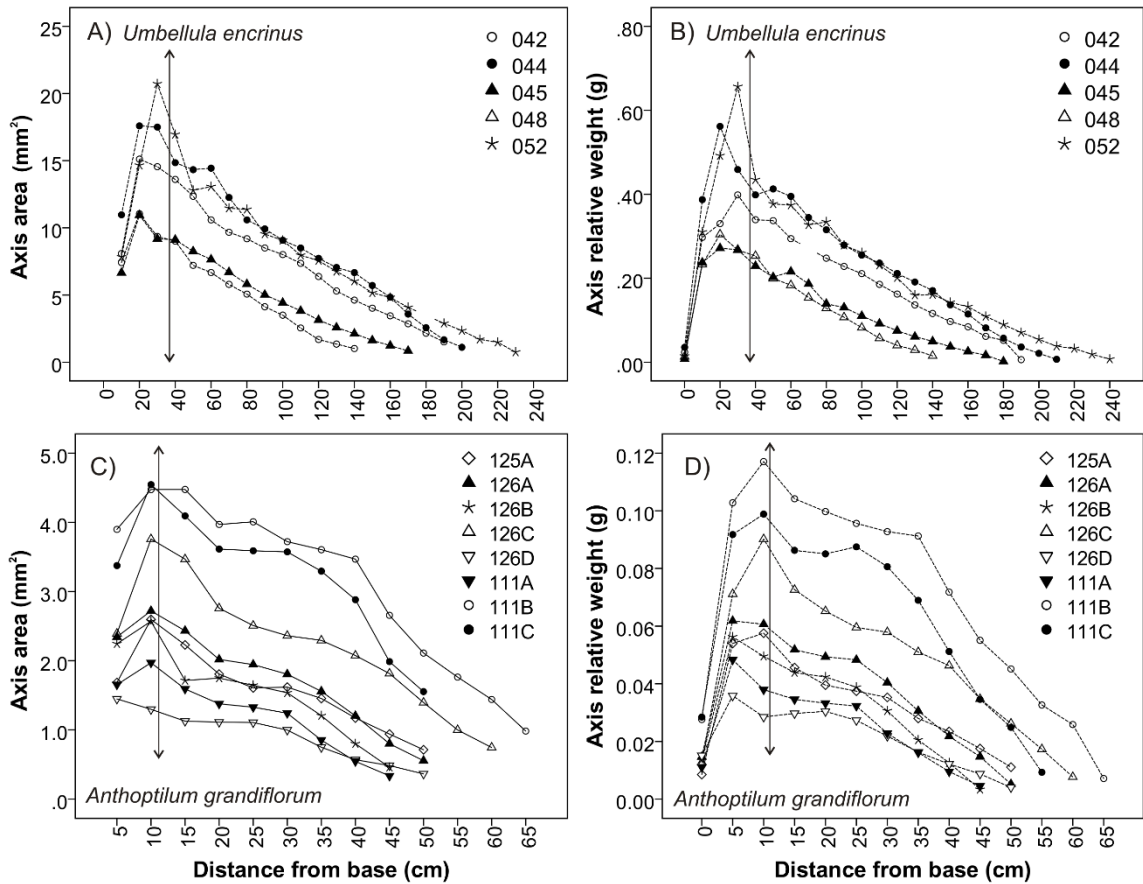


Figure 5-8. Axis area and relative weight in relation to distance from base in five colonies of *Umbellula encrinus* (A-B), and eight colonies of *Anthoptilum grandiflorum* (C-D). The vertical arrows indicate maximum peduncle length among the studied colonies.

5.3.1.2 *Anthoptilum grandiflorum*

The axis of *A. grandiflorum* also has a mainly smooth surface (Fig. 5-9). It is mostly cylindrical, varying between approximately round and elliptical in cross section.

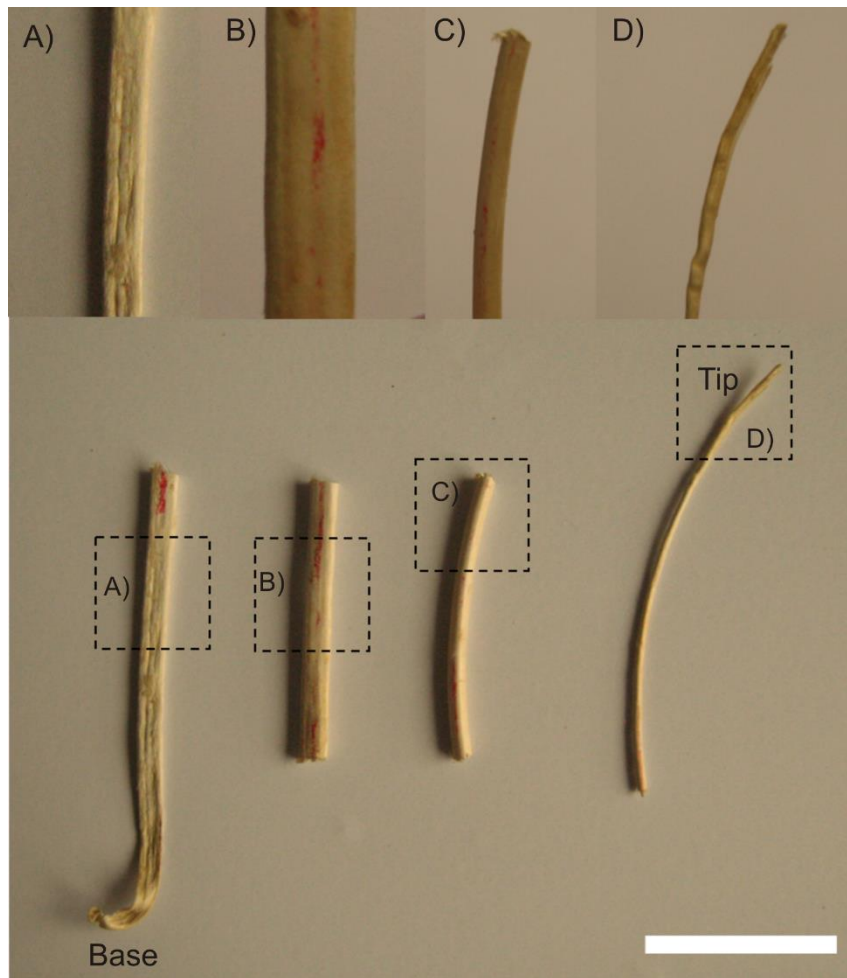


Figure 5-9. Pieces of axis showing surface at different sections of a same specimen of *Anthoptilum grandiflorum* from base to tip. Pencil marking is seen in red. Scale bar = 2 cm.

In the first ~5-20 cm (19-35% of colony size) the axis is flat, with an elliptical cross section (Figs. 5-9 to 5-11). From 15-25 cm from the base up to its apical region, shape changes to round-oval in cross section (Figs. 5-9 to 5-11).

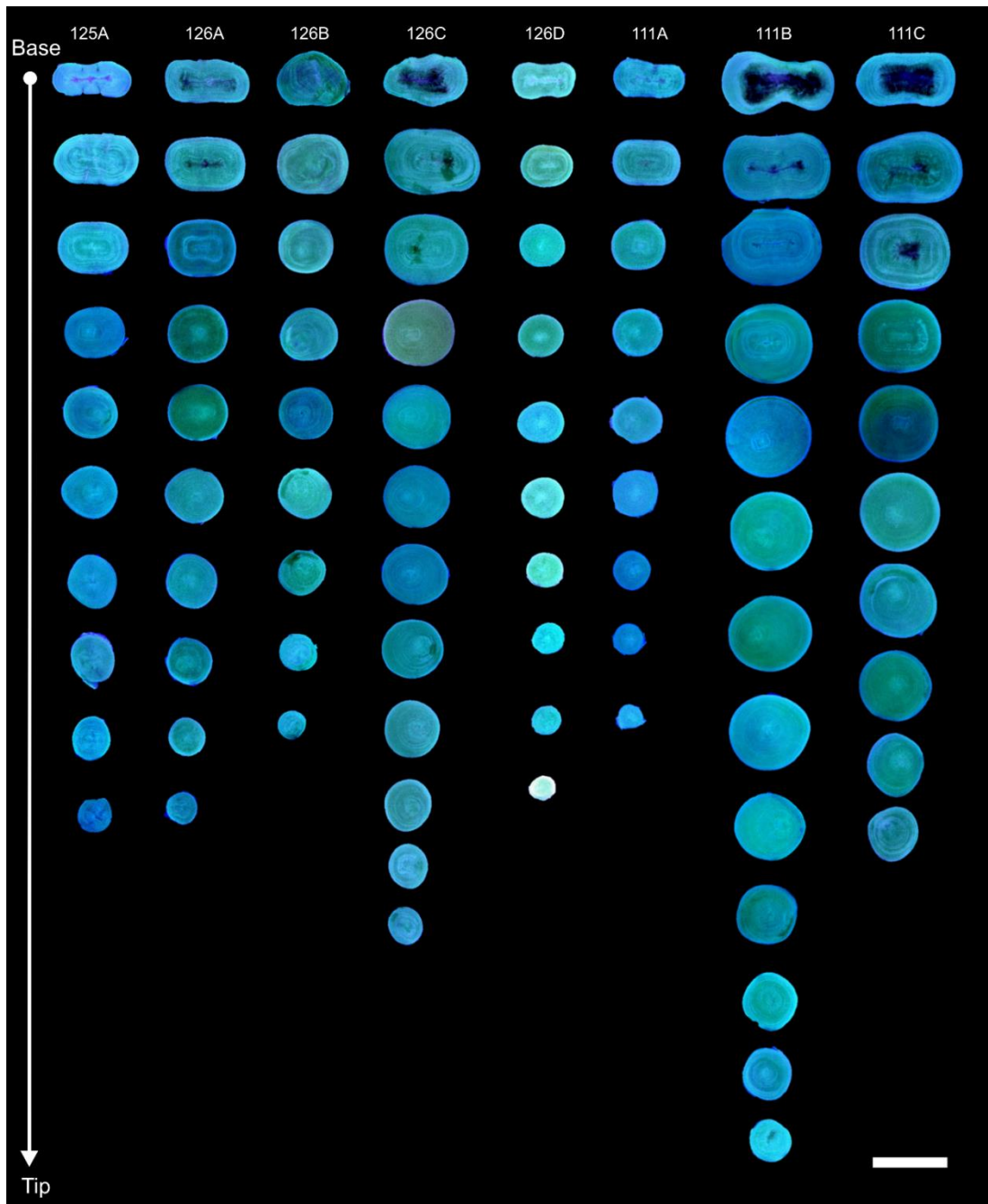


Figure 5-10. Cross sections of the internal axis of eight *Anthoptilum grandiflorum* colonies along a gradient (every 5 cm) from the base to the distal tip. Cross sections were photographed under UV light. Scale bar = 2 mm.

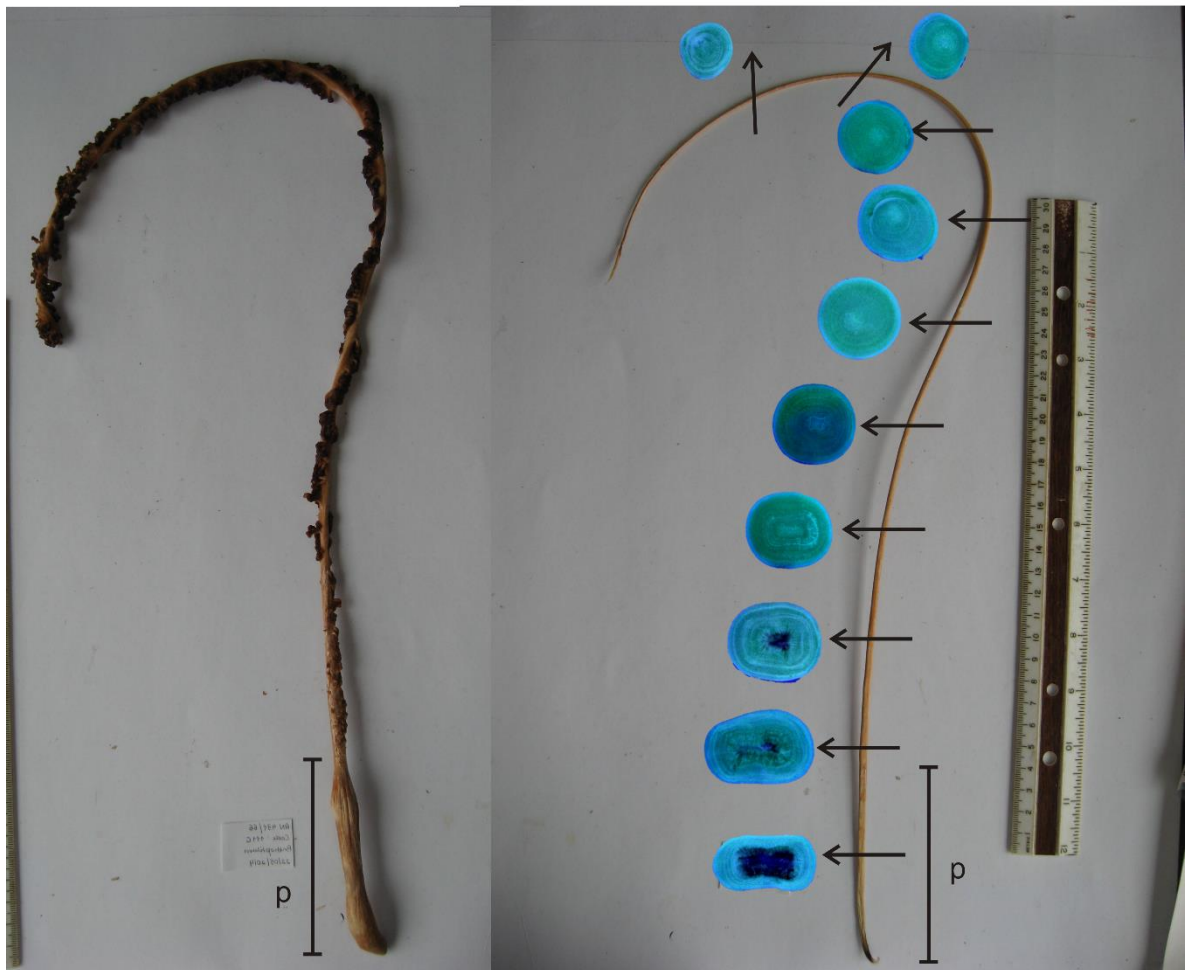


Figure 5-11. *Anthoptilum grandiflorum*: whole colony and its extracted axis before being sectioned, showing position of cross sections (arrows) along the axis, and in relation to the peduncle (p).

Axis area was the largest at 10 cm in all colonies except 126D (5 cm), and from there it decreased with distance from base (Figs. 5-8C and 5-10). Axis area at the base was much larger than at the tip, with the apical axis cross-sectional area representing 17-34% of the largest area measured near the base (Figs. 5-8C and 5-10, Table 5-4). In the

analyzed colonies, peduncle length ranged 8.7-10.5 cm, which shows that axis area was the largest near the transition between the peduncle and the rachis.

Similarly to the pattern observed for axis area, axis weight was the highest at the first 10-15 cm. However, both base and tip had the lowest axis weights, which were very similar in these two regions (Fig. 5-8D). Although growth rings were also seen in the axis of *A. grandiflorum*, they were not very evident (Fig. 5-10).

5.3.2 Axis carbonate characterization along a vertical gradient

The X-ray diffraction analysis showed that the carbonate portion of the axis in both *U. encrinus* and *A. grandiflorum* is composed of magnesian calcite $(\text{Ca,Mg})\text{CO}_3$ (Appendix 5-1 and 5-2). In both species the axis is mostly composed of carbonate material, which corresponds in average to $71 \pm 0.8\%$ of the axis in *U. encrinus* and $65 \pm 2.7\%$ in *A. grandiflorum* (Fig. 5-12A-B). On average, the axis of *U. encrinus* had twice more water than that of *A. grandiflorum*. (Fig. 5-12A-B).

The lowest carbonate proportion was found at the base and tip regions of the axis in both species, which therefore presented a higher organic content. However, in *U. encrinus* the carbonate proportion was much lower at the distal tip than at the base, with a trend of carbonate proportion decreasing with distance from base (Fig. 5-12C, E). Conversely, carbonate proportion in the axis of *A. grandiflorum* was higher at the tip region, but differences base-tip were not as striking as in *U. encrinus* (Fig. 5-12D, F).

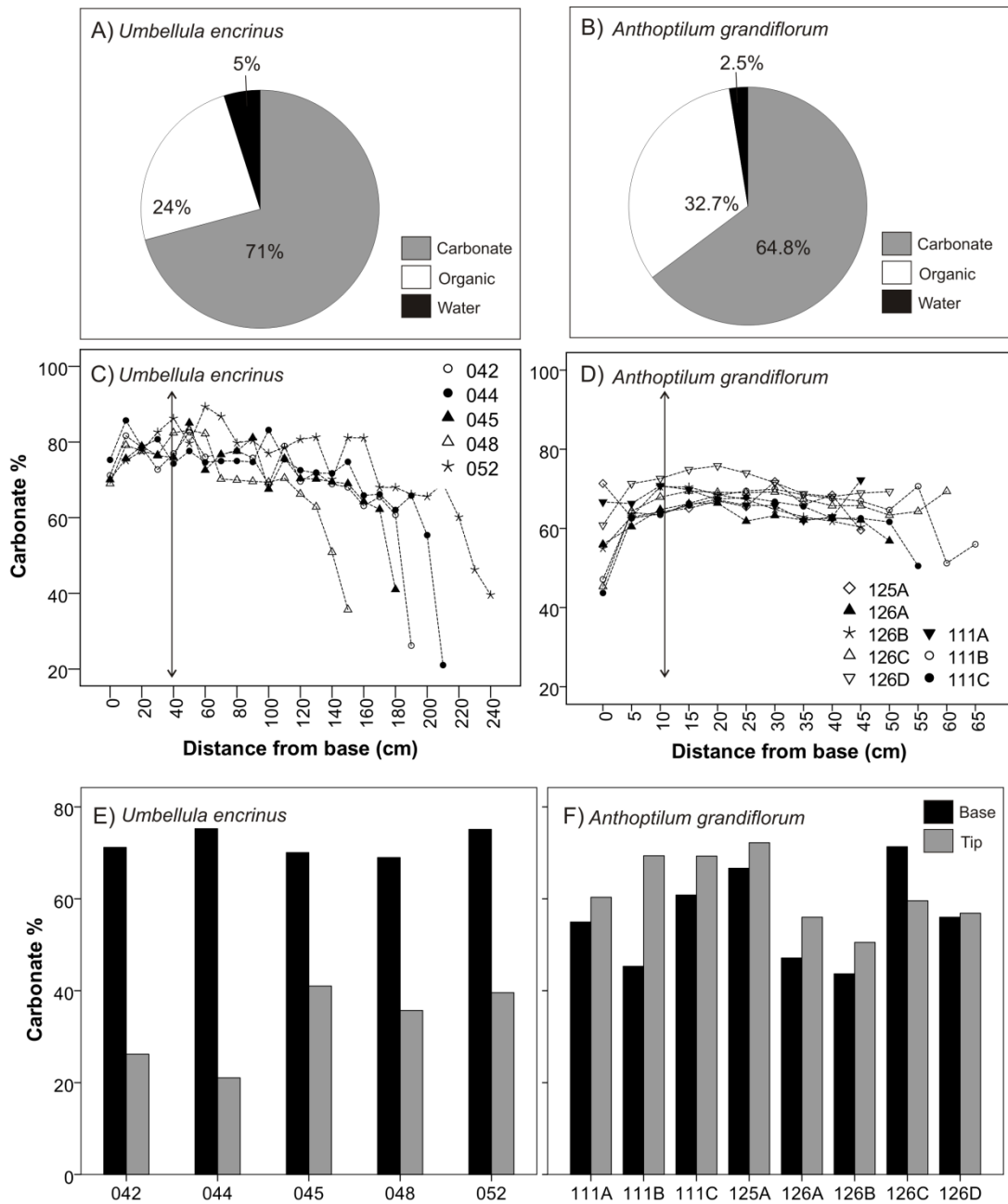


Figure 5-12. Axis composition in *Umbellula encrinus* and *Anthoptilum grandiflorum*: proportion of axis components (A-B), carbonate proportion in relation to distance from base (C-D), and carbonate proportion at base and tip. The vertical arrows in C and D indicate maximum peduncle length among the studied colonies.

5.4 Discussion

5.4.1 Carbonate composition

The carbonate composition of the axis in *U. encrinus* and *A. grandiflorum* agrees with that of other sea pens, including *Veretillum cynomorium* (Ledger & Franc, 1978), *Halipterus willemoesi* (Wilson et al., 2002), *H. finmarchica* (Chapter 2), *Pennatula grandis* Ehrenberg, 1834 (Chapter 4), and *Pennatula aculeata* Danielssen, 1860 (data not shown). Bayer and Macintyre (2001) found Mg-Calcite as the most common mineral component in the axes and holdfasts of gorgonians; although aragonite (several families) and hydroxyapatite (family Gorgoniidae) were also found in several species.

The percentage of carbonate material in the axis of sea pens has rarely been addressed. In *A. grandiflorum* ~65% of the axis was composed of CaCO₃, while in *U. encrinus* ~71% of the axis was made of carbonate material. These percentages are smaller than those estimated for other biogenic carbonate structures/organisms where CaCO₃ can represent >90% of the structure, such as the skeletons of scleractinians (Silliman, 1846), gorgonians (Lewis et al., 1992), mollusk shells (Michio & Hiromichi, 2013), fish otoliths (Campana et al., 1997), etc. However, in sea pens a relatively high proportion of organic material in the axis might be beneficial by allowing them to reach some degree of flexibility, which is not the case in these other calcareous organisms and structures. In both species calcareous sclerites common to octocorals are absent, except for tiny calcareous corpuscles that can be found in the peduncle area (Williams, 1995). In this sense, the axis is the main calcium carbonate source in these two sea pens. The higher organic content of the axis in *A. grandiflorum* might be related to its unique question

mark shape, which by itself might require additional flexibility, in comparison to *U. encrinus*. Observations of *U. encrinus in situ* indicate that this sea pen stands erect despite its large size (see Fig. 5-6C, and Chapter 3).

The distribution of the carbonate component in the axis was also different between these two species. In *U. encrinus* the carbonate proportion was highly reduced at the tip in comparison to the base and overall axis. Velimirov and Böhm (1976) also found a decrease in carbonate proportion at the tip of tropical gorgonians, in comparison to the base. Conversely, in *A. grandiflorum* carbonate proportion was higher at the tip than at the base in all but one colony. The studied specimens of *U. encrinus* were very tall (160-210 cm), and are more exposed to drag forces than *A. grandiflorum* (Wainwright & Dillon, 1969). This could explain a higher need for flexibility towards the tip in *U. encrinus*, and strength at the base. At the same time, the reduced diameter at the tip would in theory already increase flexibility (e.g. Wainwright, 1988). In Caribbean gorgonians Lewis et al. (1992) found that protein proportion increased towards the base, as observed in *U. encrinus*.

5.4.2. Changes in axis metrics and growth rates along the axis

In both species, axis area was larger at the base than at the tip, however weights were very similar between these two regions. This is probably not related to a different composition of the regions because the two species showed opposite patterns regarding proportion of carbonate at base versus tip, but similar patterns of axis metrics. It is possible that this reflects the difference in the way metrics were obtained. The measurement of axis weight comprised a ~2-3 cm segment of the axis (where area can

vary), while the measurement of area only considered the tip of the segment. By re-examining fig. 5-8, it is possible to notice that the lowest relative weights (fig. 5-8B, D) were those in the first segment (0-10 cm). After this segment, weight has a pattern that is more comparable to area.

Axis cross-sectional area (also diameter and radius) also decreased with distance from base in both species, but the degree of tapering was much higher in *U. encrinus* than in *A. grandiflorum*. This pattern is common in other groups of corals, including other sea pens and gorgonians. Because the tip of the colony is the area in contact with the highest current velocities, having thinner axes at this region might help to cope with hydrodynamic forces, by offering less resistance to currents (Wainwright & Dillon, 1969). In this sense, the tall sizes of *U. encrinus* might require a more significant tapering than the shorter colonies of *A. grandiflorum*.

In both species, this decrease in axis cross-sectional area started at ~20-30 cm, with the largest area being found at ~20 cm, which in most colonies was still the peduncle area. While more flexibility might be important towards the apical region of the axis, strength towards the base is also essential to support the colony. Axis radius and diameter have an impact in overall axis stiffness, with a small increase in these metrics leading to an increase in flexural stiffness (Wainwright, 1988).

The cross-sectional asymmetry of the four lobes in *U. encrinus* (when compared to one another) suggests that the four lobes (sides) of the axis are not subject to the same forces all along. Some lobes were longer than others, indicating a faster growth, and usually two lobes were more similar to one another than to the two other lobes.

It is possible that current direction (unidirectional currents) has an influence on the differential lobe size and shape in *U. encrinus*. Unidirectional flow has been shown to influence colony symmetry (Mass & Genin, 2008, Kaandorp et al., 1996, Chindapol et al., 2013), and cross-sectional skeletal symmetry (Noé & Dullo, 2006) in other coral species. The side with lobes facing the currents might develop more than the opposite side (e.g. Chindapol et al., 2013), and despite the twisting of the axis (and changing lobe positioning), the side that accreted more material earlier remains larger.

In the shallow-water coral *Pocillopora verrucosa* (Ellis & Solander, 1786), asymmetric growth resulting from the influence of unidirectional currents has been associated to the flux of nutrients brought by these currents (e.g. Mass & Genin, 2008). In the case of *U. encrinus*, it is possible that the asymmetry of the lobes is a response to the physical/mechanical influence of the currents, rather than to food delivery. However, this hypothesis remains to be tested.

In terms of growth rings, the average number of growth rings decreased with distance from base, as expected. Towards the tip of the axis, the organic content was more visible in the core region, and rings were not visible in this portion. The decrease in the number of growth rings towards the tip of the axis is logical considering the tapering showed by the axis from the base to the tip (Wainwright & Dillon, 1969).

Growth rates were variable along the axis of a single colony, but overall growth rate ranges were similar between the different studied colonies. No obvious trends in relation to changes in radial growth rates along the axis were identified, but for some colonies there was a tendency of radial growth rates decreasing with distance from base, or increasing with age. This pattern was also identified in the analysis of colonies of *U.*

encrinus where a single average growth rate measurement (single location in the axis) was estimated for several colonies, and it could be related to an increase in the number of feeding polyps and consequent feeding rate with increased age (Chapter 3).

This is the first study to estimate changes in growth rates and skeletal metrics and morphology along whole sea pen colonies. Other studies have reported changes in skeletal morphology and growth rates in other octocorals such as bamboo corals (Noé & Dullo, 2006, Noé et al., 2008). Growth rates are known to vary depending on ontogenetic stage (Sebens, 1987).

Together these studies indicate that although average growth rates are a useful measure to better understand how fast these organisms grow, living organisms are complex in their biology and interactions with the environment, and changes in growth with ontogenetic stage are not surprising, but rather expected. This is what was observed in the skeleton of *U. encrinus*, although no overall clear pattern was identified towards specific growth rates intervals for specific regions of the skeleton.

5.4.3 Twisting of axis in *U. encrinus*

This is the first study to report in detail the twisting along the axis of a sea pen. It is still uncertain why and how the axis in *U. encrinus* twists. In most analyzed colonies, twisting started after the first 50 cm of colony height, which shows that the portion of axis laying inside the peduncle of these specimens did not twist, since peduncle length in all analyzed colonies was < 50 cm long (see table 5-2).

One of the colonies (sample 048) showed twisting above 20 cm, and in this colony peduncle length was 23 cm. This suggests that in this colony twisting started at the

intersection peduncle-stalk (joint). This sample was the smallest colony (156 cm), but size does not explain its early twisting, since sample 045 was the second smallest (187 cm), and twisting started much later, at 80 cm. Samples 045 and 048 came from the same environment and depth, had comparable heights, and yet twisting started at quite distinct heights. Based on these data, the timing for the axis to start twisting can be colony-specific.

In the first known description of *Umbellula*, Ellis (1753) already reported that the axis twists and suggested that twisting was probably due to some sort of physical damage caused to the colony. In a taxonomic study of the genus, Dolan (2008) reported the twisting of axis in a few colonies of *Umbellula carpenteri* K lliker, 1880. She suggested that twisting was probably due to contraction, although she did not clarify whether a natural contraction or following sampling and fixation.

Twisting of the axis in *U. encrinus* is almost certainly not accidental or rare. During a video survey in Scott Inlet (Baffin Bay, NW Atlantic) using a remotely operated vehicle (ROV), a colony of *U. encrinus* was observed bending over the substrate at an angle of $\sim 177^\circ$, showing a very conspicuous twisting of the distal part of the stalk (Fig. 5-4B). Additionally, during ROV video transects *U. encrinus* has been observed to partially rotate its stalk on a time scale of seconds, and colonies of the sea whip *Stylatula elongata* (Gabb, 1862) at Cobb Seamount (Northeast Pacific), and *Pennatula* sp. (Orphan Knoll, NW Atlantic) were also witnessed to rotate their bodies *in situ* (BMN, personal observation). However, it is unknown how twisting of the stalk and axis might be related.

Other corals show rotation of their bodies. The axis of the gorgonian *Astrogorgia rubra* Thomson & Henderson, 1906 is horny, spirally twisted (Thomson & Henderson,

1906), and in Caribbean gorgonians the early alignment of the blade differs from the final alignment, indicating a change in orientation over time (Wainwright & Dillon, 1969).

Although most *U. encrinus* seen *in situ* shows some degree of bending, very tall colonies (>2 m) have also been observed almost in a 90° position (e.g. Fig. 5-4C, Chapter 3). Twisting of the axis might be a strategy to cope with a combination of a tall and thin body and exposition to increased drag forces as the colony grows taller. For instance, a body/skeleton having a low torsional stiffness (not resisting the torsion when a force is applied) can help to reduce the flow-induced drag in several organisms/structures (Etnier, 2003, Etnier & Vogel, 2000), and this could be an advantage to *U. encrinus*.

Additionally, increasing chances of encountering food might also be a reason for the twisting seen in the skeleton of *U. encrinus*, as suggested for the body rotation performed by the sea pen *Ptilosarcus gurneyi* (Best, 1983, 1988), and some gorgonians (Jeyasuria & Lewis, 1987). Twisting the axis in *U. encrinus* might therefore be a response to both coping with drag forces and/or increasing chances of food capture, or other factors not discussed here; but corroboration of these hypotheses depends on specific experiments designed to better understanding the twisting of the axis in this species.

5.4.4 Comparing the axes of *U. encrinus* and *A. grandiflorum*

In Pennatulacea, axes of different shapes can occur in species of the same genus, in different colonies of a same species, and in a same colony as showed for *A. grandiflorum* (Table 5-5). Axis shape does not seem to be particularly related to attainable colony size. For instance, *Umbellula* species with quadrangular axes can be both short

(e.g. *U. carpenteri*; < 10 cm) and tall (e.g. *U. encrinus*; 100-230 cm) (Dolan, 2008), and species of tall *Umbellula* can also have cylindrical axes (Dolan, 2008).

Four genera of Pennatulacea (*Actinoptilum*, *Amphibelemnon*, *Echinoptilum*, *Renilla*) completely lack an internal axis (Williams, 1995, López-González et al., 2000), which is present in ~ 90% of the 36 extant Pennatulacea genera (Williams, 1995, 2011, 2015, López-González et al., 2000).

In *A. grandiflorum* the axis changed from elliptical to round, with instances where the core of the axis was quadrangular, but the main axis was elliptical. Thomson and Henderson (1906) reported a relatively quadrangular shape at the base of the axis in *Anthoptilum murrayi* Kölliker, 1880. In *Pennatula phosphorea* Linnaeus, 1758 the axis also changes the shape with distance from base, being more squared at the intersection between stalk and rachis, and cylindrical above and below it (Musgrave, 1909). As the organism grows, drag forces increase since water flow becomes faster further away from the bottom (Wainwright & Koehl, 1976, Wainwright, 1988). It is therefore expected that the geometry and the material properties of the joint elements change in response to this increase in drag forces (Wainwright & Koehl, 1976, Best, 1983).

In *U. encrinus* the axis did not show great changes in geometry along its length, with the basic quadrangular shape and four-fold symmetry remaining the same with distance from base in the studied specimens. The main change observed along the axis of *U. encrinus* was that the grooves between lobes were “shallower” in the first cm of the axis than with distance from base (see fig. 5-5). Furthermore, some colonies had more pronounced lobes than others.

In the analyzed specimens from both species we observed that the axis was the thickest at around the same position. In the analyzed specimens of *A. grandiflorum*, maximum axis area was observed at ~10 cm, which is approximately the transition zone between peduncle and rachis. In the sea pen *Ptilosarcus gurneyi*, Best (1985) observed that thickness and rigidity of the axis in the joint region (intersection peduncle-rachis) helped to prevent bending at the joint. Furthermore, small increases in size largely increase beam stiffness (Etnier, 2003).

In *U. encrinus*, maximum averaged axis area was found at ~ 20-30 cm from the base, which was near the peduncle-rachis transition in the two smallest specimens; in the largest specimen (sample 052; 215 cm) the peduncle-rachis transition occurred at ~39 cm from the base, and maximum axis area was at 30 cm. However, because there is a 10 cm difference between the measured areas, it is possible that an even larger area would be found between 30 and 40 cm, which would be close to the peduncle-rachis transition.

The axis of sea pens can be considered biological beams, which can be defined as structures that are long relative to their width (Etnier, 2001). According to the engineering beams theory, beams with elliptical sections are more torsionally compliant, and they are stiffer in the direction of the major axis of the ellipse; while cylindrical sections are equally rigid on all sides (Wainwright, 1988). In *A. grandiflorum*, the peduncle-rachis transition zone is very conspicuous, showing an evident muscular bulb, which is absent in *U. encrinus*. The axis in *A. grandiflorum* is flat (elliptical in cross section) in the first 15-20 cm of the colony. In certain sea fans, the axis is also elliptical near the base, such as in *Gorgonia* sp. (Wainwright & Koehl, 1976), and in *Leptogorgia lütkeni* (Wright & Studer, 1889) (Williams & Lindo, 1997). An elliptical axis gives resistance to side-ways bending

(an advantage for fan shaped colonies) and low resistance to bending with the flow normal to the fan (Wainwright & Koehl, 1976). *A. grandiflorum* has a characteristic question-mark, concave shape, with a very developed spongy tissue and transverse musculature of the body wall in the bulb area (Musgrave, 1909). The flat axis - in the first cm - might be related to the unusual question mark shape presented by this species, where an elliptical shape would give more stability to an axis that changes from a straight to a curved position along its height.

Studies on the biomechanics of sea pens are rare, with the most recent study having been conducted at least 30 years ago (e.g. Magnus, 1966, Best, 1985). Biomechanical studies on different morphological types of sea pens such as *U. encrinus* and *A. grandiflorum* might provide more insights on how these deep-water organisms interact with the environment. Advancing the knowledge about the biology and geochemistry of the skeleton in these organisms can help to better understand their relationship to the environment.

Table 5-5. Shape of axis in some Pennatulacea genera with an internal axis (quadrangular and cylindrical). Here cylindrical includes forms between round and elliptical

(Wainwright, 1988). Presence of axis in the genus does not mean that all species in the genus have an axis. *Flattened, ** not whole axis investigated, *** mostly.

Family	Genus	■	●	Reference
Anthoptilidae	<i>Anthoptilum</i>			Hickson (1916), Williams (1995)
Chunellidae	<i>Amphiacme</i>			Williams (1995)
	<i>Calibelemnon</i>			Williams (1995)
	<i>Chunella</i>			Williams (1995)
	<i>Porcupinella</i>			López-González and Williams (2011)
	<i>Funiculina</i>			Hickson (1916), Williams (1995)
Funiculidae	<i>Funiculina</i>			Hickson (1916), Williams (1995)
Halipteridae	<i>Halipteris</i>			Williams (1995)
Kophobelemnidae	<i>Kophobelemnon</i>			Williams (1995)
	<i>Malacobelemnon</i>	*		Williams (1995)
	<i>Sclerobelemnon</i>			Hickson (1916)
Pennatulidae	<i>Pennatula</i>			Hickson (1916)
	<i>Pteroeides</i>		**	Hickson (1916)
	<i>Ptilosarcus</i>			Birkeland (1974)
	<i>Gyrophyllum</i>			Williams (1995)
Protoptilidae	<i>Distichoptilum</i>			Hickson (1916)
Pteroeididae	<i>Crassophyllum</i>			Williams (1995)
	<i>Gyrophyllum</i>			Williams (1995)
	<i>Protoptilum</i>			Mastrototaro et al. (2015)
	<i>Pteroides</i>		**	Hickson (1916)
	<i>Sarcoptilus</i>			Williams (1995)
Stachyptilidae	<i>Stachyptilum</i>			Kölliker (1880)
	<i>Gilibelemnon</i>			López-González and Williams (2002)
Scleroptilidae	<i>Scleroptilum</i>			Williams (1995)
Umbellulidae	<i>Umbellula</i>			Williams (1995)
Veretillidae	<i>Cavernularia</i>			Hickson (1916)
	<i>Cavernulina</i>			Veena and Kaladharan (2012)
	<i>Lituaria</i>			Hickson (1916)
	<i>Veretillum</i>			Hickson (1916)
Virgulariidae	<i>Acanthoptilum</i>			Williams (2007)
	<i>Grasshoffia</i>			Williams (2015)
	<i>Scytalium</i>	***		Williams (1995)
	<i>Scytaliopsis</i>			Williams (1995)
	<i>Stylatula</i>			Williams (1995, 2007)
	<i>Virgularia</i>			Williams (1995)

Acknowledgements

We thank Glenn Piercey, Michael Shaffer, and Brian Loveridge (CREAIT, Memorial University) for assistance with sectioning, and Wanda Aylward (CREAIT, Memorial University) for the X-ray diffraction analysis. Kent Gilkinson (Fisheries and Oceans Canada) for the samples and location data. Research is funded by the Natural Sciences and Engineering Research Council of Canada (NSERC) (doctoral scholarship to BMN) and Canadian Healthy Oceans Network (CHONe).

5.5 References

Baillon, S., J. Hamel & A. Mercier, 2014. Diversity, distribution and nature of faunal associations with deep-sea pennatulacean corals in the Northwest Atlantic. PLoS ONE 9: e111519.

Baillon, S., M. English, J. Hamel & A. Mercier, 2016. Comparative biometry and isotopy of three dominant pennatulacean corals in the Northwest Atlantic. Acta Zoologica: in press.

Baillon, S., J. Hamel, V. E. Wareham & A. Mercier, 2012. Deep cold-water corals as nurseries for fish larvae. Frontiers in Ecology and the Environment 10: 351-356.

Baker, K. D., V. E. Wareham, P. V. R. Snelgrove, R. L. Haedrich, D. A. Fifield, E. N. Edinger & K. D. Gilkinson, 2012. Distributional patterns of deep-sea coral assemblages in three submarine canyons off Newfoundland, Canada. Marine Ecology Progress Series 445: 235-249.

Bayer, F. M. & I. G. Macintyre, 2001. The mineral component of the axis and holdfast of some gorgonacean octocorals (Coelenterata: Anthozoa), with special reference to the family Gorgoniidae. Proceedings of the Biological Society of Washington 114: 309-345.

Best, B. A., 1988. Passive suspension feeding in a sea pen: effects of ambient flow on volume flow rate and filtering efficiency. The Biological Bulletin 175: 332-342.

Best, B. A., 1985. An integrative analysis of passive suspension feeding: the sea pen *Ptilosarcus gurneyi* as a model organism. PhD thesis, Duke University, Durham, United States.

- Best, B., 1983. Mechanics of orientation in sea pens - a rotational one link joint. *Journal of Biomechanics* 16: 297-297.
- Birkeland, C., 1974. Interactions between a sea pen and seven of its predators. *Ecological Monographs* 44: 211-232.
- Brodeur, R. D., 2001. Habitat-specific distribution of Pacific ocean perch (*Sebastes alutus*) in Pribilof Canyon, Bering Sea. *Continental Shelf Research* 21: 207-224.
- Campana, S. E., S. R. Thorrold, C. M. Jones, D. Günther, M. Tubrett, H. Longerich, S. Jackson, N. M. Halden, J. M. Kalish & P. Piccoli, 1997. Comparison of accuracy, precision, and sensitivity in elemental assays of fish otoliths using the electron microprobe, proton-induced X-ray emission, and laser ablation inductively coupled plasma mass spectrometry. *Canadian Journal of Fisheries and Aquatic Sciences* 54: 2068-2079.
- Chindapol, N., J. A. Kaandorp, C. Cronemberger, T. Mass & A. Genin, 2013. Modelling growth and form of the scleractinian coral *Pocillopora verrucosa* and the influence of hydrodynamics. *PLoS Computational Biology* 9: e1002849.
- Dolan, E., 2008. Phylogenetics, systematics and biogeography of deep-sea Pennatulacea (Anthozoa: Octocorallia): evidence from molecules and morphology. PhD thesis, University of Southampton, Southampton, England.
- Etnier, S. A., 2001. Flexural and torsional stiffness in multi-jointed biological beams. *The Biological Bulletin* 200: 1-8.
- Etnier, S. A., 2003. Twisting and bending of biological beams: distribution of biological beams in a stiffness mechanospace. *Biological Bulletin* 205: 36-46.

Etnier, S. A. & S. Vogel, 2000. Reorientation of daffodil (*Narcissus*: Amaryllidaceae) flowers in wind: drag reduction and torsional flexibility. *American Journal of Botany* 87: 29-32.

Franc, S., A. Huc & G. Chassagne, 1974. Ultrastructural and physicochemical study of the skeletal axis of *Veretillum cynomorium* Pall. (Cnidarian, Anthozoan): cells, calcite, collagen. *Journal of Microscopy* 21: 93-110.

Hickson, S. J., 1916. The Pennatulacea of the Siboga Expedition: with a general survey of the order. Late EJ Brill.

Jeyasuria, P. & J. C. Lewis, 1987. Mechanical properties of the axial skeleton in gorgonians. *Coral Reefs* 5: 213-219.

Kaandorp, J. A., C. P. Lowe, D. Frenkel & P. M. Sloom, 1996. Effect of nutrient diffusion and flow on coral morphology. *Physical Review Letters* 77: 2328.

Kölliker, R. A., 1880. Report on the Pennatulida, dredged by H.M.S. Challenger during the years 1873-1876. *Voyage of the Challenger, Zoology* 1:1-41, pl. 1-11.

Ledger, P. W. & S. Franc, 1978. Calcification of collagenous axial skeleton of *Veretillum cynomorium* Pall (Cnidaria Pennatulacea). *Cell and Tissue Research* 192: 249-266.

Lewis, J. C., T. F. Barnowski & G. J. Telesnicki, 1992. Characteristics of carbonates of gorgonian axes (Coelenterata, Octocorallia). *The Biological Bulletin* 183: 278-296.

López-González, P. J., J. Gili & G. C. Williams, 2000. On some veretillid pennatulaceans from the eastern Atlantic and western Pacific Oceans (Anthozoa: Octocorallia), with a review of the genus *Cavernularia*, and descriptions of new taxa. *Journal of Zoology* 250: 201-216.

López-González, P. J. & G. C. Williams, 2002. A new genus and species of sea pen (Octocorallia: Pennatulacea: Stachyptilidae) from the Antarctic Peninsula. *Invertebrate Systematics* 16: 919-929.

López-González, P. & G. Williams, 2011. A new deep-sea pennatulacean (Anthozoa: Octocorallia: Chunellidae) from the Porcupine Abyssal Plain (NE Atlantic). *Helgoland Marine Research* 65: 309-318.

Magnus, D. B. E., 1966. On the ecology of a seapen (Octocorallia, Pennatularia) in the Red Sea. *Veröff. Inst. Meeresforsch. Bremerhaven* 10: 369-379.

Malecha, P. W. & R. P. Stone, 2009. Response of the sea whip *Halipteris willemoesi* to simulated trawl disturbance and its vulnerability to subsequent predation. *Marine Ecology Progress Series* 388: 197-206.

Mass, T. & A. Genin, 2008. Environmental versus intrinsic determination of colony symmetry in the coral *Pocillopora verrucosa*. *Marine Ecology Progress Series* 369: 131-137.

Mastrototaro, F., G. Chimienti, F. Capezzuto, R. Carlucci & G. Williams, 2015. First record of *Protoptilum carpenteri* (Cnidaria: Octocorallia: Pennatulacea) in the Mediterranean Sea. *Italian Journal of Zoology* 82: 61-68.

Michio, S. & N. Hiromichi, 2013. Mollusk shell structures and their formation mechanism. *Canadian Journal of Zoology* 91: 349-366.

Musgrave, E. M., 1909. Experimental observations on the organs of circulation and powers of locomotion in pennatulids. *Quarterly Journal of Microscopical Science* 54: 443-482.

Noé, S. & W. -. Dullo, 2006. Skeletal morphogenesis and growth mode of modern and fossil deep-water isidid gorgonians (Octocorallia) in the West Pacific (New Zealand and Sea of Okhotsk). *Coral Reefs* 25: 303-320.

Noé, S., L. Lembke-Jene & W. -. Dullo, 2008. Varying growth rates in bamboo corals: sclerochronology and radiocarbon dating of a mid-Holocene deep-water gorgonian skeleton (*Keratoisis* sp.: Octocorallia) from Chatham Rise (New Zealand). *Facies* 54: 151-166.

Schneider, C. A., W. S. Rasband & K. W. Eliceiri, 2012. NIH Image to ImageJ: 25 years of image analysis. *Nature Methods* 9: 671-675.

Sebens, K. P., 1987. The ecology of indeterminate growth in animals. *Annual Review of Ecology and Systematics* 18: 371-407.

Silliman, B., 1846. On the chemical composition of the calcareous corals. *American Journal of Science* 1: 189-199.

Soong, K., 2005. Reproduction and colony integration of the sea pen *Virgularia juncea*. *Marine Biology* 146: 1103-1109.

Thomson, J. A. & W. D. Henderson, 1906. An account of the alcyonarians collected by the Royal Indian Marine Survey Ship Investigator in the Indian Ocean. Order of the Trustees of the Indian Museum.

Troffe, P. M., C. D. Levings, G. E. Piercey & V. Keong, 2005. Fishing gear effects and ecology of the sea whip *Halipteris willemoesi* (Cnidaria: Octocorallia: Pennatulacea) in British Columbia, Canada: preliminary observations. *Aquatic Conservation: Marine and Freshwater Ecosystems* 15: 523-533.

Veena, S. & P. Kaladharan, 2012. First record of *Cavernulina orientalis* (Thomson & Simpson, 1909) (Octocorallia: Pennatulacea: Veretillidae) from the Bay coast of Visakhapatnam, Andhra Pradesh. *Zootaxa* 3204: 61-64.

Velimirov, B. & E. L. Böhm, 1976. Calcium and magnesium carbonate concentrations in different growth regions of gorgonians. *Marine Biology* 35: 269-275.

Wainwright, S. A., 1988. Axis and circumference: the cylindrical shape of plants and animals. Harvard University Press, Cambridge, Mass.

Wainwright, S. A. & J. R. Dillon, 1969. On the orientation of sea fans (genus *Gorgonia*). *The Biological Bulletin* 136: 130-139.

Wainwright, S. A. & M. A. R. Koehl, 1976. The nature of flow and the reaction of benthic Cnidaria to it. In Mackie, G. O. (ed), *Coelenterate ecology and behavior: [selected papers]* International Symposium on Coelenterate Biology. Plenum Press, New York: 5-21.

Wareham, V. E. & E. N. Edinger, 2007. Distribution of deep-sea corals in the Newfoundland and Labrador region, Northwest Atlantic Ocean. *Bulletin of Marine Science* 81: 289-313.

Williams, G. C., 1995. Living genera of sea pens (Coelenterata: Octocorallia: Pennatulacea): illustrated key and synopses. *Zoological Journal of the Linnean Society* 113: 93-140.

Williams, G. C., 2007. New Species of the Pennatulacean Genera *Acanthoptilum* and *Stylatula* (Octocorallia: Virgulariidae) from New Zealand and the Campbell Plateau: Both Genera Previously Considered Endemic to the West Coast of the Americas and Atlantic Ocean. *Proceedings of the California Academy of Sciences* 58: 339-348.

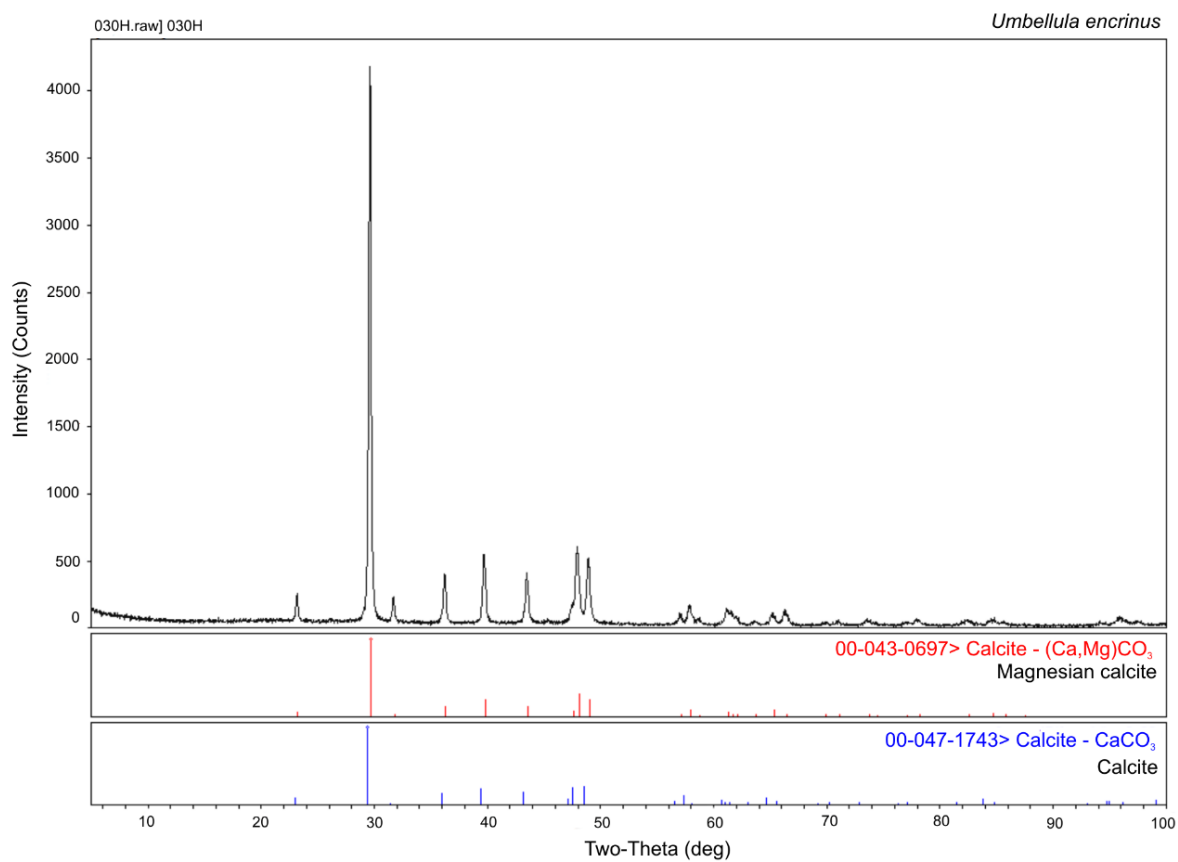
Williams, G. C., 2011. The global diversity of sea pens (Cnidaria: Octocorallia: Pennatulacea). PLoS ONE 6: 1-11.

Williams, G. C., 2015. A new genus and species of pennatulacean octocoral from equatorial West Africa (Cnidaria, Anthozoa, Virgulariidae). ZooKeys: 39-50.

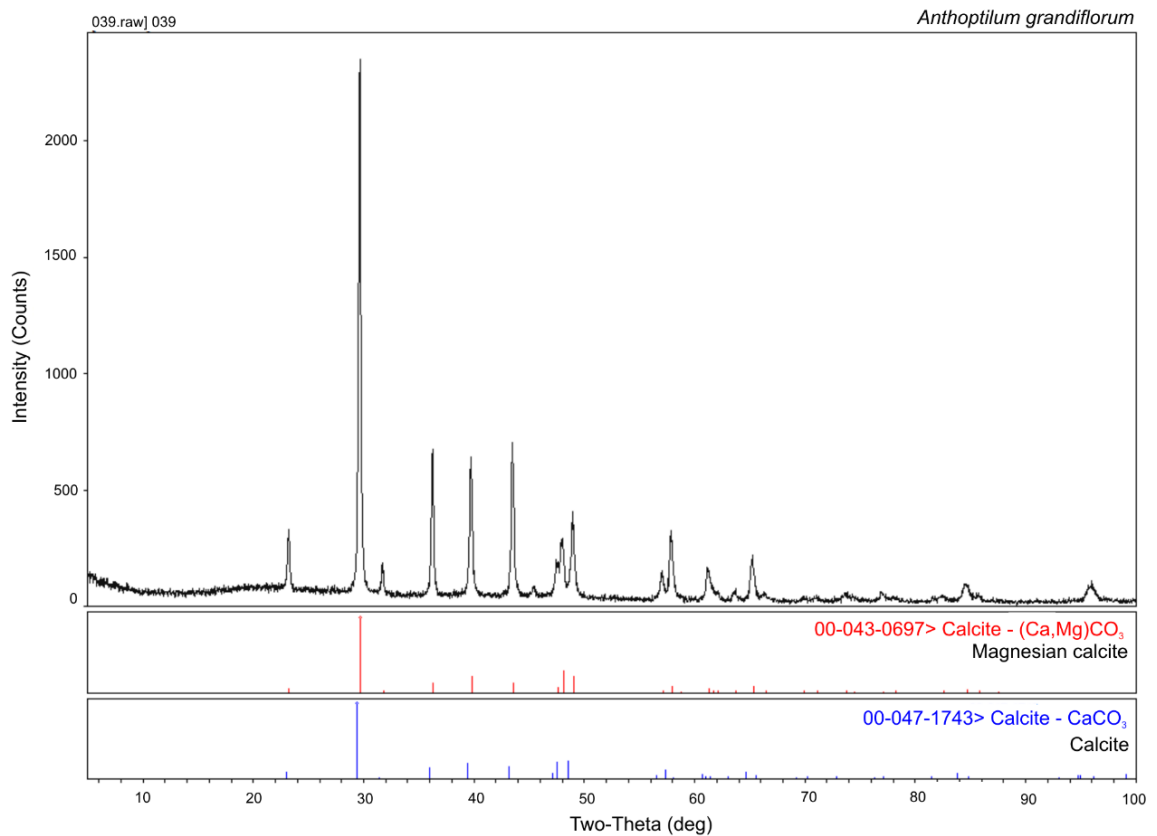
Williams, G. C. & K. G. Lindo, 1997. A review of the octocorallian genus *Leptogorgia* (Anthozoa: Gorgoniidae) in the Indian Ocean and Subantarctic, with description of a new species and comparisons with related taxa. Proceedings of the California Academy of Sciences 49: 499-521.

Wilson, M. T., A. H. Andrews, A. L. Brown & E. E. Cordes, 2002. Axial rod growth and age estimation of the sea pen, *Halipteris willemoesi* Kölliker. Hydrobiologia 471: 133-142.

Appendix 5-1 X-Ray Diffraction analysis for the carbonate portion of the axis in *Umbellula encrinus*. Overlap between the axis in *U. encrinus* axis (black), magnesian calcite (red), and calcite (blue). Note that the axis of *U. encrinus* follows the same pattern as magnesian calcite.



Appendix 5-2 X-Ray Diffraction analysis for the carbonate portion of the axis in *Anthoptilum grandiflorum*. Overlap between the axis in *A. grandiflorum* (black), magnesian calcite (red), and calcite (blue). Note that the axis of *A. grandiflorum* follows the same pattern as magnesian calcite.



6. Growth in the cold-water gorgonians *Primnoa pacifica* Kinoshita, 1907 and *Primnoa resedaeformis* (Gunnerus, 1763) (Cnidaria: Octocorallia) in relation to environmental variables⁵

Abstract

Growth rates in the octocorals *Primnoa pacifica* and *Primnoa resedaeformis* from several locations were obtained from new data and data from the literature, compared, and investigated in relation to environmental variables. Age was estimated by counting the number of annual growth rings in the stem, and growth rates were estimated based on the relationship between age and colony height, and stem diameter. Additionally, we described the size structure of *P. pacifica* colonies from two sites at the Strait of Georgia (British Columbia, Canada), from where colony skeletons were also analyzed for ¹⁴C. There were significant relationships between diametric growth rates and chlorophyll a and depth, but only non-significant trends were observed with other environmental variables. The ¹⁴C analysis could not be used to corroborate frequency of ring formation for colonies from the Strait of Georgia because live-collected colonies were too young to have incorporated bomb-¹⁴C. However, by using the ¹⁴C data we estimated that some of the dead-collected colonies had been laying on the bottom for at least 40 years. This study showed that growth rates in *P. pacifica* and *P. resedaeformis* are not different from each

⁵For submission to Deep Sea Research I.

other as previously suggested in the literature, and that they can be influenced by environmental factors such as surface primary productivity.

6.1 Introduction

The study of deep-water corals has intensified in the past decade, mostly because of concerns related to their vulnerability to bottom fisheries and other anthropogenic threats (e.g. Thrush & Dayton, 2002, Troffe et al., 2005, Althaus et al., 2009, Heifetz et al., 2009, Durán Muñoz et al., 2012, Roberts & Cairns, 2014). Several deep-water coral species create habitat for other invertebrates and fish (Krieger & Wing, 2002, Buhl-Mortensen & Mortensen, 2003, 2005, Metaxas & Davis, 2005, Du Preez & Tunnicliffe, 2011), are long-lived and slow growing (Sherwood et al., 2005a, Roark et al., 2006, 2009 Tracey et al., 2007, Sherwood & Edinger, 2009), although growth rates seem to be highly variable among individuals and taxa.

Growth rates have been estimated in several deep-water coral species, especially scleractinians, black corals, and octocorals including primnoids (family Primnoidae), precious corals (family Corallidae), and bamboo corals (family Isididae). Many of these taxa have skeletons where growth rings can be identified and used to determine longevity and growth rates, as an alternative to tagging and monitoring techniques that are challenging to apply in deep-water settings. Furthermore, using the skeleton to estimate growth allows drawing a more general picture of the whole life of the specimen, rather than estimating growth based on a few years of monitoring.

Additionally, the rigid skeletons of many deep-water coral species have been proved to be an important source of environmental information, making these animals proxies of environmental change (Sherwood et al., 2011, 2014, Aranha et al., 2014, Robinson et al., 2014). In this context, deep-water corals have been successfully used to

make inferences about past oceanographic conditions. However, although our knowledge on their potential as palaeoceanographic proxies and on their growth rates has improved in the past decade, there is still a paucity of information on the influences of environmental factors on these organisms' growth (Roberts et al., 2009).

Although relationships between deep-water coral growth rates and environmental factors have often been investigated in certain cold-water corals such as *Lophelia pertusa* (Linnaeus, 1758) (Orejas et al., 2008, Brooke & Young, 2009, Gass and Roberts, 2011), in octocoral taxa these studies are still sparse. Thresher (2009) found a negative correlation between growth rates and depth, and a positive correlation with water temperature in bamboo corals. Recently, Farmer et al. (2015) found no correlation between growth rates and temperature in the bamboo coral *Keratoisis* sp., and no statistically significant relationships between growth rates and 20 environmental variables tested (although trends were observed).

The octocorals *Primnoa pacifica* Kinoshita, 1907 and *Primnoa resedaeformis* (Gunnerus, 1763) have been the subject of several growth rates studies in the past years (Risk et al., 2002, Mortensen & Buhl-Mortensen, 2005, Sherwood et al., 2005a, Matsumoto, 2007, Sherwood & Edinger, 2009, Aranha et al., 2014). In both species growth rings are deposited annually and longevities can reach several hundred years (Risk et al., 2002, Sherwood et al., 2005a, 2006, Sherwood & Edinger, 2009). These studies have indicated that growth rates in *P. pacifica* from the Northeast (NE) Pacific are faster than in *P. resedaeformis* from the Northwest (NW) Atlantic, and temperature (Matsumoto, 2007), current strength (Sherwood & Edinger, 2009), and food availability (Aranha et al.,

2014) have all been suggested to influence growth rates in these species. However, none of these hypotheses have been fully investigated.

In this context, the objective of this study was to compare growth rates in *P. pacifica* and *P. resedaeformis* using published data and new data, and to investigate relationships between colony growth rates and environmental variables. We also took an opportunity to use video data collected using a remotely operated vehicle (ROV) to study the abundance and size-frequency distribution of *P. pacifica* colonies from two sites in the Strait of Georgia (British Columbia, Canada), from where colonies were also collected for the growth study.

6.2 Material and methods

6.2.1 Study area and sampling

A total of 15 colonies of *P. pacifica* were collected in 4-5 November 2011 at two sites in the Strait of Georgia: Coral Knoll and Sabine Channel (NE Pacific) (Figs. 6-1 and 6-2), which are ~23 km apart from each other. Colonies were sampled at depths ranging 224-270 m, using the ROV ROPOS aboard the Canadian Coast Guard Ship (CCGS) *Vector*. Once onboard, colonies were photographed, measured, and then frozen at -20 °C.

Data on an additional 13 colonies hosted at the National Museum of Natural History (NMNH, Smithsonian Institution) were incorporated in the study, including five colonies of *P. pacifica*, one colony of *Primnoa pacifica* var. *willeyi*, and seven colonies of *P. resedaeformis*. Data on latitude, longitude and depth were obtained from the Smithsonian database. One colony of *P. resedaeformis* from the Smithsonian collection

(USNM 12261) has been recorded from a depth of 3186 m, south of Georges Bank (NW Atlantic, Fig. 6-1). Although to our knowledge this is the deepest record of a *Primnoa* colony (usually found at depths < 1000 m; Cairns and Bayer, 2005), the geographic coordinates place this observation in a site where according to the General Bathymetric Chart of the Oceans (GEBCO) the depth is 3013 m. Furthermore, the calcite saturation depth at this region is >4500 m (Feely et al., 2004). Therefore we have no concrete reason to doubt the validity of this record.

Growth data on additional *P. pacifica* and most *P. resedaeformis* were obtained from the literature, and two *P. resedaeformis* colonies from the Labrador region (no specific coordinates or depth available) were also added to the dataset. Data from Matsumoto (2007) included diametric growth rates for eight colonies (ten growth estimates) of *P. pacifica* from Japanese waters. Growth rates per colony were only available in the form of a graph. For this reason we estimated stem diameter and age from figure 4 in the published manuscript using ImageJ to precisely scale the axes, and calculated diametric growth rates per colony afterwards. Our estimated minimum and maximum growth rates (0.19-0.37 mm·yr⁻¹) matched those reported by Matsumoto (2007). Therefore, we feel that using these estimates is reliable and better than only using the average rate.

In total, 95 growth rates records of *Primnoa* spp. (40 *P. pacifica* and 55 *P. resedaeformis*) were included in the study, from the following locations: Japan (N = 11), Alaska (N = 3), British Columbia: Dixon Entrance (N = 5), Chatam Sound (N = 1), Knight Inlet (N = 1), Coral Knoll (N = 7), and Sabine Channel (N = 8), Washington State, USA (Olympic Coast Marine Sanctuary, OCNMS, N = 4) in the Pacific, and East of

Hudson Strait (N = 15), Labrador (N = 2), Banquereau Bank (N = 1), The Gully (N = 1), Mount Desert Island (N = 1), Northeast Channel (N = 32), Georges Bank (N = 1), south of Georges Bank (N = 1), and Virginia Beach (N = 1) in the NW Atlantic (Fig. 6-1, Appendix 6-1).

6.2.2 Video analysis (Strait of Georgia): abundance and size structure

Video data recorded using the ROV ROPOS at the Coral Knoll and Sabine Channel sites were also analyzed in order to determine the size-frequency distribution of *P. pacifica* at these sites. Transects were video-recorded using a forward HD video camera (Insite Pacific Zeus) with the ROV flying at a speed of 0.5-1 knots at ~0.5-1 m from the bottom. Two green lasers 10 cm apart were projected for size estimation. At the Coral Knoll site (dive R1512) the transect had a zig-zag pattern and followed a length of ~3 km, at depths ranging between 160-440 m. At the Sabine Channel site (dive R1513) two nearly parallel transect lines (~0.6 and 0.4 km each) were followed, at depths ranging between 65-270 m. Surveyed area was calculated as the average width of the field of view from 25 random video frames at each site multiplied by transect length. Average surveyed area in the Coral Knoll was 15600 m², and 5100 m² in the Sabine Channel.

A snapshot from each video frame containing *P. pacifica* colonies (alive or dead) was produced using the software VLC. These snapshots were visualized in imageJ, and the projected green lasers (10 cm apart) seen in the video were used to estimate colony height and width. Colonies with tissue but laying on the floor were considered dead, and those mostly without tissue but standing were considered partially alive. Proportion of dead versus alive colonies was also determined.

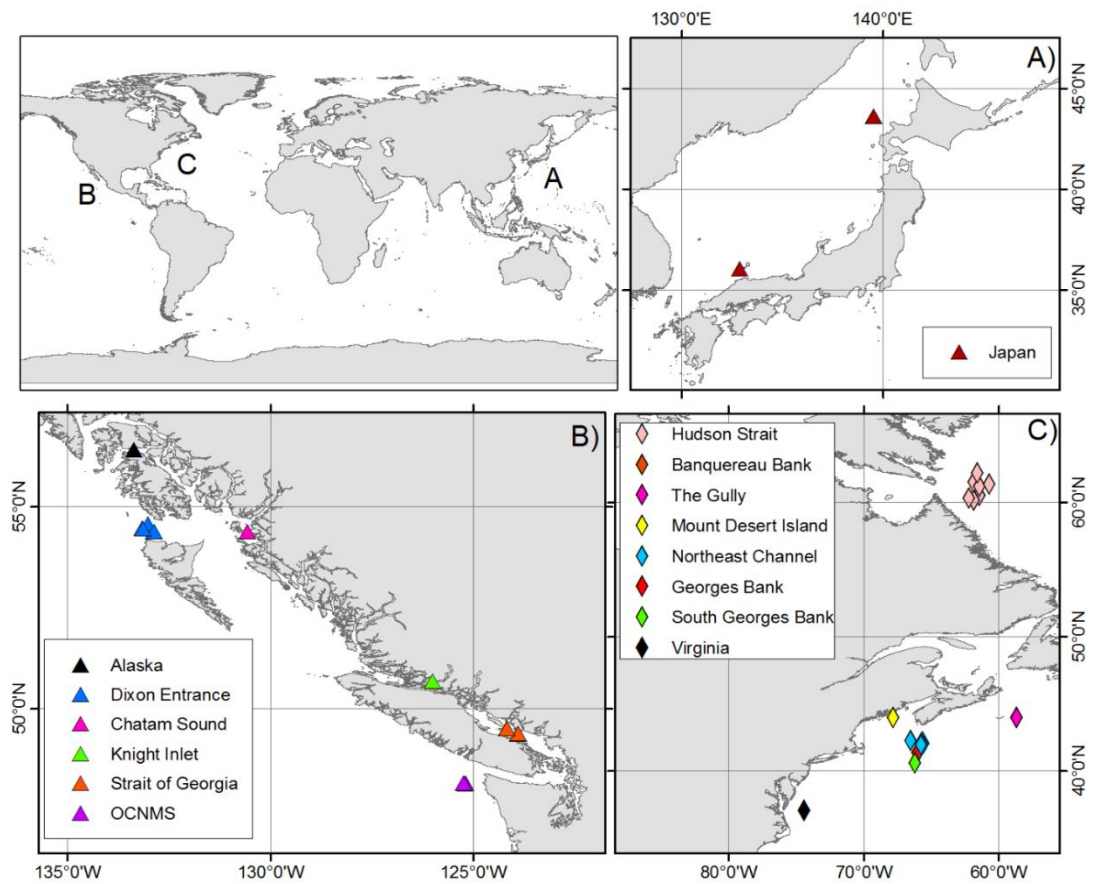


Figure 6-1. Map of sample locations for *Primnoa pacifica* and *P. resedaeformis* colonies included in this study.

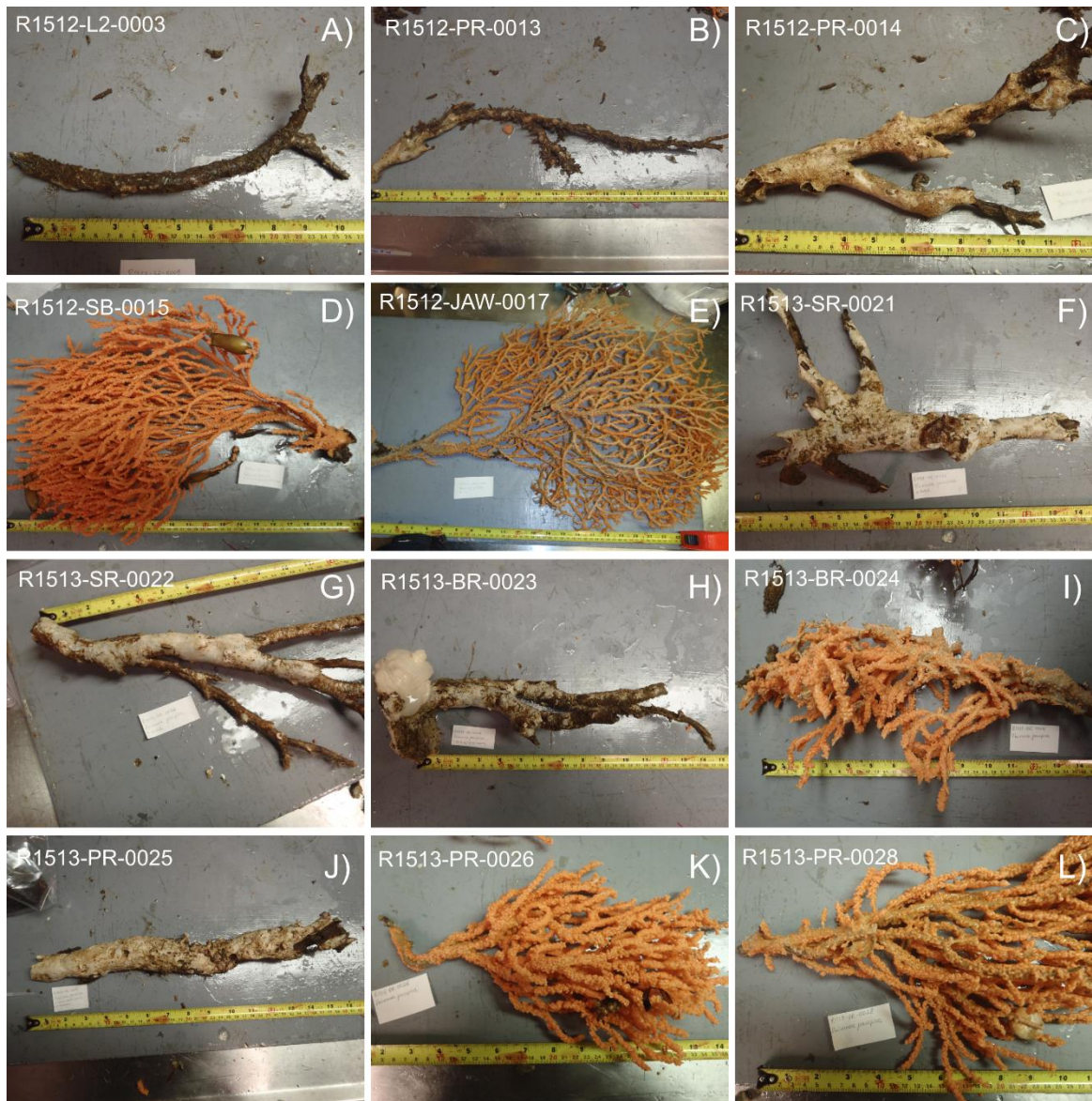


Figure 6-2. Colonies of *Primnoa pacifica* collected in 2011 at the Coral Knoll (A-E) and Sabine Channel (F-L) in the Strait of Georgia (NE Pacific) using the ROV ROPOS.

6.2.3 Growth rates and ^{14}C analysis

To estimate growth rates, the base of each colony was cross sectioned using a rock saw. These were polished using grinding paper (600/P1200 grit size) and photographed

under UV light in stereomicroscope. Age was estimated by counting rings from the photographs at three non-consecutive times and averaged. The software GIMP 2.8 was used to improve ring visibility, and ImageJ (Schneider et al., 2012) was used to measure axis radius and diameter.

Growth rates were estimated as radial and diametric rates by dividing the axis radius and diameter by the average number of rings. Because the stem of *Primnoa* is not perfectly circular, the largest radius and diameters were measured from the gorgonin portion of the stem. Cross sections that had an outer layer of calcite surrounding the gorgonin portion were not included in the estimates of radius and diameter. However, to avoid underestimating age in these colonies, we used the calculated growth rates based on the gorgonin to extrapolate total colony age when including the calcite portion (Sherwood et al., 2006, Aranha et al., 2014).

Among the published studies incorporated to our dataset there were cases where growth rates were estimated as radial rates, and cases where diametric growth rates were estimated instead. For the studies that have only provided radial rates, we extrapolated diametric rates by multiplying radial growth rates by two. However, we acknowledge that since the stem in these gorgonians is frequently asymmetric and not perfectly round in shape, this approach is subject to inaccuracies. Nevertheless, this inconsistency in terms of the metric chosen among these studies forced us to extrapolate. Because of the asymmetry of the axis, in this study we opted for reporting diametric rates, instead of radial rates.

Stem radius for samples from Aranha et al. (2014) were given as gorgonin band zone and as basal radius. When investigating relationships between stem diameter and age

we used their radius and age data based on the measurements including the calcite region and the extrapolated age. Diameter for this dataset was obtained by summing maximum and minimum basal radius.

Previous studies have already confirmed the annual nature of growth rings in both *P. pacifica* (Risk et al., 2002) and in *P. resedaeformis* (Sherwood et al., 2005a). We opted for performing ^{14}C analyses on dead specimens of *P. pacifica* from the Strait of Georgia region aiming to gain knowledge on *post-mortem* time on bottom. Live colonies were also analyzed for comparison. To this end, cross sections of the base of 11 colonies were embedded in 5% HCl until complete dissolution of the CaCO_3 . Gorgonin rings from the outer, middle, and inner regions of the axis were then peeled apart and isolated for the ^{14}C analysis (cf. Sherwood et al., 2005a).

^{14}C analyses were performed at two institutions: the Radiocarbon Dating Center at the Australian National University (ANU) and at the Center for Accelerator Mass Spectrometry at the Lawrence Livermore National Laboratory (LLNL), USA. In the case of samples analyzed at ANU, $\delta^{13}\text{C}$ values are the AMS machine quoted values, and were used to correct the age. In the case of samples analyzed at the LLNL, $\delta^{13}\text{C}$ values are the assumed values (-15‰) according to Stuiver and Polach (1977).

In both cases, the quoted age is in ^{14}C years using the Libby half-life of 5568 years and following the conventions of Stuiver and Polach (1977). Radiocarbon concentration is given as percent Modern Carbon and conventional radiocarbon age (both institutions), and in $\Delta^{14}\text{C}$ (LLNL). We calculated $\Delta^{14}\text{C}$ values for samples analyzed at the ANU using the equation:

$$\Delta^{14}\text{C} = \left(\left(\frac{\text{Percent Modern Carbon}}{100} \right) \times \left(\frac{\text{EXP}(1950 - \text{Calendar Year})}{8267} \right) - 1 \right) \times 1000$$

Calendar year was 2011 (year of collection) for all samples, including those dead-collected. We acknowledge that the resulting $\Delta^{14}\text{C}$ values for these dead-collected samples is therefore underestimated. Sample preparation backgrounds have been subtracted based on measurements of samples of ^{14}C -free CO_2 (coal for LLNL). For the samples from ANU, backgrounds were scaled relative to sample size based on coal as a background material.

A marine reservoir correction was applied to samples from colonies collected partially or entirely dead. We calculated the average reservoir age of the five points closest to the Strait of Georgia sampling sites, yielding an average reservoir age of 710 ± 91 ^{14}C years (McNeely et al., 2006) (Table 6-1). This average was subtracted from the ^{14}C ages, and converted to calendar years in the CALIB Radiocarbon Calibration Program 7.0.4 (<http://calib.qub.ac.uk/calib/>) using the IntCal13 calibration curve (Reimer et al., 2013).

6.2.4 Environmental data

Relationships between growth rates and environmental variables in the two *Primnoa* species were investigated. For the samples from the Strait of Georgia latitude, longitude and depth were obtained from the ROPOS Integrated Real-time Logging System (IRLS).

Table 6-1. Location and reservoir age used for ^{14}C calibration from McNeely et al. (2006) for samples collected in the Strait of Georgia (British Columbia, Canada).

Longitude	Latitude	Locality	DeltaR	Res. age	^{14}C age	Species
123.95'W	49.2' N	Departure Bay, BC	440 ± 50	800 ± 50	890 ± 50	<i>Macoma nasuta</i>
124'W	49.5' N	Georgia Strait, BC	510 ± 40	840 ± 40	960 ± 40	<i>Macoma</i> sp.
124.17'W	49.49'N	Comox, BC	380 ± 50	640 ± 50	860 ± 50	<i>Crepidula fornicata</i>
124.2'W	49.27'N	Nanoose Bay, BC	370 ± 50	630 ± 50	850 ± 50	<i>Mya arenaria</i>
123.7'W	48.92'N	Chemainus Bay, BC	380 ± 50	640 ± 50	860 ± 50	<i>Balanus</i> sp.
Average				710		

Certain samples from the Smithsonian collection did not have precise latitude and longitude, but had a specific indication of the sampling locality (e.g. Kupreanof Island, Alaska). However, samples with no latitude and longitude and a too-broad sampling location (e.g. Southeastern Alaska) were excluded from the environmental data analysis, and only kept for the overall comparison between growth rates in the two species. When depths were given as ranges, the mid-point of the reported ranges was used.

Average bottom temperature and dissolved oxygen for the available data between the years 1955-2012 (1 degree pixel resolution) were retrieved from the World Ocean Atlas 2013 (Locarnini et al., 2013, Garcia et al., 2014), using the data point closest to each *Primnoa* locality. Additionally, data on bottom temperature and salinity were obtained from the World Ocean Database (Boyer et al., 2013) and from the Ocean Data Inventory (Bedford Institute of Oceanography <http://www.bio.gc.ca/science/data-donnees/base/run-courir-en.php>) by averaging the ~10 closest data points to *Primnoa* samples. Dissolved oxygen for the SoG samples was obtained from the oxygen sensor on ROPOS CTD profiler (SBE 19plusV2).

Surface data on chlorophyll a and particulate organic carbon (POC) (as proxies for phytoplankton biomass) were downloaded from <http://oceancolor.gsfc.nasa.gov/> and extracted in ArcMap 10.1 using Marine Geospatial Ecology Tools (Roberts et al., 2010). Annual chlorophyll a and POC for the period of 2002-2014 were obtained from the Aqua Moderate Resolution Imaging Spectroradiometer Sensor (MODIS) L3 product database. The 9 km scale resolution was used, with cell sizes of 1/12 geographic degree at the Equator.

Annual averaged surface salinity for the years 1990-2010 were obtained from the Simple Ocean Data Assimilation (SODA) analysis database 2.2.4 (Carton and Giese, 2008). Data were downloaded from the National Center for Atmospheric Research website and extracted in ArcMap using Multidimension Tools. These data had a pixel resolution of 0.25° x 0.4°.

Finally, ocean surface velocity data (absolute magnification) were obtained from the Ocean Surface Currents Analyses (OSCAR) project. Data were directly imported and extracted in ArcMap using the NOAA OSCAR tool in the Marine Geospatial Ecology Tools extension. These data were used as an average of measurements taken every five days from 1992-2004, with a spatial resolution of 1/3 of a degree. Environmental data specifications are summarized in Table 6-2.

Not all environmental data were available from all sites from where colonies have been collected. As a result, only data on 81 colonies could be included in the analysis of growth rates in relation to environmental data.

Table 6-2. Specifications of environmental data used in this study

Environmental data	Source	Spatial resolution	Years
Bottom temperature (°C)	WOA	1°	1955-2012
Bottom temperature (°C)	WOD/BIO	10 closest points	1933-2014
Dissolved oxygen (ml.l ⁻¹)	WOA	1°	1955-2012
Bottom salinity (PSU)	WOD/BIO	10 closest points	1933-2014
Chlorophyll a (mg.m ⁻³)	Oceancolor	1/12°	2002-2014
POC (mg.m ⁻³)	Oceancolor	1/12°	2002-2014
Surface salinity (PSU)	SODA	0.25° x 0.4°	1990-2010
Surface velocity (m.s ⁻¹)	OSCAR	1/3°	1992-2004

WOA: World Ocean Atlas, WOD: World Ocean Database, BIO: Bedford Institute of Oceanography, SODA: Simple Ocean Data Assimilation, OSCAR: Ocean Surface Currents Analyses

6.2.5 Data analysis

Descriptive statistics (skewness and kurtosis) were used to study the size distribution of *P. pacifica* in the Strait of Georgia. If the skewness (g₁) and kurtosis (g₂) divided by their standard errors are ≥ 2 , it indicates the presence of a dominant size class in the population (c.f. Gori et al., 2011). Growth rates between the two *Primnoa* species were compared using a one-way analysis of covariance (ANCOVA) in order to account for depth as a co-variate (Kabacoff, 2015). Relationships between colony growth rates and environmental variables were investigated using general linear models (GLM) including all variables in the model plus interaction terms between depth and bottom variables (oxygen, salinity, and temperature).

The original model would have included the following predictor variables: depth, surface chlorophyll a, latitude, dissolved oxygen, current velocity, surface salinity, bottom salinity, bottom temperature, and the interactions oxygen: depth, salinity: depth, bottom temperature: depth, and bottom temperature: latitude. Because of the large number of

predictors, an “all subsets” regression analysis was performed in order to pre-select those that best fitted the model, with the adjusted R^2 used as a stopping rule (Kabacoff, 2015), not including the interactions. Furthermore, because of the interaction added to the model, the predictor variables were re-scaled by centering them (centering = each observation – mean), an approach suggested to be used when dealing with multiple regressions with interactions (Aiken & West, 1991, Quinn & Keough, 2002).

The proxies of primary productivity (chlorophyll a and POC) are highly correlated, and their inclusion in a single model could cause a problem of multicollinearity (Quinn & Keough, 2002). As a result, we used Akaike Information Criterion (AIC) values to select a single productivity variable among these (Kabacoff, 2015). Chlorophyll a was the variable showing the lowest AIC values, and therefore it was selected to represent productivity in the model.

The presence of influential observations was explored using Cook’s distance (D_i) influential plots, with $D_i > 1$ as the threshold to consider an observation as influential (Quinn & Keough, 2002, Kabacoff, 2015). All statistical analyses were performed in RStudio version 0.99.484, using the `Anova()` function in the *car* package (Type III sum of squares), and the package *leaps* in the all subsets regression analysis. Assumptions of homogeneity of variance, independence of residuals, and normality were assessed before running the analyses (Kabacoff, 2015). Error is given as standard deviation (SD).

6.3 Results

6.3.1 Video analysis (Strait of Georgia): abundance and size structure

A total of 109 colonies of *P. pacifica* (alive and dead) were observed during the video analysis, most of them at the Sabine Channel (N=96), with only 13 colonies being identified at the Coral Knoll site. From these, two colonies could not be measured at the Coral Knoll and 59 at the Sabine Channel, because either the scaling lasers were not close enough to the colonies or because the angle of the colony didn't allow for size determination. Based on the estimated surveyed area, density of *P. pacifica* at the two sites was 0.019 colonies·m⁻² (Sabine Channel), and 0.0008 colonies·m⁻² (Coral Knoll).

A high proportion of colonies were partially or completely dead, with several branches or the entire colony lacking tissue and polyps (Fig. 6-3). Partial or total mortality was identified in all the observed colonies in the Coral Knoll, and in 51% of the colonies in the Sabine Channel.

In the Coral Knoll, colony height and width ranged between 27-132 cm and 9-122 cm (N= 11), respectively. In the Sabine Channel, colony height and width ranged between 17.6-181 cm and 9-157 cm (N= 17, alive colonies only), respectively. Further descriptive statistics were only calculated for live colonies. Therefore colonies from the Coral Knoll were not included, as only dead or partially alive colonies were identified at this site. The descriptive statistics indicated that the size distribution of *P. pacifica* colonies in the Sabine Channel is positively skewed and dominated by colonies of small size (Fig. 6-4).

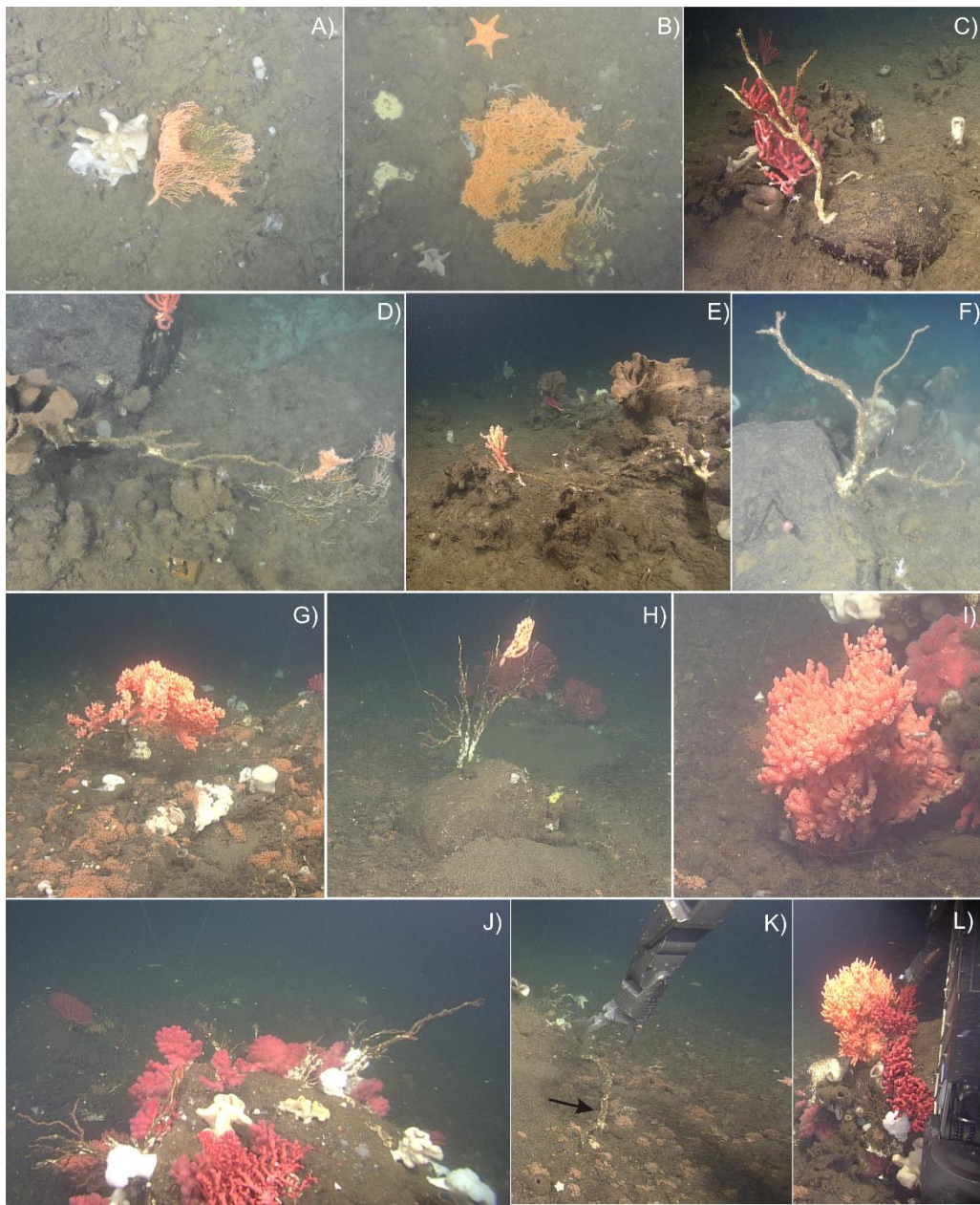


Figure 6-3. *In situ* colonies of *Primnoa pacifica* at the Coral Knoll (A-F) and Sabine Channel (G-L), Strait of Georgia, British Columbia (NE Pacific). High suspension of sediments can be noticed in several photos. Colonies of *Paragorgia arborea* (Linnaeus, 1758) are also seen (C-D, H-J, and L: dark red colonies).

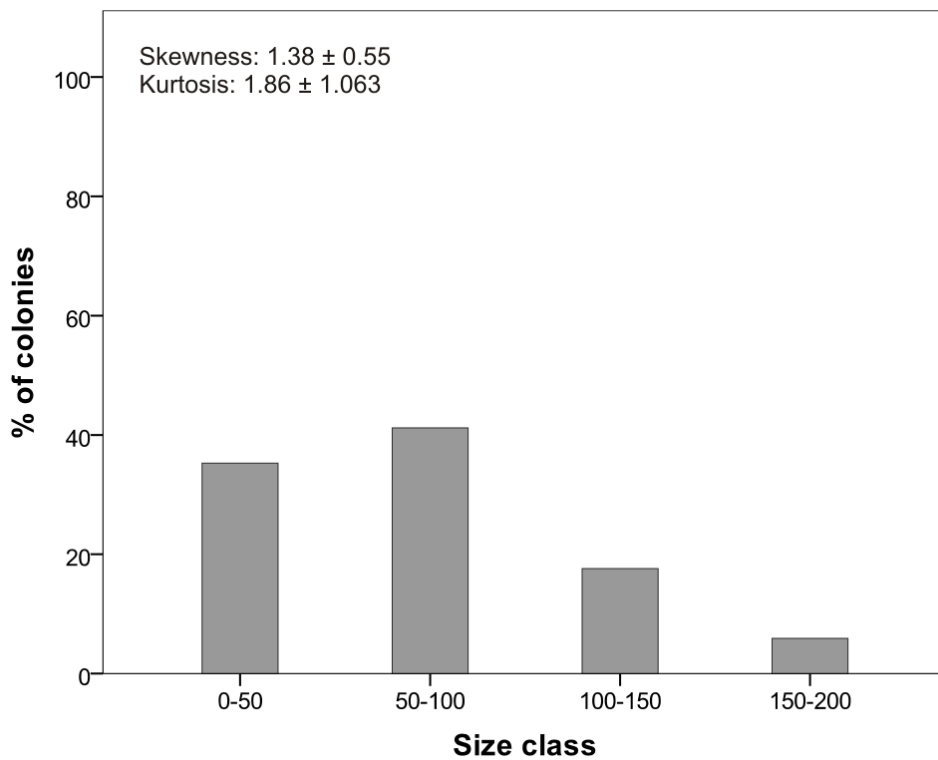


Figure 6-4. Size frequency distribution of *Primnoa pacifica* colonies (N=17) in the Sabine Channel (Strait of Georgia, NE Pacific).

6.3.2 ¹⁴C analysis

Most samples collected in the 2011 cruise (*P. pacifica*) were already dead or only partially alive at the time of sampling (Fig. 6-2). Samples had a mix of pre-bomb (before 1958) and post-bomb ¹⁴C values (Table 6-3). All dead-collected samples had only pre-bomb ¹⁴C values (although two samples only had one observation each) (Fig. 6-5). Samples collected alive had either observations with both pre- and post-bomb values or only post-bomb values (Fig. 6-5). Our ¹⁴C data could not be used to corroborate ring formation periodicity in *P. pacifica* for the region because colonies collected alive were

too young to have incorporated the peak in the ^{14}C concentration following atomic bomb tests.

The fact that all dead-collected samples had only pre-bomb values indicates that they had been dead on the bottom for at least 50 years, since they have been collected in 2011, with the post-bomb phase starting in 1958. Our interpretation is that the highest ^{14}C post-bomb values indicate that the associated portion of the skeleton was produced during the 1970s regional peak in ^{14}C , according to reference ^{14}C chronologies produced for the NE Pacific based on fish data (Kerr et al., 2004, Piner et al., 2005, Fig. 6-5). For instance, for sample R1512-PR-0013 to have its highest ^{14}C value match the regional bomb- ^{14}C reference curves (Kerr et al., 2004, Piner et al., 2005), its latest gorgonin would have growth in ~1960, and the core (oldest part of the sample) would have been laid down in ~1920 (Fig. 6-5). Therefore this sample should have been dead on the bottom for ~50 years, since collection occurred in 2011. Our estimations suggest that, for the analyzed samples, *post-mortem* time on the bottom ranged 40-81 years (Table 6-4).

Table 6-3. ^{14}C concentration and ages per sample of *Primnoa pacifica*, including ^{14}C reservoir corrected ages (^{14}C age – reservoir) and calibrated ages in calendar years.

Sample	Ring	Year*	CAMS #	Fraction modern	±	$\Delta^{14}\text{C}$	±	^{14}C age	±	^{14}C age reservoir corrected (710 years)	±	Notes	Calibrated age
LLNL													
R1512-L2-0003	1	-	167806	1.0184	0.0031	18.4	3.1	>Modern	na	na	na	dead	na
R1512-L2-0003	19	-	167807	0.9028	0.0027	-97.2	2.7	820	25	110	25	dead	1693-1919
R1512-L2-0003	39	-	167808	0.9044	0.0028	-95.6	2.8	805	25	95	25	dead	1696-1917
R1512-PR-0013	39	-	167809	0.9541	0.0029	-45.9	2.9	375	25	-335	25	dead	na
R1512-PR-0013	20	-	167810	0.9048	0.0027	-95.2	2.7	805	25	95	25	dead	1696-1917
R1512-PR-0013	5	-	167811	0.9024	0.0026	-97.6	2.6	825	25	115	25	dead	1691-1923
R1512-PR-0013	1	-	167812	0.8996	0.0027	-100.4	2.7	850	25	140	25	dead	1680-1938
R1512-0017-JAW	1	2011	167813	0.9860	0.0040	-14.0	4.0	115	35	-595	35	alive	na
R1512-0017-JAW	14	1997	167814	1.0169	0.0033	16.9	3.3	>Modern	na	na	na	alive	na
R1512-0017-JAW	25	1986	167815	0.9991	0.0030	-0.9	3.0	Modern	na	na	na	alive	na
R1513-BR-0024	2	1971	167816	1.0210	0.0031	21.0	3.1	>Modern	na	na	na	alive	na
R1513-BR-0024	15	1956	167817	1.0016	0.0030	1.6	3.0	>Modern	na	na	na	alive	na
R1513-BR-0024	29	1944	167818	0.9227	0.0028	-77.3	2.8	645	25	-65	25	dead	na
R1513-SR-0026 PC1	1	2011	167819	0.9928	0.0032	-7.2	3.2	Modern	na	na	na	alive	na
R1513-SR-0026 PC1	10	2001	167820	1.0052	0.0031	5.2	3.1	>Modern	na	na	na	alive	na
R1513-SR-0026 PC1	16-17	1995	167821	1.0032	0.0031	3.2	3.1	>Modern	na	na	na	alive	na
R1513-SR-0026 PC2	1	2011	167822	1.0136	0.0031	13.6	3.1	>Modern	na	na	na	alive	na

Sample	Ring	Year*	CAMS #	Fraction modern	±	Δ ¹⁴ C	±	¹⁴ C age	±	¹⁴ C age reservoir corrected (710 years)	±	Notes	Calibrated age
R1513-SR-0026 PC2	10	2001	167823	1.0076	0.0031	7.6	3.1	>Modern	na	na	na	alive	na
R1513-SR-0026 PC2	15	1996	167824	1.0108	0.0031	10.8	3.1	>Modern	na	na	na	alive	na
R1513-PR-0028	2	2009	167825	1.0048	0.0027	4.8	2.7	>Modern	na	na	na	alive	na
R1513-PR-0028	7	2004	167826	1.0001	0.0030	0.1	3.0	Modern	na	na	na	alive	na
R1513-PR-0028	14	1997	167827	1.0157	0.0031	15.7	3.1	>Modern	na	na	na	alive	na
R1513-SR-0033**	1	-	167828	0.9941	0.0030	-5.9	3.0	Modern	na	na	na	dead	na
R1513-SR-0033**	19	-	167829	1.0038	0.0030	3.8	3.0	>Modern	na	na	na	dead	na
R1513-SR-0033**	36	-	167830	0.9671	0.0033	-32.9	3.3	270	30	-440	30	dead	na
ANU lab													
R1512-0014-inner	15	-	30807	0.89303	0.0033	-113.5	0.3	910	30	200	30	dead	1658-1949
R1513-0021-inner	39	-	30806	0.88556	0.0071	-121.0	0.7	980	70	270	70	dead	1493-1949
R1513-0023-inner	16	-	30812	0.89869	0.0031	-107.9	0.3	860	30	150	30	dead	1670-1943
R1513-0023-middle	29	-	30813	0.89531	0.0029	-111.3	0.3	890	30	180	30	dead	1666-1949
R1513-0023-out	44	-	30814	0.93239	0.0029	-74.5	0.3	560	25	-150	25	dead	
R1513-0025-inner	2	-	30809	0.87544	0.0029	-131.0	0.3	1070	30	360	30	dead	1466-1624
R1513-0025-middle	50	-	30810	0.87547	0.0052	-131.0	0.5	1070	50	360	50	dead	1461-1630
R1513-0025-out	79	-	30811	0.88153	0.0030	-125.0	0.3	1015	30	305	30	dead	1521-1644

*Precise year for dead-collected samples unknown. *0022 in our database

Table 6-4. Estimation of time *post-mortem* on the bottom for colonies of *Primnoa pacifica* from the Strait of Georgia (NE Pacific). na = not applicable.

Sample id	Site	Status	Age*	Year of death**	Years on bottom
R1512-L2-0003	Coral Knoll	Dead	40	1971	40
R1512-PR-0013	Coral Knoll	Dead	30	1961	50
R1512-PR-0014	Coral Knoll	Dead	54	1951	60
R1512-JAW-0017	Coral Knoll	Alive	34	2011	na
R1513-SR-0021	Sabine Channel	Dead	69	1930	81
R1513-SR-0022/33	Sabine Channel	Dead	37	2011	na
R1513-BR-0023	Sabine Channel	Dead	85	1960	51
R1513-BR-0024	Sabine Channel	Dead (partially)	28	1971	40
R1513-PR-0025	Sabine Channel	Dead	78	1950	61
R1513-PR-0026	Sabine Channel	Alive	25	2011	na
R1513-PR-0028	Sabine Channel	Alive	23	2011	na

*Age determined from ring counting. **See text for explanation on year of death estimation for dead-collected samples.

Dead collected *P. pacifica* skeletons were already eroded and colonized by other organisms, including encrusting and other sessile organisms such as sponges, hydroids, sea anemones, polychaete tubes, and bryozoans (Fig. 6-6). One of the skeletons had foraminiferans between the more exposed gorgonin rings.

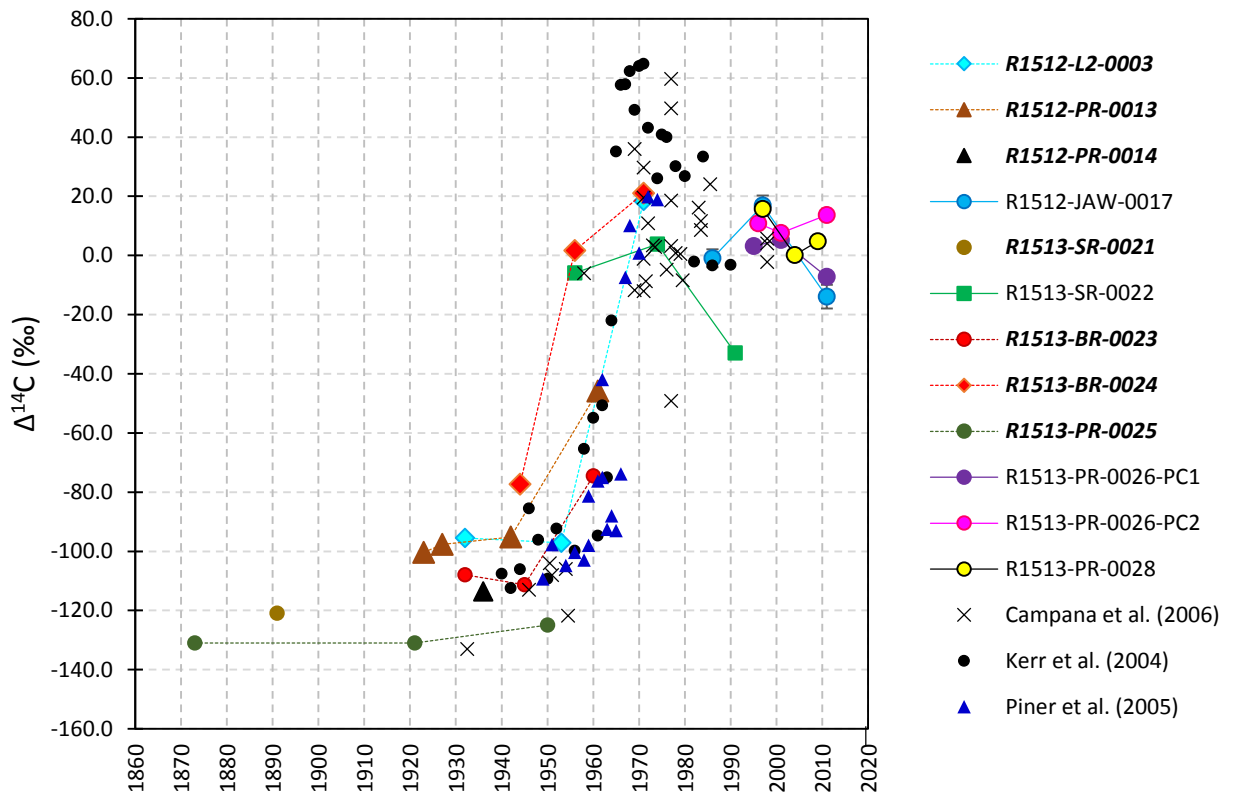


Figure 6-5. $\Delta^{14}\text{C}$ in relation to year (ring count) in colonies of *Primnoa pacifica* from the Strait of Georgia (NE Pacific), from otoliths of yelloweye rockfish from Southeast Alaska (Kerr et al., 2004), canary rockfish from the Oregon coast (Piner et al., 2005), and from dorsal spines of spiny dogfish from the NE Pacific (Campana et al., 2006). Sample identifications in bold as well as dashed lines in the figure represent dead-collected colonies. For these colonies, year of the outermost ring was estimated based on the expected year for the ^{14}C value associated to that ring. Sample R1513-BR-0024 was partially alive when sampled. PC1 and PC2 are different pieces of the same colony. Different symbols refer to different samples.

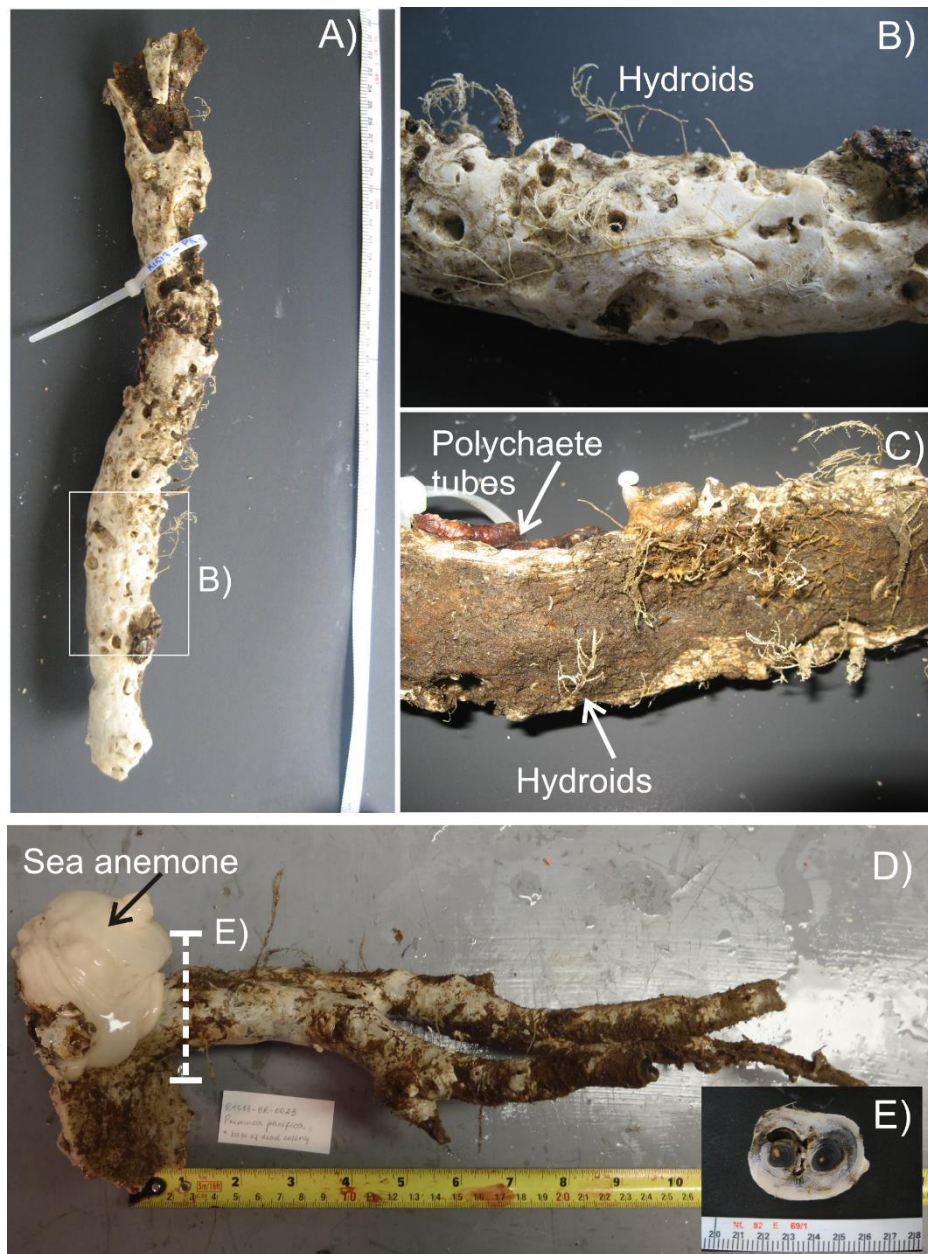


Figure 6-6. Skeletons of dead-collected *Primnoa pacifica* showing bioerosion in two colonies (A-C, and D-E). Skeleton shown in C is part of A (side not seen). Note cross section of D shown in E), with a hole containing the arm of a brittle star.

6.3.3 Colony metrics versus age relationships

The relationship colony height-age for *P. pacifica* could only be estimated for eight colonies (Fig. 6-7A). A very tall colony (~230 cm) from the Smithsonian collection (USNM 58084) was included in the plot, but its age is probably underestimated as ring counting for this sample was not taken from the thickest portion of the colony, which was very eroded. A logarithmic curve best described this relationship (Fig. 6-7A, $R^2 = 0.83$). In terms of *P. resedaeformis*, data on 46 colonies (4 newly estimated, 9 from Sherwood & Edinger, 2009, and 33 from Mortensen & Buhl-Mortensen, 2005) indicate that the relationship colony height-age for this species has a logarithmic shape (Fig. 6-7A, $R^2 = 0.64$).

For *P. pacifica* the relationship between stem diameter and colony age was better described than between colony height and age, as more observations on stem diameter were available than on colony height. In both species this relationship was better described (higher R^2) by a power model (similar to exponential) (Fig. 6-7B). This relationship was stronger for *P. pacifica* than for *P. resedaeformis* (Fig. 6-7B).

6.3.4 Growth rates

Growth rings were well visible, especially when observed under UV light or slightly wet (Fig. 6-8). Linear growth rates could only be estimated for nine *P. pacifica* and 47 *P. resedaeformis* colonies, due to unknown height of several specimens. Linear growth rates averaged $1.76 \pm 0.59 \text{ cm}\cdot\text{yr}^{-1}$ in *P. pacifica* (N=9), and $1.9 \pm 0.54 \text{ cm}\cdot\text{yr}^{-1}$ in *P. resedaeformis* (N=47).

The analysis of 15 specimens from the Strait of Georgia yielded an average diametric growth rate of $0.41 \pm 0.09 \text{ mm}\cdot\text{yr}^{-1}$ with a maximum mean age of 85 years for a dead-collected colony. The average growth rates for samples from the Coral Knoll was $0.41 \text{ mm}\cdot\text{yr}^{-1}$, and $0.40 \text{ mm}\cdot\text{yr}^{-1}$ for the Sabine Channel. When adding data from the literature and the NMNH specimens, the average diametric growth rate for *P. pacifica* was $0.45 \pm 0.21 \text{ mm}\cdot\text{yr}^{-1}$ (N=40). In contrast, the analysis of published data and NMNH specimens of *P. resedaeformis* showed a slower average diametric growth rate of $0.42 \pm 0.017 \text{ mm}\cdot\text{yr}^{-1}$ (N=58).

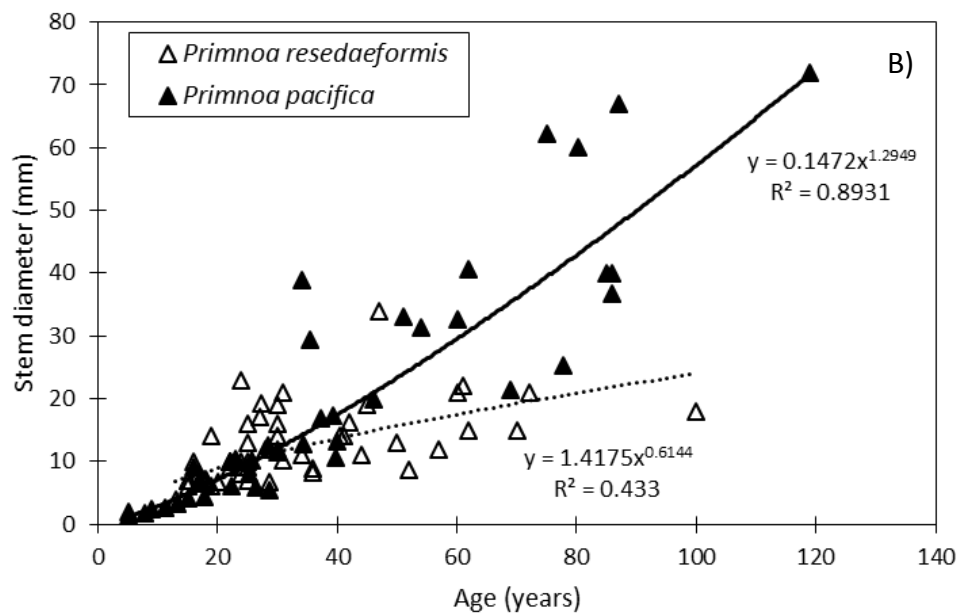
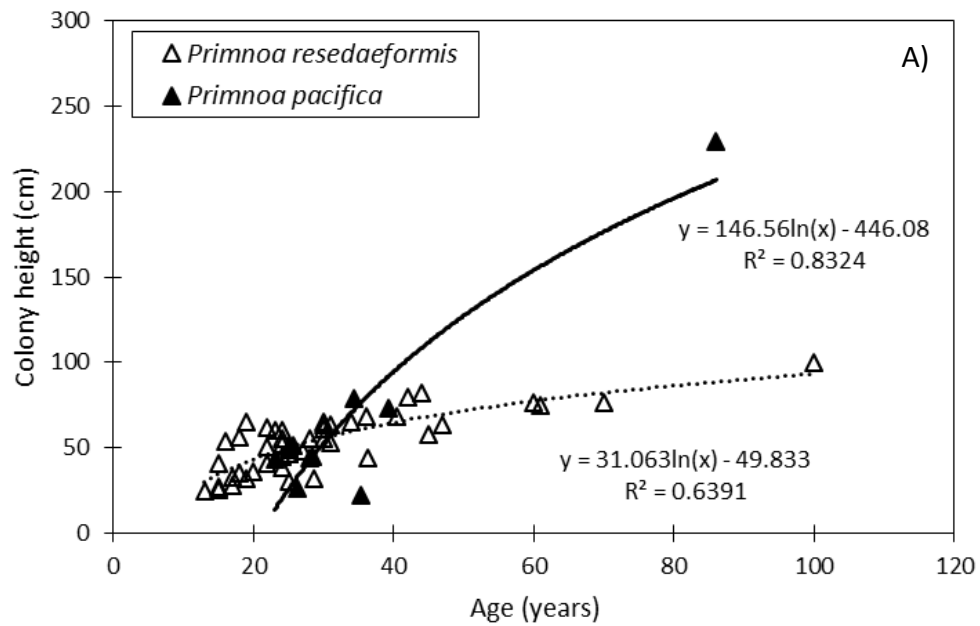


Figure 6-7. Relationship between A) colony height versus colony age, and B) stem diameter versus colony age in *Primnoa pacifica* and *Primnoa resedaeformis*.

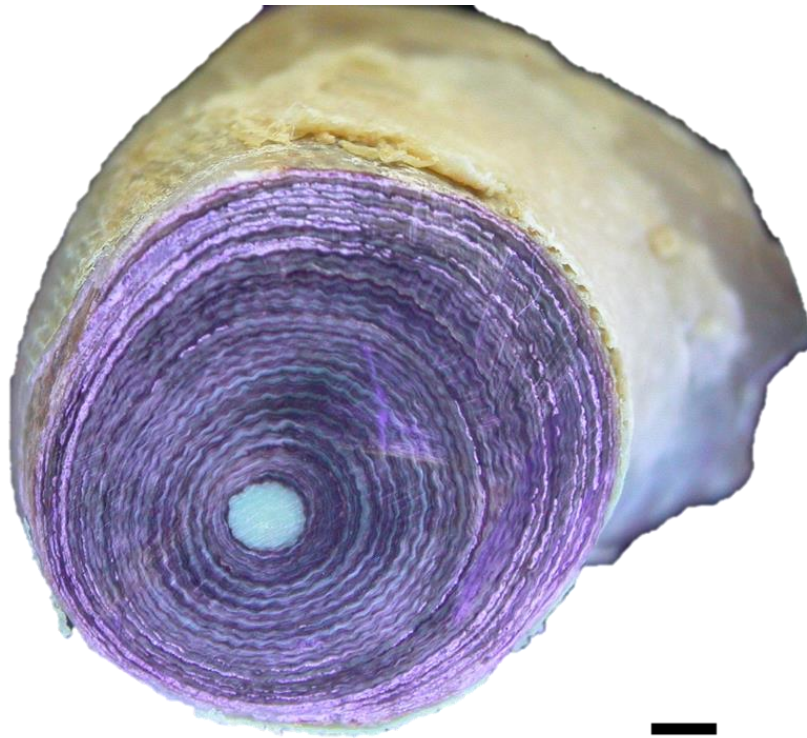


Figure 6-8. Cross section of the base of *Primnoa pacifica* under UV light where alternating bands of calcite (pale) and gorgonin (dark) rings, as well as the calcite core can be identified. Sample 12261 USNM. Scale bar = 1 mm.

Although average diametric growth rates in *P. pacifica* were slightly higher than in *P. resedaeformis*, they were not statistically different ($F = 0.56$, $p=0.46$, $N = 91$), after controlling for depth, which was significant ($F=10.55$, $p<0.05$, $df = N = 91$). The *P. resedaeformis* record from the site at 3186 m was removed from this analysis, as it was identified as an influential observation ($D_i > 1$) with an important impact in the analysis. However, diametric growth rates for this colony averaged $0.31 \text{ mm}\cdot\text{yr}^{-1}$, being comparable to growth rates from other locations. We acknowledge that despite controlling for depth, the different locations from where samples were collected could not be

controlled. Location was therefore only distinguished in terms of Pacific versus Atlantic (or species).

Furthermore, colony size could not be controlled, as this information was not available for several samples, particularly the ones dead-collected and the ones from the NMNH. When looking at each specific location it can be seen that the slowest growth rates were from a colony from Japanese waters ($0.19 \text{ mm}\cdot\text{yr}^{-1}$), and the fastest growth rates were from a colony from Dixon Entrance ($1.16 \text{ mm}\cdot\text{yr}^{-1}$), although in average they grew faster at the OCNMS area (Fig. 6-9).

6.3.5 Growth rates versus environmental variables

Because growth rates between the two species were not significantly different, we pooled the data for the environmental analyses. The “all subsets” regression analysis indicated that the best model should retain as predictor variables: chlorophyll a, dissolved oxygen, depth, and latitude. The interaction oxygen-depth was also included in the final model. This interaction was statistically significant (Table 6-5), and therefore the relationship between diametric growth rates and oxygen concentration varies with depth, and cannot be interpreted separately. There were statistically significant relationships between growth rates and chlorophyll a and depth, but not between growth rates and latitude (Table 6-5, Fig. 6-10).

In terms of the variables not included in the GLM analysis, there was a positive trend between diametric growth rates and bottom temperature data from the World Ocean Database and from the World Ocean Atlas (Fig. 6-11). Although there was no clear trend between growth rates and bottom salinity, growth rates decreased with increased surface

salinity (Fig. 6-11). Particulate organic carbon showed the same patterns as chlorophyll a (highly correlated variables), and there was a negative trend on the relationship between growth rates and surface current velocity (Fig. 6-11).

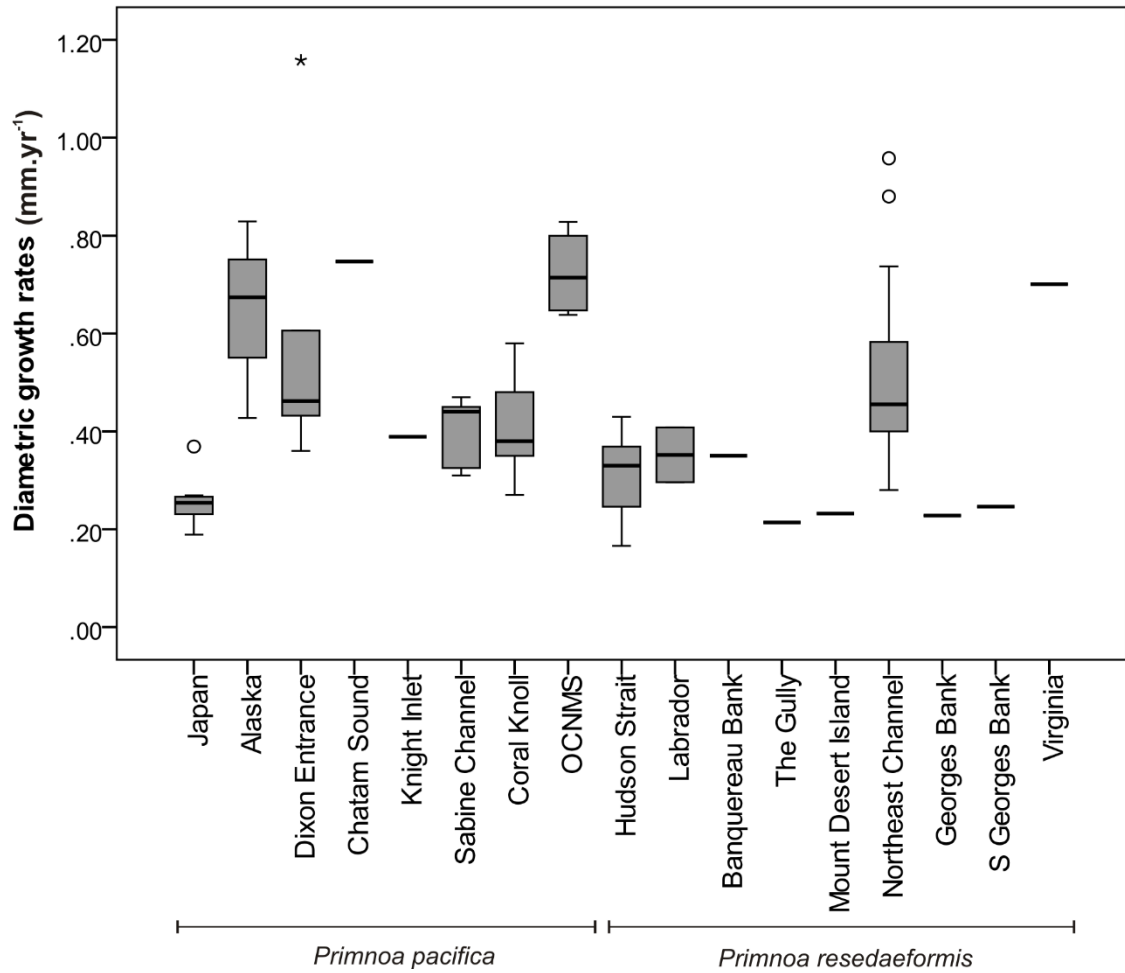


Figure 6-9. Growth rates in *Primnoa pacifica* and *Primnoa resedaeformis* by location.

Black horizontal bars inside the boxes represent the median, boxes are limited by minimum and maximum values, circles are outliers, and stars are extreme values.

Table 6-5. Results from the statistical analysis on diametric growth rates in *Primnoa* spp. in relation to environmental variables.

Variable	Df	F-value	p-value
Chlorophyll a	1,76	33.2	1.69e-7
Oxygen	1,76	54.6	1.61e-10
Depth	1,76	6.12	0.02
Latitude	1,76	0.79	0.38
<i>Interaction</i>			
Oxygen: depth	1,76	7.43	0.008

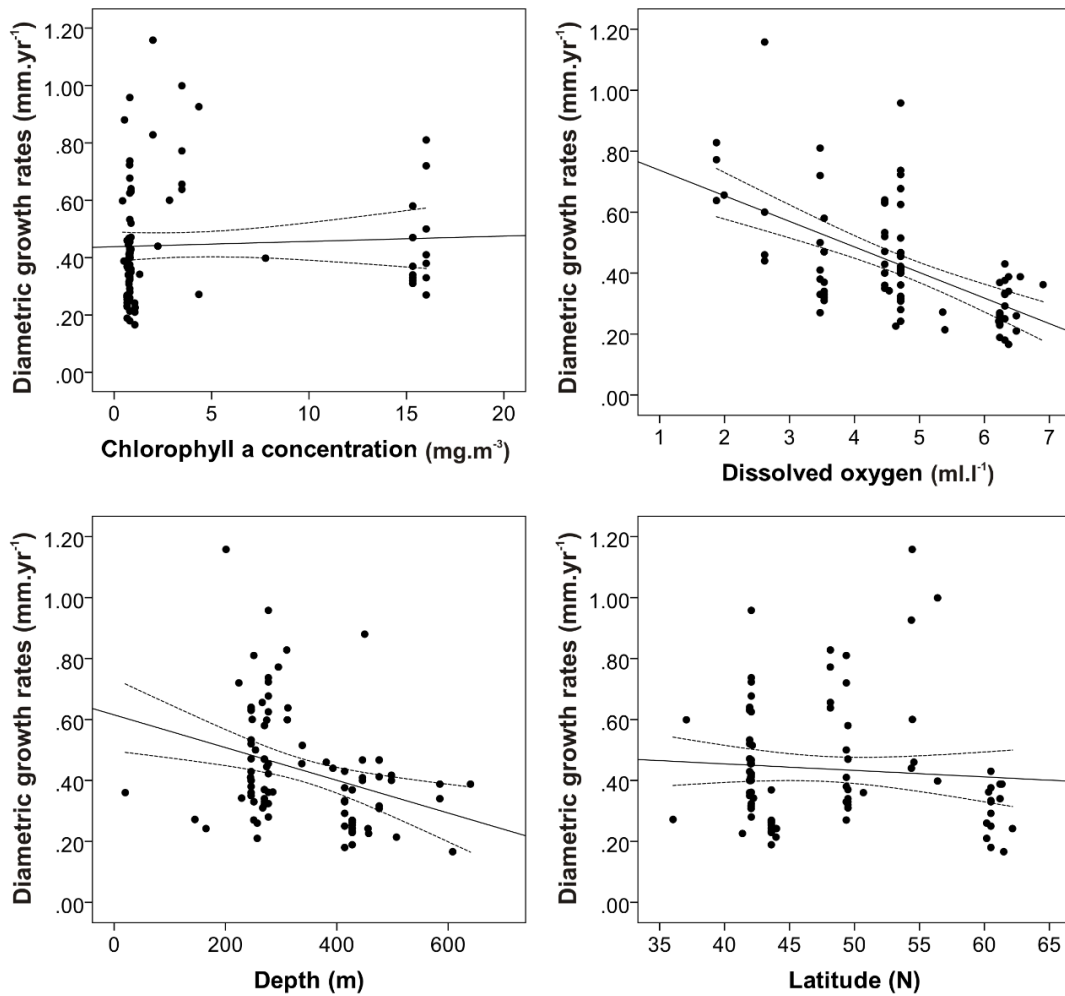


Figure 6-10. Diametric growth rates in *Primnoa pacifica* and *P. resedaeformis* in relation to chlorophyll a, dissolved oxygen, depth, and latitude.

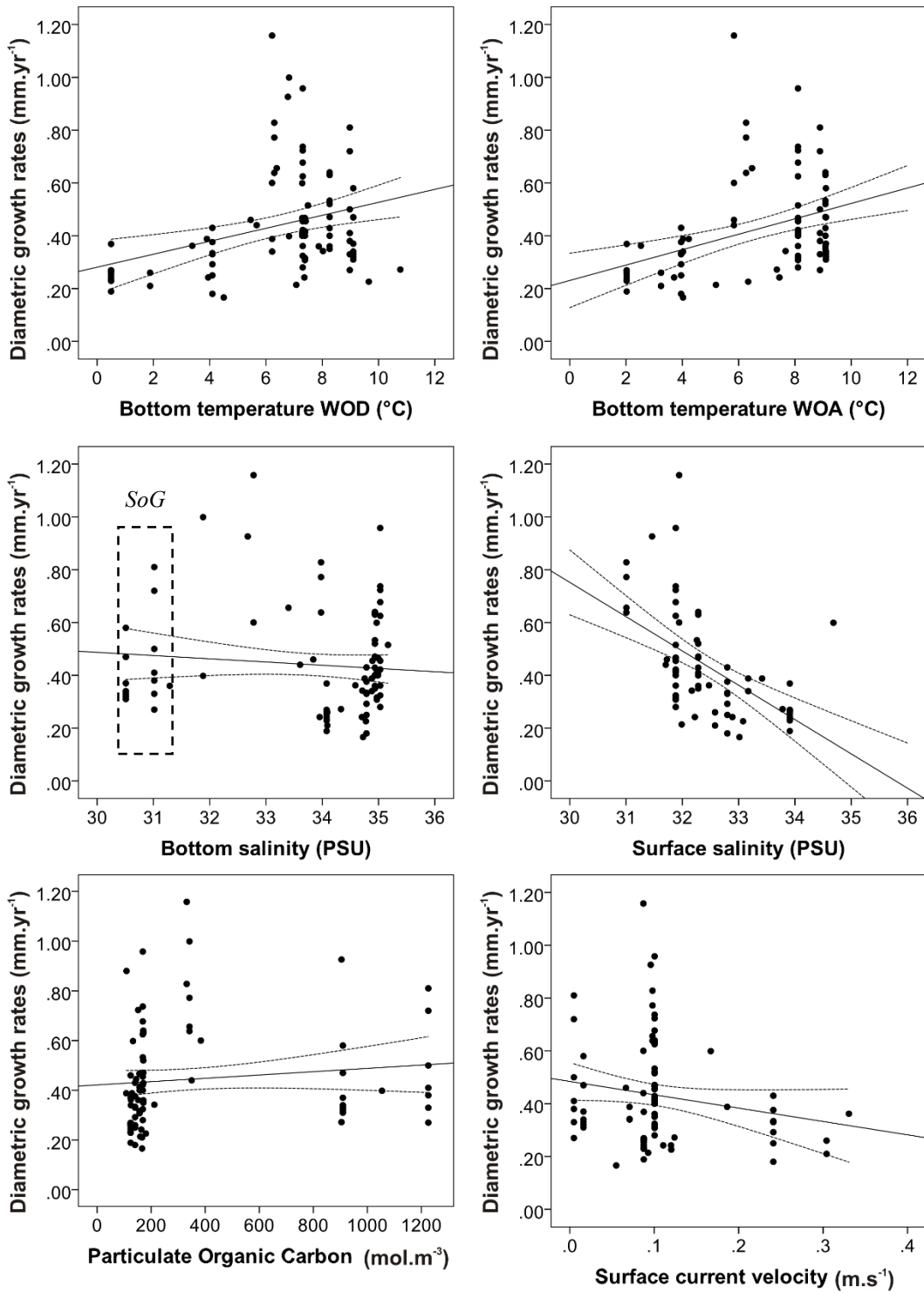


Figure 6-11. Diametric growth rates in *Primnoa* spp. in relation to environmental variables not included in the GLM model: bottom temperature (world ocean database – WOD, and world ocean atlas - WOA), bottom salinity, surface salinity from the SODA database (not available for the Strait of Georgia – SoG site), particulate organic carbon (POC), and surface current velocity. Figure in previous page.

6.4 Discussion

6.4.1 Video analysis (Strait of Georgia): abundance and size structure

The density of *P. pacifica* colonies in the two studied sites in the Strait of Georgia ranged 0.0008-0.02 colonies·m⁻². As an overall observation from the video analysis, colonies of the gorgonian *Paragorgia arborea* were much more abundant at both sites (data not shown). These two genera are often reported to co-occur, but their proportions vary among sites. At Dixon Entrance (British Columbia), Neves et al. (2014) reported a biotope called “*Primnoa*”, which consisted of aggregations of gorgonians, mainly *P. pacifica*, with sparse colonies of *P. arborea* in densities ≥ 0.5 colonies·m⁻². In the Northeast Channel (off Nova Scotia, NW Atlantic), colonies of *P. resedaeformis* had higher densities than *P. arborea* (Watanabe et al., 2009). Densities of *P. resedaeformis* reported by these authors (0.13 colonies·m⁻²) were much higher than the maximum densities calculated in this study (0.02 colonies·m⁻²). But in terms of size, our maximum size of *P. pacifica* was 181 cm, which is similar to that reported by Watanabe et al. (2009) for *P. resedaeformis* in the Atlantic.

The fact that most colonies of *P. pacifica* observed during the video analysis were dead or partially dead indicates that these colonies were under some form of pressure. Fishing gear was found during the video surveys, and several colonies were seen turned on the floor still with tissue, or entangled in fishing gear. Physical contact with fishing gear could be an important cause of the high mortality seen at these sites, although other causes cannot be excluded at the moment. Mortality was also observed in colonies of *P. arborea*, but not yet quantified.

The descriptive statistics indicated that the population of *P. pacifica* in the Sabine Channel is dominated by colonies of small size, which can be related to the high mortality observed (i.e. the oldest colonies are no longer present). Nevertheless, the largest colony observed from the video analysis was 181 cm in length, which should be ~100 years old based on linear growth rates of $1.8 \text{ cm}\cdot\text{yr}^{-1}$ estimated for *P. pacifica* in the Sabine Channel. Colonies of *P. pacifica* and *P. resedaeformis* are known to reach longevities at the scale of centuries (e.g. Risk et al., 2002, Sherwood & Edinger, 2009), so our extrapolated age is in the known range for the species.

6.4.2 ^{14}C data

The results on the ^{14}C analysis on the live-collected samples from the Strait of Georgia region could not be used to corroborate the annual nature of rings in *P. pacifica* because live-collected samples were too young to have incorporated the peak in ^{14}C . The ^{14}C analysis on dead-collected samples could not confirm ring formation periodicity because the actual date of colony death was unknown.

Rather, the results from the ^{14}C analysis of dead-collected colonies allowed us to make inferences in terms of *post-mortem* time laying on the bottom prior to sampling. Other studies have indicated a high resilience of *Primnoa* spp. skeletons. Sherwood et al. (2006) indicated that *P. resedaeformis* gorgonin might suffer little or no diagenesis over long periods of time (e.g. > 1000 years). Similarly, there was no skeletal degradation in *P. resedaeformis* calcite over a period of 14 months under experimental conditions (Edinger and Sherwood, 2012). Furthermore, using ^{14}C data Aranha et al. (2014) showed that dead-collected colonies of *P. pacifica* had remained dead on the bottom for at least 50 years before being collected. In this context, our interpretations of colonies of *P. pacifica* laying on the bottom for ~55 years in average seems supported by these other studies.

6.4.3 Colony metrics versus age relationships

The relationship between colony height and age in both species had a logarithmic shape, as already reported by Mortensen & Buhl-Mortensen (2005) in their study on *P. resedaeformis*. On the other hand, the relationship between stem diameter and colony age was not logarithmic, as also remarked by these authors. Aranha et al. (2014) indicated that the relationship between axis radius and colony age had a logarithmic pattern. However, they based the curves on individual locations with a small number of observations. By looking at a more general pattern of all locations and species pooled together we found that a power curve best described this relationship (higher R^2).

As the colony grows in height, more strength at the base is required in order to support the colony. In this sense, an asymptote will be reached in the relationship colony

height-age (time), while the stem should grow at a faster rate as the colony increases in height.

6.4.4 Growth rates

P. pacifica and *P. resedaeformis* are very similar in morphology, reaching similar sizes, with similar colors and overall appearance. The basic taxonomic distinction between the two species is the presence/absence of a spine in the basal sclerites (scales) from the polyp area (Cairns & Bayer, 2005). In terms of reproduction, the two species seem to have similar characteristics such as gonochorism and broadcast spawning (Mercier & Hamel, 2011, Waller et al., 2014). These species also have similar feeding habits as they both feed on fresh phytodetritus and microzooplankton (Sherwood et al., 2005b, 2008).

Our analysis of diametric growth rates from almost 100 observations showed that contrary to what has been suggested in previous studies, the faster growth rates identified in colonies of *P. pacifica* are not statistically higher than those found in *P. resedaeformis*. Growth rates in colonies of the same species was shown to be very variable. In *P. pacifica* average diametric growth rates ranged from 0.19 mm·yr⁻¹ in Japan to 1.2 mm·yr⁻¹ in Dixon Entrance. High variability in growth rates in a same species has been suggested by other authors to indicate that intrinsic factors might be more important into controlling growth rates than environmental factors (Farmer et al., 2015).

In terms of the influence of environmental factors on colony growth rates, our GLM analyses showed that these relationships were significant for chlorophyll a and depth, but not for latitude. The relationships between growth rates and oxygen varies with

depth (significant interaction), and cannot be interpreted separately. Roberts et al. (2009) highlights that it is not depth itself (hydrostatic pressure) that influences the distribution of cold-water corals, but rather the changes in temperature associated with changes in depth. In the growth context, it is possible that oxygen changes associated to depth do have an influence on growth, since the relationship between growth and bottom temperature was not statistically significant (although there was a positive trend).

Temperature has been suggested to influence growth rates in *P. pacifica* (Matsumoto, 2007). However, colonies from Japan had slow diametric growth rates and had the lowest temperature ranges (average 0.5 °C, compared to 7 °C from the NE Pacific), and those were still similar to some of the rates estimated for Atlantic *Primnoa* colonies (see fig. 6-9). This seems to indicate that the very low temperatures of these Japanese waters were not the cause of the growth rates seen in the Japanese *Primnoa*. Colonies of *Primnoella scotiae* Thomson & Ritchie, 1906 (also a primnoid coral) from Antarctica had average diametric growth rates of 0.053 mm·yr⁻¹ (Peck & Brockington, 2013) which are extremely slow compared to the average 0.24 mm·yr⁻¹ of *P. pacifica* from Japan (Matsumoto, 2007). Peck & Brockington (2013) suggested that these very slow growth rates in *P. scotiae*, like in other invertebrates (Peck, 2016), are probably related to the sub-zero temperatures common throughout the year in Antarctica. In this sense, as indicated by Matsumoto (2007), there might be a temperature threshold that will influence growth rates in these corals. However, based on the available growth rates and temperature data analyzed so far, this threshold has not yet been identified for *Primnoa* colonies.

The significant positive relationship between growth rates and chlorophyll a might show the link between surface particles, feeding, and growth. As mentioned before, the diet of *Primnoa* spp. includes particulate organic matter from the surface, which strengthens the plausibility of the relationship between surface chlorophyll a and growth in these benthic organisms. When examining the plot on this relationship, a clear pattern is not readily identified. That is because of a cluster of samples from the Strait of Georgia region, where chlorophyll a is very high, but growth rates are not extraordinary. If these values are excluded from the plot, the relationship becomes clearer. Productivity is the ultimate environmental factor suggested by Aranha et al. (2014) to influence growth rates in these octocorals, rather than temperature and currents alone. Our data corroborates the hypothesis of a relationship between colony growth rates and productivity in the studied colonies of *Primnoa*.

Current strength has also been suggested to influence growth rates in deep-water corals, by providing access to food. Primnoids in the coasts of North America have their distribution associated with strong currents (Bryan & Metaxas, 2006). However, the relationship between growth rates and surface current velocity was not statistically significant, with at best a weak negative trend. Obviously, a minimum bottom current strength is necessary in order to provide food to these sessile organisms, but surface velocity does not seem to have a direct influence in these corals' growth.

The relationship between growth rates and bottom salinity also was not significant, with a very weak negative trend being observed. However, when examining surface salinity, a much more clear negative trend could be identified, probably because no surface salinity data was available for samples from the Strait of Georgia area

(influenced by the large Fraser River), where bottom salinity was the lowest of all surveyed sites. Salinity is an important variable influencing the distribution of cold-water octocorals (Yesson et al., 2012, Greathead et al., 2014). Most coral observations had bottom salinity values between 34.5 and 35 PSU, which is the usual salinity range for cold-water octocorals (Yesson et al., 2012).

Farmer et al. (2015) also found a trend of growth rates decreasing with depth, salinity and bottom current speed in *Keratoisis* sp., although none of the relationships were statistically significant. These authors have indicated that biological factors might be more important than environmental variables in the growth control in *Keratoisis* spp. Based on our results, environmental factors do influence growth rates in *Primnoa* spp., although in some cases only trends could be identified.

Several complications could have reduced the power of our analyses. First, we note the inconsistency of publications regarding radial and diametric growth rates, as we extrapolated diametric growth to include all published observations. For future studies on coral growth rates, we recommend authors to provide both estimates, to make them available for comparison. Additionally, an indication of how radius and diameter were measured (e.g. longest vs. shortest) is also an important information to accompany these data. Secondly, growth rates have been estimated by different teams, mainly using the ring counting technique, which is not free of errors. Finally, in many cases specimens might be older than the environmental data available, which therefore will not encompass the full life span of those specimens.

Acknowledgements

We thank CCGS *Vector* captain and crew, chief scientist Dr. Sally Leys, Vincent Lecours, Jackson Chu, and the ROPOS team Keith Tamburri, Josh Chernov, and Ray Morgan for the assistance in the field. We also thank Dr. Stephen Cairns and Tim Coffer (National Museum of Natural History, Smithsonian Institution) for the access to the invertebrate collection, loan and use of the NMNH specimens. Brian Loveridge (CREAIT, Memorial University of Newfoundland) for the access to the rock saw and Dr. Graham Layne and Glenn Piercey (CREAIT) for the low speed saw. We also thank Stewart Fallon (Australian National University) and Tom Guilderson (Lawrence Livermore National Laboratory) for the radiocarbon analyses. This study was funded by the Natural Sciences and Engineering Research Council (NSERC) (doctoral scholarship to BMN), Canadian Healthy Oceans Network (CHONe) and NSERC ship time to EE and SL.

6.6 References

- Aiken, L. S. & S. G. West, 1991. Multiple regression: testing and interpreting interactions. SAGE Publications, Newbury Park, California.
- Althaus, F., A. Williams, T. A. Schlacher, R. J. Kloser, M. A. Green, B. A. Barker, N. J. Bax, P. Brodie & SchlacherHoenlinger M. A., 2009. Impacts of bottom trawling on deep-coral ecosystems of seamounts are long-lasting. *Marine Ecology Progress Series* 397: 279-294.
- Aranha, R., E. Edinger, G. Layne & G. Piercey, 2014. Growth rate variation and potential paleoceanographic proxies in *Primnoa pacifica*: Insights from high-resolution trace element microanalysis. *Deep Sea Research Part II: Topical Studies in Oceanography* 99: 213-226.
- Boyer, T. P., J. I. Antonov, O. K. Baranova, C. Coleman, H. E. Garcia, A. Grodsky, D. R. Johnson, R. A. Locarnini, A. V. Mishonov, T. D. O'Brien, C. R. Paver, J. R. Reagan, D. Seidov, I. V. Smolyar & M. M. Zweng, 2013. World Ocean Database 2013, NOAA Atlas NESDIS 72, Silver Spring, MD.
- Brooke, S. & C. Young, 2009. In situ measurement of survival and growth of *Lophelia pertusa* in the northern Gulf of Mexico. *Marine Ecology Progress Series* 397: 153-161.
- Bryan, T. L. & A. Metaxas, 2006. Distribution of deep-water corals along the North American continental margins: Relationships with environmental factors. *Deep Sea Research Part I: Oceanographic Research Papers* 53: 1865-1879.

Buhl-Mortensen, L. & P. B. Mortensen, 2003. Crustaceans associated with the deep-water gorgonian corals *Paragorgia arborea* (L., 1758) and *Primnoa resedaeformis* (Gunn., 1763). *Journal of Natural History* 38: 1233-1247.

Buhl-Mortensen, L. & P. Mortensen, 2005. Distribution and diversity of species associated with deep-sea gorgonian corals off Atlantic Canada. In Freiwald, A. & J. M. Roberts (eds), . Springer Berlin Heidelberg: 849-879.

Cairns, S. D. & F. M. Bayer, 2005. A review of the genus *Primnoa* (Octocorallia: Gorgonacea: Primnoidae), with the description of two new species. *Bulletin of Marine Science* 77: 225-256.

Campana, S. E., C. Jones, G. A. McFarlane & S. Myklevoll, 2006. Bomb dating and age validation using the spines of spiny dogfish (*Squalus acanthias*). *Environmental Biology of Fishes* 77: 327-336.

Carton, J. A. & B. S. Giese, 2008. A reanalysis of ocean climate using Simple Ocean Data Assimilation (SODA). *Monthly Weather Review* 136: 2999-3017.

Du Preez, C. & V. Tunnicliffe, 2011. Shortspine thornyhead and rockfish (Scorpaenidae) distribution in response to substratum, biogenic structures and trawling. *Mar Ecol Prog Ser* 425: 217-231.

Durán Muñoz, P., M. Sayago-Gil, T. Patrocinio, M. González-Porto, F. J. Murillo, M. Sacau, E. González, G. Fernández & A. Gago, 2012. Distribution patterns of deep-sea fish and benthic invertebrates from trawlable grounds of the Hatton Bank, north-east Atlantic: effects of deep-sea bottom trawling. *Journal of the Marine Biological Association of the United Kingdom* 92: 1509-1524.

Edinger, E. N. & O. A. Sherwood, 2012. Applied taphonomy of gorgonian and antipatharian corals in Atlantic Canada: experimental decay rates, field observations, and implications for assessing fisheries damage to deep-sea coral habitats. *Neues Jahrbuch für Geologie und Paläontologie-Abhandlungen* 265: 199-218.

Farmer, J. R., L. F. Robinson & B. Hönisch, 2015. Growth rate determinations from radiocarbon in bamboo corals (genus *Keratoisis*). *Deep Sea Research Part I: Oceanographic Research Papers* 105: 26-40.

Feely, R. A., C. L. Sabine, K. Lee, W. Berelson, J. Kleypas, V. J. Fabry & F. J. Millero, 2004. Impact of anthropogenic CO₂ on the CaCO₃ system in the oceans. *Science* 305: 362-366.

Garcia, H. E., R. A. Locarnini, T. P. Boyer, J. I. Antonov, O. K. Baranova, M. M. Zweng, J. R. Reagan & D. R. Johnson, 2014. *World Ocean Atlas 2013, Volume 3: Dissolved Oxygen, Apparent Oxygen Utilization, and Oxygen Saturation*. S. Levitus, Ed., A. Mishonov Technical Ed.; NOAA Atlas NESDIS 75, 27 pp.

Gass, S. E. & J. M. Roberts, 2011. Growth and branching patterns of *Lophelia pertusa* (Scleractinia) from the North Sea. *Journal of the Marine Biological Association of the United Kingdom* 91: 831-835.

Gori, A., S. Rossi, C. Linares, E. Berganzo, C. Orejas, M. Dale & J. Gili, 2011. Size and spatial structure in deep versus shallow populations of the Mediterranean gorgonian *Eunicella singularis* (Cap de Creus, northwestern Mediterranean Sea). *Marine Biology* 158: 1721-1732.

Greathead, C., J. M. González-Irusta, J. Clarke, P. Boulcott, L. Blackadder, A. Weetman & P. J. Wright, 2014. Environmental requirements for three sea pen species:

relevance to distribution and conservation. ICES Journal of Marine Science: Journal du Conseil 72: 576-586.

Heifetz, J., R. P. Stone & S. K. Shotwell, 2009. Damage and disturbance to coral and sponge habitat of the Aleutian Archipelago. Marine Ecology Progress Series 397: 295-303.

Kabacoff, R., 2015. R in action: data analysis and graphics with R. Manning, Shelter Island.

Kerr, L. A., A. H. Andrews, B. R. Frantz, K. H. Coale, T. A. Brown & G. M. Cailliet, 2004. Radiocarbon in otoliths of yelloweye rockfish (*Sebastes ruberrimus*): a reference time series for the coastal waters of southeast Alaska. Canadian Journal of Fisheries and Aquatic Sciences 61: 443-451.

Krieger, K. J. & B. L. Wing, 2002. Megafauna associations with deepwater corals (*Primnoa* spp.) in the Gulf of Alaska. Hydrobiologia 471: 83-90.

Locarnini, R. A., A. V. Mishonov, J. I., T. P. Antonov, H. E. Boyer, O. K. Garcia, M. M. Baranova, C. R. Zweng, J. R. Paver, D. R. Reagan, H. Johnson M. & D. Seidov, 2013. *World Ocean Atlas 2013, Volume 1: Temperature*. S. Levitus, Ed., A. Mishonov Technical Ed.; NOAA Atlas NESDIS 73, 40 pp.

Matsumoto, A. K., 2007. Effects of low water temperature on growth and magnesium carbonate concentrations in the cold-water gorgonian *Primnoa pacifica*. Bulletin of Marine Science 81: 423-435.

McNeely, R., A. S. Dyke & J. R. Southon, 2006. Canadian marine reservoir ages, preliminary data assessment. Open File 5049: 3.

Mercier, A. & J. Hamel, 2011. Contrasting reproductive strategies in three deep-sea octocorals from eastern Canada: *Primnoa resedaeformis*, *Keratoisis ornata*, and *Anthomastus grandiflorus*. *Coral Reefs* 30: 337-350.

Metaxas, A. & J. Davis, 2005. Megafauna associated with assemblages of deep-water gorgonian corals in Northeast Channel, off Nova Scotia, Canada. *Journal of the Marine Biological Association of the United Kingdom* 85: 1381-1390.

Mortensen, P. B. & L. Buhl-Mortensen, 2005. Morphology and growth of the deep-water gorgonians *Primnoa resedaeformis* and *Paragorgia arborea*. *Marine Biology* 147: 775-788.

Neves, B. M., C. Du Preez & E. Edinger, 2014. Mapping coral and sponge habitats on a shelf-depth environment using multibeam sonar and ROV video observations: Learmonth Bank, northern British Columbia, Canada. *Deep Sea Research Part II: Topical Studies in Oceanography* 99: 169-183.

Orejas, C., A. Gori & J. M. Gili, 2008. Growth rates of live *Lophelia pertusa* and *Madrepora oculata* from the Mediterranean Sea maintained in aquaria. *Coral Reefs* 27: 255-255.

Peck, L. S., 2016. A cold limit to adaptation in the sea. *Trends in Ecology & Evolution* 31: 13-26.

Peck, L. S. & S. Brockington, 2013. Growth of the Antarctic octocoral *Primnoella scotiae* and predation by the anemone *Dactylanthus antarcticus*. *Deep Sea Research Part II: Topical Studies in Oceanography* 92: 73-78.

Piner, K. R., O. S. Hamel, J. L. Menkel, J. R. Wallace & C. E. Hutchinson, 2005. Age validation of canary rockfish (*Sebastes pinniger*) from off the Oregon coast (USA) using

the bomb radiocarbon method. *Canadian Journal of Fisheries and Aquatic Sciences* 62: 1060-1066.

Quinn, G. P. & M. J. Keough, 2002. *Experimental design and data analysis for biologists*. Cambridge University Press, Cambridge, UK; New York.

Reimer, P., E. Bard, A. Bayliss, J. Beck, P. Blackwell, C. B. Ramsey, C. Buck, H. Cheng, R. L. Edwards, M. Friedrich, P. Grootes, T. Guilderson, H. Haflidason, I. Hajdas, C. Hatté, T. Heaton, D. Hoffmann, A. Hogg, K. Hughen, K. Kaiser, B. Kromer, S. Manning, M. Niu, R. Reimer, D. Richards, E. Scott, J. Southon, R. Staff, C. Turney & J. v. d. Plicht, 2013. IntCal13 and Marine13 radiocarbon age calibration curves 0–50,000 years cal BP. *Radiocarbon* 55: 1869-1887.

Risk, M. J., J. M. Heikoop, M. G. Snow & R. Beukens, 2002. Lifespans and growth patterns of two deep-sea corals: *Primnoa resedaeformis* and *Desmophyllum cristagalli*. *Hydrobiologia* 471: 125-131.

Roark, E. B., T. P. Guilderson, R. B. Dunbar & B. L. Ingram, 2006. Radiocarbon-based ages and growth rates of Hawaiian deep-sea corals. *Marine Ecology Progress Series* 327: 1-14.

Roark, E. B., T. P. Guilderson, R. B. Dunbar, S. J. Fallon & D. A. Mucciarone, 2009. Extreme longevity in proteinaceous deep-sea corals. *Proceedings of the National Academy of Sciences* 106: 5204-5208.

Roberts, J. M. & S. D. Cairns, 2014. Cold-water corals in a changing ocean. *Current Opinion in Environmental Sustainability* 7: 118-126.

Roberts, J. J., B. D. Best, D. C. Dunn, E. A. Treml & P. N. Halpin, 2010. *Marine Geospatial Ecology Tools: An integrated framework for ecological geospatial processing with*

ArcGIS, Python, R, MATLAB, and C++. *Environmental Modelling & Software* 25: 1197-1207.

Roberts, J. M., A. Wheeler, A. Freiwald & S. Cairns, 2009. *Cold-water corals: the biology and geology of deep-sea coral habitats*. Cambridge University Press, Cambridge, UK; New York.

Robinson, L. F., J. F. Adkins, N. Frank, A. C. Gagnon, N. G. Prouty, E. Brendan Roark & T. v. de Flierdt, 2014. The geochemistry of deep-sea coral skeletons: A review of vital effects and applications for palaeoceanography. *Deep Sea Research Part II: Topical Studies in Oceanography* 99: 184-198.

Schneider, C. A., W. S. Rasband & K. W. Eliceiri, 2012. NIH Image to ImageJ: 25 years of image analysis. *Nature Methods* 9: 671-675.

Sherwood, O. A. & E. N. Edinger, 2009. Ages and growth rates of some deep-sea gorgonian and antipatharian corals of Newfoundland and Labrador. *Canadian Journal of Fisheries and Aquatic Sciences* 66: 142-152.

Sherwood, O. A., T. P. Guilderson, F. C. Batista, J. T. Schiff & M. D. McCarthy, 2014. Increasing subtropical North Pacific Ocean nitrogen fixation since the Little Ice Age. *Nature* 505: 78-81.

Sherwood, O. A., R. E. Jamieson, E. N. Edinger & V. E. Wareham, 2008. Stable C and N isotopic composition of cold-water corals from the Newfoundland and Labrador continental slope: Examination of trophic, depth and spatial effects. *Deep Sea Research Part I: Oceanographic Research Papers* 55: 1392-1402.

Sherwood, O. A., M. F. Lehmann, C. J. Schubert, D. B. Scott & M. D. McCarthy, 2011. Nutrient regime shift in the western North Atlantic indicated by compound-specific

$\delta^{15}\text{N}$ of deep-sea gorgonian corals. Proceedings of the National Academy of Sciences 108: 1011-1015.

Sherwood, O. A., D. B. Scott & M. J. Risk, 2006. Late Holocene radiocarbon and aspartic acid racemization dating of deep-sea octocorals. *Geochimica et Cosmochimica Acta* 70: 2806-2814.

Sherwood, O. A., D. B. Scott, M. J. Risk & T. P. Guilderson, 2005a. Radiocarbon evidence for annual growth rings in the deep-sea octocoral *Primnoa resedaeformis*. *Marine Ecology Progress Series* 301: 129-134.

Sherwood, O. A., J. M. Heikoop, D. B. Scott, M. J. Risk, T. P. Guilderson & R. A. McKinney, 2005b. Stable isotopic composition of deep-sea gorgonian corals *Primnoa* spp.: a new archive of surface processes. *Marine Ecology Progress Series* 301: 135-148.

Stuiver, M. & H. A. Polach, 1977. Discussion: reporting of ^{14}C data. *Radiocarbon* 19: 355-363.

Thresher, R. E., 2009. Environmental and compositional correlates of growth rate in deep-water bamboo corals (Gorgonacea; Isididae). *Marine Ecology Progress Series* 397: 187-196.

Thrush, S. F. & P. K. Dayton, 2002. Disturbance to marine benthic habitats by trawling and dredging: implications for marine biodiversity. *Annual Review of Ecology and Systematics* 33: 449-473.

Tracey, D. M., H. Neil, P. Marriott, A. H. Andrews, G. M. Cailliet & J. A. Sánchez, 2007. Age and growth of two genera of deep-sea bamboo corals (family Isididae) in New Zealand waters. *Bulletin of Marine Science* 81: 393-408.

Troffe, P. M., C. D. Levings, G. E. Piercey & V. Keong, 2005. Fishing gear effects and ecology of the sea whip *Halimeteris willemoesi* (Cnidaria: Octocorallia: Pennatulacea) in British Columbia, Canada: preliminary observations. *Aquatic Conservation: Marine and Freshwater Ecosystems* 15: 523-533.

Waller, R. G., R. P. Stone, J. Johnstone & J. Mondragon, 2014. Sexual reproduction and seasonality of the Alaskan Red Tree Coral, *Primnoa pacifica*. *PLoS ONE* 9: e90893.

Watanabe, S., A. Metaxas, J. Sameoto & P. Lawton, 2009. Patterns in abundance and size of two deep-water gorgonian octocorals, in relation to depth and substrate features off Nova Scotia. *Deep Sea Research Part I: Oceanographic Research Papers* 56: 2235-2248.

Yesson, C., M. L. Taylor, D. P. Tittensor, A. J. Davies, J. Guinotte, A. Baco, J. Black, J. M. Hall-Spencer & A. D. Rogers, 2012. Global habitat suitability of cold-water octocorals. *Journal of Biogeography* 39: 1278-1292.

Appendix 6-1. Sample identification and associated information. Latitude (N) and longitude (W) are in decimal degrees. Depth in meters, height in cm, age in years. Rgrowth: radial growth rates ($\text{mm}\cdot\text{yr}^{-1}$), Dgrowth: diametric growth rates ($\text{mm}\cdot\text{yr}^{-1}$), Lgrowth: linear growth rates ($\text{cm}\cdot\text{yr}^{-1}$).

Sample identification	Location	Latitude	Longitude	Depth	Height	Age \pm SD	Rgrowth	Dgrowth	Lgrowth	Source
<i>Primnoa pacifica</i>										
R1512-L2-0003	Coral Knoll	49.3704	-123.8970	251	na	40 \pm 0	0.19	0.33	na	This study
R1512-SR-0008	Coral Knoll	49.3743	-123.8920	245	51	26 \pm 0.47	0.25	0.40	1.99	This study
R1512-BR-0009	Coral Knoll	49.3744	-123.8917	224	na	16 \pm 2.16	0.29	0.56	na	This study
R1512-PR-0013	Coral Knoll	49.3705	-123.8971	254	na	30 \pm 1.63	0.26	0.38	na	This study
R1512-PR-0014	Coral Knoll	49.3704	-123.8970	251	na	54 \pm 0.82	0.32	0.58	na	This study
R1512-SB-0015	Coral Knoll	49.3704	-123.8969	251	na	22 \pm 0.47	0.15	0.27	na	This study
R1512-JAW-0017	Coral Knoll	49.3743	-123.8919	246	79	34 \pm 2.05	0.24	0.37	2.30	This study
R1513-SR-0021	Sabine channel	49.4961	-124.1701	267	na	69 \pm 2.05	0.18	0.31	na	This study
R1513-SR-0022	Sabine channel	49.4959	-124.1702	270	na	37 \pm 3.3	0.30	0.45	na	This study
R1513-BR-0023	Sabine channel	49.4959	-124.1703	270	na	85 \pm 0.47	0.32	0.47	na	This study
R1513-BR-0024	Sabine channel	49.4959	-124.1703	270	44.7	28 \pm 0.94	0.25	0.44	1.58	This study
R1513-PR-0025	Sabine channel	49.4958	-124.1700	270	na	78 \pm 1.7	0.16	0.33	na	This study
R1513-PR-0026	Sabine channel	49.4958	-124.1700	270	na	25 \pm 1.25	0.15	0.32	na	This study
R1513-PR-0028	Sabine channel	49.4955	-124.1696	270	43	23 \pm 2.94	0.25	0.45	1.87	This study
R1513-SR-0033	Sabine channel	49.4955	-124.1696	270	73	39 \pm 1.7	0.27	0.44	1.86	This study
A	Dixon Entrance	na	na	na	na	na	0.18	0.36	1.96	A
B	Japan	43.6000	139.5417	428	na	5	0.13	0.26	na	B ¹
B	Japan	43.6000	139.5417	428	na	5	0.18	0.37	na	B ¹
B	Japan	43.6000	139.5417	428	na	8	0.12	0.23	na	B ¹
B	Japan	43.6000	139.5417	428	na	9	0.13	0.26	na	B ¹
B	Japan	43.6000	139.5417	428	na	11	0.11	0.23	na	B ¹

Sample identification	Location	Latitude	Longitude	Depth	Height	Age±SD	Rgrowth	Dgrowth	Lgrowth	Source
B	Japan	43.6000	139.5417	428	na	13	0.13	0.25	na	B ¹
B	Japan	43.6000	139.5417	428	na	18	0.12	0.24	na	B ¹
B	Japan	43.6000	139.5417	428	na	29	0.09	0.19	na	B ¹
B	Japan	43.6000	139.5417	428	na	40	0.13	0.27	na	B ¹
B	Japan	43.6000	139.5417	428	na	15	0.13	0.27	na	B ¹
R1156-0004	Dixon Entrance	54.5690	-133.0230	381	na	22	0.23	0.46	na	C
R1153-0003	Dixon Entrance	54.3790	-132.8610	393	na	46	0.22	0.43	na	C
R1155-0013	Dixon Entrance	54.4560	-133.1550	248	na	119	0.30	0.61	na	C
R1155-0012	Dixon Entrance	54.4440	-133.1420	201	na	34	0.58	1.16	na	C
R1162-0015	OCNMS	48.1430	-125.1820	310	na	75	0.41	0.83	na	C
R1162-0016	OCNMS	48.1430	-125.1820	312	na	51	0.32	0.64	na	C
R1165-0002	OCNMS	48.1350	-125.1830	295	na	87	0.39	0.77	na	C
R1165-0005	OCNMS	48.1470	-125.2380	266	na	62	0.33	0.66	na	C
USNM 44058	Kupreanof Island	56.3940	-133.3686	na	na	86±2.87	0.50	0.67	na	D
USNM 52199	Chatam Sound	54.3831	-130.5664	na	na	80±2.05	0.46	0.75	na	D
USNM 85281	Japan	36.0341	132.8687	145	26	26±0.47	0.14	0.22	0.99	D
USNM 1024425	Alaska	na	na	274	22	35±0.47	0.30	0.83	0.62	D
USNM 1120445	Knight Inlet	50.6842	-125.9970	20	na	17±2.16	0.18	0.39	na	D
<i>P. pacifica var.willeyi</i>										
USNM 58084	Kupreanof Island	56.3940	-133.3686	na	229	86±3.27	0.20	0.43	2.66	D
<i>Primnoa resedaeformis</i>										
USNM 4524	NE Channel	42.1300	-65.5800	338	na	60±0.94	0.26	0.54	na	D
USNM 4534	Mount Desert Isl.	43.9921	-67.7666	165	32	29±0.94	0.12	0.23	1.12	D
USNM 4544	NE Channel	42.2279	-66.5095	229	na	41±0.82	0.17	0.34	na	D
USNM 4582	Georges Bank	41.3749	-65.9628	457	68	36±0.82	0.10	0.23	1.89	D
USNM 4589	Banquereau Bank	na	na	274	68	40±0.94	0.22	0.35	1.69	D
USNM 54269	Virginia	37.0600	-74.4017	311	na	27±0.94	0.30	0.70	na	D
USNM 12261	S Georges Bank	40.5717	-66.1500	3186	44	36±2.63	0.15	0.25	1.21	D

Sample identification	Location	Latitude	Longitude	Depth	Height	Age±SD	Rgrowth	Dgrowth	Lgrowth	Source
1525-1	E Hudson Strait	60.4980	-61.3950	414	na	50	na	na	na	E
1525-3	E Hudson Strait	60.4980	-61.3950	414	100	100	0.09	0.18	1.00	E
1525-4	E Hudson Strait	60.4980	-61.3950	414	na	72	0.15	0.29	na	E
1525-5	E Hudson Strait	60.4980	-61.3950	414	53.01	31	0.17	0.33	1.71	E
1525-6	E Hudson Strait	60.4980	-61.3950	414	60.03	23	0.22	0.43	2.61	E
1525-7	E Hudson Strait	60.4980	-61.3950	414	60	24	0.19	0.38	2.50	E
1525-8	E Hudson Strait	60.4980	-61.3950	414	54.96	24	0.17	0.33	2.29	E
1525-10	E Hudson Strait	60.4980	-61.3950	414	81.84	44	0.13	0.25	1.86	E
1526-1	E Hudson Strait	60.1760	-61.7900	257	na	50	0.13	0.26	na	E
1526-2	E Hudson Strait	60.1760	-61.7900	257	na	57	0.11	0.21	na	E
1534	E Hudson Strait	61.4880	-61.8190	608	na	52	0.08	0.17	na	E
1536-1	E Hudson Strait	61.2020	-61.3780	585	34.92	18	0.19	0.39	1.94	E
1536-2	E Hudson Strait	61.2020	-61.3780	585	36	20	0.17	0.34	1.80	E
1539	E Hudson Strait	60.3230	-62.1490	285	na	18	0.18	0.36	na	E
1567	E Hudson Strait	62.1610	-61.5370	456	na	62	0.12	0.24	na	E
2370-10	E Hudson Strait	61.3500	-60.6830	640	79.8	42	0.19	0.39	1.90	E
F	NE Channel	na	na	450	na	>300	0.44	0.88	na	F
HUD 2001-55, VG 13	NE Channel	42.0063	-65.6930	337	41	22	0.23	0.45	1.86	G ²
ROPOS 2001, R636	NE Channel	42.0465	-65.5745	498	38	24	0.21	0.42	1.58	G ²
ROPOS 2001, R636	NE Channel	42.0465	-65.5745	498	41	15	0.20	0.40	2.73	G ²
ROPOS 2001, R637	NE Channel	42.0475	-65.5767	476	28	17	0.21	0.41	1.65	G ²
ROPOS 2001, R637	NE Channel	42.0475	-65.5767	476	27	15	0.23	0.47	1.80	G ²
ROPOS 2001, R637	NE Channel	42.0475	-65.5767	476	25.5	15	0.23	0.47	1.70	G ²
ROPOS 2001, R637	NE Channel	42.0475	-65.5767	476	24.5	13	0.15	0.31	1.88	G ²
ROPOS 2001, R637	NE Channel	42.0475	-65.5767	476	32	19	0.16	0.32	1.68	G ²
ROPOS 2001, R640	NE Channel	41.9975	-65.6480	446	61	30	0.23	0.47	2.03	G ²
ROPOS 2001, R640	NE Channel	41.9975	-65.6480	446	62	22	0.20	0.41	2.82	G ²
ROPOS 2001, R640	NE Channel	41.9975	-65.6480	446	56	18	0.20	0.40	3.11	G ²

Sample identification	Location	Latitude	Longitude	Depth	Height	Age±SD	Rgrowth	Dgrowth	Lgrowth	Source
NED 2001-037, Set 77	The Gully	43.9642	-58.6017	507	86	na	na	na	na	G ²
NED 2001-037, Set 77	The Gully	43.9642	-58.6017	507	76	70	0.11	0.21	1.09	G ²
NED 2002-037, Set 46	NE Channel	42.0573	-65.6353	277	75	61	0.18	0.36	1.23	G ²
NED 2002-037, Set 46	NE Channel	42.0573	-65.6353	277	63	47	0.36	0.72	1.34	G ²
NED 2002-037, Set 46	NE Channel	42.0573	-65.6353	277	63	31	0.34	0.68	2.03	G ²
NED 2002-037, Set 46	NE Channel	42.0573	-65.6353	277	45	24	0.48	0.96	1.88	G ²
NED 2002-037, Set 46	NE Channel	42.0573	-65.6353	277	50.5	22	0.23	0.45	2.30	G ²
NED 2002-037, Set 46	NE Channel	42.0573	-65.6353	277	65	19	0.37	0.74	3.42	G ²
NED 2002-037, Set 46	NE Channel	42.0573	-65.6353	277	65	34	0.16	0.32	na	G ²
NED 2002-037, Set 46	NE Channel	42.0573	-65.6353	277	50	25	0.14	0.28	2.00	G ²
NED 2002-037, Set 46	NE Channel	42.0573	-65.6353	277	54	16	0.31	0.63	3.38	G ²
NED 2002-037, Set 46	NE Channel	42.0573	-65.6353	277	58	45	0.21	0.42	1.29	G ²
HUD 2001-55, VG 15	NE Channel	42.0158	-65.6842	321	53	na	na	na	na	G ²
Fisher B	NE Channel	41.9332	-65.7250	246	65	30	0.27	0.53	2.17	G ²
Fisher B	NE Channel	41.9332	-65.7250	246	55	30	0.20	0.40	1.83	G ²
Fisher B	NE Channel	41.9332	-65.7250	246	49	25	0.20	0.40	1.96	G ²
Fisher B	NE Channel	41.9332	-65.7250	246	63	30	0.32	0.63	2.10	G ²
Fisher B	NE Channel	41.9332	-65.7250	246	55	28	0.21	0.43	1.96	G ²
Fisher B	NE Channel	41.9332	-65.7250	246	48	27	0.31	0.63	1.78	G ²
Fisher B	NE Channel	41.9332	-65.7250	246	46	25	0.32	0.64	1.84	G ²
Fisher B	NE Channel	41.9332	-65.7250	246	33	17	0.24	0.47	1.94	G ²
Fisher B	NE Channel	41.9332	-65.7250	246	30	25	0.18	0.36	1.20	G ²
Fisher B	NE Channel	41.9332	-65.7250	246	46	25	0.26	0.52	1.84	G ²
Fisher B	NE Channel	41.9332	-65.7250	246	76	60	0.18	0.35	1.27	G ²
sample #1	Labrador	na	na	na	44	28	0.20	0.41	1.57	This study
sample #2	Labrador	na	na	na	52	24	0.15	0.30	2.17	This study

References: A: Andrews et al. (2002), B: Matsumoto (2007), C: Aranha et al. (2014), D: USNM, E: Sherwood & Edinger (2009), F: Risk et al. (2002); G: Mortensen & Buhl-Mortensen (2005). ¹Data estimated from graph in the published manuscript. ²Raw data for individual colonies obtained from the authors. SD shown for new estimates of age only.

7. Morphology, growth rates, and trace element composition of dense bamboo coral forests in a muddy Arctic environment⁶

Abstract

Keratoisis is a genus of bamboo coral commonly reported in the Northwest (NW) Atlantic as fishing bycatch or by *in situ* observations. In 1999, a scientific trawl survey recovered fragments of *Keratoisis* sp. in Southeast Baffin Bay, but colonies had never been seen *in situ* at this location until 2013, when a Remotely Operated Vehicle (ROV) was used to survey the area. Here we report the presence of dense forests of *Keratoisis* sp. in a muddy environment at depths > 900 m. Colonies were found as dense patches up to ~ 55 m long along the ROV track and were estimated to reach ~ 1 m in height. At this location, *Keratoisis* sp. appears to have branched root-like structures probably used for anchorage on mud. The majority of colonies were alive, but fragments of dead colonies were also observed, especially in the path of the 1999 bottom trawl tow. Based on visual observation, the dense stands of *Keratoisis* sp. in this environment seem to form structure and habitat for other invertebrates and fishes in an otherwise mainly muddy environment. A trace elements analysis of the calcitic skeleton yielded results similar to those obtained from other gorgonians and sea pens found in the literature, but trace element cyclicity was not an effective tool for defining ring formation periodicity. The number of growth rings

⁶ This chapter was partially published in Neves, B. M., E. Edinger, C. Hillaire-Marcel, E. Saucier, S. C. France, M. A. Treble & V. E. Wareham, 2014. Deep-water bamboo coral forests in a muddy Arctic environment. *Marine Biodiversity* 45: 867-871. The molecular analysis was performed by E. Saucier and S. France. The sections on growth rates and geochemistry are still unpublished.

identified in the gorgonin portion of the two skeletons was 43 and 59, with radial growth rates of 0.01 and 0.02 mm·yr⁻¹ assuming rings to be formed annually (as in *Keratoisis grayi*). By extrapolating to the whole stem including the calcite, the maximum number of rings in these specimens was estimated to be 103 and 120, which might indicate that these colonies are slow growing and long-lived.

7.1 Introduction

Bamboo corals (Octocorallia: Isididae) are cosmopolitan long-lived gorgonians occurring on hard or soft substrates to depths of >4000 m (Roberts et al., 2009). In the Northwest (NW) Atlantic, one of the most common bamboo corals is *Keratoisis grayi* (Wright, 1869) (senior synonym of *K. ornata*), which has been reported in the Newfoundland and Labrador region (Wareham & Edinger, 2007, Murillo et al., 2011, Baker et al., 2012) and in the Southeast (SE) Baffin Bay (DFO, 2007).

In Newfoundland and Labrador *K. grayi* has been observed both *in situ* (Edinger et al., 2011; Baker et al., 2012) and as a result of fisheries observer data (Wareham and Edinger, 2007, Murillo et al. 2011). Sparse skeletal fragments of *Keratoisis* sp. were retrieved from SE Baffin Bay (between Greenland and Canada) during a 1999 trawl survey in which the trawl broke and was lost on the bottom (DFO, 2007).

In this area there is a gap in fishing effort along the shelf slope (Fig. 7.1B): shrimp trawling on the continental shelf mostly occurs shallower than 500 m (Tim Siferd, pers. comm. 2014), while trawling and gillnetting for Greenland Halibut *Reinhardtius hippoglossoides* (Walbaum, 1792) mostly occurred below 1000 m (Treble et al., 2003, Jørgensen & Hammeken Arboe, 2013).

In 2012 several live colonies were recovered in a boxcore at the same area (E. Kenchington, pers. comm. 2012). A Remote Operated Vehicle (ROV) dive in Aug 2013 permitted the observation and sampling of *Keratoisis* sp. bamboo corals on a muddy sea floor at depths > 900 m. Here we report the distribution of these bamboo corals and estimated radial growth rates based on two samples obtained with the ROV. Furthermore,

because of the potential of gorgonians as palaeoceanographic proxies, we also determined the trace element composition of the skeleton in these octocorals using Secondary Ion Mass Spectrometry (SIMS) and assessed its applicability to estimate palaeotemperatures.

7.2 Material and methods

7.2.1 Data sampling

The surveyed location is on the lower slopes of the Disko trough-mouth fan, in SE Baffin Bay (67°58.32'N, 59°30.98'W) (Fig. 7-1A). The coral habitat was surveyed using a Super Mohawk™ ROV deployed from the Canadian Coast Guard Ship (CCGS) *Amundsen* on 7-8 August 2013. A CTD cast was conducted in the surrounding area (67°8'N, 59°43'W) to a maximum of 901 m. Multibeam sonar data (15 m pixels) were collected before the ROV dive using a Kongsberg Simrad™ EM302 multibeam sonar system, with the resulting bathymetry and slope data suggesting an overall flat environment (Fig. 7-1C).

The ROV video survey was designed to cross the path of the 1999 trawl survey (Fig. 7-1C). The video survey covered a ~1.3 km track of sea floor at a speed of 0.5 knots. The extent of bamboo coral patches was calculated by determining the geographic coordinates at the beginning and end of each patch seen in the video, and the distance was measured using ArcMap 10.1. The ROV lacked scaling lasers at the time of this expedition; therefore an aluminum ruler was used to estimate colony size by holding the ruler adjacent to a coral colony, and determining polyp size (Fig. 7-3D). Polyp size was later used as a scale to estimate colony height throughout the dive.

Coral fragments, including both tissue and skeleton, were sampled for species identification using the ROV arms and a storage bag specifically adapted for this ROV, which does not have permanent storage units for sampling. Samples were frozen at -20 °C following collection, and subsamples were later transferred to 95% ethanol.

Genus morphological identification was performed following terminology and identification keys by Deichmann (1936). We identified the samples as *Keratoisis* sp. based on branches arising from the internodes (calcareous regions), and on the presence of a hollow axis (Deichmann, 1936). However, the subfamily Keratoisidinae and specifically the genus *Keratoisis* are undergoing further taxonomic revisions (Watling et al., 2011, France, 2007). Therefore, a molecular analysis was also performed to confirm identity.

7.2.2 Molecular analysis

The molecular analysis was performed by Esprit Saucier and Dr. Scott Grant (Neves et al., 2014). DNA was extracted from two preserved specimens (Baff1 & Baff 2) using a CTAB protocol (Berntson & France 2001) and DNA stocks were diluted for PCR to a working concentration of $\approx 40\text{ng}\cdot\mu\text{L}^{-1}$. The 5' end (the first ≈ 700 bp) of the ≈ 3 kbp-long mitochondrial gene mtMutS (formerly called msh1; Bilewitch and Degnan 2011) was amplified and sequenced, and is hereafter referred to as mtMutS -5'. Polymerase chain reaction (PCR) was used to amplify the gene region with primers specifically designed to target that region in Keratoisidinae corals (Co3BAM5657f: GCTGCTAGTTGGTATTGGCT; Brugler and France 2008 & MutCHRY3458r: TGAAGYAAAAGCCACTCC; Pante et al. 2012).

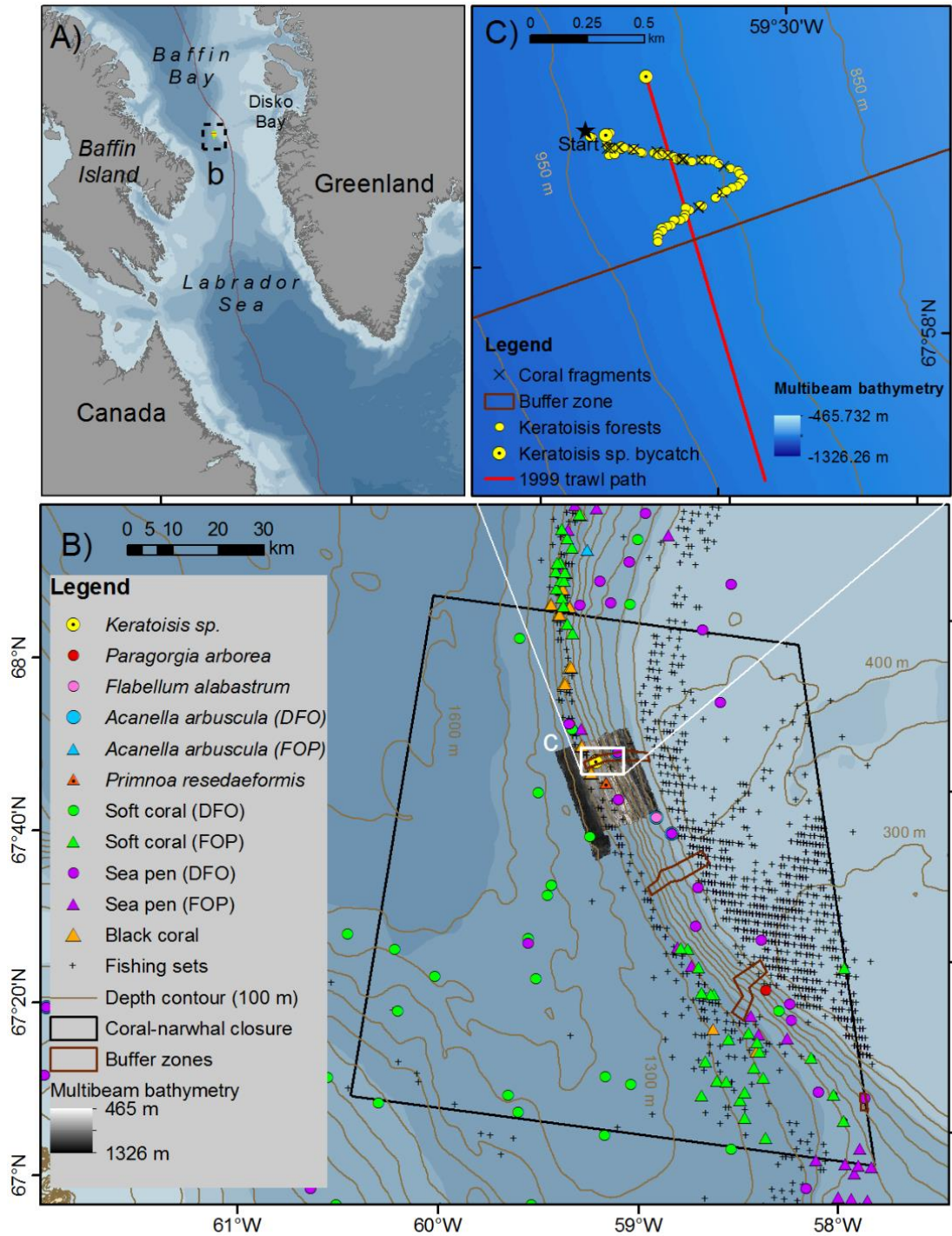


Figure 7-1. A) location of surveyed area (rectangle) showing Canada's Exclusive Economic Zone (EEZ), B) fishing effort (shrimp and Greenland Halibut; 2004-2005; Edinger et al. 2007) and coral records from Fisheries and Oceans Canada (DFO) scientific surveys (circles; 1999, 2001, 2006, 2008, 2010, 2012) and the Fisheries Observer Program (FOP) datasets (2005-2007) (triangles, Gass & Willison, 2005, Wareham, 2009) near the surveyed area (positional error ~ 100 m), C) location of *Keratoisis* sp. from previous surveys, *Keratoisis* sp. forests observed in this study, and fragments of dead colonies in relation to the 1999 trawl path. Buffer zones represent areas of long-term monitoring. Figure shown in the previous page.

Because species in the subfamily Keratoisidinae have a different mitochondrial gene arrangement in the region of mtMutS compared to other octocorals (Brugler and France 2008), a forward primer anchored in the *cox3* gene was used to amplify the mtMutS-5' rather than the *nad4L* primer used to amplify the same region for most octocorals. Half-volume (25uL) reactions were used for PCR amplification following the manufacturer's protocols. TaKaRa Ex TaqTM polymerase and associated reagents (TaKaRa Bio Inc.) were used for the PCR. PCR products were sent to Eurofins Genomics (Huntsville, Alabama, USA) for sequencing. The raw DNA sequence traces were examined and edited using Sequencher v. 4.7 (Gene Codes). The haplotype sequence was submitted to NCBI's GenBank (GenBank acc. # KP091541).

7.2.3 Skeleton carbonate composition

In order to determine the carbonate composition of the skeleton in *Keratoisis* sp., an X-Ray diffraction (XRD) analysis was performed at the Earth Resources Research and Analysis (TERRA) facility, Memorial University of Newfoundland. A Rigaku Ultima-IV with a Cu source used in Bragg-Brentano configuration was used for this analysis. A portion of the internode region of the skeleton was crushed using a mortar and pestle, and ~1 g of this material was used in the analysis.

7.2.4 Growth rings and apparent rates

In order to estimate longevity and growth rates, transversal sections from two fragments of *Keratoisis* sp. were obtained from the node region (Fig. 7-2) using a rock saw. These sections were embedded in epoxy and polished using a Struers® polishing (TegraForce-5, TegraPol-31) machine. Following polishing, cracks were formed in the gorgonin region (node), and for this reason Crazy Glue™ was used to fill in the cracks, to avoid problems due to surface topography when performing trace element microanalysis with SIMS (section 7.2.5).

Cross sections were photographed under optical microscope, and the number of growth rings in the gorgonin portion of the stem were counted from the photographs using the software GIMP 2.8. Rings were counted at 3 non-consecutive times and averaged. By assuming growth rings to be formed annually (as in *Keratoisis grayi* from the Grand Banks region; Sherwood & Edinger, 2009) we estimated radial growth rates for the portion of the gorgonin where growth rings could be identified. From these growth rates we extrapolated the number of rings expected in the calcite region (c.f. Aranha et al.,

2014), assuming constant growth rates. We compared the number of extrapolated growth rings in the calcite to the number of trace element cycles for each element. Radial growth rates were estimated rather than diametric growth rates for comparison with published data on other *Keratoisis* sp. colonies.

7.2.5 Trace element analysis

Although growth rings are known to be formed annually in *K. grayi* from the Grand Banks region (Sherwood & Edinger, 2009), we acknowledge that confirming the frequency of ring formation in the studied specimens of *Keratoisis* sp. would be ideal to determine longevity and growth rates. A ^{14}C analysis of the gorgonin portion of the skeleton (Sherwood & Edinger, 2009, Chapter 6) could not be accomplished because there was not enough material available for the analysis, as the stems and rings were considerably thin.

As an attempt to better understand the geochemical composition of the stem in the studied *Keratoisis* sp. and perhaps find indications of ring formation periodicity, a trace elements analysis of the stem was performed. A Cameca IMS 4f Secondary Ion Mass Spectrometer at Memorial University of Newfoundland was used to determine ratios of Mg, Sr, Ba, and Na to Ca.

The same cross sections used to estimate growth rates were analyzed for trace elements. For each fragment, both sides of the cross sections were analyzed: one side had only calcite (side A), while the other side had the gorgonin internode and the calcite surrounding it (side B). Because branches were sampled fragmented and mixed between sampled sites, we cannot be sure whether these samples belong to the same colony or not.

Mounted polished cross sections were gold coated (300Å) prior to SIMS analysis. SIMS transects were only performed across the calcite zones. In samples that only contained calcite (side A), transects started at the core of the sample, and ended at the edge. In samples containing both gorgonin and calcite (side B), transect lines started at the limit zone between gorgonin and calcite, and ended at the edge of the sample; therefore these transects were shorter than the ones at sides containing calcite only (side A).

SIMS transects were not run in the exact same position in sides A and B of each fragment. For this reason, when graphing the results of the SIMS analysis, trace element ratios from side A and B of a sample are only tentatively aligned from the edge to the core, and spots do not necessarily correspond to the same position in the stem. Individual SIMS spots were ~25 µm apart, the resolution allowed by the instrument. Detailed procedures can be found in Aranha et al. (2014).

7.2.6 Palaeotemperature estimation

Based on the Mg/Ca ratios obtained from the trace element analysis, we estimated water temperature for the location where *Keratoisis* sp. was sampled. To this end, we used the equation on the relationship between Mg/Ca and seawater temperature determined from the skeleton of the gorgonian *Primnoa resedaeformis* by Sherwood et al. (2005) as follows:

$$\text{Mg/Ca (mmol}\cdot\text{mol}^{-1}) = 5 (\pm 1.4)T (\text{°C}) + 64 (\pm 10) \quad (1)$$

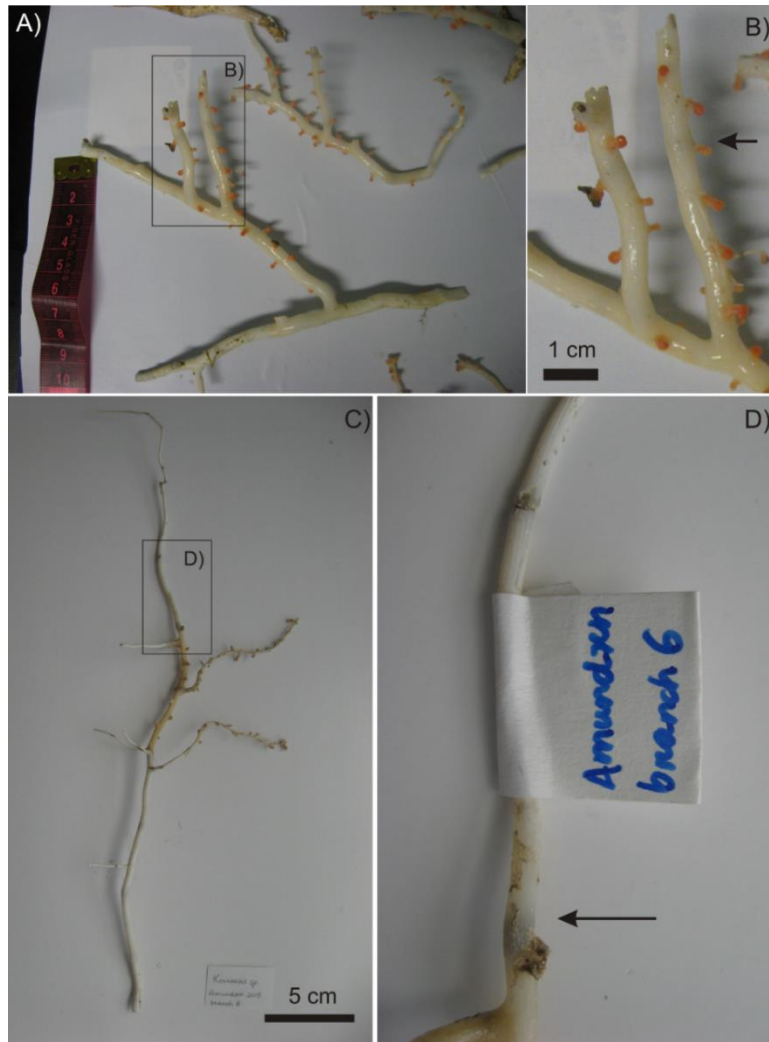


Figure 7-2. Fragments of *Keratoisis* sp. used to estimate growth rates and for the trace elements analysis. A-B) sample 1, C-D) sample 2. Arrows point to locations from where cross sections were made. Note orange polyps still present in both samples.

7.3 Results

7.3.1 Molecular analysis

The two *Keratoisis* samples sequenced yielded the same mtMutS -5' haplotype ("kerD2d", Neves et al., 2014). This sequence is different from those attributed to *K. grayi* (Wright, 1869) the species previously reported by DFO to comprise the mound or reef at this location, and so we refer to it as *Keratoisis* sp. "kerD2d". Bamboo corals with mtMutS -5' haplotype kerD2d have previously been collected in the NW Atlantic from 584 m depth on Whale Bank, south of Newfoundland (SCF, unpublished data), and from 1982 m on Retriever Seamount, in the New England Seamounts chain (GenBank acc. #EF060045).

7.3.2 *Keratoisis* forests

Colonies of *Keratoisis* sp. "kerD2d" were observed as dense patches up to ~ 55 m long, at depths of 905-947 m, in a muddy environment (Fig. 7-3A-C). Bottom temperature at 900 m was 1.1 °C. The vast majority of colonies were alive (Fig. 7-3A-E), although fragments of dead colonies were also observed spread over the bottom in certain areas (Fig. 7-3G), especially in the path of the 1999 scientific trawl survey (DFO, 2007).

Colonies were estimated to reach ~ 1 m in height, and have branched root-like structures that likely serve for anchoring in the muddy bottom (Fig. 7-3F). Colonies are considered dense because their appearance was very crowded, such that individual colonies could not be distinguished (Fig. 7-3A-C). Average colony density (colonies·m⁻²)

could not be calculated from the ROV video because individual colony bases could not be distinguished and because the ROV lacked laser scales to precisely estimate covered area.

Other invertebrates such as sponges, anemones, and crinoids, as well as fish, including the Greenland Halibut, were observed among the coral colonies (Fig. 7-3C).

7.3.3 Carbonate composition of the skeleton

The XRD analysis confirmed that the carbonate composition in the skeleton of *Keratoisis* sp. “kerD2d” is magnesian calcite (Appendix 7-1).

7.3.4. Growth rings and apparent rates

Growth rings could be identified in the gorgonin portion of the axis of *Keratoisis* sp. “kerD2d” (Fig. 7-4). However, because we used Krazy Glue™ to seal the cracked region between the gorgonin and the calcite for the SIMS analysis, the glue made the rings in part of the cross section more difficult to visualize. A total of 59 rings were identified in sample 1 (gorgonin only radius = 1.04 mm), and 43 in sample 2 (gorgonin only radius = 0.5 mm).

By assuming rings to be formed annually, radial growth rates of 0.018 and 0.010 mm·yr⁻¹ were estimated from the gorgonin portion of these colonies. The extrapolation of these growth rates estimated from the gorgonin to the whole radius (gorgonin + calcite) yielded a longevity of 120 years for sample 1, while an extrapolation of 103 years was obtained for sample 2.

Growth rates in the studied specimens of *Keratoisis* sp. “kerD2d” were plotted with published *Keratoisis* growth rates for comparison (Fig. 7-5).

7.3.5. Trace element analysis

Trace element averages were 2.4 mmol·mol⁻¹ (Sr/Ca), 77.7 mmol·mol⁻¹ (Mg/Ca), 29.2 mmol·mol⁻¹ (Na/Ca), and 0.01 mmol·mol⁻¹ (Ba/Ca) (Table 7-1). Mg/Ca and Na/Ca ratios decreased with distance from core, but no trends were observed for Sr/Ca and Ba/Ca (Figs. 7-6 and 7-7). In sample 1, Sr/Ca, Mg/Ca, and Na/Ca values from sides A and B were quite different in magnitude (Figs. 7-6 and 7-7), while in sample 2 values were more similar (Figs. 7-6 and 7-7).

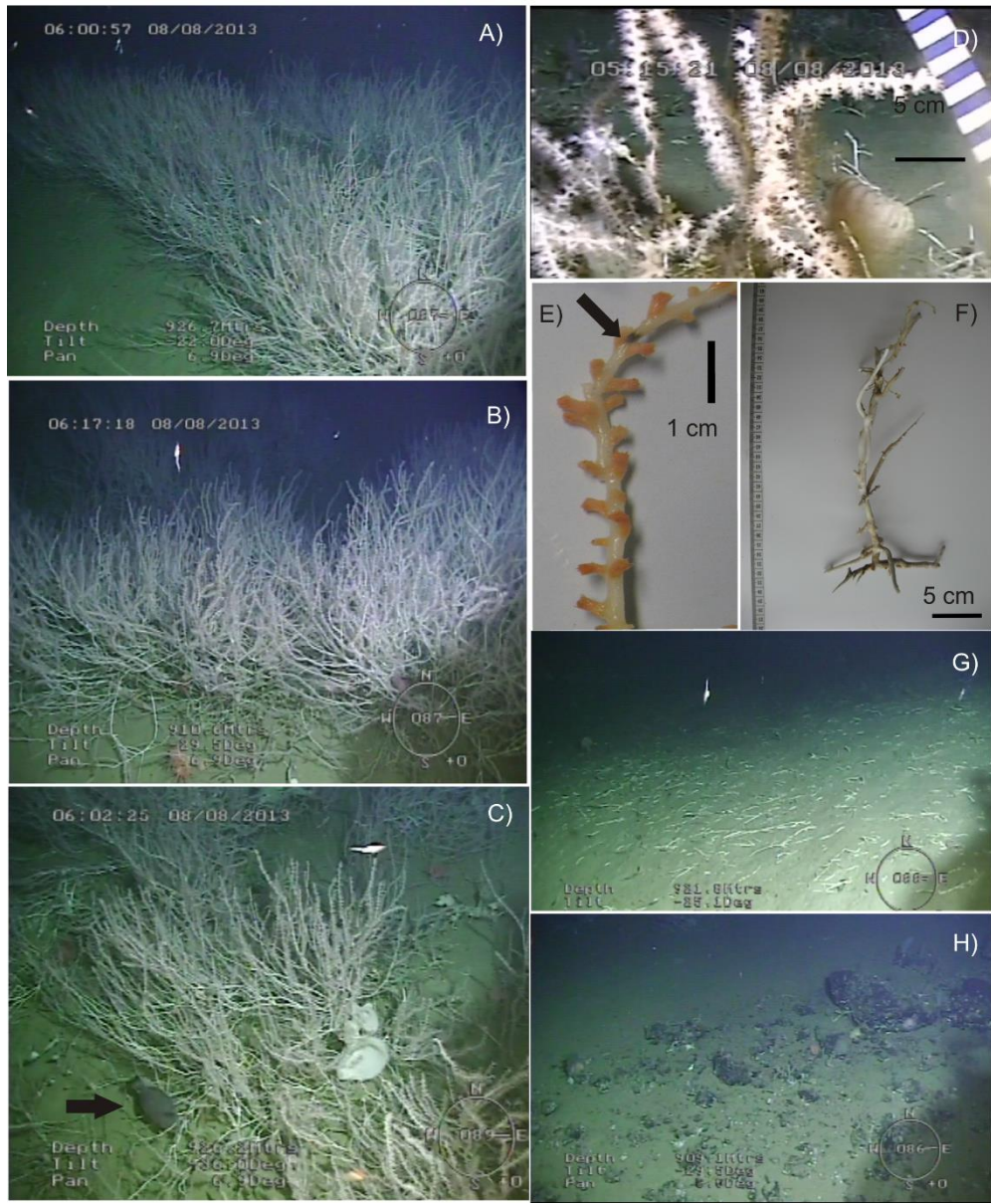


Figure 7-3. A-C) Forests of *Keratoisis* sp. “kerD2d” (arrow in C points to a flatfish), D) close up of polyps showing ruler used to estimate size, E) polyps and node (arrow), F) branched root-like structures, G) coral fragments close to the 1999 trawl path, and H) sparse rocks.

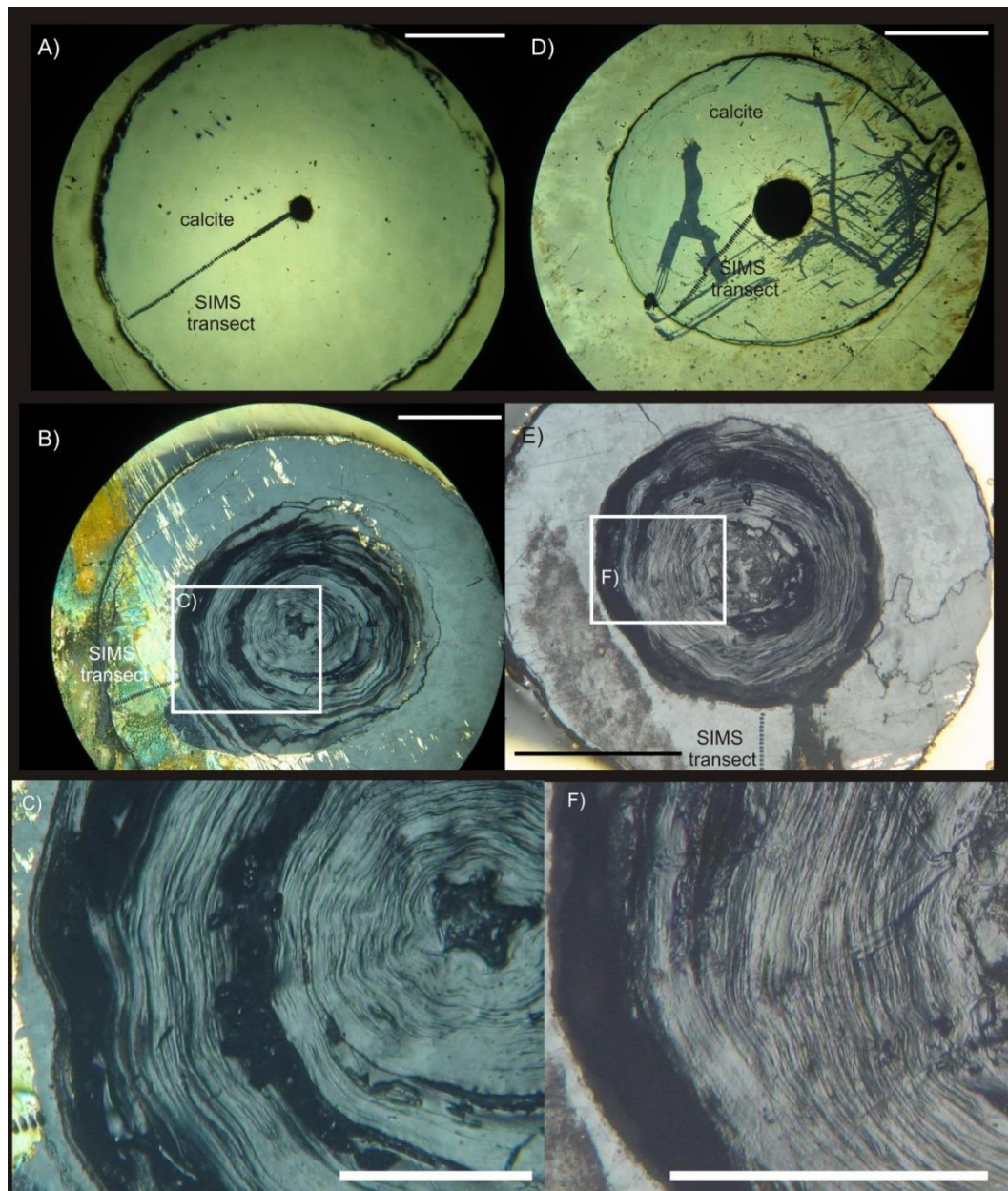


Figure 7-4. Cross section of the stem in *Keratoisis* sp. "kerD2d". A-C: sample 1, D-E: sample 2. Grey spots/stains in A and B are from the impregnated polishing liquid. Residues of the gold coating can still be seen in the samples (B and E), which were completely covered with gold before using acetone to dissolve the Krazy Glue™. Scale bars = 1 mm (A-B, D-E), and 0.5 mm (C and F).

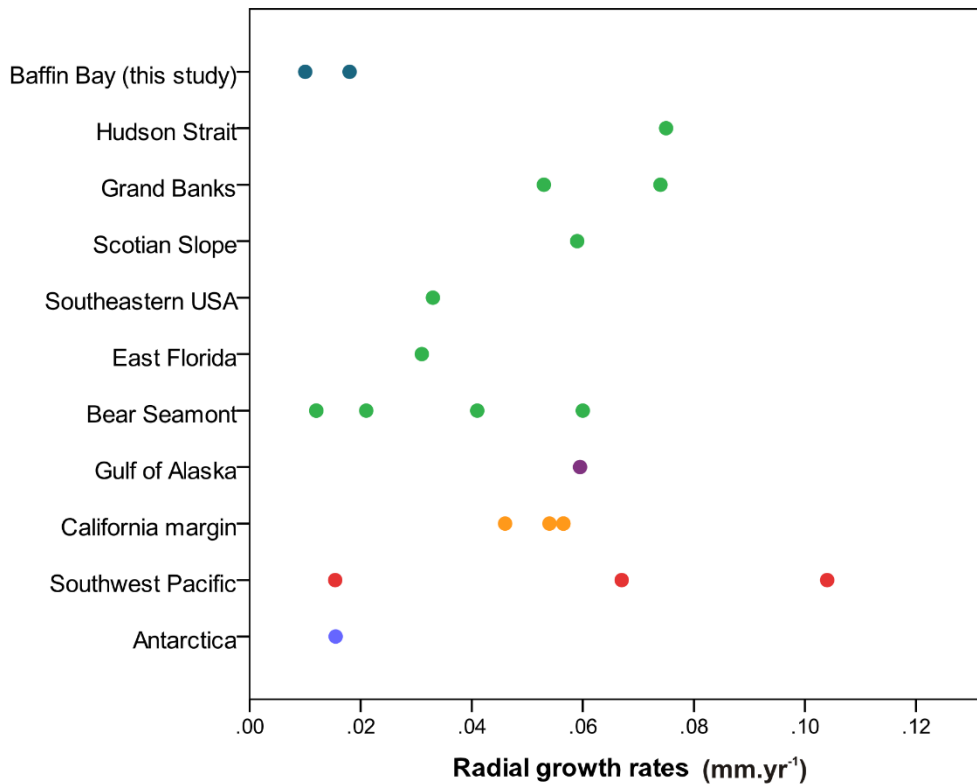


Figure 7-5. Comparison of radial growth rates among specimens of the genus *Keratoisis* from this study and published data. Growth rates from Andrews et al. (2009), Sherwood & Edinger (2009), Thresher (2009), Thresher et al. (2009), Hill et al. (2011), Sinclair et al. (2011), and Farmer et al. (2015). Values from Hudson Strait to Bear Seamount (green dots) are all from the North Atlantic region.

Table 7-1. Summary of trace element ratios (mmol·mol⁻¹) for the calcite of *Keratoisis* sp. “kerD2d”.

Me/Ca	Minimum	Maximum	Average ± SD
Sr/Ca	2.1	2.6	2.4 ± 0.09
Mg/Ca	65.6	113	77.7 ± 10.1
Na/Ca	21.2	45.6	29.2 ± 4.8
Ba/Ca	0.008	0.023	0.01 ± 0.00

In sample 1 (sides A and B) there was a negative correlation between Mg/Ca and Sr/Ca (1a Pearson's $r = -0.8$, 1b Pearson's $r = -0.18$), while a positive correlation was identified in sample 2 (2a Pearson's $r = 0.39$, 2b Pearson's $r = 0.67$) (Fig. 7-8).

The number of trace element cycles in the transects was not similar to the extrapolated number of growth rings for the calcite area (Table 7-2). The average number of peaks in trace element ratios in relation to the number of rings for sample 1b was 6.5, and for sample 2b was 6. Based on these samples, no clear trend can be identified in relation to trace elements and number of rings.

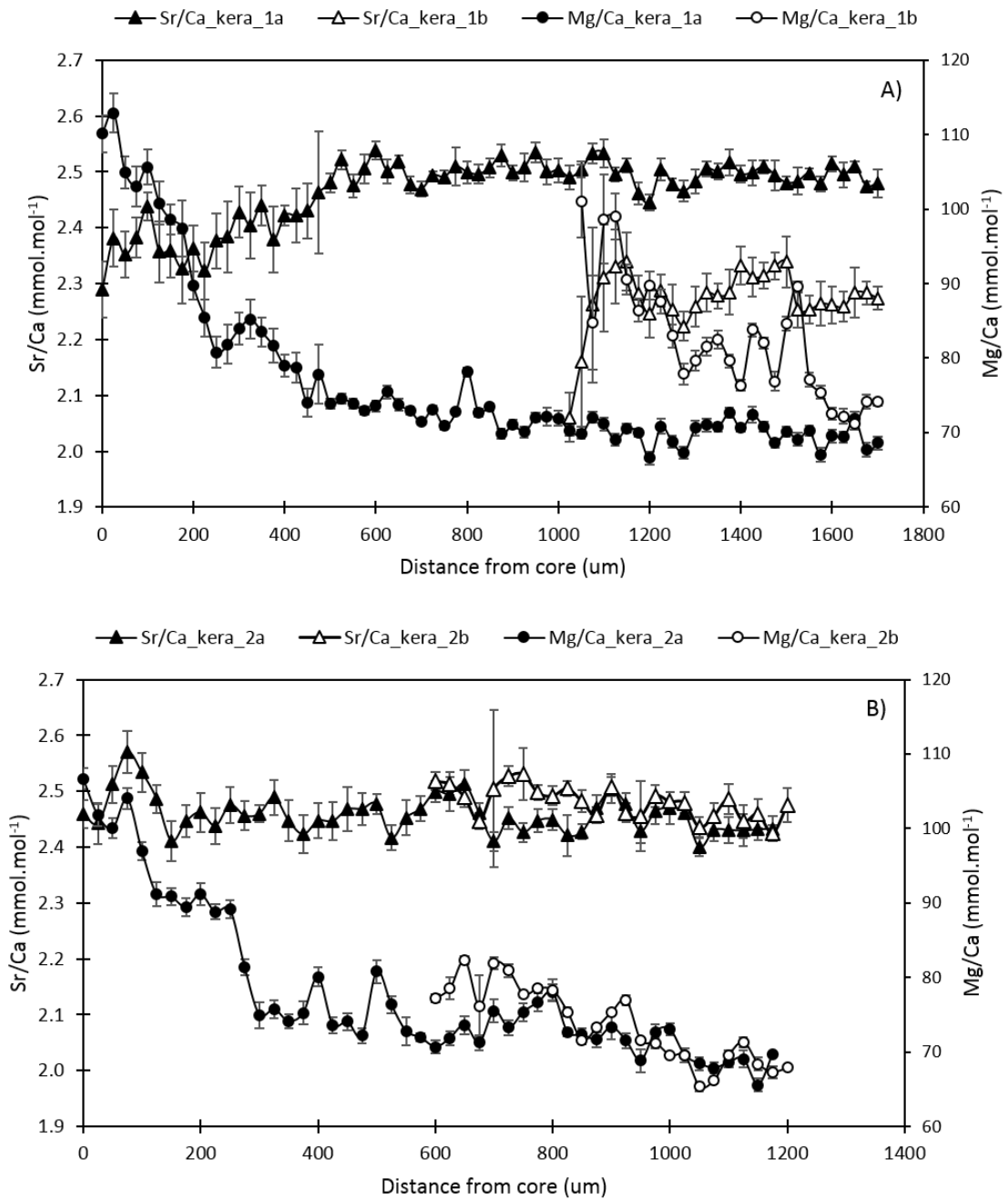


Figure 7-6. Trace elements/Ca ratios (Sr/Ca, Mg/Ca) in the calcite of *Keratoisis* sp. “kerD2d” in relation to distance from core for sample 1 (A) and 2 (B). Error bars are 1SD. Where error bars are not seen the error is smaller than the marker.

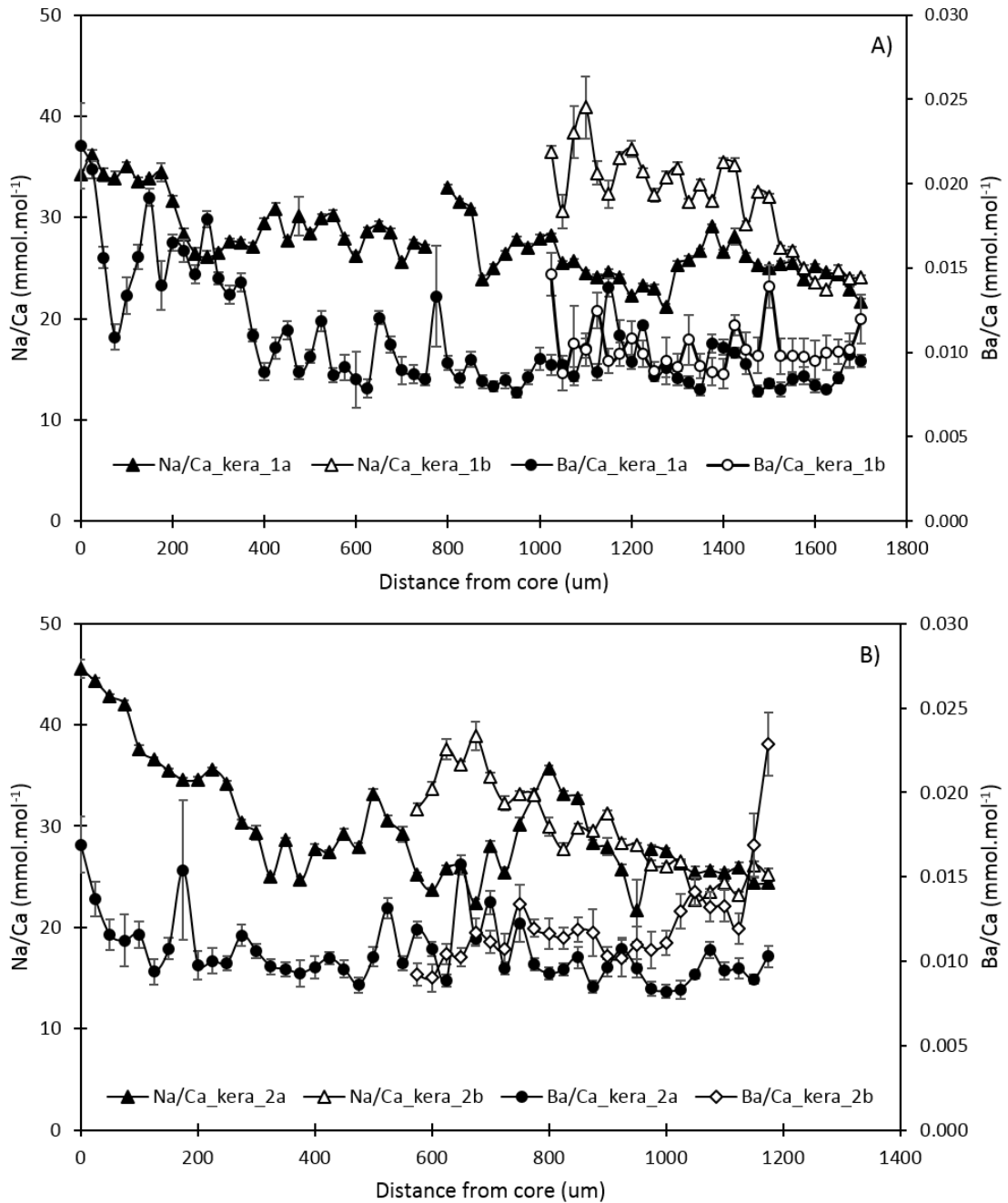


Figure 7-7. Trace elements/Ca ratios (Na/Ca, Ba/Ca) in the calcite of *Keratoisis* sp. “kerD2d” in relation to distance from core for sample 1 (A) and 2 (B). Error bars are 1SD. Where error bars are not seen the error is smaller than the marker.

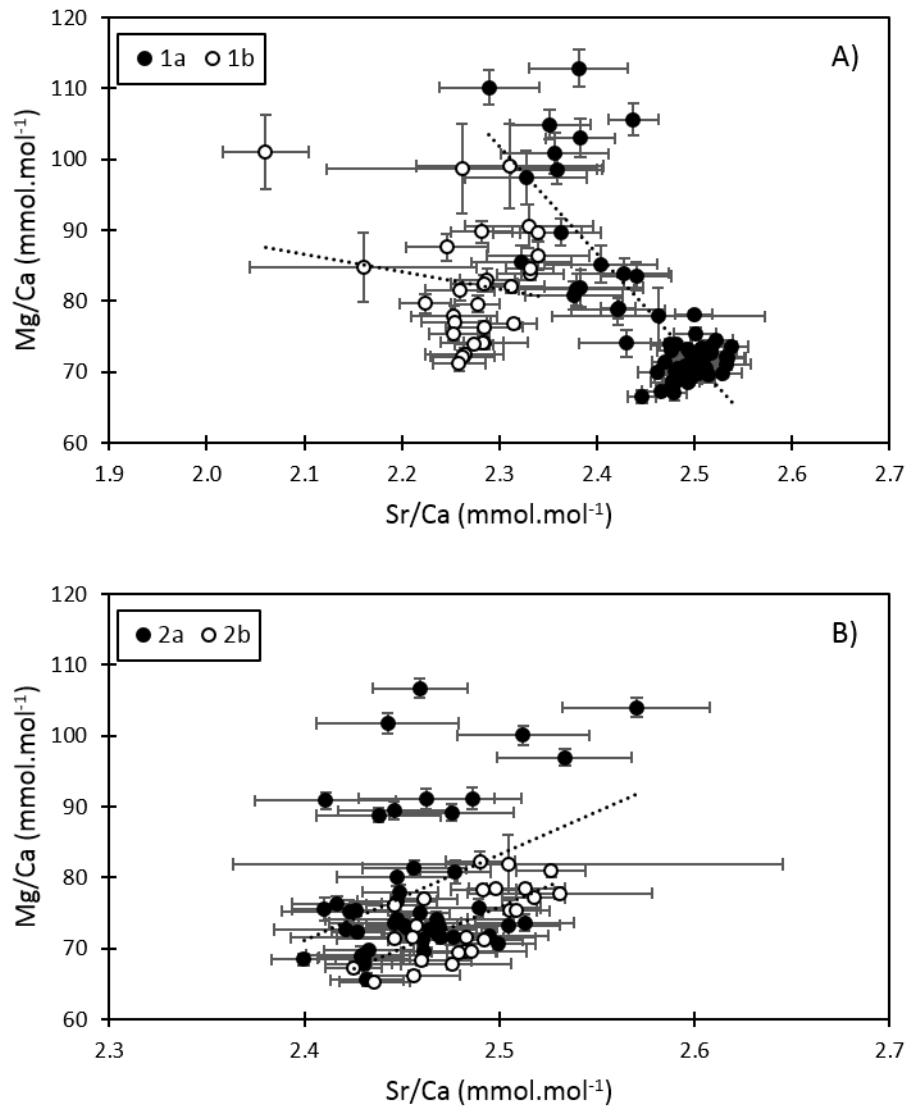


Figure 7-8. Relationships between Mg/Ca and Sr/Ca in the calcite of *Keratoisis* sp.

“kerD2d” stem in sample 1 (A) and 2 (B). Error bars are 1SD.

Table 7-2. Number of peaks in the trace elements in relation to the extrapolated number of growth rings in *Keratoisis* sp. “kerD2d”.

Sample id	Sr/Ca	Mg/Ca	Ba/Ca	Na/Ca	Average	Rings	Extrapolated	
						Gorgonin	Calcite	Total
1a	21	19	20	18	19.5	na	102.5	102.5
1b	5	6	8	7	6.5	59	43.5	102.5
2a	11	14	14	10	12.25	na	120	120
2b	7	5	5	7	6	43	77	120

7.3.6 Palaeotemperature estimation

Based on the equation by Sherwood et al. (2005), the calculated average water temperature ranged 2.6 ± 2.2 and 3.7 ± 1.6 °C for sample 1 (sides a and b, respectively), and 2.8 ± 2.1 and 1.9 ± 1 °C for sample 2 (sides a and b, respectively; Table 7-3, Fig. 7-9). In both samples, the calculated temperature (as the Mg/Ca profiles showed in fig. 7-6) decreased from the core to the edge of the sample, with the half closest to the edge having much more constant averaging 1.3-1.5 °C (samples 1a and 2a respectively; Fig. 7-9).

Table 7-3. Estimated water temperature (°C) from Mg/Ca ratios from the calcite of *Keratoisis* sp. “kerD2d” according to the equation by Sherwood et al. (2005).

Sample id	Minimum	Maximum	Average \pm SD
1a	0.5	9.8	2.6 ± 2.2
1b	1.4	7.4	3.7 ± 1.6
2a	0.3	8.5	2.8 ± 2.1
2b	0.3	3.7	1.9 ± 1.0

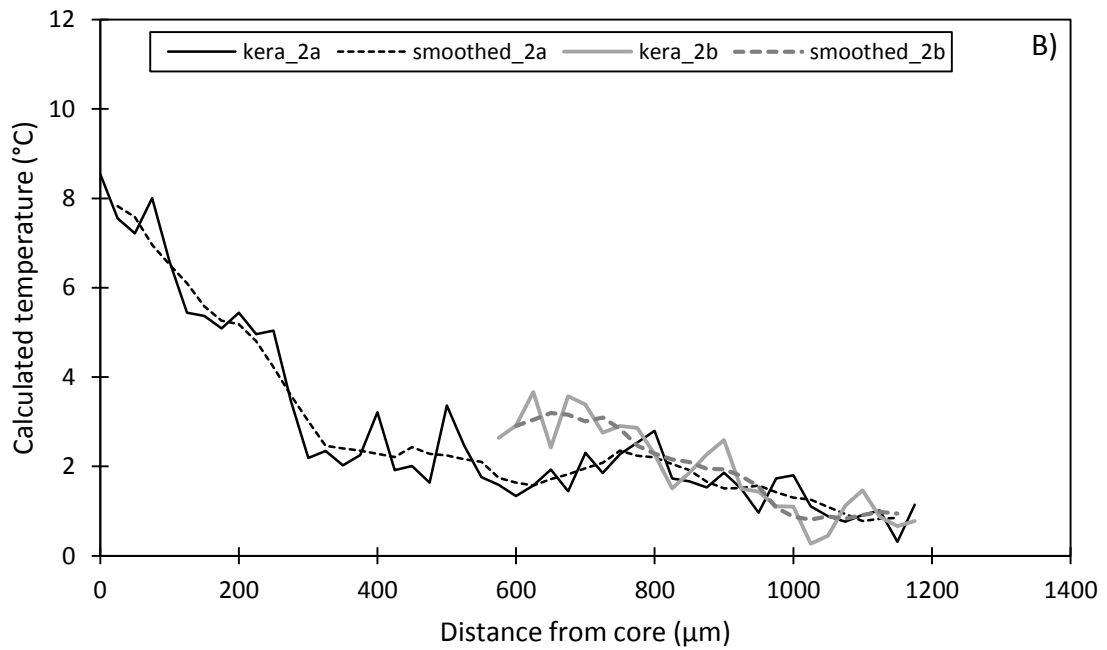
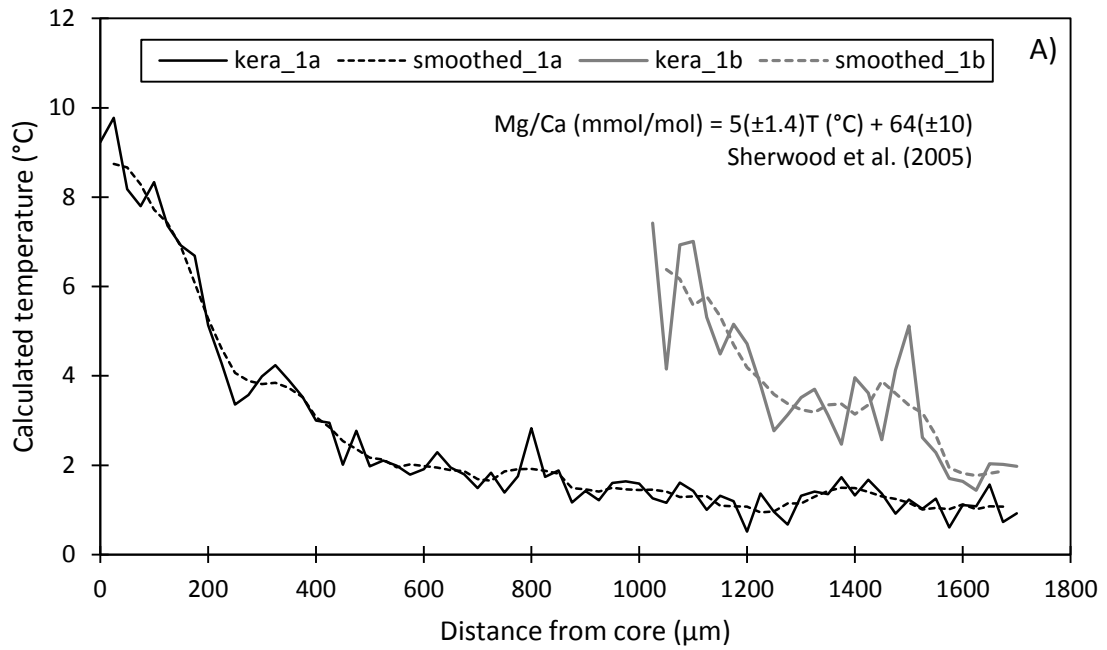


Figure 7-9. Estimated water temperature (°C) from Mg/Ca ratios from A) samples 1a-b, and B) samples 2a-b of *Keratoisis* sp. “kerD2d”, according to the equation by Sherwood et al. (2005). Smoothed lines produced using a moving average (5 intervals).

7.4 Discussion

7.4.1 Forests

The forests of *Keratoisis* sp. “kerD2d” described in this study are different from other *Keratoisis* observed *in situ* in the Newfoundland region, where they are commonly found attached to hard substrates by a single point of attachment, in a way that even when densely distributed, colonies can be distinguished from one another (Edinger et al., 2011). Interestingly, the bamboo coral *Isidella lofotensis* Sars, 1868 has been reported from East Greenland at depths of 751-807 m, also so densely distributed that individual colonies could not be distinguished (Mayer & Piepenburg, 1996).

The specific reasons for colonies being so particularly crowded are still to be investigated. NASA satellite data on surface chlorophyll a from the last 11 years (2002-2013) indicates that primary productivity in the area is not particularly high in comparison to surrounding locations (Appendix 7-2), and therefore an exceptional food availability should not be expected to explain the high density of *Keratoisis* sp. “kerD2d” in the area. On the other hand, their predisposition to a life on highly available soft sediments allowed by the root-like branches probably increases their chances of growing successfully.

Branched root-like structures as those observed in *Keratoisis* sp. “kerD2d” also occur in other species of deep-water octocorals, such as *Radicipes gracilis* (Verrill, 1884) and *Acanella arbuscula* (Johnson, 1862), and are considered to be related to a life on soft substrates (Deichmann, 1936, Bayer, 1973). Colonies appeared to be anchored directly in the mud, and were not seen attached to the sparse rocks observed (Fig. 7.3H). However,

the possibility that corals were initially attached to hard substrates and subsequently buried under mud cannot be excluded at the moment.

Because the base of the stem in these colonies is not very thick and not attached to a single point, having an overall thin and light body might actually allow the colony to better sustain itself above the soft sediment. Furthermore, colonies of *Keratoisis* spp. have hollow stems (Deichmann, 1936) that make colonies lighter, which may be an advantage in this setting. As mentioned earlier, *Keratoisis* spp. can also be found attached to hard substrates (e.g. bedrock, boulders) by a single point of attachment (Edinger et al., 2011), and in these colonies the stem is thicker and robust. The variation in colony growth forms might be related to local environmental conditions (e.g. substrate availability, and current strength/direction), which are still to be investigated.

Delicate chrysogorgiids (family Chrysogorgiidae) that inhabit soft bottoms can initiate growth attached to small objects (e.g. shell fragments). If these objects turn out to be too small as the colony grows, the colony has the ability to produce branching structures that anchor the colony in the soft bottom (Bayer, 1973), similarly to the observed in *Keratoisis* sp. “kerD2d”. At this point we cannot determine whether *Keratoisis* sp. “kerD2d” is a variation of a same *Keratoisis* species which live attached to hard substrates and have thicker branches, or if it is a different species.

Bottom temperature at 900 m was 1.1 °C, which is colder than the lower temperatures generally associated with occurrences for *Keratoisis* in southern Newfoundland (Baker et al., 2012), and for most cold-water gorgonian coral species (i.e. ≥ 4 °C (Tendal, 1992, Roberts et al., 2006). This is important, and it highlights the

possibility of colonies of *Keratoisis* being found at other sites in Baffin Bay, despite very low temperatures.

The surveyed location has been closed to Greenland Halibut fisheries since 2008 to protect narwhal overwintering grounds and corals located deeper than 500 m (Fig. 7.1B; DFO, 2007), although shrimp trawling on the continental shelf still occurs in environments shallower than 500 m (Tim Siferd, Fisheries and Oceans Canada, pers. comm. 2014).

The dense stands of *Keratoisis* sp. “kerD2d” at this location suggest they form structured habitat for other organisms, in this otherwise muddy environment (cf. Buhl-Mortensen et al., 2010). By contrast, the destruction of corals within the path of the 1999 trawl and lack of macroscopic evidence of recovery, emphasize the fragility of these coral habitats. In light of predicted expansion of bottom-contact fishing in Arctic waters (cf. Christiansen et al., 2014), previously undiscovered Arctic coral biodiversity urgently requires future investigation.

7.4.2 Growth rings and apparent rates

The calcite composition of the internode in *Keratoisis* sp. “kerD2d” was not surprising, as it has already been shown for other members of the family (e.g. Bostock et al., 2015). Assuming rings to be formed annually, we estimate an average radial growth rate of $0.014 \text{ mm}\cdot\text{yr}^{-1}$ in these specimens. These rates are considerably slower than those obtained by Sherwood & Edinger (2009) from *Keratoisis grayi* from the Southwest Grand Banks and East Hudson Strait areas ($0.053\text{-}0.075 \text{ mm}\cdot\text{yr}^{-1}$). But Farmer et al. (2015) found that growth rates in *Keratoisis* spp. from the Bear Seamount (NW Atlantic) ranged

0.012-0.078 mm·yr⁻¹, with two specimens with radial growth rates of 0.012 mm·yr⁻¹ during some period of their lives. Our oldest estimates of longevity were of ~60 years considering the gorgonin portion only, and 120 years when extrapolating to the calcite region as well, which is not uncommon for deep-water isidids (e.g. Sherwood & Edinger, 2009, Thresher 2009, Thresher et al., 2009).

Despite the very slow growth rates and the very low temperatures associated to the environment where samples were collected, a relationship between these two variables might not be real. Farmer et al. (2015) found no evidence of the influence of temperature on growth rates in *Keratoisis* spp. Instead, these authors suggested that ontogenetic factors are likely to be the main drivers of growth rates in these organisms. For instance, their two specimens growing at a similar rate to what we estimated here from ~1 °C were collected from sites where temperatures were 3.3 and 4.2 °C, and *Keratoisis* from locations with temperatures of -0.4 and 2 °C had growth rates of 0.015 mm·yr⁻¹ (Thresher, 2009).

7.4.3 Trace elements analysis

In terms of the trace elements analysis, the ratios for *Keratoisis* sp. “kerD2d” were similar to those found in the axis of the sea pens *Halopteris finmarchica* (Sars, 1851) (Chapter 2) and *Umbellula encrinus* Linnaeus, 1758 (Chapter 3), with only Sr/Ca showing slightly higher ratios in *Keratoisis* sp. “kerD2d” than in these two other species. But considering that these are different species from different depths and possible different life stages, it is expected to find some variation in these ratios simply due to vital effects (Gagnon et al., 2007, Robinson et al., 2014). The Sr/Ca values from *Keratoisis* sp.

were closer to those obtained from the calcite of the gorgonian *Primnoa pacifica* Kinoshita, 1907 (Aranha et al., 2014), and similar in magnitude to those from *Keratoisis* sp., *Paragorgia* spp., and *Lepidisis* spp. from New Zealand (Bostock et al., 2015), which might be related to the nature of the skeleton in these species. Whereas the axis of *Umbellula encrinus* can be up to 71% carbonate material with a large fraction of organic material (Chapter 5), the carbonate portion of the skeletons in these gorgonians is almost pure carbonate (Bostock et al., 2015, Appendix 7-1).

While there was a negative correlation between Mg/Ca and Sr/Ca in sample 1 and in the sea pens (Chapters 2-3), a positive correlation between these variables was found for sample 2, which is usually not expected based on a known negative relationship between these two variables in biogenic calcite (Kinsman, 1969, Hart & Cohen, 1996, Mitsuguchi et al., 2003). However, in benthic Foraminifera both Sr/Ca and Mg/Ca had positive relationships with water temperature (Rathburn & De Deckker, 1997), and in some deep-sea corals Sr is not negatively correlated with Mg (Sinclair et al., 2006). By examining the supplementary material data from Bostock et al. (2015) on *Keratoisis* spp. from New Zealand, the relationship Sr/Ca-Mg/Ca did not have a negative correlation (inter-colony comparison), but rather an undefined pattern.

Although fragments still had live polyps on them, it is possible that the fragment showing the positive Mg/Ca-Sr/Ca relationship came from a partially dead colony, where the polyps were no longer influencing skeletal deposition. In fact, some of the samples were collected from a cluster of fragments laying on the sea floor. Therefore, these results could also be interpreted as a potential evidence of diagenetic alteration in sample 2.

Alternatively, the presence of a negative relationship in one sample, but a positive relationship in another sample can perhaps indicate that in this coral and setting Sr and Mg precipitation might not be mainly controlled by environmental variables. The precipitation of Sr in several carbonates has been related to factors other than environmental, such as growth rates and age, or even photosynthetic activity of zooxanthellae in the case of shallow-water corals (de Villiers et al., 1995, Stecher et al., 1996, Cohen et al., 2001, Heikoop et al., 2002). In other cases Mg/Ca ratios were independent of growth rates (Mitsuguchi et al., 2003), being strongly related or influenced by water temperature. Both Mg/Ca and Na/Ca ratios decreased with distance from the core, and Sr/Ca ratios increased with distance from core only in sample 1.

The better correspondence in the magnitude of trace element ratio values between sides A and B in sample 2 than in sample 1 might simply reflect a better alignment of transects in the two sides of the former. This would indicate an intra-colony variation in the trace element ratios, which highlights the importance of sampling from different parts of the organism. Intra-colony variation has been reported for the isotopic composition of other bamboo corals (Hill et al., 2011). It is possible that our samples represent fragments from different parts of a colony, and the difference in the trace element ratios between samples could be associated to the vital effects reported by Hill et al. (2011).

Differently from the results on the trace element analysis in sea pens, the number of peaks in the trace element ratios in the calcite of *Keratoisis* sp. “kerD2d” was not comparable to the number of growth rings estimated from the gorgonin portion. This indicates a non-correspondence between the pattern in trace elements distribution in the

calcite and in the gorgonin portion of the skeleton, but this can also be a result of ring width being thinner than the SIMS spots.

7.4.4 Palaeotemperature estimation

Although average water temperature estimated from Mg/Ca ratios ranged 1.94-3.67 °C, the full range included temperatures of up to 7 °C in the first μm of the sample, with a marked decrease with distance from core. Thresher et al. (2004) also found a decrease in Mg/Ca ratios with distance from core in *Keratoisis* sp., and a consequent decrease in estimated water temperature. It is unlikely that at our study site and depth (900 m) temperature in the past 100 years has reached 7 °C. For instance, in East Davis Strait mean water temperature between 1950 and 2000 (at 66.67°N, 56.68°W) had a maximum value <4.5 °C at 500 m (Tang et al., 2004); and bottom temperature data for the region (up to 50 km from the study site) between the years 1928-1990, for depths ranging 500-1345 m had a maximum temperature of 3.7 °C in September (N= 15, Boyer et al., 2013).

On the other hand, when only considering temperatures estimated from the Mg/Ca ratios determined for the half closest to the edge, temperature averaged 1.3-1.5 °C (samples 1a and 2a, respectively), which are close to the bottom temperatures at the time of collection (1.1 °C). This could indicate that Mg/Ca ratios in this coral are not a function of temperature in the first years of life, when other factors might have a stronger influence on this ratio (e.g. growth rates). We have also applied our Mg/Ca data to a recently published palaeotemperature equation based on Mg/Ca ratios from the skeletons

of isidid octocorals from the southern hemisphere (Thresher et al., 2016). Despite the fact that this equation was produced based on organisms more closely related to our *Keratoisis* sp. (same family), the average estimated temperature was one degree colder than that estimated using the primnoid equation by Sherwood et al. (2005). This difference of one degree is smaller than the margin of error in the isidid palaeotemperature equation (Thresher et al., 2016).

Therefore, the skeleton of *Keratoisis* “kerD2d” might have a potential as a palaeoceanographic proxy, although this interpretation should be taken with caution, as more knowledge on the influence of ontogeny and vital effects on the precipitation of calcite in this coral is still needed. Microanalysis certainly seems valuable in assessing *Keratoisis* “kerD2d” in this environment, where the later growth zones may provide the most accurate records of palaeotemperature.

Acknowledgements

We thank the Captain and crew of CCGS *Amundsen* and the Canadian Coast Guard, chief scientist Louis Fortier, ROV pilots Ian Murdock and Trevor Shepherd. We also thank Glenn Piercey for the SIMS analysis. This manuscript was improved by the comments of three anonymous reviewers. This study was funded by the Natural Sciences and Engineering Research Council of Canada (NSERC) doctoral scholarship to BMN, NSERC Discovery Grant to CHM, Canadian Healthy Oceans Network (CHONe), a university-government partnership dedicated to biodiversity science for the sustainability

of Canada's three oceans, Network of Centres of Excellence of Canada ArcticNet, and the NSERC MRS grant to the Canadian Scientific Submersible Facility (CSSF).

7.6 References

Andrews, A. H., R. P. Stone, C. C. Lundstrom & A. P. DeVogelaere, 2009. Growth rate and age determination of bamboo corals from the northeastern Pacific Ocean using refined ^{210}Pb dating. *Marine Ecology Progress Series* 397: 173-185.

Aranha, R., E. Edinger, G. Layne & G. Piercey, 2014. Growth rate variation and potential paleoceanographic proxies in *Primnoa pacifica*: Insights from high-resolution trace element microanalysis. *Deep Sea Research Part II: Topical Studies in Oceanography* 99: 213-226.

Baker, K. D., V. E. Wareham, P. V. R. Snelgrove, R. L. Haedrich, D. A. Fifield, E. N. Edinger & K. D. Gilkinson, 2012. Distributional patterns of deep-sea coral assemblages in three submarine canyons off Newfoundland, Canada. *Marine Ecology Progress Series* 445: 235-249.

Bayer, F. M., 1973. Colonial organization in octocorals. In Boardman, R. S., A. H. Cheetham & W. A. Oliver (eds), *Animal colonies: Development and function through time*. Dowden, Hutchinson, and Ross, Stroudsburg, PA: 69-93.

Berntson, E. A. & S. C. France, 2001. Generating DNA sequence information from museum collections of octocoral specimens (Phylum Cnidaria: Class Anthozoa). *Bulletin of the Biological Society of Washington* 10: 119-129.

Bilewitch, J. P. & S. M. Degnan, 2011. A unique horizontal gene transfer event has provided the octocoral mitochondrial genome with an active mismatch repair gene that has potential for an unusual self-contained function. *BMC Evolutionary Biology* 11: 228.

Bostock, H. C., D. M. Tracey, K. I. Currie, G. B. Dunbar, M. R. Handler, S. E. M. Fletcher, A. M. Smith & M. J. M. Williams, 2015. The carbonate mineralogy and distribution of habitat-forming deep-sea corals in the southwest pacific region. *Deep Sea Research Part I: Oceanographic Research Papers* 100: 88-104.

Boyer, T. P., J. I. Antonov, O. K. Baranova, C. Coleman, H. E. Garcia, A. Grodsky, D. R. Johnson, R. A. Locarnini, A. V. Mishonov, T. D. O'Brien, C. R. Paver, J. R. Reagan, D. Seidov, I. V. Smolyar & M. M. Zweng, 2013. *World Ocean Database 2013*, NOAA Atlas NESDIS 72, Silver Spring, MD.

Brugler, M. R. & S. C. France, 2008. The mitochondrial genome of a deep-sea bamboo coral (Cnidaria, Anthozoa, Octocorallia, Isididae): genome structure and putative origins of replication are not conserved among octocorals. *Journal of Molecular Evolution* 67: 125-136.

Buhl-Mortensen, L., A. Vanreusel, A. J. Gooday, L. A. Levin, I. G. Priede, P. Buhl-Mortensen, H. Gheerardyn, N. J. King & M. Raes, 2010. Biological structures as a source of habitat heterogeneity and biodiversity on the deep ocean margins. *Marine Ecology* 31: 21-50.

Christiansen, J. S., C. W. Mecklenburg & O. V. Karamushko, 2014. Arctic marine fishes and their fisheries in light of global change. *Global Change Biology* 20: 352-359.

Cohen, A. L., G. D. Layne, S. R. Hart & P. S. Lobel, 2001. Kinetic control of skeletal Sr/Ca in a symbiotic coral: Implications for the paleotemperature proxy. *Paleoceanography* 16: 20-26.

de Villiers, S., B. K. Nelson & A. R. Chivas, 1995. Biological controls on coral Sr/Ca and $\delta^{18}\text{O}$ reconstructions of sea surface temperatures. *Science* 269: 1247-1249.

- Deichmann, E., 1936. The Alcyonaria of the western part of the Atlantic Ocean. *Memoirs of the Museum of Comparative Zoology* 53: 1-317.
- DFO, 2007. Development of a closed area in NAFO OA to protect Narwhal overwintering grounds, including deep-sea corals. DFO CSAS Sic. Resp. 2007/002
- Edinger, E. N., O. A. Sherwood, D. J. W. Piper, V. E. Wareham, K. D. Baker, K. D. Wilkinson & D. B. Scott, 2011. Geological features supporting deep-sea coral habitat in Atlantic Canada. *Continental Shelf Research* 31: S69-S84.
- Farmer, J. R., L. F. Robinson & B. Hönisch, 2015. Growth rate determinations from radiocarbon in bamboo corals (genus *Keratoisis*). *Deep Sea Research Part I: Oceanographic Research Papers* 105: 26-40.
- France, S. C., 2007. Genetic analysis of bamboo corals (Cnidaria: Octocorallia: Isididae): does lack of colony branching distinguish *Lepidisis* from *Keratoisis*? *Bulletin of Marine Science* 81: 323-333.
- Gagnon, A. C., J. F. Adkins, D. P. Fernandez & L. F. Robinson, 2007. Sr/Ca and Mg/Ca vital effects correlated with skeletal architecture in a scleractinian deep-sea coral and the role of Rayleigh fractionation. *Earth and Planetary Science Letters* 261: 280-295.
- Gass, S. E. & J. H. M. Willison, 2005. An assessment of the distribution of deep-sea corals in Atlantic Canada by using both scientific and local forms of knowledge: 223-245.
- Hart, S. R. & A. L. Cohen, 1996. An ion probe study of annual cycles of Sr/Ca and other trace elements in corals. *Geochimica et Cosmochimica Acta* 60: 3075-3084.

Heikoop, J. M., D. D. Hickmott, M. J. Risk, C. K. Shearer & V. Atudorei, 2002. Potential climate signals from the deep-sea gorgonian coral *Primnoa resedaeformis*. *Hydrobiologia* 471: 117-124.

Hill, T.M., H.J. Spero, T. Guilderson, M. Lavigne, D. Clague, S. Macallelo, & N. Jang, 2011. Temperature and vital effect controls on bamboo coral (Isididae) isotope geochemistry: A test of the “lines method”. *Geochemistry, Geophysics, Geosystems* 12(4): Q4008.

Jørgensen, O.A. & N. Hammeken Arboe, 2013. Distribution of the commercial fishery for Greenland halibut and northern shrimp in Baffin Bay. Pinngortitaleriffik, Greenland Institute of Natural Resources Technical Report no. 91.

Kinsman, D. J. J., 1969. Interpretation of Sr²⁺ concentrations in carbonate minerals and rocks. *Journal of Sedimentary Research* 39: 486-508.

Mayer, M. & D. Piepenburg, 1996. Epibenthic community patterns on the continental slope off East Greenland at 75 N. *Marine Ecology Progress Series* 143: 151-164.

Mitsuguchi, T., E. Matsumoto & T. Uchida, 2003. Mg/Ca and Sr/Ca ratios of *Porites* coral skeleton: Evaluation of the effect of skeletal growth rate. *Coral Reefs* 22: 381-388.

Murillo, F.J., M.P. Durán, A. Altuna & A. Serrano, 2011. Distribution of deep-water corals of the Flemish cap, Flemish pass, and the Grand banks of Newfoundland (Northwest Atlantic Ocean): Interaction with fishing activities. *ICES Journal of Marine Science: Journal du Conseil* 68(2): 319-332.

Neves, B. M., E. Edinger, C. Hillaire-Marcel, E. Saucier, S. C. France, M. A. Treble & V. E. Wareham, 2014. Deep-water bamboo coral forests in a muddy arctic environment. *Marine Biodiversity* 45(4): 867-871.

Pante, E., S.C. France, A. Couloux, C. Cruaud, C.S. McFadden, S. Samadi & L. Watling, 2012. Deep-sea origin and in-situ diversification of chrysogorgiid octocorals. PLoS ONE 7(6): e38357. doi:10.1371/journal.pone.0038357.

Rathburn, A. E. & P. De Deckker, 1997. Magnesium and strontium compositions of recent benthic Foraminifera from the Coral Sea, Australia and Prydz Bay, Antarctica. Marine Micropaleontology 32: 231-248.

Roberts, J. M., A. J. Wheeler & A. Freiwald, 2006. Reefs of the deep: the biology and geology of cold-water coral ecosystems. Science 312: 543-547.

Roberts, J. M., A. Wheeler, A. Freiwald & S. Cairns, 2009. Cold-water corals: the biology and geology of deep-sea coral habitats. Cambridge University Press, Cambridge, UK; New York.

Robinson, L. F., J. F. Adkins, N. Frank, A. C. Gagnon, N. G. Prouty, E. Brendan Roark & T. v. de Flierdt, 2014. The geochemistry of deep-sea coral skeletons: A review of vital effects and applications for palaeoceanography. Deep Sea Research Part II: Topical Studies in Oceanography 99: 184-198.

Sherwood, O.A., Heikoop, J.M., Sinclair, D.J., Scott, D.B.; Risk, M.J., Shearer, C. & Azetsu-Scott, K., 2005. Skeletal Mg/Ca in *Primnoa resedaeformis*: relationship to temperature. In: Freiwald, A., Murray, J.M. (Eds.), Cold-Water Corals and Ecosystems. Springer, Berlin, pp. 1061-1079.

Sherwood, O. A. & E. N. Edinger, 2009. Ages and growth rates of some deep-sea gorgonian and antipatharian corals of Newfoundland and Labrador. Canadian Journal of Fisheries and Aquatic Sciences 66: 142-152.

Sinclair, D., B. Williams & M. Risk, 2006. A biological origin for climate signals in corals—Trace element “vital effects” are ubiquitous in Scleractinian coral skeletons.

Geophysical Research Letters 33.

Sinclair, D. J., B. Williams, G. Allard, B. Ghaleb, S. Fallon, S. W. Ross & M. Risk, 2011. Reproducibility of trace element profiles in a specimen of the deep-water bamboo coral *Keratoisis* sp. *Geochimica et Cosmochimica Acta* 75: 5101-5121.

Stecher, H. A., D. E. Krantz, C. J. Lord, G. W. Luther & K. W. Bock, 1996. Profiles of strontium and barium in *Mercenaria mercenaria* and *Spisula solidissima* shells.

Geochimica et Cosmochimica Acta 60: 3445-3456.

Tang, C. C. L., C. K. Ross, T. Yao, B. Petrie, B. M. DeTracey & E. Dunlap, 2004. The circulation, water masses and sea-ice of Baffin Bay. *Progress in Oceanography* 63: 183-228.

Tendal, O. S., 1992. The North Atlantic distribution of the octocoral *Paragorgia arborea* (L., 1758) (Cnidaria, Anthozoa). *Sarsia* 77: 213-217.

Thresher, R., S. R. Rintoul, J. A. Koslow, C. Weidman, J. Adkins & C. Proctor, 2004. Oceanic evidence of climate change in southern Australia over the last three centuries. *Geophysical Research Letters* 31: L07212.

Thresher, R. E., 2009. Environmental and compositional correlates of growth rate in deep-water bamboo corals (Gorgonacea; Isididae). *Marine Ecology Progress Series* 397: 187-196.

Thresher, R. E., C. M. MacRae, N. C. Wilson & S. Fallon, 2009. Feasibility of age determination of deep-water bamboo corals (Gorgonacea; Isididae) from annual cycles in

skeletal composition. *Deep Sea Research Part I: Oceanographic Research Papers* 56: 442-449.

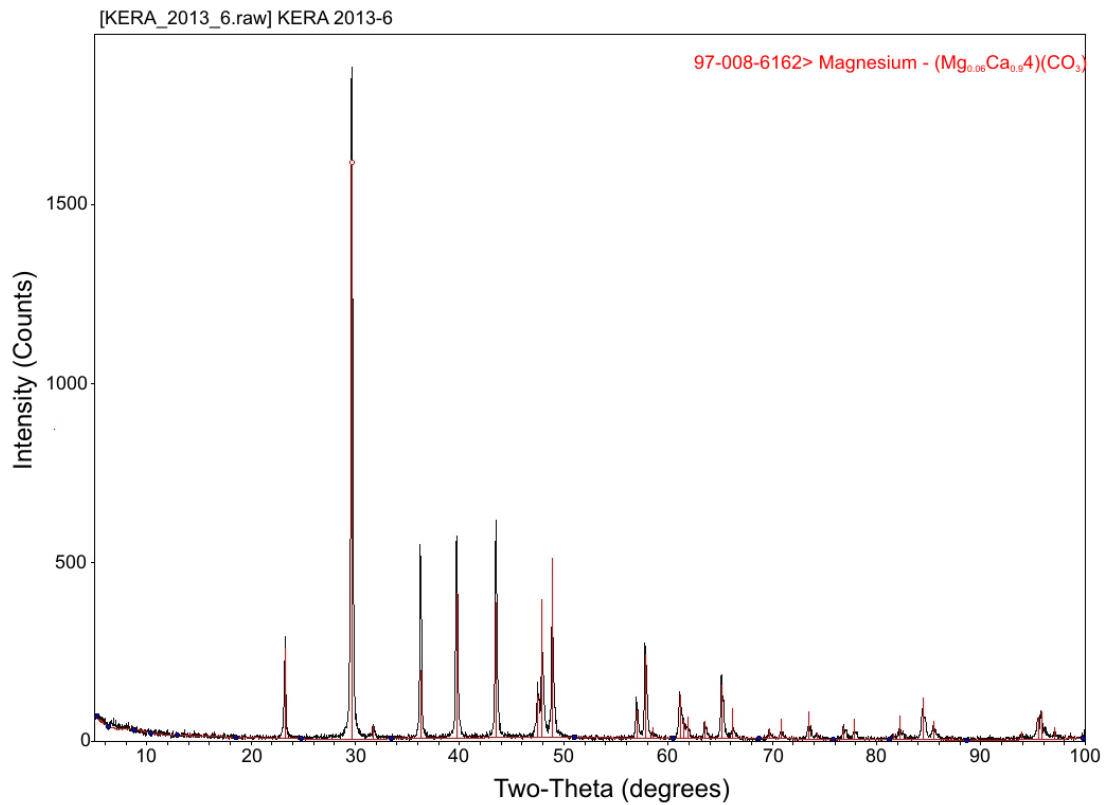
Treble, M.A., W.B. Brodie, & D. Power, 2003. Summary of data from the offshore Canadian commercial fishery for Greenland halibut. NAFO SCR Doc. 03/50. Serial No. N4868: 19.

Wareham, V. E., 2009. Updates on deep-sea coral distributions in the Newfoundland and Labrador and Arctic Regions, Northwest Atlantic. In Gilkinson, K. & E. Edinger (eds), *The ecology of deep-sea corals of Newfoundland and Labrador waters: biogeography, life history, biogeochemistry, and relation to fishes*. Canadian Technical Report on Fisheries Aquatic Sciences. 2830: vi + 136 p.

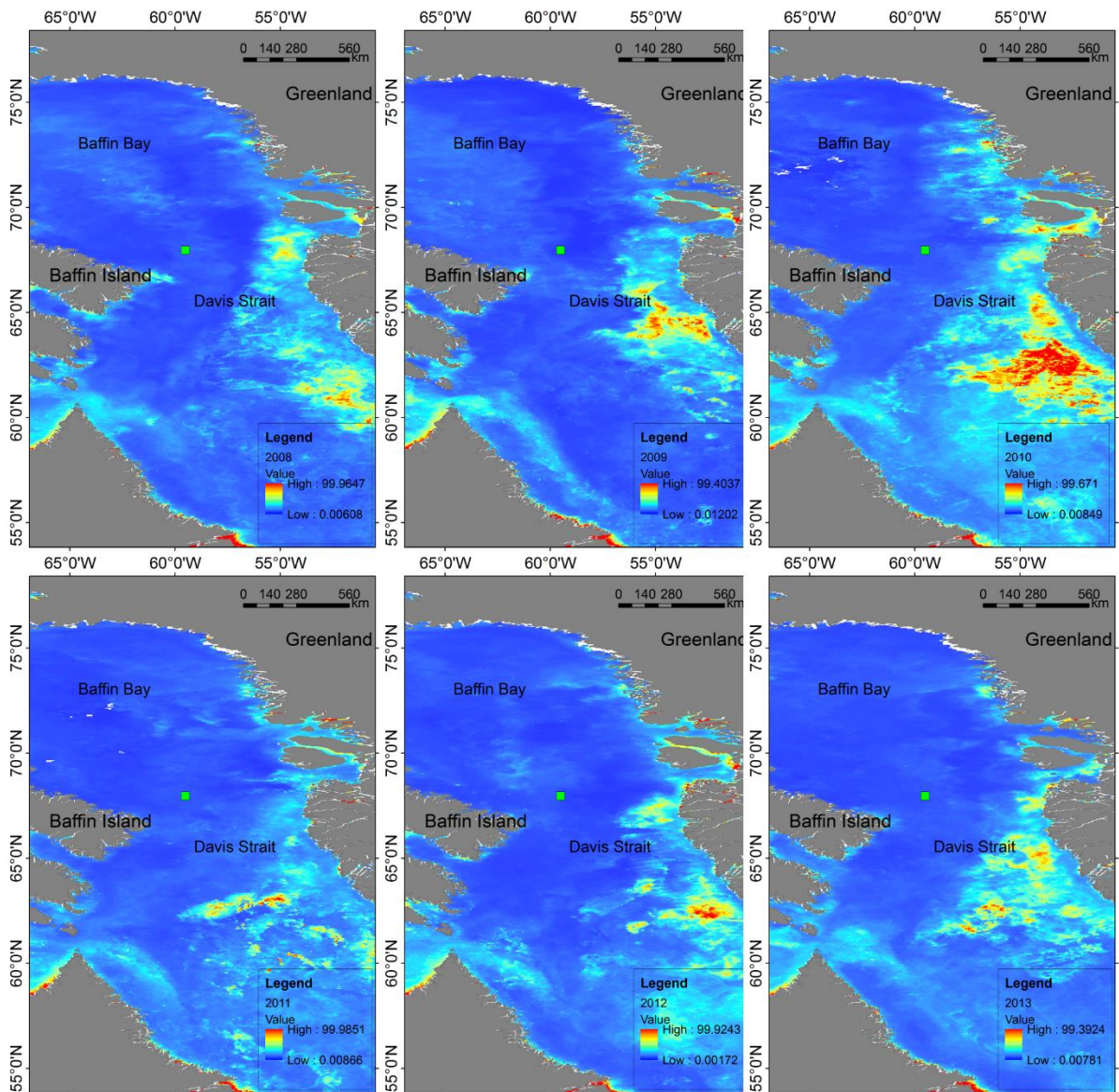
Wareham, V. E. & E. N. Edinger, 2007. Distribution of deep-sea corals in the Newfoundland and Labrador region, Northwest Atlantic Ocean. *Bulletin of Marine Science* 81: 289-313.

Watling, L., S. C. France, E. Pante & A. Simpson, 2011. Chapter Two - Biology of Deep-Water Octocorals. In Michael Lesser (ed), *Advances in Marine Biology*. Academic Press: 41.

Appendix 7-1 X-Ray Diffraction analysis for the carbonate portion of the stem in *Keratoisis* sp. (“kerD2d”). Overlap between the stem in *Keratoisis* sp. (black) and magnesian calcite (red). Note that the stem of *Keratoisis* sp. follows the same pattern as magnesian calcite.



Appendix 7-2 Annual surface chlorophyll a from the MODIS sensor in the Aqua satellite for the years 2008-2013, for Baffin Bay near the sampled site (central green square). Red represents the highest values for chlorophyll a, while dark blue represents the lowest values. Data from NASA Goddard Space Flight Center, Ocean Biology Processing Group (2015).



8. General conclusions

8.1 Growth rates

Overall, average radial growth rates in sea pens were similar among different genera from different locations and depths. Species as morphologically different as the feather-shaped *Pennatula grandis* Ehrenberg, 1834, the whip-shaped *Halipteris finmarchica* (Sars, 1851) and the tall *Umbellula encrinus* Linnaeus, 1758 all have similar radial growth rates. However, they are slower than the potential estimated for the gorgonians *Primnoa* spp. (Fig. 8.1A). Faster radial growth rates in *Primnoa pacifica* Kinoshita, 1907 and *Primnoa resedaeformis* (Gunnerus, 1763) than in sea pens are probably related to the thickest stems produced by these gorgonians, which can have much wider diameters than sea pens.

On the other hand, when looking at linear growth rates, *H. finmarchica* and *U. encrinus* had faster growth rates than *P. grandis* and *Primnoa*, which had more comparable ranges (Fig. 8.1B). All these species have growth rings and longevities reaching decades and/or centuries (Chapters 2-6). *Primnoa* spp. can reach sizes >2 m, but so can *U. encrinus* (Chapters 3 and 5) and species in the genus *Halipteris* (e.g. Brodeur, 2001).

Sea pens and gorgonians have very different growth forms and life styles: sea pens are unbranched, and have a muscular peduncle that anchors them in the substrate (mostly soft), while most gorgonians live directly attached to hard substrates and can display varied shapes and forms. Therefore, comparing growth rates in these quite distinct organisms is interesting from the point of view of summarizing growth rates in

octocorals, but interpretations about the differences/similarities in growth rates among these taxa should be taken cautiously.

Growth rates in the two compared species of *Primnoa* (*P. pacifica* and *P. resedaeformis*) were not statistically different, which contrasts to previous studies where they have been suggested to be different (e.g. Sherwood & Edinger, 2009, Aranha et al., 2014). In these previous studies, the average growth rates from different locations and usually from a low number of observations were compared.

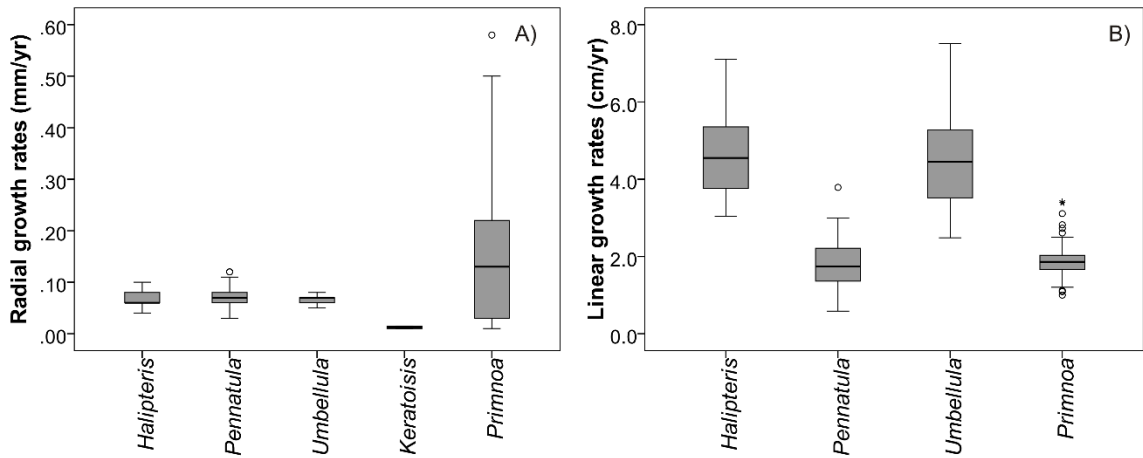


Figure 8-1. A) radial and B) linear growth rates in the four genera included in this study, including *Halipteris finmarchica*, *H. willemoesi* (Wilson et al., 2002), *Pennatula grandis*, *Umbellula encrinus*, *Keratoisis* sp. (radial growth rates only), *Primnoa pacifica* and *P. resedaeformis*.

Colony size seems to have an important influence in growth rates in these organisms, and by not controlling for it extreme growth rates in two specimens might be erroneously associated to external factors, when it might not be the case. Rates might be different because of ontogeny, and not mainly because of environmental conditions. That

being said, environmental factors do influence these organisms, and in several of the analyses I performed, certain environmental variables had a statistically significant relationship to growth rates. However, none of them was obvious and striking, in any of the studied species.

In Chapter 4 I showed that diametric growth rates in *P. grandis* were very similar to those estimated for other sea pens (*Halipteris* spp. and *U. encrinus*), but that linear growth rates were slower than those and similar to *Ptilosarcus gurneyi* (Gray, 1860) a shallow-water sea pen also belonging to the family Pennatulidae (Birkeland, 1974). Although a similar morphology between these two species might explain similar growth rates, the similarity with *Primnoa* spp. cannot be attributed to comparable morphologies. Mortensen & Buhl-Mortensen (2005) showed that based on their data on *Primnoa resedaeformis* (Gunnerus, 1763), changes in colony height with age had a logarithmic pattern, which was also the case when I included additional data from other *P. resedaeformis* colonies. However, when examining growth rates in relation to colony height no clear patterns were identified, differently from the observed for the sea pens. While in *Primnoa* spp. it seems that growth rates might not really change over time based on the available data, a change was observed for the sea pens. At this point my hypothesis is that growth rates might be species-specific or taxa-specific.

Roberts et al. (2009) compiled growth rates for cold-water corals, including scleractinians and gorgonians. At that time, a list of 17 publications contained information on cold-water octocoral growth rates focusing on five gorgonian genera from deep-water environments. Since then, at least 15 additional published studies and grey literature have added knowledge on growth rates in cold-water octocorals (Appendix 8-1).

This large number of studies on this topic added to the new data resulting from this thesis provided an opportunity to draw an overall picture of growth rates in octocorals. To this end, I compiled over 550 records of growth rates from polar, cold, temperate, and tropical octocorals, from shallow and deep-water environments. Temperature classes were roughly based on the Köppen climate classification. Each record representing one individual colony or the average of several colonies, depending on the availability of the data. Maximum growth rates were used when referring to rates in different parts of the same colony. When average and maximum growth rates were given, I used average rates in the comparison.

From these data it can be seen that growth rates are very comparable among polar, cold, temperate, and tropical octocorals (Fig. 8-2), and among species (Fig. 8.3-8.4). For instance, Yoshioka & Yoshioka (1991) showed that averaged linear growth rates in 13 species of shallow-water plexaurid gorgonians from Puerto Rico ranged 0.8-4.5 cm·yr⁻¹. In Singapore, average growth rates in shallow-water octocorals ranged 2.3-7.9 cm·yr⁻¹ (Goh & Chou, 1995), and in Japan, the shallow-water *Melithaea japonica* (Verrill, 1865) (published as *M. flabellifera*) grew in average 0.3-1.1 cm·yr⁻¹ (Matsumoto, 2004). Deep-water colonies of *Primnoa resedaeformis* had linear growth rates of 0.6-3.5 cm·yr⁻¹ (Mortensen & Buhl-Mortensen, 2005, Sherwood & Edinger, 2009, Chapter 6), and *Primnoella scotiae* Thomson & Ritchie, 1906 from Antarctica had extremely slow average linear growth rates of 0.12 cm·yr⁻¹ (Peck & Brockington, 2013).

It is important to mention that certain colonies of *P. scotiae* had maximum rates reaching ~18 cm·yr⁻¹ (Peck & Brockington, 2013), or twice the maximum rates estimated for *U. encrinus* in Chapter 3. A Kruskal-Wallis test on average rates displayed in figs. 8-3

and 8-4 showed that both radial (Kruskal-Wallis chi-squared = 33.7, p-value= 2.3e-07, N= 473) and linear (Kruskal-Wallis chi-squared = 120.9, p-value= 2.2e-16, N= 435) growth rates are significantly different among temperature classes.

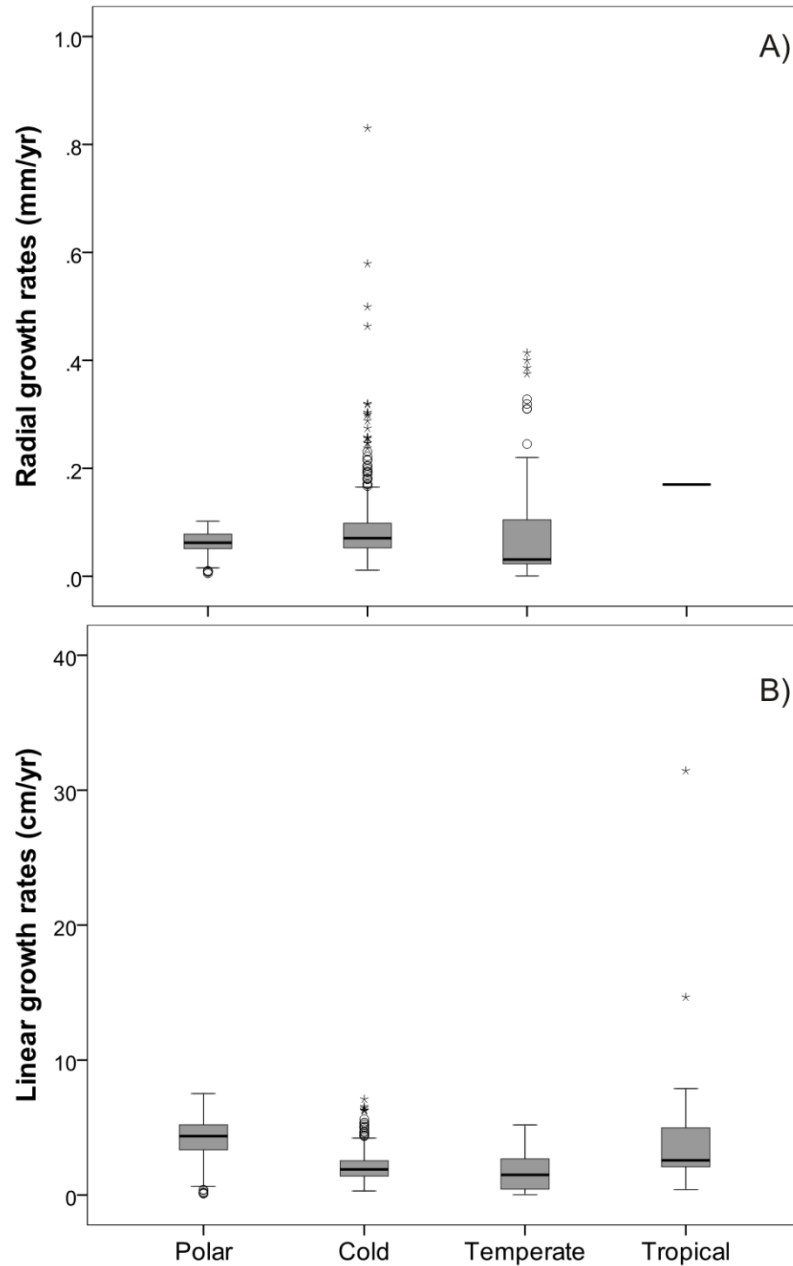


Figure 8-2. Growth rates in octocorals from shallow and deep waters by temperature classes: A) radial growth, and B) linear growth.

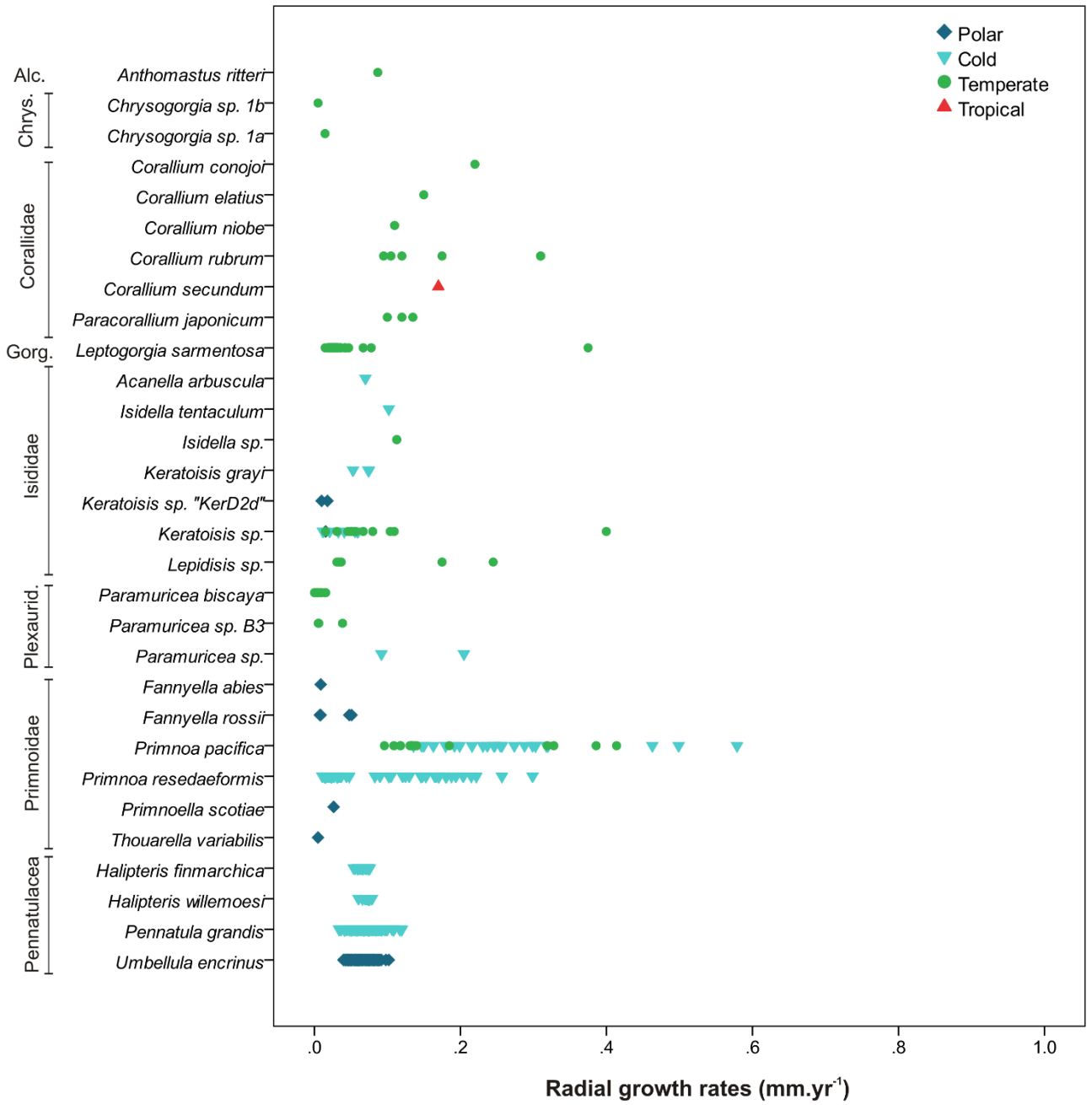


Figure 8-3. Radial growth rates in octocoral species from shallow and deep-water. Stars (*) indicate new data produced as a result of this thesis. Alc: Alcyoniidae, Chrys: Chrysogorgiidae, Gorg: Gorgoniidae, and Plexaurid: Plexauridae. When radial growth rates were not available, diametric growth rates were used as a proxy by dividing them by 2. Radial growth rates for *Paragorgia arborea* are not shown for a better visualization of the data ($0.83 \text{ mm}\cdot\text{yr}^{-1}$, Sherwood & Edinger, 2009). Figure shown in the previous page.

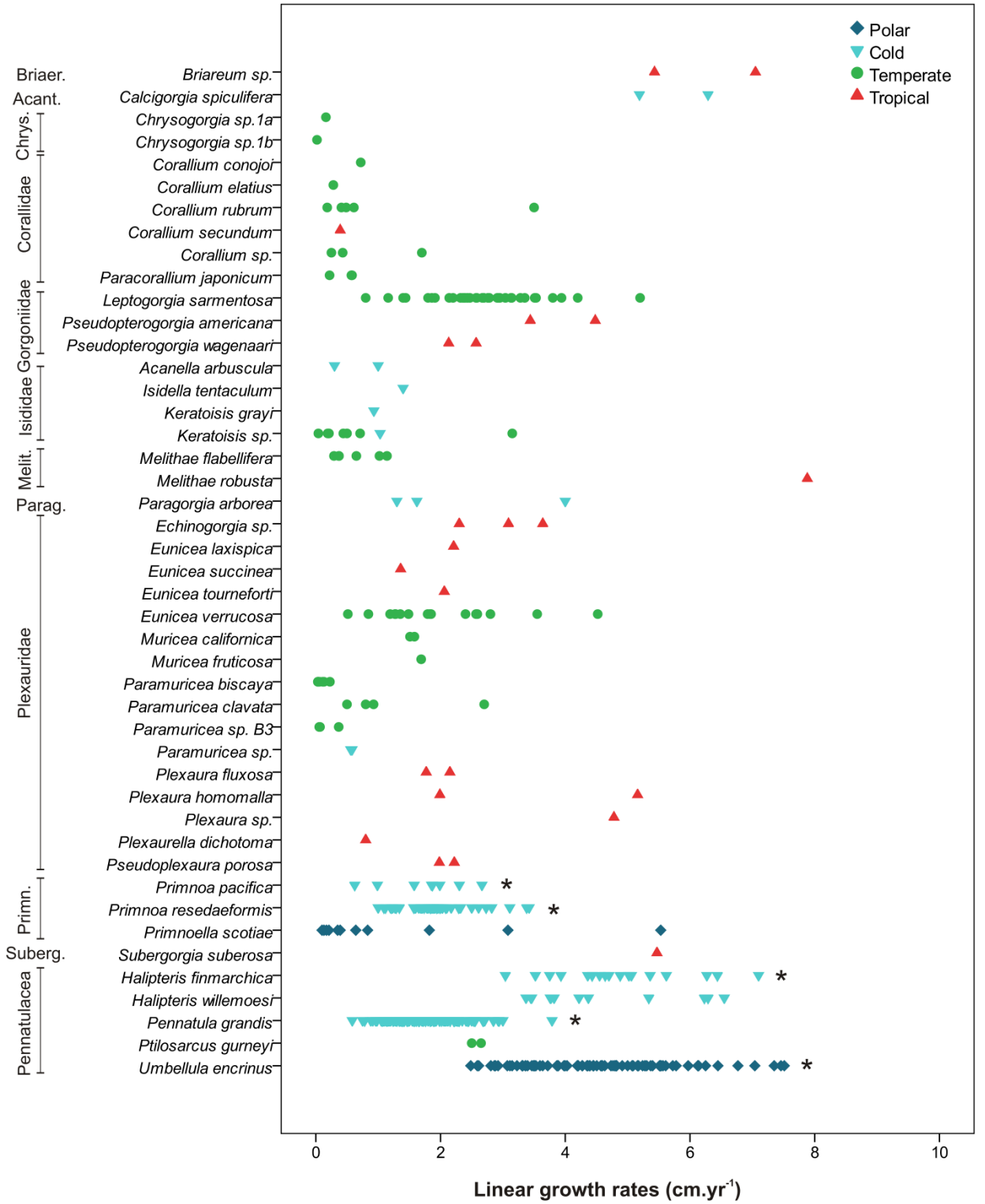


Figure 8-4. Linear growth rates in octocoral species from shallow and deep-water. Stars (*) indicate new data produced as a result of this thesis. Briar: Briareidae, Acant: Acanthogorgiidae, Chrys: Chrysogorgiidae, Gorg: Gorgoniidae, Melit: Melithaeidae, Parag: Paragorgiidae, Primn: Primnoidae, and Suberg: Subergorgiidae. Linear growth rates for *Pseudopterogorgia acerosa* are not shown for a better visualization of the data (31 cm·yr⁻¹, Cadena & Sánchez, 2010). Figure shown in the previous page.

Organisms living in cold-water environments where temperature can reach negative values for half of the year might have very slow growth rates, and probably these low temperatures explain the minimum average rates found in *P. scotiae* from Antarctica, which are the slowest linear growth rates estimated for an octocoral to date (0.12 cm·yr⁻¹, Peck & Brockington, 2013). At the same time, as outlined above the species has the potential to grow at much faster rates. Recently, Martinez-Dios et al. (2016) also estimated very slow growth rates for deep-water Antarctic octocorals, corroborating the study by Peck & Brockington (2013). Our *Keratoisis* sp. “kerD2d” from Baffin Bay also had very slow growth rates, in contrast to the sea pen *U. encrinus* from the same region. Therefore, growth rates in these octocorals might be influenced by other factors rather than temperature alone.

One limitation of this comparison is the data restriction on linear growth rates for many deep-water species, which limits a better comparison between them and their shallow-water counterparts. Similarly, radial and diametric growth rates estimates are usually more restricted for shallow-water tropical taxa, whose studies have been mainly focused on measurement of size increments over time (linear growth rates).

Additionally, we did not control for taxonomic level, depth or colony height (age). Most estimations of octocoral growth rates assume a constant growth during the organism lifespan. However, in this comparison between different species with different life strategies, I could not control for the fact that growth rates might actually change along the life span and be more characteristic of specific age intervals. In several octocorals growth rates have been shown to decrease with colony age (e.g. Grigg, 1974, Mistri & Ceccherelli, 1993, Matsumoto, 2004, Sartoretto & Francour, 2012). Conversely, in the soft coral *Anthomastus ritteri* Nutting, 1909 initial growth is very slow, following a faster growth and reaching of an asymptote (Cordes et al., 2001). In the case of sea pens, growth rates were slower in smaller (younger) colonies as well (Chapters 2-4). In other cases, no relationship has been identified between growth rates and colony age (Thresher, 2009).

The data presented throughout this thesis showed that significant relationships between growth rates and environmental factors were found for some species. However, in any of the cases this relationship was very strong and showing an obvious trend. On the other hand, for all sea pens studied there was a relationship between growth rates and colony height. This seems to indicate that in these organisms colony size or life stage might actually dictate growth rates more than environmental factors, especially under more “acceptable” conditions where water temperature is not extreme, and minimum conditions of food availability required to grow exist.

As I showed in the *Primnoa* study (Chapter 6), colonies from the Strait of Georgia did not have faster growth rates than colonies from other locations, despite the very high surface chlorophyll a in the region. Colonies from this area had similar growth rates to colonies from other areas, indicating that despite a higher food availability at this site

(assuming a strong surface-bottom flux) colonies did not grow faster. However, the overall analysis including all *Primnoa* observations yielded a significant relationship between these two variables. It is possible that colonies from this site were coping with other factors that demanded a trade-off between them and growth, keeping them at a normal growth rate instead of pushing them to the limits of growth. Higher food availability might have a certain influence on growth rates, but ontogeny might actually dictate when it is time to grow faster or slow down.

8.2 Validation of ring formation periodicity

One challenge in the study of longevity in deep-water octocorals is related to the difficulties associated with confirming ring formation periodicity. Although the use of trace elements and ^{14}C analyses to this end could not prove the frequency of ring formation, my attempts were not in vain. To my knowledge, both trace element and ^{14}C analyses of sea pens skeletons were performed for the first time as a result of this work (Chapters 2-4).

While the trace element analysis of the axes in *H. finmarchica* and in *U. encrinus* did not confirm ring formation periodicity, it showed that number of rings and trace element peaks are comparable. This indicates that the physical and chemical characteristics of the axis are correlated. With some refinement of the technique, the axis of sea pens might be a source of environmental information. The EDX analysis was also helpful in characterizing the distribution of elements in the axis, and it can be used in the sclerochronology of sea pens.

The ^{14}C analysis performed in the axis of two *P. grandis* colonies from the Canadian Museum of Nature and from one *U. encrinus* colony from Jones Sound both showed a similar pattern to that observed in the calcite of other deep-water corals whose growth rings were confirmed to be formed annually (c.f. Sherwood et al., 2008). In these other corals, gorgonin was used for the ^{14}C analysis. However, in sea pens it is very challenging to isolate enough organic material from the axis for a ^{14}C analysis. Isolating enough calcite for this study was not straightforward, and considering that calcite makes between 65-85% (Chapters 4 and 5) of the axis shows the limitation of extracting enough organic material that would be meaningful for this analysis (e.g. by extracting material from core, middle, and edge regions). The comparable patterns between my data and those for other deep-water corals in terms of calcite is encouraging, because it strongly suggests that the calcite in the skeleton of sea pens comes from the same water mass as the calcite in the gorgonians, and that rings are formed in the same frequency, which is annual.

Although in my study it was not possible to keep sea pens in a tank and follow growth ring formation after a given period of time (e.g. 2 years), this should not be exceptionally challenging to accomplish, provided live colonies can be maintained for prolonged periods. This is one of the future directions to be followed in the field of sclerochronology of sea pens.

8.3 Morphology and growth in sea pens and *Keratoisis* sp. “kerD2d”

Although studying the axis of sea pens and the stem of gorgonians provide excellent ways of understanding more about growth rates in deep-water species, examining other parts of the colony can also help to better understand how these animals grow. This is what I have done especially for the sea pen *P. grandis*, which has several morphological traits suitable for comparison. For instance, by simply examining relationships between peduncle length proportion and total colony height, rather than peduncle length only, as well as density of polyp leaves rather than number of polyp leaves only, shed a light on the allometry of growth in these organisms: these different parts of the colony do not grow at the same rate as the rest of the colony. This result comes from the interpretation of the negative relationship observed between both peduncle length proportion and density of polyp leaves and colony height, but also from the slope values (<1) in the allometric equation used to test these relationships.

The skeleton of sea pens had rarely been addressed in the literature before this study, in which I showed that magnesian calcite is the carbonate component of the axis all studied sea pen species. The carbonate proportion varying between 65-85% of total axis weight is also a new information about the axis in these organisms. The changes in morphology, metrics (area, radius, weight), and carbonate proportion along the axes of *U. encrinus* and *A. grandiflorum* show the complexity of these skeletons, which record information through the colony's life span. These organisms might prove to be very interesting models in the field of biomechanics in the future. Furthermore, a comparison

to colonies of small size (young colonies) will also help to better understand changes in the skeleta with age.

In terms of gorgonians, the report of the dense forests of the bamboo coral *Keratoisis* sp. “kerD2d” in Baffin Bay was important from the conservation perspective. However, the observation that those colonies grow probably directly on mud through root-like branches that support the colony in soft substrate was also interesting from the perspective of growth. Root-like branches are common in bamboo corals (family Isididae) and chrysogorgiids (Family Chrysogorgiidae) (Deichmann, 1936). But colonies of *Keratoisis grayi* at other sites in the Northwest Atlantic grow attached to hard substrates (Edinger et al., 2011), through a single point of attachment, not root-like branches. The causes for different growth strategies in *Keratoisis* spp. is an interesting topic to be investigated.

In Baffin Bay these corals are so densely distributed that it is difficult to tell colonies apart (Chapter 7). We still do not know why and how these colonies grow so close to each other in this area. Because of the root-like branch system, my hypothesis is that colonies grow not only vertically, but they keep expanding laterally because substrate is largely available, and root-like branches allow for this lateral growth. Future video surveys in this site might help us to elucidate some of the questions related to these forests, including: 1) Are colonies entirely associated to a soft substrate or is there a hard substrate component not yet identified? 2) What is the extent of these forests? 3) Why are they so dense? Are they several colonies or fewer individuals that grow to the sides? 4) How old are these colonies, and are rings formed annually like in *K. grayi* from Newfoundland waters?

I made attempts to answer to the last question but I was not 100% successful. First of all, these densely arranged colonies have thin stems where visualization of growth rings is more challenging than in bamboo corals with wider stems. For the fragments obtained I simply could not obtain enough gorgonin material (in weight) for a ^{14}C analysis. Rings are thin and delicate, and therefore very difficult to work with for this type of analysis. After polishing a cross section on a lapidary wheel, rings were easier to visualize. I performed a trace element analysis on the calcite portion of the skeleton, and tried to make a correspondence between the number of peaks visualized and the number of rings. Differently from the sea pens, I found no clear correspondence. This might be related to the size of SIMS spots, which were sometimes larger than growth rates for one year (ring). If rings are formed annually as in *K. grayi* from the Grand Banks (Sherwood & Edinger, 2009), these colonies have longevities > 100 years, which is not uncommon for the genus (e.g. Sherwood & Edinger, 2009, Farmer et al., 2015). Additionally, if our estimates are correct, these colonies have some of the slowest growth rates reported for gorgonians.

8.4 Final considerations

We now know much more than we did only a few decades ago on sclerochronology, growth rates, and distribution of octocorals. The increasing access to equipment that allows us to survey deep-water environments is immensely contributing to the understanding of deep-water coral ecological importance and vulnerability. Based on

my thesis, some of the questions and future directions that I believe are important for a better understanding of octocoral growth are listed below.

- **More environmental data required.** Having access to samples from sites where bottom environmental data has been obtained over a large temporal scale. This will help to further understand, in a more precise way, how changes in environmental conditions influence growth rates in these organisms. In this way, the use of surface data to test the influence of environmental conditions in these benthic organisms can also be fully assessed and calibrated.
- **How fast do tropical deep-water octocorals grow and how old are they?** Studies on deep-water octocoral growth have been largely focused on high latitude regions. Studies on tropical deep-water octocorals are lacking in the literature, and an assessment of how fast these octocorals grow in these environments can add important knowledge on the influence of environmental conditions on these organisms' growth over a larger spatial scale.
- **How variable are growth rates in cosmopolitan deep-water octocoral species?** Dedicated studies on cosmopolitan species or species with wide geographic distributions might also help to better understand the influence of environmental factors on these organisms. While growth rates in certain genera of wide geographic distributions have been estimated, a comparison between these data is always risky due to different techniques employed, possible species-specific variations, different temporal scales studied, etc. Having growth rates estimated

using similar techniques, and with the same focus might be very valuable to reduce any bias that could result from these studies.

- **Going back to the beginning: how to validate frequency of ring formation in more challenging taxa?** The development of dating techniques and other techniques and strategies for confirming the periodicity of ring formation are particularly important to study species with decadal longevities, such as sea pens. Furthermore, better understanding the meaning of “inter-annual” rings or frequencies other than annual in the deep-sea is another important step.
- **What triggers growth ring formation in different taxa of deep-water octocorals, and how does the process occur at the skeletal level?** Studies on the basic understanding of how growth rings are formed, as well as calcification rates in deep-water species are also required for a better understanding of the biology of these organisms.
- **How does colony morphology change as the coral grows?** Although in several octocoral species juveniles and adults look alike, in some species this is not the case. Even when obvious changes in colony morphology through life stages cannot be readily identified, changes in the proportions of colony parts do occur (e.g. allometry in *Pennatula grandis*). In some cases colonies might suffer obvious morphological changes as they grow (e.g. Mosher and Watling, 2009). Examining and comparing colony morphology through different life stages in other octocoral species is therefore a field to be explored in order to better understand growth in these organisms (Watling et al., 2011).

- **How will climate change influence growth and calcification processes in deep-water octocorals?** Several growth processes might be influenced by increased water temperatures and ocean acidification. Calcification is one of the obvious processes that might be affected by a decreased water pH. Decrease in calcification and changes in the morphology of sclerites in octocorals have been identified under acidic conditions in laboratory (Bramanti et al., 2013, Cerrano et al., 2013); although sclerites seem to be more resilient, as they are protected by tissue (Gabay et al., 2014). Increased water temperatures can have adverse effects on shallow-water corals, especially zooxanthellate species (e.g. Prada et al., 2010); but knowledge on their impact on growth and specifically on deep-water octocorals is still limited in the literature (Roberts & Cairns, 2014). The effects of increased temperature and lowered pH in octocorals have been started to be explored in gorgonians, but not in sea pens yet, and this is an important future direction towards a better understanding of the vulnerability of these organisms to climate change.

8.5 References

Aranha, R., E. Edinger, G. Layne & G. Piercey, 2014. Growth rate variation and potential paleoceanographic proxies in *Primnoa pacifica*: Insights from high-resolution trace element microanalysis. *Deep Sea Research Part II: Topical Studies in Oceanography* 99: 213-226.

Birkeland, C., 1974. Interactions between a sea pen and seven of its predators. *Ecological Monographs* 44: 211-232.

Bramanti, L., J. Movilla, M. Guron, E. Calvo, A. Gori, C. Dominguez-Carrió, J. Grinyó, A. Lopez-Sanz, A. Martinez-Quintana, C. Pelejero, P. Ziveri & S. Rossi, 2013. Detrimental effects of ocean acidification on the economically important Mediterranean red coral (*Corallium rubrum*). *Global Change Biology* 19: 1897-1908.

Brodeur, R. D., 2001. Habitat-specific distribution of Pacific ocean perch (*Sebastes alutus*) in Pribilof Canyon, Bering Sea. *Continental Shelf Research* 21: 207-224.

Cadena, N. J. & J. A. Sánchez, 2010. Colony growth in the harvested octocoral *Pseudopterogorgia acerosa* in a Caribbean coral reef. *Marine Ecology* 31: 566-573.

Cerrano, C., U. Cardini, S. Bianchelli, C. Corinaldesi, A. Pusceddu & R. Danovaro, 2013. Red coral extinction risk enhanced by ocean acidification. *Scientific Reports* 3: 1457.

Cordes, E. E., J. W. Nybakken & G. VanDykhuisen, 2001. Reproduction and growth of *Anthomastus ritteri* (Octocorallia: Alcyonacea) from Monterey Bay, California, USA. *Marine Biology* 138: 491-501.

- Deichmann, E., 1936. The Alcyonaria of the western part of the Atlantic Ocean. *Memoirs of the Museum of Comparative Zoology* 53: 1-317.
- Edinger, E. N., O. A. Sherwood, D. J. W. Piper, V. E. Wareham, K. D. Baker, K. D. Gilkinson & D. B. Scott, 2011. Geological features supporting deep-sea coral habitat in Atlantic Canada. *Continental Shelf Research* 31: S69-S84.
- Farmer, J. R., L. F. Robinson & B. Hönisch, 2015. Growth rate determinations from radiocarbon in bamboo corals (genus *Keratoisis*). *Deep Sea Research Part I: Oceanographic Research Papers* 105: 26-40.
- Gabay, Y., M. Fine, Z. Barkay & Y. Benayahu, 2014. Octocoral tissue provides protection from declining oceanic pH. *PLoS ONE* 9: e91553.
- Goh, N. K. C. & L. M. Chou, 1995. Growth of five species of gorgonians (Subclass Octocorallia) in the sedimented waters of Singapore. *Marine Ecology* 16: 337-346.
- Grigg, R. W., 1974. Growth rings: annual periodicity in two gorgonian corals. *Ecology* 55: 876-881.
- Martinez-Dios, A., C. Dominguez-Carrió, R. Zapata-Guardiola & J. Gili, 2016. New insights on Antarctic gorgonians' age, growth and their potential as paleorecords. *Deep Sea Research Part I: Oceanographic Research Papers* 112: 57-67.
- Matsumoto, A., 2004. Heterogeneous and compensatory growth in *Melithaea flabellifera* (Octocorallia: Melithaeidae) in Japan. *Hydrobiologia* 530: 389-397.
- Mistri, M. & V. U. Ceccherelli, 1993. Growth of the Mediterranean gorgonian *Lophogorgia ceratophyta* (L., 1758). *Marine Ecology* 14: 329-340.

Mortensen, P. B. & L. Buhl-Mortensen, 2005. Morphology and growth of the deep-water gorgonians *Primnoa resedaeformis* and *Paragorgia arborea*. *Marine Biology* 147: 775-788.

Mosher, C. V. & L. Watling, 2009. Partners for life: a brittle star and its octocoral host. *Marine Ecology Progress Series* 397: 81-88.

Peck, L. S. & S. Brockington, 2013. Growth of the Antarctic octocoral *Primnoella scotiae* and predation by the anemone *Dactylanthus antarcticus*. *Deep Sea Research Part II: Topical Studies in Oceanography* 92: 73-78.

Prada, C., E. Weil & P. M. Yoshioka, 2010. Octocoral bleaching during unusual thermal stress. *Coral Reefs* 29: 41-45.

Roberts, J. M. & S. D. Cairns, 2014. Cold-water corals in a changing ocean. *Current Opinion in Environmental Sustainability* 7: 118-126.

Roberts, J. M., A. Wheeler, A. Freiwald & S. Cairns, 2009. Cold-water corals: the biology and geology of deep-sea coral habitats. Cambridge University Press, Cambridge, UK; New York.

Sartoretto, S. & P. Francour, 2012. Bathymetric distribution and growth rates of *Eunicella verrucosa* (Cnidaria: Gorgoniidae) populations along the Marseilles coast (France). *Scientia Marina* 76: 349-355.

Sherwood, O. A. & E. N. Edinger, 2009. Ages and growth rates of some deep-sea gorgonian and antipatharian corals of Newfoundland and Labrador. *Canadian Journal of Fisheries and Aquatic Sciences* 66: 142-152.

Sherwood, O. A., E. N. Edinger, T. P. Guilderson, B. Ghaleb, M. J. Risk & D. B. Scott, 2008. Late Holocene radiocarbon variability in Northwest Atlantic slope waters. *Earth and Planetary Science Letters* 275: 146-153.

Thresher, R. E., 2009. Environmental and compositional correlates of growth rate in deep-water bamboo corals (Gorgonacea; Isididae). *Marine Ecology Progress Series* 397: 187-196.

Watling, L., S. C. France, E. Pante & A. Simpson, 2011. Chapter Two - Biology of Deep-Water Octocorals. In Michael Lesser (ed), *Advances in Marine Biology*. Academic Press: 41.

Yoshioka, P. M. & B. B. Yoshioka, 1991. A comparison of the survivorship and growth of shallow-water gorgonian species of Puerto Rico. *Marine Ecology Progress Series* 69: 253-260.

Appendix 8-1 Published octocoral growth rates.

Year	Class	Depth	Class	Location	Suborder	Family	Species	Source
1974	Temp	14-20	Shallow	California	Holaxonia	Plexauridae	<i>Muricea fruticosa</i>	Grigg (1974)
1974	Temp	13-16	Shallow	Washington	Subsessiliflorae	Pennatulidae	<i>Ptilosarcus gurneyi</i>	Birkeland (1974)
1975	Temp	14-17	Shallow	California	Holaxonia	Plexauridae	<i>Muricea californica</i>	Grigg (1975)
1985	Temp	na	Shallow	Spain	Holaxonia	Plexauridae	<i>Paramuricea clavata</i>	Gili & Garcia (1985)
1986	Temp	na	Shallow	Spain	Scleraxonia	Coraliiidae	<i>Corallium rubrum</i>	García-Rodríguez & Massó (1986)
1990	Temp	600	Deep	Florida	Scleraxonia	Coraliiidae	<i>Corallium niobe</i>	Druffel et al. (1990)
1990	Tropical	0-15	Shallow	Panama	Holaxonia	Plexauridae	<i>Plexaura</i> A.	Lasker (1990)
1991	Tropical	10.6	Shallow	Puerto Rico	Holaxonia	Plexauridae	<i>Eunicea laxispica</i>	Yoshioka & Yoshioka (1991)
1991	Tropical	10.6	Shallow	Puerto Rico	Holaxonia	Plexauridae	<i>Eunicea succinea</i>	Yoshioka & Yoshioka (1991)
1991	Tropical	10.6	Shallow	Puerto Rico	Holaxonia	Plexauridae	<i>Eunicea tourneforti</i>	Yoshioka & Yoshioka (1991)
1991	Tropical	6.7-10.6	Shallow	Puerto Rico	Holaxonia	Plexauridae	<i>Plexaura fluxosa</i>	Yoshioka & Yoshioka (1991)
1991	Tropical	10.6	Shallow	Puerto Rico	Holaxonia	Plexauridae	<i>Plexaura homomalla</i>	Yoshioka & Yoshioka (1991)
1991	Tropical	10.6	Shallow	Puerto Rico	Holaxonia	Plexauridae	<i>Plexaurella dichotoma</i>	Yoshioka & Yoshioka (1991)
1991	Tropical	6.7-10.6	Shallow	Puerto Rico	Holaxonia	Plexauridae	<i>Pseudoplexaura porosa</i>	Yoshioka & Yoshioka (1991)
1991	Tropical	6.7-10.6	Shallow	Puerto Rico	Holaxonia	Plexauridae	<i>Pseudopterogorgia americana</i>	Yoshioka & Yoshioka (1991)
1991	Tropical	6.7-10.6	Shallow	Puerto Rico	Holaxonia	Plexauridae	<i>Pseudopterogorgia wagnaari</i>	Yoshioka & Yoshioka (1991)
1991	Tropical	6.7-10.6	Shallow	Puerto Rico	Holaxonia	Plexauridae	<i>Pseudoptorgorgia acerosa</i>	Yoshioka & Yoshioka (1991)
1992	Tropical	5-8	Shallow	Panama	Scleraxonia	Briareidae	<i>Briareum asbestinum</i>	Brazeau & Lasker (1992)
1993	Temp	16-27	Shallow	Italy	Holaxonia	Gorgoniidae	<i>Leptogorgia sarmentosa</i>	Mistri & Cecchereli (1993)
1994	Temp	29-39	Shallow	Italy	Holaxonia	Plexauridae	<i>Paramuricea clavata</i>	Mistri & Cecchereli (1994)
1995	Tropical	12-14	Shallow	Singapore	Holaxonia	Plexauridae	<i>Echinogorgia</i> sp. A	Goh & Chou (1995)
1995	Tropical	12-14	Shallow	Singapore	Holaxonia	Plexauridae	<i>Echinogorgia</i> sp. C	Goh & Chou (1995)
1995	Tropical	12-14	Shallow	Singapore	Holaxonia	Plexauridae	<i>Echinogorgia</i> sp. D	Goh & Chou (1995)
1995	Tropical	12-14	Shallow	Singapore	Scleraxonia	Melithidae	<i>Melithae robusta</i>	Goh & Chou (1995)

Year	Class	Depth	Class	Location	Suborder	Family	Species	Source
1995	Tropical	12-14	Shallow	Singapore	Scleraxonia	Subergorgiidae	<i>Subergorgia suberosa</i>	Goh & Chou (1995)
1997	Tropical	16-22	Shallow	Panama	Holaxonia	Plexauridae	<i>Plexaura homomalla</i>	Kim & Lasker (1997)
1998	Temp	15-27	Shallow	NW Mediterranean	Holaxonia	Plexauridae	<i>Paramuricea clavata</i>	Coma et al. (1998)
1999	Temp	na		Italy	Scleraxonia		<i>Corallium rubrum</i>	Cerrano et al. (1999)
2001	Cold	20.5-26	Shallow	Alaska	Holaxonia	Acanthogorgiidae	<i>Calcigorgia spiculifera</i>	Stone & Wing (2001)
2001	Temp	300-450	Deep	California	Alcyoniina	Alcyoniidae	<i>Anthomastus ritteri</i>	Cordes et al. (2001)
2002	Cold	263	Deep	Dixon Entrance	Holaxonia	Primnoidae	<i>Primnoa resedaeformis</i>	Andrews et al. (2002)
2002	Temp	10-47	Shallow	France	Scleraxonia	Coraliidae	<i>Corallium rubrum</i>	Garrabou & Harmelin (2002)
2002	Cold	142-248	Deep	Gulf of Alaska	Holaxonia	Halipteridae	<i>Halipterus willemoesi</i>	Wilson et al. (2002)
2002	Cold	450	Deep	NE Channel	Holaxonia	Primnoidae	<i>Primnoa resedaeformis</i>	Risk et al. (2002)
2004	Temp	1-5	Shallow	Japan	Scleraxonia	Melithidae	<i>Melithae flabellifera</i>	Matsumoto (2004)
2004	Temp	15-62	Shallow	Mediterranean	Scleraxonia	Coraliidae	<i>Corallium rubrum</i>	Marschal et al. (2004)
2005	Temp	1482	Deep	California	Scleraxonia	Coraliidae	<i>Corallium</i> sp.	Andrews et al. (2005)
2005	Temp	1425	Deep	California	Holaxonia	Isididae	<i>Keratoisis</i> sp.	Andrews et al. (2005)
2005	Temp	25-35	Shallow	Italy	Scleraxonia	Coraliidae	<i>Corallium rubrum</i>	Bramanti et al. (2005)
2005	Cold	246-542	Deep	NE Channel	Holaxonia	Primnoidae	<i>Primnoa resedaeformis</i>	Mortensen & Buhl-Mortensen (2005)
2005	Cold	50	Shallow	Norway	Scleraxonia	Paragorgiidae	<i>Paragorgia arborea</i>	Mortensen & Buhl-Mortensen (2005)
2005	Cold	na	Deep	New Zealand	Scleraxonia	Paragorgiidae	<i>Paragorgia arborea</i>	Mortensen & Buhl-Mortensen (2005) ¹
2006	Tropical	450	Deep	Makapuu, Oahu	Scleraxonia	Coraliidae	<i>Corallium secundum</i>	Roark et al. (2006)
2006	Temp	594-770	Deep	New Zealand	Holaxonia	Isididae	<i>Keratoisis</i> sp.	Noé & Dullo (2006)
2007	Temp	350-505	Deep	Japan	Holaxonia	Primnoidae	<i>Primnoa pacifica</i>	Matsumoto (2007)
2007	Cold	720	Deep	NE Atlantic	Holaxonia	Primnoidae	Primnoid sp.	Noé et al. (2007)
2007	Temp	935	Deep	New Zealand	Holaxonia	Isididae	<i>Keratoisis</i> sp.	Tracey et al. (2007)
2007	Temp	690-800	Deep	New Zealand	Holaxonia	Isididae	<i>Lepidisis</i> sp.	Tracey et al. (2007)
2007	Temp	874-1030	Deep	New Zealand	Holaxonia	Isididae	<i>Lepidisis</i> sp.	Tracey et al. (2007)

Year	Class	Depth	Class	Location	Suborder	Family	Species	Source
2007	Temp	638-840	Deep	New Zealand	Holaxonia	Isididae	<i>Lepidisis</i> sp.	Tracey et al. (2007)
2007	Temp	1000	Deep	Tasmania	Holaxonia	Isididae	<i>Keratoisis</i> sp.	Thresher et al. (2007)
2008	Temp	594-770	Deep	New Zealand	Holaxonia	Isididae	<i>Keratoisis</i> sp.	Noé et al. (2008)
2009	Temp	1425-1574	Deep	Davidson Seamount	Holaxonia	Isididae	<i>Keratoisis</i> sp.	Andrews et al. (2009)
2009	Cold	874	Deep	Gulf of Alaska	Holaxonia	Isididae	<i>Isidella tentaculum</i>	Andrews et al. (2009)
2009	Cold	746	Deep	Gulf of Alaska	Holaxonia	Isididae	<i>Keratoisis</i> sp.	Andrews et al. (2009)
2009	Cold	526	Deep	NW Atlantic	Holaxonia	Isididae	<i>Acanella arbuscula</i>	Sherwood & Edinger (2009)
2009	Cold	601-1193	Deep	NW Atlantic	Holaxonia	Isididae	<i>Keratoisis ornata</i>	Sherwood & Edinger (2009)
2009	Cold	414	Deep	NW Atlantic	Scleraxonia	Paragorgiidae	<i>Paragorgia arborea</i>	Sherwood & Edinger (2009)
2009	Cold	814-850	Deep	NW Atlantic	Holaxonia	Plexauridae	<i>Paramuricea</i> sp.	Sherwood & Edinger (2009)
2009	Cold	257-640	Deep	NW Atlantic	Holaxonia	Primnoidae	<i>Primnoa resedaeformis</i>	Sherwood & Edinger (2009)
2009	Temp	1140-1150	Deep	Tasmania	Holaxonia	Isididae	<i>Isidella</i> sp.	Sherwood et al. (2009)
2009	Temp	1000-1366	Deep	Tasmania	Holaxonia	Isididae	<i>Lepidisis</i> sp.	Sherwood et al. (2009)
2009	Temp		Deep	Australia	Holaxonia	Isididae	<i>Keratoisis</i> sp.	Thresher (2009)
2009	Temp	850-1000	Deep	Tasmania	Holaxonia	Isididae	<i>Keratoisis</i> sp.	Thresher et al. (2009)
2009	Polar		Deep	Antarctica	Holaxonia	Isididae	<i>Keratoisis</i> sp.	Thresher (2009)
2010	Tropical	9	Shallow	Caribbean	Holaxonia	Plexauridae	<i>Pseudopterogorgia acerosa</i>	Cadena & Sánchez (2010)
2010	Temp	36-42	Shallow	Mediterranean	Scleraxonia	Coralliidae	<i>Corallium rubrum</i>	Gallmetzer et al. (2010)
2011	Temp	1295-2136	Deep	California	Holaxonia	Isididae	<i>Keratoisis</i> sp.	Hill et al. (2011)
2011	Temp	30-32	Shallow	Mediterranean	Holaxonia	Gorgoniidae	<i>Leptogorgia sarmentosa</i>	Rossi et al. (2011)
2011	Cold	549	Deep	SE US slope	Holaxonia	Isididae	<i>Keratoisis</i> sp.	Sinclair et al. (2011)
2012	Temp	20-40	Shallow	France	Holaxonia	Plexauridae	<i>Eunicella verrucosa</i>	Sartoretto & Francour (2012)
2013	Polar	4-12	Shallow	Antarctica	Holaxonia	Primnoidae	<i>Primnoella scotiae</i>	Peck & Brockington (2013)
2013	Temp	108	Deep	Japan	Scleraxonia	Coralliidae	<i>Corallium conojoi</i>	Luan et al. (2013)
2013	Temp	200-300	Deep	Japan	Scleraxonia	Coralliidae	<i>Corallium elatius</i>	Luan et al. (2013)
2013	Temp	94-212	Deep	Japan	Scleraxonia	Coralliidae	<i>Paracorallium japonicus</i>	Luan et al. (2013)

Year	Class	Depth	Class	Location	Suborder	Family	Species	Source
2013	Temp	16-20	Shallow	Thyrrhenian Sea	Holaxonia	Plexauridae	<i>Eunicella verrucosa</i>	Munari et al. (2013)
2014	Temp	1049	Deep	Gulf of Mexico	Calcaxonia	Chrysogorgiidae	<i>Chrysogorgia</i> sp.1a	Prouty et al. (2014)
2014	Temp	1094	Deep	Gulf of Mexico	Calcaxonia	Chrysogorgiidae	<i>Chrysogorgia</i> sp.1b	Prouty et al. (2014)
2014	Temp	882-1852	Deep	Gulf of Mexico	Holaxonia	Plexauridae	<i>Paramuricea biscaya</i>	Prouty et al. (2014)
2014	Temp	1040-1050	Deep	Gulf of Mexico	Calcaxonia	Plexauridae	<i>Paramuricea</i> sp.B3	Prouty et al. (2014)
2014	Cold	201-393	Deep	Dixon Entrance	Holaxonia	Primnoidae	<i>Primnoa pacifica</i>	Aranha et al. (2014)
2014	Temp	266-312	Deep	Washington	Holaxonia	Primnoidae	<i>Primnoa pacifica</i>	Aranha et al. (2014)
2015	Cold	847-1079	Deep	Bear Seamount	Holaxonia	Isididae	<i>Keratoisis</i> sp.	Farmers et al. (2015)
2015	Cold	1195-1402	Deep	Bear Seamount	Holaxonia	Isididae	<i>Keratoisis</i> sp.	Farmers et al. (2015)
2015	Cold	1826-2008	Deep	Bear Seamount	Holaxonia	Isididae	<i>Keratoisis</i> sp.	Farmers et al. (2015)
2015	Temp	805	Deep	East Florida	Holaxonia	Isididae	<i>Keratoisis</i> sp.	Farmers et al. (2015)
2015	Cold	347-1210	Deep	NW Atlantic	Subsessiliflorae	Halipteridae	<i>Halipterus finmarchica</i>	Chapter 2
2015	Cold	320	Deep	Scotian slope	Holaxonia	Isididae	<i>Keratoisis</i> sp.	Farmer et al. (2015)
2016	Polar	243	Deep	Antarctica	Calcaxonia	Primnoidae	<i>Fannyella abies</i>	Martinez-Dios et al. (2016)
2016	Polar	332-408	Deep	Antarctica	Calcaxonia	Primnoidae	<i>Fannyella rossii</i>	Martinez-Dios et al. (2016)
2016	Polar	525	Deep	Antarctica	Calcaxonia	Primnoidae	<i>Thouarella variabilis</i>	Martinez-Dios et al. (2016)
2016	Cold	188-1203	Deep	NW Atlantic	Sessiliflorae	Umbellulidae	<i>Umbellula encrinus</i>	Chapter 3
2016	Cold	52-1451	Deep	NW Atlantic	Subsessiliflorae	Pennatulidae	<i>Pennatula grandis</i>	Chapter 4
2016	Cold	20-270	Deep	NW Atlantic	Calcaxonia	Primnoidae	<i>Primnoa pacifica</i>	Chapter 6
2016	Cold	165-3186	Deep	NW Atlantic	Calcaxonia	Primnoidae	<i>Primnoa resedaeformis</i>	Chapter 6
2016	Polar	900	Deep	Baffin Bay	Holaxonia	Isididae	<i>Keratoisis</i> sp. “kerD2d”	Chapter 7

¹Growth rates reported by these authors as personal communication.